Role of Metabolism Controlled Histone Posttranslational Modifications in Cancer Biology

Mengqing Gao

THÈSE

Pour obtenir le grade de

DOCTEUR DE L'UNIVERSITE GRENOBLE ALPES

Préparée dans le cadre d'une cotutelle entre la Communauté Université Grenoble Alpes et Shanghai Jiao Tong University

Spécialité : **Biologie Cellulaire**

Arrêté ministériel : le 6 janvier 2005 – 25 mai 2016

Présentée par

Mengqing GAO

Thèse dirigée par **Saadi KHOCHBIN** et **Jianqing MI**
codirigée par **Sophie ROUSSEAUX**

Préparée au sein des **Centre de recherche UGA- INSERM U 1209-CNRS UMR 5309/ l'Institut pour l'avancée des biosciences (IAB)** dans **l'Ecole Doctorale Chimie et Sciences du Vivant**

Role of Metabolism Controlled Histone Posttranslational Modifications in Cancer Biology

Rôle des modifications post-traductionnelles des histones contrôlées par le métabolisme dans la biologie du cancer

Thèse soutenue publiquement le « **16 Juin 2021** »,
devant le jury composé de :

Dr. Uwe SCHLATTNER
Professeur, Université Grenoble Alpes, Président
Dr. Eric GILSON
Professeur, Université Côte d'Azur, Rapporteur
Dr. Zdenko HERCEG
Directeur de recherche, IARC de Lyon, Rapporteur
Dr. Geneviève ALMOUZNI
Directeur de recherche, CNRS de Paris, Examinatrice

CONTENT

ACKNOWLEDGEMENT

I would like to thank Uwe Schlattner, Eric Gilson, Zdenko Herceg, and Geneviève Almouzni to be members of the jury and evaluate my work.

I thank my supervisor, Saadi Khochbin for his wonderful ideas and extensive suggestions throughout the project. As a beginner, I have been exposed to too many expert thoughts, and have received too much patience from him. I would like to thank my co-supervisor, Sophie Rousseaux for her suggestions and her tremendous help in bioinformatics. I would like to thank my joint supervisor, Jianqing Mi, who not only supported the scientific project, but also attached me to the clinical knowledge. I would like to thank my PhD committee members, Carlo Petosa and Sophie Park, who evaluated my work each year and gave advice.

I would like to thank all the colleagues in SK team. I thank Domenico Iuso, who expressed numerous basic concepts in biology and taught plenty of general ideas about research. I thank Tao Wang, who is a walking encyclopedia and always gave answers. I thank Sophie Barral, Sandrine Benitski-Curtet, Florent Chuffart and Ekaterina Flin who helped me with the experiments and the data analysis. I thank Anne-Laure Vitte, Fayçal Boussouar, Thierry Buchou, Michel Pabion, Alexandra Vargas, Clovis Chabert, Ariadni Liakopoulou, Mélanie Petrier, and the previous colleagues, Naghmeh Hoghoughi, Azadeh Hajmirza to talk, to discuss, and to help.

I would like to thank every colleague in IAB, I thank Sara El Kennani, Xue Yang, Tao Jia, Alex Casanova, Francesco Ielasi, Valentina Lukinovic, Oliver Destaing, Sabeen Ikram, Nicolas Reynoird etc. I remember every single piece of help they provided, and every single piece of joy they brought about in the institute. I would like to thank every working stuff in IAB, Anne-Sophie Ribba, Mylène Pezet, Jacques Mazzega, Dalenda Benmedjahed, Hélène Medjkane, Amélie Fauconnet etc. who ensure the platforms and the whole institute to run properly. I thank UGA working stuffs, the CSV secretary Magali Pourtier and a lot of other employees to deal with the students' affairs.

I would like to thank all the collaborators for their contributions. I thank Lisa Bargier and Denis Puthier from Aix Marseille Université to support the tremendous work of sequencing. I would like to thank Yingming Zhao and Zhongyi Cheng, who provided the important antibodies in my work. I thank Minjia Tan and Lulu Pan from Shanghai Institute of Materia Medica for helping with the work by mass spectrometry, I thank Heinz Neumann and Martin Spinck from Max-Planck-Institute of Molecular Physiology to support the work of CobB.

I would like to thank my colleagues in Shanghai, Jin Wang, Duohui Jing, Lijun Peng, Mengping Xi, Caicike Bayin, Sisi Wang, Wenqian Xu, Wanyan Ouyang, Shanshan Guo, Gaoxian Song who make the lab function and bring joys to the lab. I thank every working stuff in Shanghai Institute of Hematology who serves the institute and provides convenience for students.

Finally, I thank my family, my parents and my siblings who support and care me all the way here. I thank my boyfriend who gives love, patience, comforts and keeps me company throughout the ups and downs in my life. I thank my precious friends Mei Kang, Hongling Diao and Xinran Wang who always stand by my side.

Thank you all.

ABSTRACT

Chromatin-based events, prominently gene transcription are the basis of cellular characteristics in normal tissues and in cancer context. Histone posttranslational modifications are parts of specific regulatory circuits controlling chromatin-based biological processes. A myriad of specific types of histone modifications, including site-specific histone acetylation and methylation, etc. have been characterized with respect to their roles in gene transcriptional regulation. A critical family of chromatin regulators bridges histone modifications and gene transcriptional output is the readers. The specificity of readers recognizing histone modifications depends not only on the modifications, but also on their combinations. Additionally, it should be noted that histone modifications are dynamic and this process is impacted by a variety of factors, including cellular metabolites.

Previously the team identified a gene FASTKD1 whose expression is associated with poor prognosis in acute lymphoblastic leukemia (ALL). During my research, we uncovered that this gene is a negative regulator of general mitochondrial activity, and more specifically controls the mitochondrial respiration. Using gene knockout cell models, we further characterized the link between mitochondrial activity with histone modifications, and highlighted the importance of fatty acid metabolism, especially β-oxidation, in mediating histone modifications. The association of mitochondrial activity-β-oxidation and histone acylations was also confirmed in patients' primary blasts.

BET family proteins are specific readers of histone acetylation and mediate transcription regulation. Previous studies uncovered that the first bromodomain of a BET protein, Brdt, recognizes diacetylated histone marks (H4K5acK8ac) but not H4K5 butyrylated histones. We noticed that FASTKD1-mediated mitochondrial activity prominently impacts non-acetylacylations but not acetylations. Using our gene knockout cell model, we could demonstrate thatthe relative level of the acetyl and acyl marks tunes the bound state of BRD4 withchromatin.We showed that an increased ratio of acyl/acetyl disfavors BRD4-chromatin interaction,resulting in a loose and dynamic bound state, while a decreased ratio favors the binding and leads to a tight interaction. The functional output of this dynamic interaction is to re-distributethe BRD4 across the genome. More specifically, dynamic BRD4-chromatin interaction causedby high acyl/acetyl ratio makes BRD4 more available to be recruited on gene transcriptionalstart sites (TSS) and mediate the stimulated expression of a subset of genes mediated by BRD4.Gene functional analysis revealed that high acyl patients or high acyl/acetyl cells displayedincreased expression of genes associated with ribosome synthesis, cell cycle and decreasedexpression of genes associated with stemness.

Based on this work, we propose that cell metabolism, through modulating the histone acetyl/acyl ratio, controls a cellular reservoir of BRD4 (and probably many bromodomain-containing proteins). High acetyl/acyl ratio favors the constitution of a reservoir of non-functional chromatin-bound BRD4. Low acetyl/acyl ratio, in contrast, increases BRD4 dynamics and makes it available for recruitment on the sites of action.

Our work not only added a new piece of evidence regarding the concept of metabolism-driven epigenetic modifications, but also emphasized on a collective and combinatorial actions of the relatively low abundant individual acylations.

Keywords: Histone Posttranslational Modification, Mitochondrial Metabolism, FASTKD1, Acute Lymphoblastic Leukemia, β-oxidation, BRD4

RESUME

Les événements contrôlés par la chromatine, notamment la transcription des gènes, sont à la base des caractéristiques cellulaires dans les tissus normaux ainsi que dans le contexte du cancer. Les modifications post-traductionnelles des histones font partie de circuits de régulations spécifiques contrôlés par la chromatine. De nombreuses modifications d'histones, notamment l'acétylation et la méthylation des histones, ont été caractérisées et leur rôle dans la régulation de la transcription a été étudié. Les facteurs régulateurs de la chromatine capables de lire ces modifications, établissent un pont entre les modifications des histones et la transcription des gènes. La spécificité de ces facteurs peut également dépendre des combinaisons de modifications d'histones. Finalement, il convient de noter que les modifications d'histones sont dynamiques et qu'elles sont influencées par divers paramètres, notamment les métabolites cellulaires.

Mon laboratoire d'accueil a précédemment identifié un gène nommé *FASTKD1* dont l'expression est associée à un mauvais pronostic dans la leucémie aiguë lymphoblastique (LAL). Au cours de mes recherches, nous avons découvert que la protéine codée par ce gène est un régulateur négatif de l'activité mitochondriale globale, et qu'elle contrôle plus spécifiquement la respiration mitochondriale. En utilisant des modèles de cellules ou le gene codant pour cette protéine est inactivé, nous avons caractérisé le lien entre l'activité mitochondriale et les modifications des histones. En particulier, nous avons mis en évidence l'importance du métabolisme des acides gras, notamment la β-oxidation, dans l'établissement des modifications d'histones par l'acylation. Cette relation entre l'activité mitochondriale, la β-oxidation et l'acylation des histones a également été confirmée dans des blastes primaires de patients atteints de LAL.

Les protéines de la famille BET reconnaissent spécifiquement l'acétylation des histones et sont impliquées dans la régulation de la transcription. Des études précédentes de mon laboratoire ont révélé que le premier bromodomaine de l'une des protéines de la famille BET, Brdt, reconnaît les marques d'histones diacétylées (H4K5acK8ac) mais pas les histones H4K5 butyrylées. A partir de ces données, mon laboratoire avait fait l'hypothèse que le rapport acetyl/acyl au niveau des histones devrait impacter la liaison des facteur de la famille BET (Brdt, BRD4, etc..) avec la chromatine. Mon travail de thèse a permis de vérifier cette hypothèse en déployant d'autres modèles cellulaires.

En effet, nous avons aussi remarqué que l'activité mitochondriale contrôlée par FASTKD1 a un impact important sur les acylations (non-acétyl) mais pas sur les acétylations. En utilisant notre modèle de cellules ou le gène codant pour ce facteur est inactivé, nous avons pu démontrer que le niveau relatif des marques acétyl et acyl au niveau des histones contrôle l'état de liaison

de BRD4 avec la chromatine. Nous avons montré qu'une augmentation du rapport acyl/acétyl diminue l'interaction BRD4-chromatine, ce qui entraîne un état de liaison lâche et dynamique, tandis qu'une diminution de ce rapport favorise une interaction forte. Le résultat fonctionnel de cette interaction dynamique est une redistribution de BRD4 à travers le génome. Plus précisément, l'interaction dynamique entre BRD4 et la chromatine causée par un rapport acyl/acétyl élevé rend la protéine BRD4 plus disponible pour être recrutée sur les sites d'initiation de transcription des gènes (TSS). Ainsi BRD4 contrôle l'expression d'un sous-ensemble de gènes. L'analyse fonctionnelle de ces gènes a révélé aussi bien chez les patients que dans nos cellules modèles, qu'un rapport acyl/acétyl élevé était associé à une expression accrue de gènes associés à la synthèse des ribosomes et au cycle cellulaire et à une expression réduite des gènes associés à l'état souche.

Sur la base de ces travaux, nous proposons que le métabolisme cellulaire, en modulant le rapport acetyl/acyl des histones, contrôle un réservoir cellulaire de BRD4 (et probablement de nombreuses autres protéines contenant un bromodomaine). Un rapport acétyl/acyl élevé favorise la constitution d'un réservoir de BRD4 non-fonctionnel lié à la chromatine. Un rapport acétyl/acyl faible, au contraire, augmente la dynamique de BRD4 et la rend disponible pour le recrutement sur les sites d'action.

Notre travail non seulement ajoute une nouvelle preuve de l'impact du métabolisme sur les modifications épigénétiques qui sous-tendent la biologie de la tumeur, mais également met l'accent sur l'action collective des acylations individuelles qui, lorsqu'on les considère chacune de manière isolée, sont relativement peu abondantes.

Mots-clés: Modifications post-traductionnelles des histones, Métabolisme mitochondrial, FASTKD1, Leucémie aiguë lymphoblastique, β-oxidation, BRD4

ABBREVIATIONS

ACC	Acetyl-CoA carboxylase
ACLY	ATP citrate lyase
ACP	Acyl-carrier protein
ACSL	Acyl-CoA ligase long chain specific
ACSS	Acyl-CoA synthetase short-chain
ALL	Acute lymphoblastic leukemia
Allo-HCT	Allogeneic hematopoietic stem cell transplantation
BD1	First bromodomain
BET	Bromodomain and extra-terminal domain containing protein
BMMC	Bone marrow mononuclear cells
BrDs	Bromodomains
C/T	Cancer-testis
CBP	CREB binding protein
ChIP	Chromatin immunoprecipitation
CHO-THF	10-formyl-tetrahydrofolate
CPT1	Carnitine palmitoyltransferase I
CrAT	Carnitine acetyltransferase
CREB	Cyclic Adenosine Monophosphate Response
DNMTi	DNMT inhibitor
DNMTs	DNA methyltransferases
DPF	Double PHD finger
DSB	Double strand breaks
dsDNA	Double strand DNA
ECAR	Extracellular acidification rate
ELISA	Enzyme linked immunosorbent assay
eRNAs	Enhancer RNAs
ETC	Electron transfer chain
EV	Empty vector
FAO	Fatty acid oxidation
FAS	Fatty acid synthesis
FASN	Fatty acid synthase
FASTKD1	FAS-induced serine/threonine kinase domain containing protein 1

FBS	Fetal bovine serum
FCCP	Carbonyl cyanide 4- (trifluoromethoxy)phenylhydrazone
FRAP	Fluorescence recovery after photobleaching
GNAT	GCN5-related N-acetyltransferases
GO	Gene ontology
GOI	Gene of interest
GSEA	Gene set enrichment analysis
GTFs	General transcriptional factors
HAT	Histone acetyltransferase
HCT	Histone crotonyltransferase
HDAC	Histone deacetylase
HDACi	HDAC inhibitor
HDCR	Histone decrotonylase
HDM	Histone demethylase
HIF-1α	Hypoxia-inducible factor 1α
HMT	Histone methyltransferase
HP1	Heterochromatin protein 1
HR	Homologous recombination
IDH	Isocitrate dehydrogenase
iPSCs	Induced pluripotent stem cells
KAT	Acyl-CoA thiolase
KDMi	KDM inhibitor
KDMs	Lysine demethylases
KMTs	Lysine methyltransferases
KO	Knockout
LDH	Lactate dehydrogenase
MCAD	Medium chain acyl-CoA dehydrogenase
MCS	Multiple cloning site
MDS	Myeodyplasic syndrome
MNase	Micrococcal nucleases
MOF	Male-absent on the first
MORF	MOZ related factor
MOZ	Monocytic leukemia zinc finger protein
MPC	Mitochondrial pyruvate carrier
MRD	Minimal residue disease

MRG	Mitochondrial RNA granules
MS	Mass spectrometry
mtDNA	Mitochondrial DNA
MTP	Mitochondrial trifunctional protein
MYST	MOZ, Ybf2/Sas3, Sas2, Tip60
NAD	Nicotinamide adenine dinucleotide
NCP	Nucleosome core particle
NES	Nucleus export signal
NFR	Nucleosome free region
NGS	Next generation sequencing
NHEJ	Non-homologous end joining
NLS	Nuclear localization signal
NMC	NUT-midline carcinoma
OAA	Oxaloacetate
OCR	Oxygen consumption rate
ORC	Origin recognition complex
ORF	Opening reading frame
OS	Overall survival
OXPHOS	Oxidative Phosphorylation
PCAF	p300/CBP-associated factor
PCC	Propionyl-CoA carboxylase
PcG	Polycomb group
PDC	Pyruvate dehydrogenase complex
PDK1	Pyruvate dehydrogenase kinase 1
PFK	Phosphofructokinase
PFS	Progression free survival
PIC	Pre-initiation complex
PKM2	Pyruvate kinase M2
PRMTs	Protein arginine methyltransferases
P-TEFb	Positive transcription elongation factor b
PTM	Post-translational modification
R/R	Replased/refractory
ROS	Reactive oxygen species
SAH	S-adenosyl homocysteine
SAHA	Vorinostat

SAM	S-adenosyl methoinine
SCAD	Short chain acyl-CoA dehydrogenase
SCFAs	Short chain free fatty acids
SDH	Succinate dehydrogenase
SEC	Super elongation complex
SEs	Super-enhancers
SETD2	SET domain-containing 2
sgRNA	Single guide RNA
SIRT	Sirtuin
SUMO	Small ubiquitin-related modifier
TADs	Topologically associating domains
TCA cycle	Tricarboxylic cycle
TFs	Transcriptional factors
Tip60	HIV Tat-interacting protein of 60 kDa
TSA	Trichostatin A
TSS	Transcription start site
VLCAD	Very long chain acyl-CoA dehydrogenase
YEATS	Yaf9, ENL, AF9, Taf14, Sas5
α-KG	α-Ketoglutarate
α-KGDH	α-Ketoglutarate dehydrogenase

LIST OF FIGURES

LIST OF TABLES

INTRODUCTION

1. Histone post-translational modifications control chromatin-dependent biological events

1.1 Chromatin is a DNA-packaging structure

1.1.1 Chromatin architecture

Chromatin is formed of DNA bound to histones. It has long been known that chromatin displays two global states : euchromatin which is associated with active or potentially active genomic regions, and heterochromatin, which is generally associated with the repressed genome. Heterochromatin comprises some structural regions of chromosomes, such as centromeres and telomeres (so-called constitutive heterochromatin). It also corresponds to a cell-type specific and developmentally-controlled transcriptionally repressed regions, known as facultative heterochromatin.

Chromatin structure undergoes temporal alterations dependent on cell cycle, most impressively it condenses during mitosis and decondenses in interphase. Later studies revealed that even in interphase, euchromatin is organized into specific areas, known as chromosome territories at nuclear scale (**Figure 1**). Recently, with the development of technologies characterizing 3D architecture of chromatin (e.g., 3C, Hi-C etc.), researchers discovered that at the megabase scale, chromosomes are segregated in two distinct compartments, designated as compartment A and B[1, 2]. Type A compartment is enriched in active chromatin, where high transcriptional activity, DNase I hypersensitivity and active histone marks are found. This compartment is likely to be in the central region of nucleus as well as in regions close to the nuclear pores. In contrast, Type B compartment is known to have inactive chromatin associated with repressive histone marks, silent genes, and late replication timing. This compartment is located close to the nuclear periphery and is associated with the nuclear lamina[3, 4]. The stability of these regions tunes the accessibility of the genomic regions to transcriptional machineries, thereby regulates cell specific gene transcription programs[5]. The additional micro-hierarchical structures composing chromosome compartments are the so-called topologically associating domains (TADs). TADs are partitioned regions with relatively defined boundaries. In TADs chromatin contacts preferentially occur within the same domain. The contacts within the same continuous chromatin region or between distant separated chromatin regions are facilitated by loop structures. Chromatin loops are kilobases structure whose formation is assisted by chromatin architectural proteins, such as CCCTC-binding factor (CTCF) (once known as an

insulator protein), cohesions and mediators. These loop structures allow the contacts between distal elements, such as promoters-enhancers, or certain DNA elements with transcriptional factors and cofactors, thereby playing an important role in gene transcription[6, 7]. Indeed, TADs are viewed as units of gene transcription[8, 9].

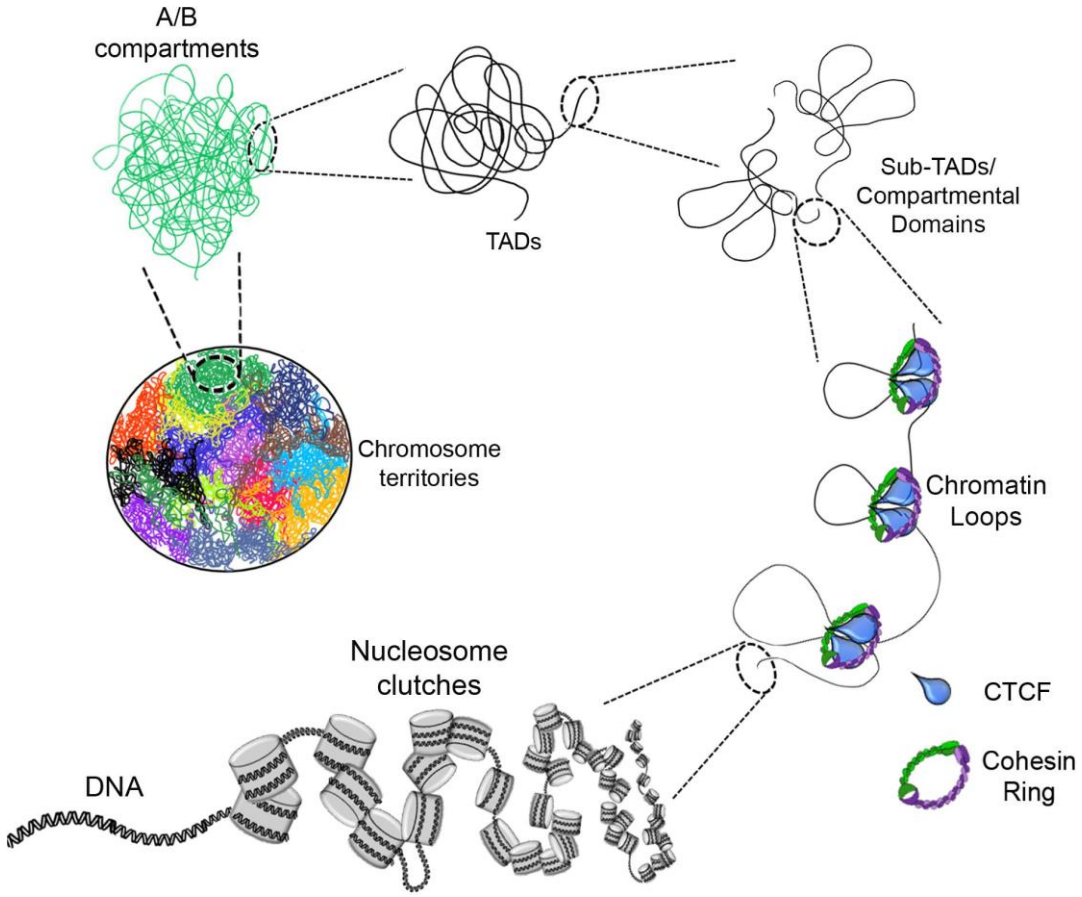

Figure 1. Hierarchical organization of chromatin.

Genome is non-randomly placed in cell nucleus. Nucleosome fibers can form loops facilitated by CTCF and the cohesin complex. Chromatin loops are ordered in TADs or sub-TADs. TADs domains are located within different types of chromatin compartments: type A active chromatin and type B inactive chromatin. At the nuclear scale, each chromosome is arranged in a relatively specific place, designated as chromosome territories. Figure taken From[3].

1.1.2 Chromatin packaging

In human cells, 2 meters of DNA must be tightly packaged into chromatin in order to fit into a micron-sized nucleus. Nucleosome is the basic unit of chromatin compaction. Each nucleosome is composed of 145-147 base pairs (bp) of DNA wrapped approximately 1.7 times around the histones core in a left-handed manner. Linker histone H1 interacts with both the dyad and entry/exit of DNA strand to further compact DNA. Adjacent nucleosomes are linked by DNA to form nucleosome arrays (so-called “beads on a string” structure observed under electron microscope). The next level of compaction is called “30nm fiber”. Two models applying “30nm fiber” have been proposed: 1) the one-start solenoid where nucleosomes are arranged in a single

helical stack, with the linker DNA slightly bent; 2) the two-start zig-zag structure where the neighboring nucleosomes extend back and forth, and are connected by a relatively straight linker. Though controversial, evidence indicated that both modes might exist in the real situation, the adoption of which depends on the length of linker DNA. A short linker DNA contributes to the formation of solenoid, while nucleosomes with long linkers tend to form zig-zag structure. As aforementioned, the chromatin fiber could be spatially ordered in the nucleus with the assistance of other chromatin bound proteins. During the mitotic cell division, these noodle-like chromatin fibers could further be folded into a highly condensed state (**Figure 2**).

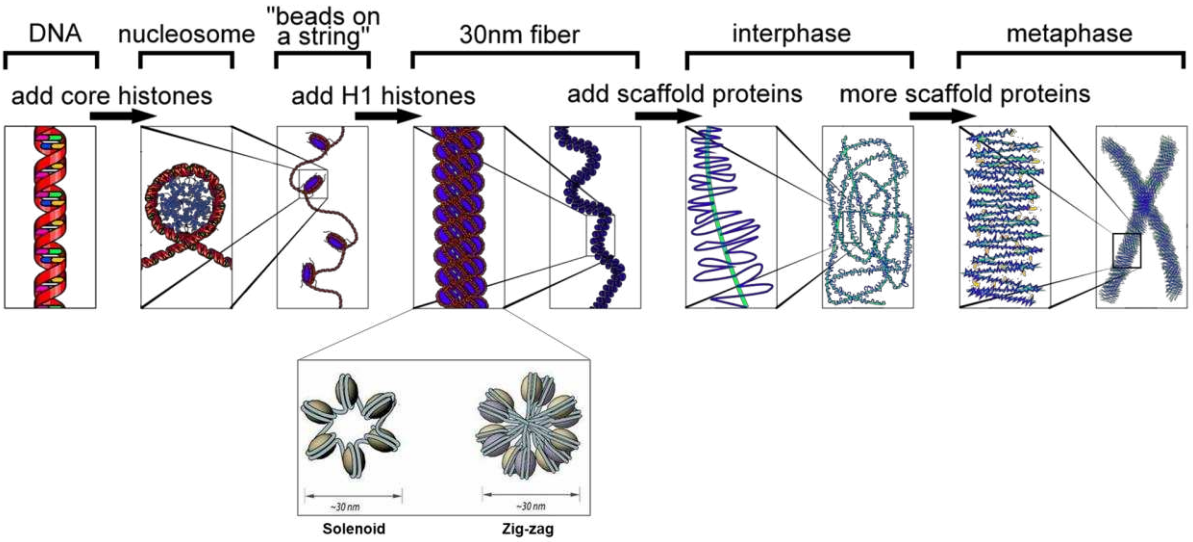

Figure 2. Chromatin Packaging.

Chromatin is highly packaged structure. Nucleosome is the basic unit of chromatin packaging. When linked, nucleosomes form the "beads on a string" structure under EM. Nucleosomes then form 30nm fiber chromatin, which can be further folded to highly condensed chromosome during metaphase. From Wikipedia.

Of note, recent studies revealed that the well-organized 30 nm fiber might merely reflect the artificial situation *in vitro* with low nucleosome concentration and low salt conditions. *In vivo* however, given 1) the physiological salt condition, 2) nucleosomes crowding[10], and 3) taking into account that nucleosomes are irregularly positioned, etc., nucleosomes arrays are not likely to fold into 30nm fiber but rather are organized in clutches and stay in an amorphous form (Figure 1)[11-13].

1.1.3 Nucleosome core particle structure

Structure of nucleosome core particle (NCP) has been determined with X-ray crystallography with near-atomic resolution (**Figure 3**)[14, 15]. Two copies of each H3, H4, H2A, and H2B form the disc-like histones core. Each core histone shares similar organization encompassing flexible N- and C-terminal tails and the histone fold, which consists of three α helices linked by two loops (α1-L1-α2-L2-α3) (**Figure 3A**). For each nucleosome, a segment of ~121bp DNA is organized around the histone fold, leaving ~13bp DNA at each entry/exit end. Interactions between core

histones and DNA are mainly mediated by the conserved domains of core histones, where 7 unique DNA binding sites are harbored in every half of nucleosome particle, corresponding to the places where the DNA major groove faces the histone octamer. At the entry/exit of nucleosome, DNA is bound by the N-terminal α helices of histone H3. Within the histone core, two H2A-H2B heterodimers interact with the symmetric $(H3\text{-}H4)_2$ heterotetramer through H2B-H4 four-helix bundle and H2A docking domain, the latter of which functions to lock H3-H4 by forming a β-sheet with C-terminus of H4, and can stabilize histone octamer by guiding H3 αN, which is interacting with DNA.

Core histones have long flexible tails containing alkaline lysine and arginine that can protrude NCP. For example, tails of H2B and H3 pass through DNA gyres and extend out of NCP randomly. Further, the N-terminal tail of H4 can contact the adjacent nucleosome via the acidic patch formed by H2A-H2B. Such interaction is crucial for the folding of nucleosome arrays and the high-order chromatin packaging. In the case of H2A, the C-terminus could serve as a docking domain that interacts with H3-H4, while the N terminal tail binds to the minor groove of DNA superhelix. Of note, these alkaline histone tails can be subject to a variety of covalent modifications. Apart from interacting with H4, the H2A-H2B acidic patch can act as a platform for many protein-nucleosomes complex interactions as well.

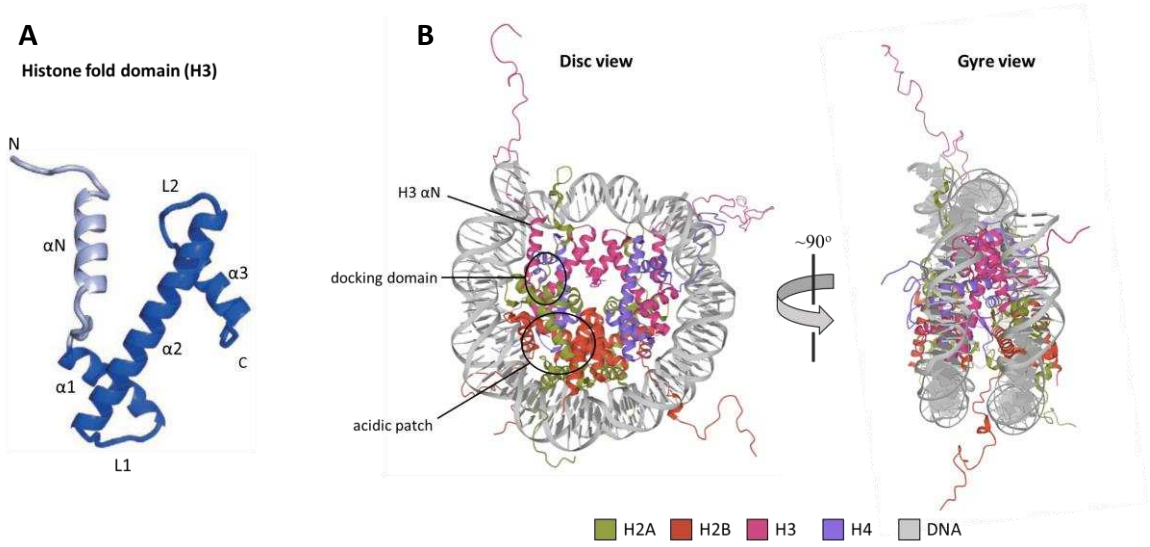

Figure 3. Nucleosome core particle structure.

A. Histone fold domains of H3. Core histones have conserved motifs of histone fold, namely α1-L1-α2-L2-α3 from N terminus to C terminus. B. Nucleosome core particle (NCP) is composed of two copies of each H2A, H2B, H3 and H4. Disc view (left) and gyre view (right) of NCP show the crucial domains and flexible tails of core histones respectively. Graphic from[16] (A) and from PDB:1KX5[17] (B).

1.1.4 Nucleosomes positioning

Around 75–90% of genomic DNA is wrapped in nucleosomes in eukaryotes. As introduced above, in order to be wrapped into nucleosomes, DNA must be bent around a histone octamer. Since DNA sequences impact histone octamer binding stability, nucleosomes might be

positioned across the genome depending on the genomic sequences. Indeed, Segal and colleagues demonstrated that dinucleotides facilitate the bending direction of DNA, where GC and AA, TT or AT are placed alternatively every 10 bp following DNA major and minor groove (**Figure 4**). Such model predicted around ~50% of nucleosomes positioning in yeast and chicken genome, indicative of a determinant role for the genomic sequence in directing nucleosome positioning[18].

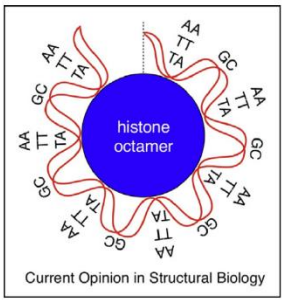

Figure 4. Sequence preference of nucleosome.
DNA is wrapped around a histone octamer following a 10bp-periodic sequences of GC/AA, TT or TA dinucleotides. From[19].

During the last decade, the heterogeneity of nucleosome positioning (referring to the relative position of nucleosomes with respect to certain genome DNA sequences) has been uncovered using high-throughput sequencing-based approaches. Up to now, the basic features of the nucleosome positioning landscape can be roughly summarized as 1) Silent genes harbor regularly-spaced, but poorly-positioned nucleosome arrays. 2) At active promoter and enhancer regions, nucleosomes are irregularly spaced. 3) At the 5' end of active genes immediately upstream and downstream of TSS, nucleosomes are strongly positioned and phased. A nucleosome-free region (NFR) at active gene TSS, separating the -1 and +1 nucleosomes, is observed (**Figure 5**)[13]. The nucleosome positioning, spacing, and phasing are controlled by the internal property of genomic sequences and the action of chromatin remodelers. Since nucleosomes are the fundamental barriers for DNA accessibility, alterations of nucleosome arrays and the resultant chromatin re-organization might impact tremendously chromatin functions.

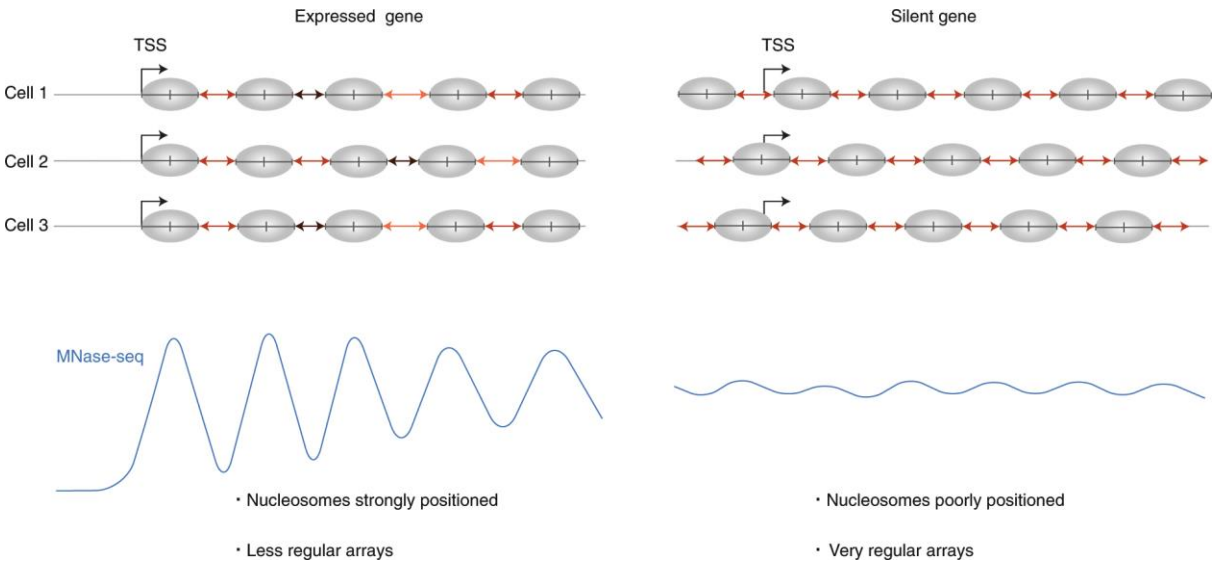

Figure 5. Nucleosome positioning.

Downstream of TSS of expressed genes, nucleosomes tend to be precisely phased, with strong positioning but less regular spacing (left panels). In contrast, in silent domains, nucleosome arrays are highly regular but poorly positioned to genomic DNA (right panels). From[13].

1.2 Gene transcription is the first highway to biological properties

Since 1950s, the discovery of DNA structure has paved the way towards understanding life. Generations of researchers built their research on this discovery and established the basics of the modern biology. What we are learning in middle schools is the central dogma of molecular biology, describing the flow of genetic information passing from DNA to RNA and then to proteins. Here I will give a brief introduction on the first level of genetic information expression in this central dogma, which is gene transcription in eukaryotes.

1.2.1 Types of RNA polymerases

Transcription is catalyzed by RNA polymerases, which produce RNAs reverse complementary to DNA template. There are three types of RNA polymerases (Pol) in eukaryotes, RNA Pol I, II, and III, with each responsible for transcribing distinct types of RNAs. RNA Pol I produces large ribosomal RNA, RNA Pol II synthesizes messenger RNA and many non-coding RNAs, while RNA Pol III transcribes transfer RNA, small ribosomal RNAs and some other small RNAs.

1.2.2 Promoters and enhancers

Two key DNA elements involved in transcription are promoters and enhancers. Promoter is a region of DNA where RNA polymerases assemble to initiate transcription. Promoter regions comprise of core promoter, proximal promoter, and distal promoter. Of them, core promoters refer to the minimal DNA region that direct the precise initiation of transcription. Core

promoters contain several sequence motifs, including TATA box (5'-TATAAA-3') (~ -30bp), initiator (± 3bp), and downstream core promoter element (DPE) (~ +30) etc., and are featured by a nucleosome-depleted region (NDR) on the TSS (transcription start site) in the case of active promoters[20].

In metazoan, core promoters can be divided into three types according to their activation status, the motifs, and the local nucleosomes architecture. The first type is known as "disperse" and "broad" promoters mainly found in housekeeping genes. These promoters are featured by constitutively activated status, dispersed distribution of transcription initiation, and a typical NDR, and often overlap CpG islands. Second type is "sharp" "focused" promoter, which possesses sharp initiation, unprecise nucleosome positions, and often contain TATA box and initiator elements. These promoters are found in cell-type-specific genes that function during differentiation. The third type is "poised" promoter, which are covered by bivalent histone histone marks (both active H3K4me3 and repressive H3K27me3). These promoters are found in embryonic stem cells, where they control developmental transcription factors and ensure the correct expression of development-associated genes in certain tissue type[20].

Enhancers are DNA sequences that can regulate the activity of their target promoters by recruiting transcription factors and cofactors. In metazoan, enhancers are relatively large elements that can be up to several hundred base pairs and are often placed distant from (e.g., kb) the target promoters. Currently, active enhancers are well-predicted by the coverage of H3K4me1 and H3K27ac and in the case of active enhancers, by the co-localization of p300/CBP[21]. Similar to promoters, active enhancers harbor NDRs. At both edges of NDR, enhancers DNA can be transcribed by RNA Pol II divergently to produce unstable enhancer RNAs (eRNAs)[22]. The existence of eRNAs reflects the active status of enhancers, although their actual functions are yet to be determined. It is noteworthy that specific subsets of large enhancers, known as locus control regions (also known as super-enhancers, SEs) were identified and became famous for their roles in controlling cell type-specific gene expression or key oncogenic program. SEs are distinguished by the co-occurrence of transcription factors binding, Mediator and Pol II co-activators[23].

In order to regulate distal promoters, enhancers should first physically contact distal promoters, which has been suggested to be enabled by the chromatin loop structure, where the interacting proteins, including Mediator complexes and cohesions, facilitate the enhancer – promoter proximity[24]. The selectivity of enhancers – promoters communication are driven by topologically associating domains (TADs), promoter – proximal tethering elements (PTEs), and the promoter DNA accessibility. More details can be found in[25].

1.2.3 Procedure of RNA Pol II transcription

Processes of transcription can be divided into three stages, initiation, elongation, and termination (**Figure 6**). Transcription initiation is the process where RNA polymerase II recognizes and interacts with promoters, and produces nascent RNA at transcription start sites (TSS). Recognition of RNA polymerases is aided by transcription factors (TFs), including general transcriptional factors (GTFs) and associated activators or coactivators. TFIID is the first GTF that interacts with DNA, followed by sequential recruitment of TFIIA, TFIIB, TFIIF, TFIIE, and TFIIH. All the recruited GTFs together with RNA Pol II, form the pre-initiation complexes (PICs) at promoter regions. The PICs are in closed form when DNA is still in a double helix state, before XBP, the translocase subunit of TFIIH, hydrolyzes ATP, through which, unwinds dsDNA and pushes DNA strand towards the catalytic center of RNA polymerase to facilitate the synthesis of nascent RNAs. After which, RNA Pol II is released from associated GTFs and promoters (termed as promoter escape) and RNA synthesis is hence elongated.

In many cases, RNA Pol II pauses after transcribing around 30-50 nucleotides downstream of TSS, which is known as promoter – proximal pause. The paused Pol II is stabilized by 5,6-dichloro-1-β-D-ribofuranosylbenzimidazole (DRB) sensitivity – inducing factor (DSIF) and negative elongation factor (NELF), which consequently, inhibits early processive transcription elongation. Release of paused RNA Pol II requires NELF, DSIF and carboxy terminal domain (CTD) of Pol II. CTD is phosphorylated by kinase CDK9, which is a subunit of positive transcription elongation factor b (P-TEFb).

Termination of transcription is less well-understood compared to initiation and elongation. Once RNA polymerases pass through Poly A signal (5'-AAUAAA-3'), newly synthesized RNA will be released from RNA Pol II, and RNA Pol II per se is released from the DNA template. Possible mechanisms are that gradual changes of CTD phosphorylation at distinct sites (e.g., Ser2 increase while Ser5 decrease) displaces RNA Pol II from DNA. Then recruited exonuclease Rat 1 pulls uncapped RNA out from RNA polymerase and degrades it.

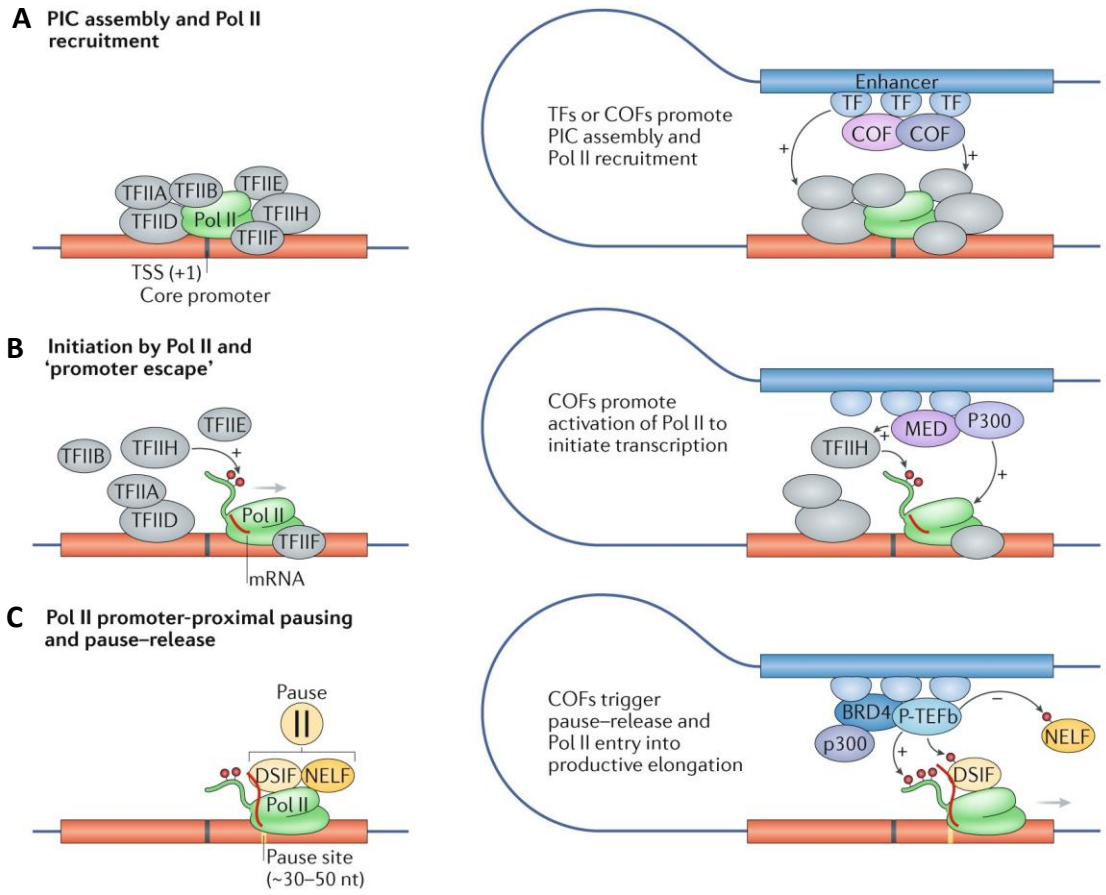

Figure 6. Gene transcription.

Transcription initiates with the assembly of Pre-initation complex (PIC) and the synthesis of nascent RNAs (**A**). RNA pol II is then phosphorylated and escapes from promoter to start transcriptional elongation (**B**). Shortly after elongation (30-50nt), RNA pol II pauses, and the processive elongation requires its CTD phosphorylated by P-TEFb (**C**). Through all these processes, enhancer can access promoters and regulate each step of transcription. TFs: Transcription factors. COFs: Cofactors. MED: Mediator. From[20].

1.3 Histone post-translational modifications impact chromatin signaling

Chromatin serves as the template for various biological processes such as transcription, DNA repair, replication, and so forth. Modifications of histones, which are the key component of chromatin, are the major regulators in such processes. Histone post-translational modifications (PTMs) refer to the chemical moieties covalently added to amino acids on histone tails or histone folds. There are various types of histone PTMs, including the well-characterized acetylation, methylation, phosphorylation (**Figure 7**), and the atypical modifications, including short chain acylation (e.g., crotonylation, butyrylation, glutarylation, succinylation, etc.), serotonylation, lipidation, etc. Histone PTMs are reversible, with certain enzymes responsible for adding (termed as "writers") or removing the groups (termed as "erasers"). Histone PTMs can directly alter chromatin structure and organization, or more importantly, recruit effector

proteins (termed as “readers”). In this section, I’ll have a general introduction about different modifications, their corresponding writers, erasers, readers, and the functions they exert.

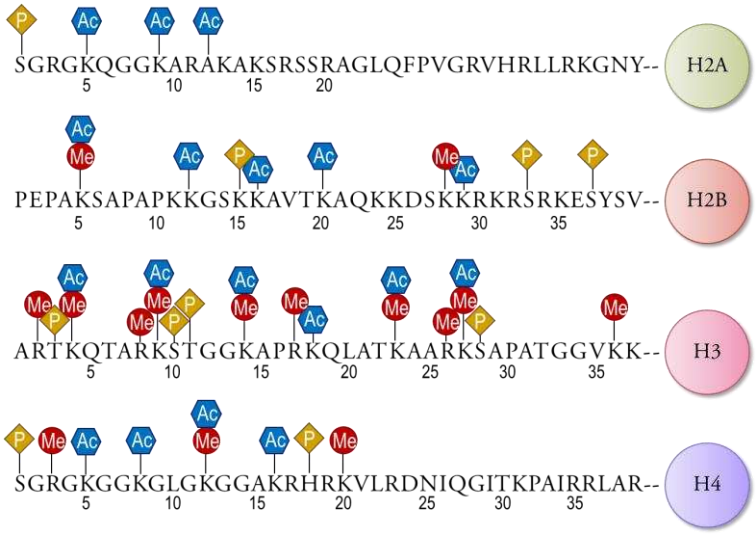

Figure 7. Histone N-terminal tail modifications.

Histone tails are subject to a variety of modifications. P: Phosphorylation. Ac: Acetylation. Me: Methylation. Adapted from[26].

1.3.1 Methylation

Histone methylation mainly occurs on the side chains of lysines or arginines on all histones (H1, H2A, H2B, H3, and H4). Lysines can be mono- (me1), di- (me2), or tri-methylated (me3) while arginines can be mono- or di-methylated. In the case of arginine di-methylation, two methyl groups can possibly be added symmetrically or asymmetrically to amino groups.

Histone methylation are catalyzed by histone methyltransferases (HMTs) with S-adenosylmethionine (SAM) as a group donor and can be removed by histone demethylases (HDMs) assisted by certain cofactors. Although histone methylation was identified in the 60s of last century, it was not until 40 years later when the first methylation modifier, SUV39H1 (KMT1A) was identified by Jenuwein and colleagues[27]. Today, two classes of lysine methyltransferases (KMTs) and one class of arginine methyltransferases (protein arginine methyltransferases, PRMTs) have been identified. Depending on the catalytic domains they possess, KMTs can further be divided into 1) SET domain containing methyltransferases, which defines the first and the major class of KMTs, and 2) KMTs which does not have a SET domain and is represented by DOT1L protein in human[28].

The first member of lysine demethylases (KDMs) LSD1/KDM1A was identified by Yang Shi and colleagues and was characterized as a FAD-dependent amine oxidase that demethylates H3K4me1 and K3K4me2. A few years later the second class of KDMs were identified and designated as jumonji C (JmjC)-domain containing protein, which use α-ketoglutarate (α-KG), oxygen and Fe (II) as cofactors to oxidize methyl groups and release formaldehyde.

Catalytic activity of HMTs and HDMs is dependent on both the site and the degree of methylation. For instance, KMT1A/B (SUV39H1/2) catalyze di- and tri-methylation of histone H3 at K9 from monomethylated state, while G9a and GLP (G9a-GLP) catalyzes mono- and di-methylation of H3K9[29]. Moreover, since some of the HMTs and HDMs are formed in protein complexes, the additional components might indeed impact the activity or specificity of the catalytic subunit. For example, SET domain containing core enzymes can only catalyze mono- and di-methylation of H3K4, while the catalysis of higher level of methylation, H3K4me3, requires the presence of holo-enzymatic complexes, which are comprised of additional interacting partners (e.g., WRAD)[30]. In addition, Polycomb repressive complexes 2 (PRC2) is a well-studied polycomb group (PcG) family protein that serve as writer for mono-, di-, and tri-methylation of H3K27. Apart from the catalytic subunit EZH1/2, PRC2 complexes comprise additional components, including SUZ12 and EED are required for the enzymatic activity, as well as accessory subunits which are either important for enhancing activity of PRC2 complexes (e.g., AEBP2 and JARID2) or might play a role in the recruitment of PRC2 to specific genomic loci (e.g., PCL protein)[31, 32].

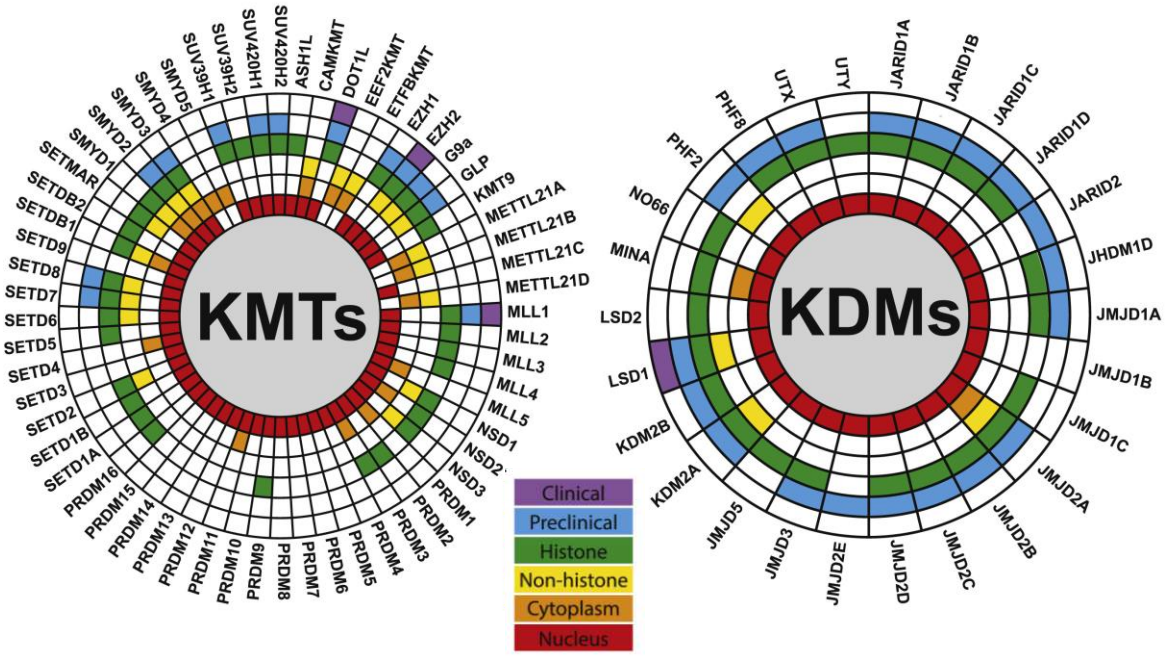

Figure 8. Writers and erasers of lysine methylation.

The graph summarizes the known KMTs (left) and KDMs (right) families with their subcellular localization. The graph also shows the potential inhibitors and their clinical status relating methylation enzymes. From [33].

Histone methylation does not alter the charge of histone protein but can impact the size and hydrophobicity of the amino acids, thereby directly influencing nucleosome structure by interfering with histone-histone or histone-DNA interactions. More importantly, histone methylation has been suggested to recruit effector proteins. “Readers” of methylation include PHD, chromo, PWWP, WD40, etc. domains containing proteins that recognize the specific

methyl groups and mediate certain outcomes. To speak roughly, in the case of gene transcription, methylation at H3K4 and H3K79 marks active transcription, in contrast, methylation at H3K9, H3K27, and H4K20 is associated with gene silencing.

Different histone methylation marks are distributed in different regions of the genome. Thanks to the advancement of high-throughput sequencing technology during the last two decades, researchers have mapped the genomic distribution of various site-specific methylations and have summarized their coverage patterns in *cis*-elements (e.g., promoters, enhancers), gene regions (e.g., exons, introns, TSS, repetitive regions), and their onsite specific roles. For instance, it is well-known that H3K4me3 is enriched in active and poised promoters, whereby it could help to recruit RNA pol II[34]. In addition, H3K27me3 and H3K9me3 are hallmarks of facultative and constitutive heterochromatin respectively, and are associated with gene silencing[29, 35].

Furthermore, mechanisms concerning the methylation targeting have begun to emerge. Specific KDMs and KMTs could directly be recruited to certain loci by transcriptional factors or RNA pol II, DNA elements, noncoding RNA etc.[28]. Functionally, histone methylation can either activate or repress gene transcription depending on the different types and their genomic locations, as well as can play a role in RNA splicing, genomic stability, and DNA damage response etc.[36].

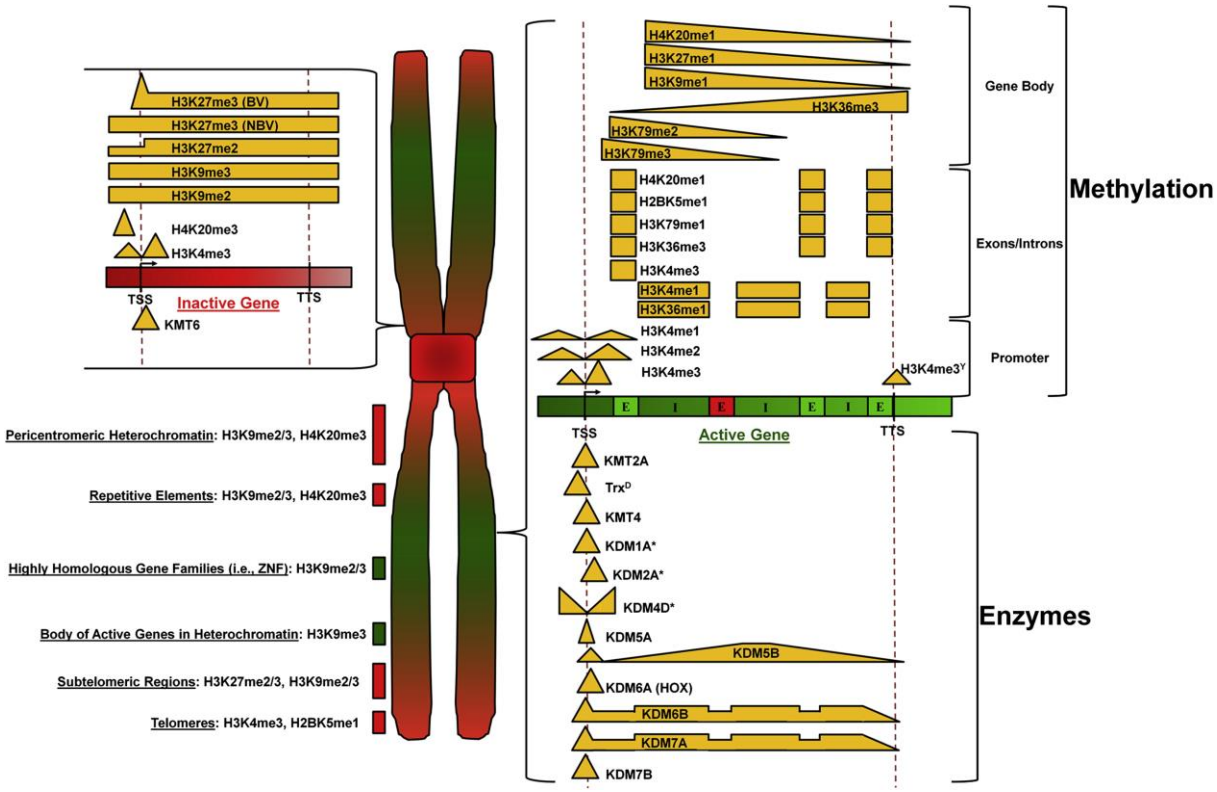

Figure 9. Distribution of histone lysine methylation and their association with gene transcription.
The graph summarizes the genomic distribution of different histone methylation, methylation modifiers, and their regulation in transcription. In general, H3K9me3, H3K27me3, H4K20me3 marks inactive genes. In contrast,

H3K27me1 enriches in gene bodies of active genes. H3K36me1 is distributed in intergenic regions whereby it might confer to the repression of cryptic transcription. More details are reviewed in [28]. From [28].

Of note, different histone methylation marks can interfere with the establishment of the other methylation marks, as well as other epigenetic modifications. For example, H3K27 methylation can be disturbed by active histone marks (e.g., H3K27ac, H3K4me3, H3K36me3 etc.). The underlying mechanism is the exclusion of PRC2 from specific chromatin loci[35, 37]. In addition, DOT1L-dependent H3K79me and SET1-dependent H3K4me can be activated by H2BK120 mono-ubiquitination[38]. Such crosstalk adds complexity of interpreting the function of histone code.

1.3.2 Phosphorylation

Histone phosphorylation corresponds to the transfer of phosphate group from ATP to amino acids, in most cases, threonine and serine of histone tails. Not surprisingly, histone phosphorylation is established by kinases and is removed by phosphatases. Histone phosphorylation has been extensively studied and has been implicated in DNA damage repair, cell cycle progression, gene transcription and chromatin architecture.

H2AX phosphorylation at Ser139 (γH2AX) is one of the early events being identified in DNA damage response process[39]. Upon DNA double strand breaks (DSBs), H2AX is phosphorylated by PI3K family members (e.g., ATR, ATM), serving as platform for the accumulation and retention of MRN, MDC1, and 53BP1 components at DSB sites, which are responsible for DNA damage repair. After proper DNA repairment, surviving cells should exit checkpoint and recover cell cycle progression. This process is possibly regulated by the phosphatase Wip1 which dephosphorylates γH2AX and could be activated by phosphorylation of H4 threonine 80 (H4T80P) in *S.cerevisiae*[40].

Another important function of histone phosphorylation is chromosome architecture, which is exemplified by well-characterized H3S10P as well as H3S28P, which are catalyzed by Aurora B, IKK, Rsk2, AKT and are important for chromatin condensation and segregation during mitosis or meiosis. In addition, phosphorylation at H3T118 has been reported to destabilize nucleosomes[41]. In addition to core histones, phosphorylation of H1 was believed to influence nucleosome structure and higher-order chromatin compaction[42].

Histone phosphorylation is also involved in gene transcription through an interplay with other histone marks. For example, H3S10P contributes to gene transcription of 14-3-3 family proteins through promoting histone acetylation[43]. Furthermore, recent study revealed that H3.3 phosphorylation can activate p300 *in trans,* which is responsible for H3K27ac at enhancers and regulates differentiation-specific gene expression[44]. H4Y88P, which is catalyzed by ACK1/TNK2, is crucial to promote androgen receptor - mediated transcription by recruiting WDR5/MLL2, which subsequently catalyzes H3K4me3[45].

Histone phosphorylation is also associated with cell stress and apoptosis. H2BSer36 phosphorylation was suggested to be involved in certain genes transcriptional regulation responsive to cell stress, while H2BSer14 phosphorylation catalyzed by PKA and PKC mediates DNA fragmentation and cell apoptosis[46].

1.3.3 Acetylation

Acetylation occurs at the ε-N of lysine side chains. While all the histones can be acetylated, acetylation on H3 and H4 is more extensively studied than on H2A or H2B. Traditionally, most of the modifications were considered at the lysine residues of N-terminal tails. However, recent studies have also included the globular domains of histones, where acetylation could probably mediate a different functional output.

Histone acetylation exhibits a high turn-over rate, with half-life (t1/2) ranging from minutes to hours[47, 48]. The dynamics of histone acetylation is regulated by histone acetyltransferases (HATs), which add acetyl groups onto histones using acetyl-CoA as donors, and by histone deacetylases (HDACs), which remove acetyl group from modified lysine and release acetate, as well as their cofactors.

Histone acetylation is one of the most prominent epigenetic code underpinning active transcription and is involved in various biological processes. In general, acetyl group neutralizes the positive charge of lysine residue and reduces interactions between histones and DNA as well as between adjacent nucleosomes. More importantly, histone acetylation recruit chromatin binding factors that either lead to transcriptional outputs or chromatin remodeling.

Herein, I'll give a brief introduction about the HATs, HDACs, readers, and the functional outputs of histone acetylation.

1.3.3.1 HATs

Histone acetyltransferases (HATs) are mainly classified into GNAT (GCN5-related N-acetyltransferases), MYST (MOZ, Ybf2/Sas3, Sas2, Tip60), p300/CBP as well as other undefined families according to their sequence homology and structural similarity. In metazoan, HATs often form complexes with other protein partners, wherein the classical HATs serve as the catalytic center. HATs complexes can have distinct specificity over nucleosomal histones compared to the free histones. It is noteworthy that different HAT complexes often have overlapping substrates *in vitro* and *in vivo*.

Table 1. Mammalian HATs members and their histone acetylation targets.

Members	Acronyms	*In vitro* substrates	*In vivo* complexes	*In vivo* substrates	Functions
GNATs family					
HAT1	KAT1	H4K5, H4K12	HAT-B complex	Newly synthesized histone H4	Histone deposition and chromatin assembly[49, 50]
KAT2A	GCN5	H3K14, H4K8, H4K16	2MDa SAGA-like complex (STAGA / TFTC / PCAF), 700kDa (ATAC)	Core histones, with preference for H3 (at K9)	Global acetylation across the genome and targeted histone acetylation at specific loci[51].
KAT2B	PCAF				
MYST family					
KAT5	TIP60	H2A, H3 and H4	NuA4 complex	Catalyze nucleosomal H2A, H4, and non-histone substrates, preference for H2A (at K5)[52].	Chromatin structure alterations, DNA damage response, cell cycle progression and transcriptional regulation, act as coactivators of corresponding factors (e.g., acetylating ATM and p53)[53, 54].
KAT8	MOF, MYST1	/	MSL complex, NSL complex	MSL complex specifically acetylates nucleosomal H4 at K16. NSL complex broadly acetylates K5, K8 and K16 on nucleosomal H4	
KAT6A	MYST3, MOZ	H3 and H4	MOZ/MORF complexes (contain ING5, MEAF6 and BRPF1/2/3 subunits)	Histone H3 at K9, K14 and K23	Acts more on locus-specific regions, might impact global H3K23ac[55, 56].
KAT6B	MORF, MYST4, QKF				

KAT7	HBO1, MYST2	H2A, H3 and H4	Form complexes with BRPF1/2/3 Or JADE1/2/3.	HBO1-BRPF complex preferentially acetylate H3, especially at K14 and K23. HBO1-JADE complex have specificity for H4K5, K8, and K12[57-59].	DNA replication licensing and transcription activation, through promoting pre-replicative complexes loading or by acetylating histones at TSS and intragenic regions respectively[60, 61].
KAT3B	p300, EP300	H3K18, H3K27, H4 N-terminal tail	/	All four core histones, among which H3K18ac, H3K27ac are preferred[62].	Transcriptional activation, the presence of p300 is one of the prominent features of active enhancers[63-65]. Acetylate a variety of non-histone substrates. Interact with a broad list of proteins[66].
KATA3A	CBP, CREBBP				

1.3.3.2 HDACs

Histone deacetylases (HDACs) remove acetyl group from ε-amino of lysine chain, producing unmodified lysines and acetate. Mammalian HDACs consist of 18 members, which can be classified into four families based on their sequence similarity and their yeast orthologues (Figure 10). Class I HDACs contains HDAC1, 2, 3, 8, which possess homology to yeast RPD3 protein; Class II HDACs are homologous to yeast HDA1, and can be further subclassified into IIa (HDAC 4, 5, 7, 9) and IIb (HDAC6, 10); Class III HDACs are known as sirtuin (SIRT) family proteins, which are homologous to yeast Sir2 and comprise of sirtuin1-7; Class IV HDACs has only one member HDAC11, which is closely related to HDACs of class I and II. In general, HDACs members perform catalysis of acetyl groups removal in an either zinc ion (Zn^{2+})-dependent (e.g., HDAC I, II, IV) or nicotinamide adenine dinucleotide (NAD+) dependent mechanism (e.g., SIRT family proteins) and they do not seem to have much preference for specific acetylated sites *in vitro*. However, different classes of HDACs tend to have distinctive roles *in vivo* due to their specific subcellular localization.

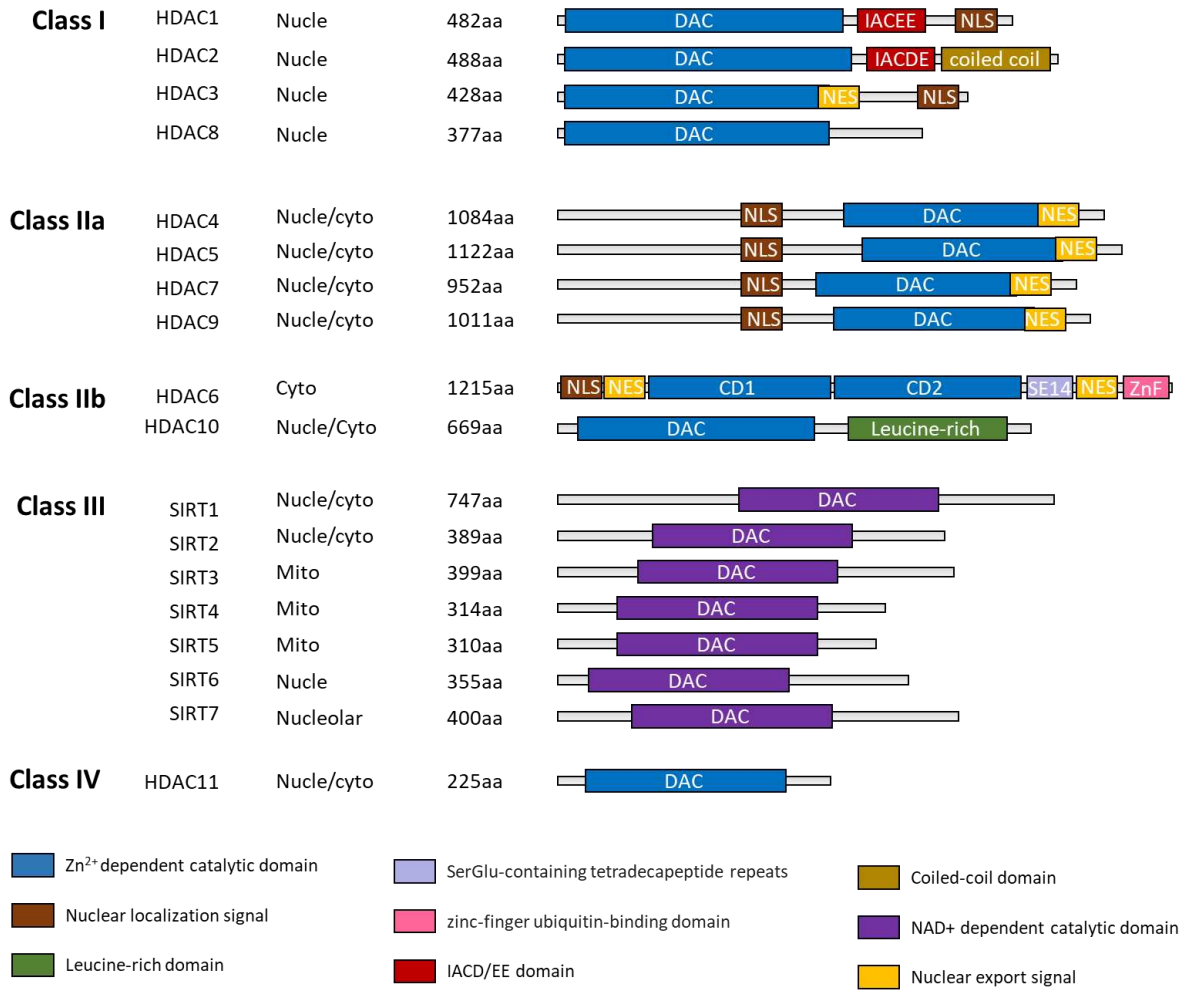

Figure 10. HDACs.

HDACs are classified into four families, Class I-IV. Class II can be further divided into IIa and IIb subclasses. The members of each family, their domains, subcellular localization are shown in the figure. DAC: Deacetylase

catalytic domain. Nucle: Nucleus. Cyto: Cytosol. Mito: Mitochondrial. NLS: Nuclear locolization signal. NES: Nucleus export signal. CD1: Catalytic domain 1. CD2: Catalytic domain 2. ZnF: Zinc-finger ubiquitin-binding domain.

HDAC1/2 (Class I) are exclusively located in nucleus due to the presence of nuclear localization signal (NLS) but lack of nuclear export signal (NES). HDAC3 who possesses both NLS and NES and HDAC8, although located predominantly in nucleus, can be found in cytoplasm[67, 68]. HDAC1 and 2 share common domains such as IAC (E/D)E motif, which is important for interacting with pocket proteins. HDAC 1 and 2 can dimerize and co-exist in many multiple protein complexes such as SIN3, NuRD, CoREST etc., HDAC3 has been characterized to interact with N-CoR/SMRT complexes through their deacetylase-activating domain (DAD), which is required for activating its inert catalytic activity[69, 70]. HDAC8 is X-linked in human and can deacetylate both histone and non-histone substrates. Its catalytic activity has been characterized to be retained with many other divalent metal ions in addition to Zn^{2+}[71, 72].

Class IIa family of HDACs possess both NLS and NES and shuttle dynamically between nucleus and cytoplasm. Whereas, class IIb HDACs are predominately located in cytoplasm due to NES. Subcellular localization of class IIa HDACs are regulated by phosphorylation of several conserved sites and the interaction proteins. For instance, phosphorylation of HDAC4 (at Ser246, 467, 632), HDAC5 (at Ser259, 497, 661), HDAC7 (at Ser155, 178, 181, 321, 344, 446,479) and HDAC9 (at Ser220, 451, 611) promotes binding of 14-3-3 family proteins, which in turn either mask NLS from importin α or unmask NES from Exportin 1 receptor (CRM-1), thereby promotes cytoplasmic localization[73].

Class IIa HDACs exhibit very weak deacetylase activity *in vitro* and their natural substrates are yet to be determined. The reduced activity is due to the amino-acid substitution from conserved histidine to tyrosine within the catalytic domain compared to class I and IIb[74]. Despite their weak deacetylase, class IIa HDACs interact with many transcriptional factors such as MEF2 proteins, Runx, NF-AT3c etc…, thereby act as transcriptional corepressors[75].

HDAC6 contains tandem catalytic domains, designated as CD1 and CD2, which display distinct catalytic activity. CD2 has broad substrate specificity over acetylated lysines, while CD1 prefers C-terminal acetyl-lysine residues[76]. Other domains possessed by HDAC6 include a ZnF ubiquitin binding domain, which binds ubiquitin and regulates various ubiquitin-dependent functions, and a SE14 which promotes cytoplasmic retention of HDAC6. HDAC6 can deacetylate important non-histone proteins such as α-tubulin, HSP90 and cortactin[77].

HDAC10 is located both in nucleus and cytoplasm. It contains a conserved HDAC domain similar to CD1 of HDAC6 and a leucine rich motif with elusive function. HDAC10 is

characterized as a weak lysine deacetylase but has a robust polyamine deacetylase activity with preference for N8-acetylspermidine[78].

Protein members of Sirtuin family share NAD+ dependent deacetylase domains but have distinct flanking C and N terminal parts, facilitating their different subcellular locations, enzymatic activities and substrates specificities. SIRT1 and 2 shuttle between cytoplasm and nucleus, SIRT3-5 reside in mitochondrion, while SIRT 6 and 7 are located in nucleus and nucleolus respectively. This family utilize acylated lysine and NAD+ as substrates and catalyze the production of unacylated lysine, 2'-O-acyl-ADP-ribose and nicotinamide (NAM). Recent studies uncovered that these family of proteins can also perform desuccinylation, deglutarylation, demalonylation etc., and can act as ADP-ribosyl-transferases and lipoamidases as well (**Figure 11**)[79].

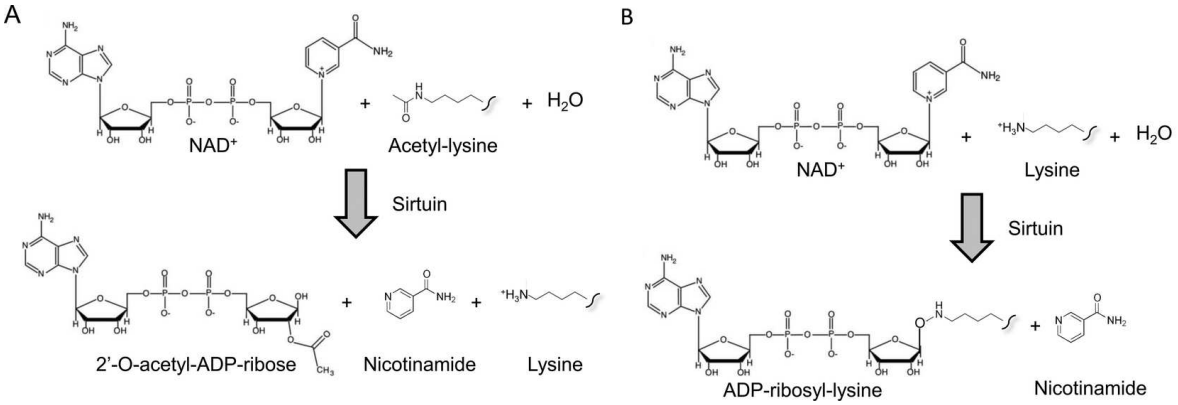

Figure 11. Sirtuins are protein deacetylase and ADP-ribosyltransferase.

A shows the NAD+ dependent deacetylase catalysis by Sirtuin. **B** shows the ADP ribosylation activity performed by Sirtuin. From[80].

Among the nuclear members, SIRT1 is the most well-studied member of sirtuin family and was firstly identified to deacetylate H3K9ac, H4K16ac and H1K26ac[81]. Later studies characterized SIRT1 as a deacetylase of non-histone substrates, including transcriptional regulators, chromatin modifiers, oncoproteins etc… SIRT1 also plays a role in gene transcription, cell senescence, stress response and energy homeostasis [82]. SIRT2 preferentially deacetylates H3K56ac and H4K16ac and other non-histone substrates (e.g., Tubulin, FOXO3A, p53 etc.)[83, 84]. SIRT3-5 are located in mitochondria and are controlling the mitochondrial metabolism by deacetylating many enzymes involved in TCA, OXPHOS etc.

SIRT6 was first identified as a mono-ADP-ribosyl-transferase using NAD+ as a substrate. Its known substrates are SIRT6 itself, PARP1 and KAP1. Its auto-deacetylation leads to autoregulation of its own activity in DNA damage repair. As a deacetylase, current evidence shows that H3K9ac, H3K18ac and H3K56ac are the targets of SIRT6, the removal of these marks is associated with gene silencing and chromatin compaction[85, 86].

SIRT7 has high specificity for H3K18ac but displays weak deacetylase activity compared to other nuclear members[87].

HDAC11 is the most recently discovered histone deacetylase and is designated to a new distinct class of HDACs, class IV. Studies found that location of HDAC11 varies in different cell type and with response to environmental cues. Although identified as robust deacetylase, HDAC11 displayed much more efficient deacylase than deacetylase activity. Recently increasing evidence has highlighted its potential role in physiology and pathophysiology[88-90].

1.3.3.3 Readers of histone acetylation

Histone acetylation was traditionally viewed as a robust chromatin regulator altering the electrostatic potential of nucleosomal histones. However, latter studies argued that this mechanism is far from enough to explain the diverse functions of histone acetylation. Indeed, later studies revealed that the major players mediating functional output of histone acetylation are factors recruited by histone marks, which are called "readers". According to the modular domains they have, readers for acetylated histones are classified into several families, including bromodomain (BrD), PHD finger domain, YEATS (Yaf9, ENL, AF9, Taf14, and Sas5) domain, and non-canonical bromodomain-containing proteins[91].

Bromodomain is the principal structural module that recognizes acetyl-lysine which can be found in many chromatin and transcription associated proteins. Although present in diverse proteins and have sequence variations, BrD modules share conserved structural fold comprising a four-helical (αZ, αA, αB, αC) bundle linked by highly variable loops (ZA and BC), which form a hydrophobic pocket (Figure 12)[92, 93]. Binding between bromodomain and acetylated lysine occurs in the way that N-acetylated lysine inserts into the pocket formed by ZA and BC loops. This interaction is stabilized by the hydrogen bond between the amide nitrogen of the conserved asparagine (Asn803 in PCAF) and the carbonyl oxygen of acetyl-lysine. Water molecules participate in the formation of hydrogen bond network as well, especially between carbonyl group of acetyl-lysine and conserved tyrosine of BrD[94]. Some of these BrD containing proteins harbor atypical bromodomains (aBrD), where the conserved Asn is replaced by Tyr, Thr or Asp, and these aBrDs may not be able to bind acetyllysine[95, 96].

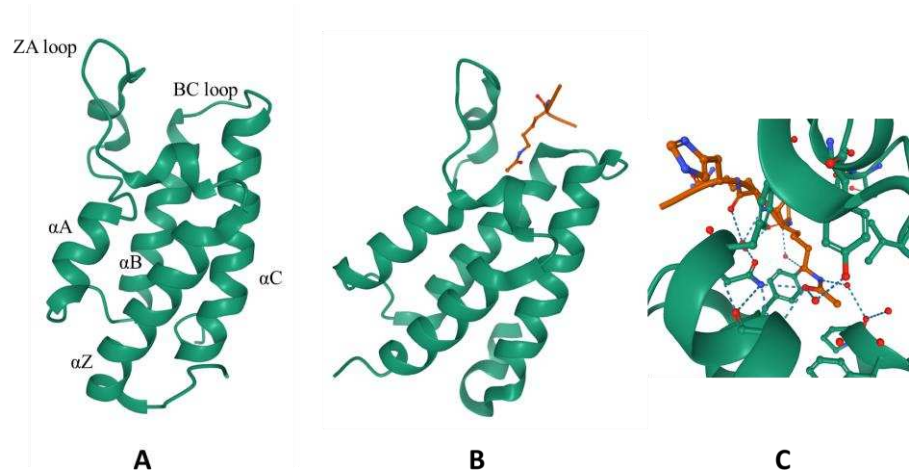

Figure 12. Bromodomain structure.

A. (PDB:1N72) shows the structure of bromodomain from p300/CBP. BrD comprises of four helix bundles (αA, αB, αC, αD), and two loops (ZA and BC). **B** and **C (**PDB:1E6I) show bromodomain from GCN5 binding with H4K16ac peptide. **C** shows hydrogen bonds formed by amide group of bromodomain and carbonyl oxygen group of acetyl-lysine. Red sphere: oxygen atom; Blue sphere: nitrogen atom; orange rods: histone peptide chain.

In human genome, 61 individual BrDs were found in 42 bromodomain containing proteins[93]. Based on their major functions, bromodomain-containing proteins can be classified into 9 groups, including HAT-containing proteins (i.e., PCAF, GCN5L2, p300/CBP, TAF1/1L) and the accessory proteins of HATs complexes (BRPF1/2/3 and BRD8), HMTs (i.e., ASH1L, MLL), chromatin remodeling factors (i.e., SWI/SNF and ISWI complexes members), AAA ATPase proteins (i.e., ATAD2, ATAD2B), BET family transcriptional coactivators (i.e., BRD2, BRD3, BRD4, BRDT), E2 SUMO/ubiquitin ligases (i.e., TRIM24, TRIM28, TRIM33A/B, TRIM66), SP family proteins of PML nuclear bodies (i.e., SP100, SP110A/C, SP140, SP140L), transcriptional corepressors (i.e., ZMYND8, ZMYND11), and WD-repeat proteins (BRWD1, BRWD3, PHIP)[95].

As noted, the BrDs containing proteins often possess additional domains in parallel with BrDs. The most common modules that flank BrD are additional BrDs. Indeed, 11 out of 46 bromodomain-containing proteins (e.g., TAF1, BET family etc.) possess double bromodomains. PBRM1 (encodes polybromo 1) even possesses six BrD modules. Besides tandem BrDs, PHD is also predominantly flanking BrD, and BrD-PHD cassette are present in various proteins including BRPF1/2/3, BAZ1/2, and TRIM24/28/33/66 etc. Other flanked domains exhibit in tandem with BrD include PWWP, SET domain (ASHL1, MLL), HATs domain, AAA ATPase domain in certain groups of bromodomain-containing proteins. These multiple domains might cooperate in function and bring about diverse regulatory chromatin regulations of BrD containing proteins.

BrDs in tandem could present an increased affinity for multiple acetylated sites. For example, two bromodomains in TAF1 form a V-shaped structure, with two binding pockets packed close

(~25Å) to each other and thereby enhances the affinity to di-acetylated or tetra-acetylated histone (H4K5/8/12/16) than mono-acetylated histone[97]. BET family proteins, which possess double BrDs preferentially bind hyperacetylated chromatin, with each BrD recognizing distinctive acetylated sites[98, 99]. Of note, the first bromodomain (BD1) of Brdt can accommodate di-acetylated lysines (H4K5acK8ac) simultaneously, while the second bromodomain (BD2) interacts with another acetylated site within the same or in different proteins[100].

PHD is a well-known histone methylation reader domain, therefore PHD-BrD tandem containing proteins tend to associate with chromatin presenting specific multivalent patterns. For example, it is reported that coupling of the second PHD and the BrD of BPTF, enhances its binding to bivalent H4K16ac and H3K4me3 in a *trans*-histone way within the same nucleosome compared to H3K4me3 alone or to the combination of H3K4me3 and H4K12ac/H4K20ac[101]. In addition, PHD-BrD region of TRIM24 recognizes combined unmodified H3K4 and H3K27ac *in cis* respectively, within the same histone tail[102]. Moreover, ZMYND8 has triple PHD-BrD-PWWP reader domains, which form a structural cassette that concomitantly interacts with histone and DNA driven by H3K14ac[103].

BrD-containing proteins such as p300/CBP, MLL, ASH1L, GCN5L2 possess additional catalytic domains and are designated as “writers that read”. Catalytic modules like acetyltransferase (ATs), methyltransferase (e.g., SET) domains facilitate the introduction of histone modifications to specific genomic sites directed by BrD recognition. For instance, bromodomain of p300/CBP binds acetylated histone tails, facilitates their recruitment to chromatin and enhances diverse core histone acetylation and gene expression[64, 93, 104, 105]. Additionally, GCN5 bromodomain was required to direct its site specific histone acetylation[106]. As a subunit of MOZ HAT complexe, the bromodomain containing protein BRPF directs the catalytic core of the complex, MOZ, to histone tails through interaction with acetylated histones via its BrDs[107].

BrDs also present in proteins involved in chromatin structural regulation. These involve chromatin remodelers and AAA ATPase proteins (e.g., ATAD2, ATAD2B). For examples, SMARCA2, SMARCA4, BRD7, BRD9 and PBRM1 are components of SWI/SNF complexes while BAZ1A/B, BAZ2A/B, BPTF and CECR2 present in ISWI complexes. BrDs in chromatin remodeling complexes associate with chromatin regions harboring acetylated histone and might contribute to their recruitment and local chromatin remodelling[108]. Bromodomain of ATAD2 was uncovered to bind diacetylated newly synthesized histones (H4K5acK12ac) and might play a role in the replication-coupled chromatin reassembly[109]. Study on Abo1 (yeast homologue of ATAD2) revealed that BrD and AAA+ pore of Abo1 bind with H3 N-terminal tail and load histone H3–H4 onto DNA for nucleosome assembly[110, 111].

Plant homeodomain (PHD) finger domain is a small module comprising of around 50-80 amino acid residues and a zinc binding motif. This domain is known to bind the N terminal tail

of histone H3, especially its methylated sites[112]. However, evidence suggests that PHD finger also displays acetyl-lysine recognition capability, as was first exemplified by double PHD finger domain of DPF3b binding to H3K14ac[113, 114]. Additionally, PHD domains in MOZ/MORF are able to recognize H3K9ac and H3K14ac, which facilitates their association with chromatin, which is important for gene transcription[115, 116]. Lately, PHD domains of MLL4 and MLL3 were identified to specifically recognize H4K16ac. This domain might mediate functional link between these proteins, MOF and H4K16ac[117].

YEATS (Yaf9, ENL, AF9, Taf14, Sas5) domain is an evolutionally conserved module from yeast to human and is found in many chromatin-associated protein complexes. The structure of YEATS domain was characterized by Yaf9, a yeast member of YEATS domain containing protein, where an immunoglobulin, β sandwich fold comprising of 8 antiparallel β-strands capped by 2 short α-helices at one end is adopted[118]. YEATS domain recognizes acetyl-lysine through a serine/threonine-lined aromatic sandwiching cage, whose binding are facilitated by relayed hydrogen bonding and multiple sets of CH-π interactions (**Figure 13**)[119].

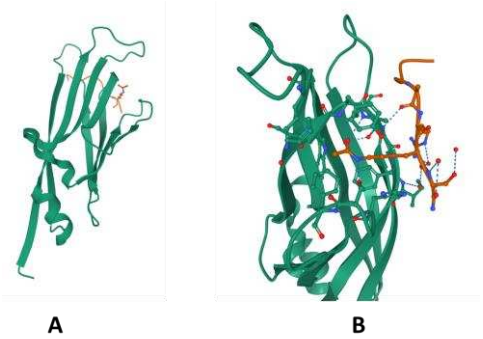

Figure 13. Structure of YEATS domain binding H3K9ac.
A. (PDB: 4TMP) The figure shows the structure of YEATS from AF9 binding with H3K9ac peptide. YEATS comprises of 8 antiparallel β-strands and 2 short α-helices. **B** The figure shows the interaction between H3K9ac and YEATS structural module.

Human genome encodes four YEATS domain-containing proteins, including AF9, ENL, GAS41 (also known as YEATS4) and YEATS2, all of which are implicated in cancer development. Specificity for acetylated histone H3 was observed among these members, with AF9/ENL binding H3K9ac, H3K18ac and H3K27ac, YEATS2 recognizing H3K27ac, and GAS41 preferentially binds acetylated H3K27, H3K14 and H3K18 as well as diacetylated H3, following protein dimerization[119-123]. Of note, recent studies found that YEATS domains act as specific acylation readers (e.g., crotonylation) and this will be discussed later in this essay.

1.3.3.4 Functional output of histone acetylation

Since its identification, histone acetylation has been extensively implicated in transcription, replication, and damage repair by directly regulating chromatin structure or by serving as platforms for recruiting chromatin modifying complexes.

Histone acetylation and Chromatin structure

Histone acetylation can alter the biochemical or physical properties of histones, therefore impacting DNA-histone, histone-histone interaction, and nucleosome dynamics as well as higher-order chromatin compaction. For instance, H3K56ac, H3K64ac, H3K122ac were suggested to disfavor the histone-DNA contacts within nucleosomes and enhance chromatin dynamics[124]. In addition, histone tails play a crucial role in inter-nucleosome interaction and chromatin fiber compaction. Bascom and colleagues revealed that acetylation at tails of all four core histones further abolishes tail-tail interactions and decreases long-range contacts[125]. Indeed, the most prominent role of H4 tail in nucleosome structure is that it interacts with acid patch of adjacent nucleosomes, acetylation at H4 tail in turn blocks such interaction and inhibits the compaction of 30-nm fiber[126, 127].

Histone acetylation further recruits and cooperates with chromatin interacting complexes to modify chromatin structure. H4K16ac inhibits nucleosome mobilization by ATP–utilizing chromatin assembly and remodeling enzyme ACF[127]. H3K56ac attracts histone chaperones such as CAF1 and Nap1, facilitating nucleosome assembly or enhancing nucleosome opening respectively[128]. H3K115 and H3K122 acetylation cooperate with SWI/SNF and RSC complexes to enhance nucleosome disassembly[129]. These are some non-exhaustive examples of the impact of histone acetylation on nucleosome/chromatin structure/organization, but there are other mechanisms that would be too long to discuss here.

Transcription activation

In general, most TFs binding free DNA need to overcome the chromatin barrier to gain access to DNA template. Chromatin structure modifications that modulate DNA accessibility can largely influence transcription initiation. Not surprisingly, less compacted chromatin at promoter and enhancer regions, which for example, are covered by specific histone modifications (e.g., H3K27ac, H4K16ac, etc.) or constituted of certain histone variants (e.g., H3.3, etc.), promotes TF binding and transcription initiation. Indeed, histone acetylation is viewed as general mark of active transcription. Consistently, nucleosomes flanking TSSs are in hyperacetylated states in actively transcribed genes[130].

In addition, histone acetylation can recruit transcriptional factors and cofactors, thereby contributing to transcriptional activation. For example, BRD4, an important histone acetylation reader, can bind promoters and recruit P-TEFb, thereby promoting CDK9-dependent, and,

transcription elongation[131, 132]. Additionally, H3K9ac was described as recruiting super elongation complex and enhancing Pol II pause release[133]. Histone variants and their modifications also play a role since for instance, H2A.Zac was found essential for enhancer RNA transcription, enhancer promoter interaction and RNA Pol II recruitment[134].

Histone acetylation is a highly dynamic mark

Histone acetylation is a highly dynamic modification. Early in the 1980s, researchers found that the half-life (t1/2) of histone acetylation ranged from minutes to hours[48]. Lately, using time-resolved approach, Weinert and colleagues identified that a subset of p300/CBP regulated sites of histone acetylation has very fast turnover rate, with half-lives of less than 1 hour for acetylation on 12 histone sites (including H2B N-terminal acetylation, H3K18/36ac and H4K8ac)[62]. Although theoretically this dynamics could result from histone turnover or continuous action of HATs and HDACs, the latter was acknowledged as the predominant cause[135]. Indeed, histone modifications and histone turnover seem to be relatively independent events[136].

Acetylation dynamics seems to be important for active transcription. Through genome-wide mapping, Wang and colleagues identified that both HATs and HDACs are enriched on highly active genes in human cells. They demonstrated that, at active genes, HDACs could indeed, remove acetylation marks in order to keep the acetylation at levels supporting transcription, while preventing promiscuous intiation[137]. Gryder and colleagues further illustrated that H3K27ac distribution at enhancer regions is balanced by an interplay between p300 and HDAC, and this balance is required for core regulatory transcription factors (CR TFs)-mediated active transcription in rhabdomyosarcoma. Hyperacetylated state might disrupt core gene regulatory network by removing RNA Pol II from core regulatory genetic elements, thereby decreasing CR TFs-mediated transcription[138].

1.3.4 Acylation

Apart from the aforementioned classical well-studied modifications, a growing body of studies have uncovered a repertoire of short chain non-acetyl acylations during last two decades, including propionylation (pr), crotonylation (cr), butyrylation (bu), succinylation (succ), β-hydroxylbutyrylation (bhb), 2-hydroxyisobytyrylation (hib), malonylation (mal), glutarylation (glu), formylation (fo), lactylation (lac) etc…, which will be designated as acylation hereafter (**Figure 14**)[139-142]. Histone acylations are dynamic and evolutionally conserved modifications, which can be detected in various species ranging from yeasts to human. Compared to acetylation, these acylations are much less abundant, with most of them covering robustly 1-5% of histone H3 and H4, in striking contrast to 15-30% by acetylation[143].

Similar to acetylation, these novel acylations appear to be driven by the corresponding CoA thioesters (acyl-CoA). Not surprisingly, acyl-CoAs level is only 1/10-1/100 of acetyl-CoA *in vivo*, in agreement with the low abundance of histone acylations. Acyl groups can be added onto histones through both enzymatic and non-enzymatic chemical reactions *in vitro*. Of those types of acylations, acidic (malonyl, succinyl and glutaryl) and β-hydroxybutyryl moieties were reported to favor non-enzymatic reaction to a greater extent than the others.

Common HATs and HDACs can add or remove acylations as well, but display different (lower, in general) efficiency compared to acetylation. An additional similarity between these acylations and acetylation is that, these acylations are distributed at TSS and enhancer regions and are associated with active gene transcription[139, 144, 145]. Currently, the function of acylations are, to a great extent, far from being understood.

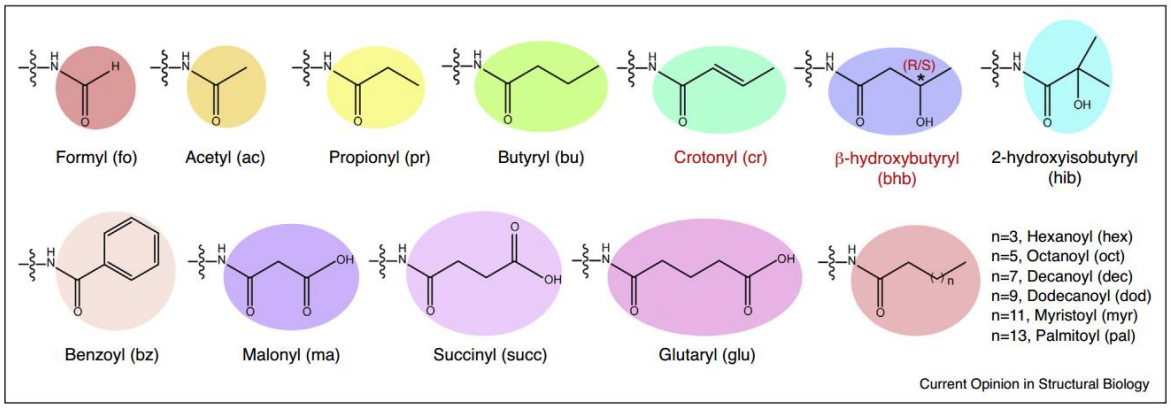

Figure 14. Histone non-acetyl acylations.

Apart from acetylation, lysines can be modified by other groups including formyl, propionyl, butyryl, crotonyl, β-hydroxybutyryl (bhb), 2-hydroxyisobutyryl, benzoyl, malonyl, sccuinyl, glutaryl, etc. Among them bhb can be R or S forms of enantiomers. From[146]

1.3.4.1 HATs for acylations

Simithy and colleagues assessed the capability of seven common HATs (i.e., p300/CBP, GCN5, PCAF, Tip60, MOF, NatA) catalyzing diverse acylations *in vitro* using mass spectrometry and found that HATs have lower affinity for longer chain acylations compared to the two-carbon acetylation. Among the acylations they tested, most HATs preserve catalytic ability for butyrylation and propionylation, but are less efficient in producing acidic acylations (e.g., malonyl, succinyl and glutaryl), in branched chain acylations (e.g., β-hydroxybutyryl) and in crotonylation [143].

p300 has promiscuous catalytic activity over various types of acylations including propinylation, byutyrylation, crotonylation, β-hydroxybutyrylation and 2-hydroxyisobutyrylation, and its catalytic activity weakens with increasing length of acyl chains [147, 148]. Crystal structure of p300 reveals that its active site can accommodate acyl chains,

however the binding conformation suitable for acyl moiety transfer might require further adaptation induced by lysine substrate binding [148].

Similar to p300/CBP, GCN5/ PCAF was shown to have acyltransferase activity[143, 149]. Structure analysis of human GCN5 binding with acyl-CoAs (i.e., butyryl-CoA, propionyl-CoA) revealed that GCN5 active sites are capable of accommodating acyl chains. However the binding with butyryl-CoA might obstruct the adoption of incoming lysine substrate, thus disfavors the catalysis to occur, which is in agreement with its almost undetectable catalytic activity for butyrylation[150]. Lately, GCN5 was found to be able to succinylate H3 at K79, thanks to its catalytic domain which is capable of binding succinyl-CoA via a distinct conformation than acetyl-CoA bound state[151].

In addition to p300/CBP and GCN5, MYST family members were described to display acyltransferases activity as well. For instance, MOF was shown to act as a histone crotonyltransferase (HCT), in a manner that is evolutionally conserved, exemplified by the yeast homologue Esa1 possessing HCT as well[152]. Similarly, Tip60 and its yeast homologue Esa1p were found to catalyze 2-hydroxyisobutyrylation[147]. More recently, Han and colleagues reported that MYST family proteins (e.g., MOF, MOZ, HBO1) possess a propionyltransferase activity which is as strong as their acetyltransferase activity. This conclusion is supported by the crystal structure revealing that MOF binds to propionyl-CoA in a manner resembling MOF-acetyl-CoA complex. However, two extra hydrophobic interactions between the propionyl group and conserved valine-314 and proline-349 residues of MOF are observed, contributing to properly place the propionyl group within catalytic domain[153].

1.3.4.2 HDACs for acylations

Recent studies discovered that class I HDACs (HDAC1, 2, 3, 8) but not class II, are the major histone decrotonylases (HDCR) in mammalian cells using their deacetylase catalytic center to direct the reaction. Among these enzymes, HDAC1 displays strongest activity and has broad specificity for various histone sites. The major amino acid difference between class I and II catalytic domain is that the latter has VRPP instead of AGG. Interestingly, when replacing the AGG in HDAC1/3 by VRPP, the authors created mutants with retained HDCR but impaired HDAC activity. The possible explanation is that the rigid crotonyl group, but not the flexible acetyl group retains the ability to reach the narrower catalytic center in the VRPP mutant[154]. HDAC2 and 3 have been reported to remove Khib both *in vitro* and *in vivo* as well[147]. In addition, HDAC3 was also characterized to display de-β-hydroxylbutyrylase activity[155]. HDAC8 was shown to remove long chain fatty acylation (e.g., myristoyl, octanoyl, dodecanoyl). However, this enzyme is inactive or shows a limited ability to hydrolyze short chain acylations (Kbu, Khib, Kcr)[156].

SIRT family (SIRT1-7) are confirmed histone deacylases and could present distinct site specificity from HDACs. Indeed, Zhang and colleagues uncovered that most of the sirtuins are capable of binding non-acetyl acyl marks, including longer alkyl chain. More specifically, SIRT5 can recognize Kglu, Ksucc, Khib, Kbhb. It should be noted that Khib and Kbhb are also recognized by SIRT3; while SIRT2 recognize Ksucc[155].

Consistent with these findings, SIRT1-3 were identified to exhibit de-crotonylase activity [154, 157]. SIRT1-3 and SIRT5 were also found to catalyze the hydrolysis of histone Kbhb. Of note, structural studies indicated that the S-form enantiomer of lysine bhb favors de-β-hydroxylbutyrylase activity compared to R-form bhb. Moreover, SIRT3 displays class selectivity and preferentially removes H3 (at K4, K9, K18, K23, K27) and H4K16 bhb but not H4K5/8/12bhb. In accord with this selectivity, structural analysis revealed that the glycine motif flanking H4K5/8/12 disfavors the recognition by SIRT3[155]. SIRT4 was shown to catalyze the removal of hydroxymethylglutarylation, SIRT5 is able to remove Kmal, Ksucc and Kglu as well[158, 159]. SIRT6 has large pocket suitable for long chain acyl groups (e.g., Kmyr)[160, 161].

1.3.4.3 Readers for acylations

It has been documented that YEATS domains of AF9 and YEATS2 have a preference for crotonyl-lysine over acetyl-lysine [162]. Structural analysis of AF9 YEATS domain reveals that it has an extended aromatic sandwich cage, which favors the π-aromatic stacking and hydrophobic contacts between crotonyl and its aromatic ring, thereby facilitates the binding and hence showing a preference for crotonyl readout[163]. Besides, double PHD finger (DPF) domains of MOZ and DPF2 have been described to accommodate different types of acyl-lysines, including Kbu, Kpr and Kcr, with best preference for Kcr. Structural basis is that Kcr is anchored in a “dead-end” pocket of first PHD finger domain through hydrophobic contacts and hydrogen bonds[164]. DPF domain of MORF was shown to bind many acylation marks including Kbu, Khib, Kac and Ksucc at K14 of H3 peptides. Molecular basis of MORF-DPF for acyl-lysine is exemplified by the butyryl moiety, where the recognition is driven by hydrophobic electrostatic interactions[165]. Most bromodomain-containing proteins are only able to bind short acetyl or propionyl groups because of restricted size of binding pockets, whereas, some non-canonical bromodomains who lack the conserved asparagine and have lager pockets, tend to accommodate longer acyl groups. Indeed, bromodomains of BRD9, CECR2 recognize butyryl-lysine, and second BrD of TAF1 can bind both butyryl-lysine and crotonyl-lysine[166].

1.3.4.4 Functional output of acylations

Histone acylations have been studied with respect to metabolic and signaling cues, including glycolysis regulation, inflammatory response, nutrient limitation or starvation, and have been

implicated in spermatogenesis and cancer[167, 168]. Similar to acetylation, histone acylations are generally associated with active transcription. *In vitro* essay demonstrated that histone non-acetyl acylations marks (i.e., butyrylation, crotonylation, β-hydroxybutyrylation, propionylation) can stimulate transcription to a comparable extent as acetylation[144, 145, 169]. Such correlation with active transcription is also observed *in vivo*, where studies documented that acylations (i.e., butyrylation, crotonylation, β-hydroxybutyrylation, 2-hydroxyisobutyrylation, lactylation) are mainly enriched at active TSS regions and enhancer regions[140-142, 144, 145]. Accordingly, to increase the level of acylations by ectopic expression of HATs, or by exposure to higher concentration of acyl-CoAs, or to decrease them by HDACs or by decreased acyl-CoA concentration resulted in enhanced transcriptional activation, or gene silencing respectively[152, 154].

Although acylations were firstly depicted to co-occur with acetylation and have similar implications in active transcription, these marks were suggested to play active roles in gene transcription, and are not merely by-products of active transcription. In spermatid cells, 29% of H4K8hib marks testis specific genes and better defines highly-expressed genes than H4K8ac[142]. In spermatogenic cells, Kac and Kbu are found to co-occur at TSS regions of highly expressed genes, however Kbu can compete with Kac and prevent Brdt from binding and might fine-tune both specific gene expression program as well as histone eviction mode during late spermatogenesis [145]. In a study of histone crotonylation by p300/CBP, introduction of p300/CBP mutants, which retain HCT but not HAT can enhance transcriptional activation under the physiological condition of low concentration of crotonyl-CoA[152]. However, another study of histone crotonylation by p300/CBP indicates that HCT and HAT activities of p300 could not be easily separable[148].

The non-redundant role of acylations is further supported by the identification of preferential histone acyl readers and writers. For instance, YEATS domain of AF9 preferentially recognizes crotonylation that links Kcr with transcriptional activation[163]. Furthermore, Taf14 YEATS domain is essential for transcriptional repression of growth-related genes under nutrient limitation in parallel with increased H3K9cr[170]. GCN5 (also known as KAT2A) preferentially binds succinyl-CoA over acetyl-CoA. When in complex with α-KGDH (α-ketoglutarate dehydrogenase), it can act as succinyltransferase and catalyze H3K79succ, which is enriched on TSS regions and is required for gene expression and cancer proliferation[151].

1.3.5 Other types of modifications

In addition to the above-mentioned modifications, histones can be subjected to other modifications such as ubiquitination (ub), sumoylation, serotonylation (ser), glycation, ADP-ribosylation, citrullination, long chain fatty acylations (lipidation) that play a role in diverse biological processes (**Figure 15**).

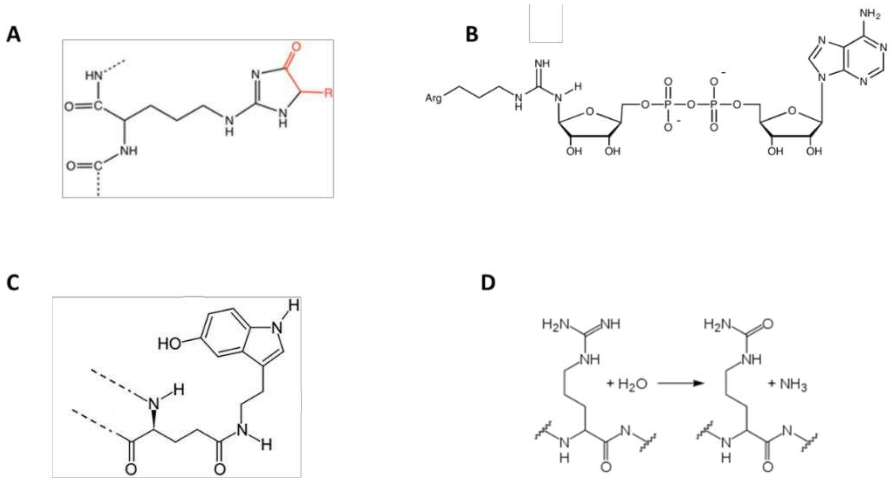

Figure 15. Other histone modifications.

A Glycation. **B** ADP-ribosylation. **C** Serotonylation. **D** Citrullination.

1.3.5.1 Ubiquitination

Histone ubiquitination is to add a ubiquitin peptide to histone lysines mainly on H2A and H2B histones. Ubiquitination is catalyzed by E3 ligases including RNF168, RING1B (RNF2, member of PCR1 complexes), BRCA1/BARD1 and RNF20/40, which are responsible for ubiquitinating H2A at K13/K15, K119, K127/129, and H2BK120 respectively. Ubiquitin can be removed by deubiquitinating enzymes (DUBs), such as ubiquitin-specific protease (USP)3/11/44/51 etc. Histone ubiquitination is predominantly involved in DNA damage repair and transcriptional regulation through recruiting and organizing DNA repair factors (e.g., 53BP1) and through cooperating with other chromatin interaction proteins[171, 172]. Of interest, there is an interplay between histone ubiquitination and other histone marks. This is exemplified by H2BK120, where mono-ubiquitination at this site activates DOT1L-dependent H3K79me and SET1-dependent H3K4me respectively[38].

1.3.5.2 Sumoylation

Histones are also substrates for small ubiquitin-related modifier (SUMO) proteins, generating sumoylation on all core histones. SUMO is added to substrates through E1-E2-E3 enzymatic cascade similar to ubiquitylation and can be cleaved by SUMO proteases. Histone sumoylation is generally associated with transcriptional repression. Shiio Y. and Eisenman R.N. reported that H4 sumoylation could recruit HP1 and HDACs, therefore mediates gene scilencing[173]. Investigators also found an interplay between histone sumoylation and other histone marks, such as histone acetylation and ubiquitination. For instance, histone sumolyation was found to occur at or adjacent to acetylation sites in yeast, suggesting a role for this modification in counteracting acetylation-mediated gene transcription[174]. Histone sumoylation can be stimulated by H2B ubiquitylation and in turn inhibits Ctk1-mediated RNA Pol II phosphorylation and transcriptional elongation[175]. Of note, functions of histone sumoylation

should be interpreted cautiously since SUMO occurs on a number of nuclear proteins other than histones, including chomatin remodelers and transcriptional coregulators[176, 177].

1.3.5.3 Serotonylation

Recently Farrelly and colleagues identified that histone tails can be serotonylated (5-hydroxytryptamine). They uncovered that transglutaminase 2 can serotonylate histone H3 that carries H3K4me3 mark, which results in the combination of H3K4me3Q5ser marks on histone tails. H3K4me3Q5ser is associated with active transcription, which could be explained by the potentiation of H3K4me3 activity in recruiting transcriptional machineries, and the fact that these dual marks enhance interactions of TFIID complexes with chromatin. H3K4me3Q5ser mark is closely linked with neuronal cell differentiation[178]. The discovery of histone serotonylation has linked the chromatin regulatory networks into neurotransmitter-dependent cellular signaling. This discovery might pave path for understanding many pathophysiological conditions concerning serotonin[179, 180].

1.3.5.4 ADP-ribosylation

Histone ADP-ribosylation refers to the addition of ADP-ribose onto a repertoire of target residues including aspartate, glutamate, lysine, arginine, serine and tyrosine and has been found to occur on all types of histones[181, 182]. Histones can be modified by single or several ADP-ribose molecules, termed as mono-ADP ribosylation (MARylation) or poly-ADP ribosylation (PARylation) respectively. Several ADP-ribose can form either linear or branched chain in the case of MARylation. Histone ADP-ribosylation is a reversible modification, which can be added by Diphteria toxin-like ADP ribosyltransferases (ARTDs; also called PARPs), and removed by ADP-ribosyl hydrolases (ARHs) and poly-ADP-ribose glycohydrolase (PARG). Domains that read ADP-ribosylation include PAR-binding motif, PAR-binding zinc finger, Macrodomains, WWE domain etc. There is also an interplay between histone ADP-ribosylation and other PTMs including acetylation, methylation, phosphorylation etc… which have been implicated in chromatin dynamics and cell fate determination[181, 183].

1.3.5.5 Citrullination

Protein citrullination is the conversion of arginine side chain to citrulline by protein (peptidyl) arginine deiminases (PADs). In human, there are 5 PAD homologues designated as PAD1-4 and PAD6 whose activity is regulated by calcium ions. Among them, PAD4 is located in nucleus and catalyzes citrullination on H2A, H3, and H4. Besides, PAD4 was also reported to catalyze demethylimination, where Arg monomethylation is hydrolyzed into citrulline and methylamide. Histone citrullination might be involved in chromatin structure regulation and is

associated with transcriptional regulation in combination with other histone PTMs such as methylation and acetylation[184, 185].

1.3.5.6 Glycation

Histone tails are susceptible to non-enzymatic covalent modifications (MECMs) on their nucleophilic side chains. One of the most prevalently occurred NECMs is glycation, where sugar (e.g., glucose, fructose) and their derivatives (e.g., ribose, methylglyoxal, MGO) are attached to histones[186, 187]. Latest studies indicate that histone glycation is reversible, with the identification of DJ-1 to be a potential histone deglycase. Histone glycation has been suggested to regulate nucleosome stability and assembly, and alter the biophysical properties of chromatin[188-190].

1.3.5.7 Lipidation

Protein lipidation (also known as fatty acylation) is the attachment of fatty acids (e.g., myristoyl (14:0), palmitoyl (16:0), stearate (18:0), oleate (18:1), arachidonate (20:4), and eicosapentaenoate (20:5)) onto proteins via thioester (S-), amide (N-) and ester (O-) bonds depending on the residues they associate with. Using unbiased proteomic analysis, Wilson and colleagues have discovered H3 variants to be substrates of S-fatty acylation[191]. Besides, Zou and colleagues reported that histone H4ser47 is subjected to O-palmitoylation catalyzed by Acyl-CoA:Lysophosphatidylcholine Acyltransferase I (LPCAT1) in response to exogenous calcium ions. H4 O-palmitoylation is associated with RNA Pol II activation and increased gene transcription[192]. In addition to histones, other chromatin interacting proteins can also undergo fatty acylation, which in turn might participate in chromatin structure and gene transcription regulation.

1.3.6 Combinatorial histone modifications

Apart from the increasing number of the types of histone modifications, an additional complexity of signaling by histone PTMs is the combination of different histone marks. A special example is the occurrence of bivalent histone marks at primed promoters, which was believed to prime the status of the subsequent active or repressed transcription. With the usage of tandem mass spectrometry, sequential MNase based ChIP, the combinations of different histone modifications have been characterized in a genome-wide scale. One study comes from Wang and colleagues, who performed a comprehensive study about the distribution of 39 histone PTMs on human genome using CD4+ T lymphocytes. They identified a common modification ‘backbone’ comprised of 17 modifications that coexist in 3286 active promoters and pointed out that these marks tend to colocalize and correlate with each other[193].

The functional interpretation of combinatorial histone marks can be tackled by reader proteins who recognize multiple modifications. The combinatorial readout of histone marks by readers comprises: 1) some reading modules recognizing several modification types within the same histone protein; 2) reader proteins possessing tandem reading modules, which facilitate the recognition of different marks on the same histones (*cis-histone*), distinct intranucleosomal (*cis-nucleosome*) or internucleosomal histones (*trans-nucleosome*). 3) reader proteins that might co-exist with additional readers or other proteins within a complex (e.g., chromatin modifier complexes), which facilitate a series of functional outputs, including the establishment of combinatorial pattern of histone marks. More information is provided in[194, 195] and summarized as **Figure 16**.

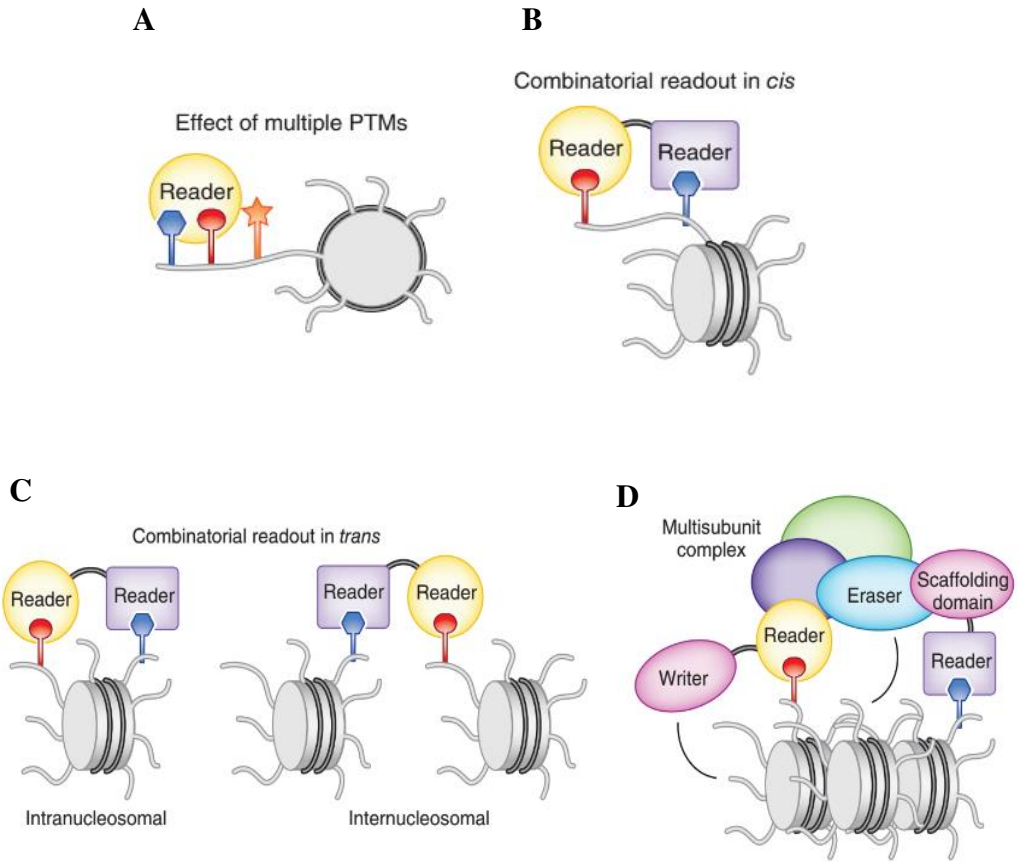

Figure 16. Combinatorial readout of histone PTMs.

The binding specificity of readers protein to histone marks can be influenced by the adjacent histone marks. For example, certain reader domains can recognize multiple PTMs simultaneously (**A**). Combined reader domains can recognize different marks on *cis*-histone (**B**), different histone proteins of *cis*-nucleosome (**C, left**) or of *trans*-nucleosomes (**C, right**). Moreover, reader proteins can form complexes with other proteins, including additional readers *in vivo*. Different subunits in the complexes therefore could exert multiple functions as a whole (**D**). From[194].

2. Histone modifications are implicated in cancer

Tumor development is a multistep process analogous to *Darwinian* evolution, where a succession of intracellular alterations contributing to several key biological capabilities are selected under environmental pressure, leading to the survival advantage, non-restricted proliferation, and dissemination of transformed cells. Two decades ago, D. Hanahan and R.A. Weinberg proposed six common hallmarks of cancer capabilities, including sustaining proliferative signaling, evading growth suppressors, resisting cell death, enabling replicative immortality, inducing angiogenesis, and activating invasion and metastasis[196]. These fundamental principles summarizing a myriad of cancer studies structured our reasoning in cancer research. Ten years later, professor Hanahan and Weinberg complemented this framework with two additional hallmarks, including energy metabolism reprogramming and immune destruction evasion[197]. They further emphasized that, underpinning these characteristics are homeostatic function of a repertoire of intracellular molecular signaling networks. Several prominent regulators (e.g., MYC, p53 etc.) participate in multiple layers of the proposed hallmarks in diverse types of cancer, and in the crosstalk between cancer cells and tumor microenvironment[197].

The oncogenic molecular signaling was originally attributed to genetic alterations. However, this concept has been challenged with the explosion and advancement of cancer studies during last few decades. One of the challenges comes from the comprehensive study on the profile of whole genome based on the next generation sequence (NGS) technology, where genome sequencing of thousands of cancers identified that more than half of human cancers harbor mutations in genes that control the epigenome. Numerous researches have been carried out on cancer epigenetics, which in turn brought forward epigenetic regulatory mechanisms being incorporated into the main themes of cancer biology. In general, epigenetic mechanisms might contribute to the means by which hallmark capabilities are acquired, or simply they may directly control the regulatory circuitry that is already known to govern them.

The classical definition of epigenetic considers the heritable changes in gene expression without DNA sequence alterations, including DNA methylation, histones and RNAs. However practically, today epigenetics considers all the signaling to chromatin mechanisms that control gene expression. In the context of cancer, the epigenetic aberrations could include mechanisms by which the driver oncogenes promote malignant transformation. Furthermore, epigenetics can directly affect cancer genetics in that it might lead to genetic mutations (e.g., deamination of 5-methylcytosine (5mC) to thymine) and cause genomic instability (e.g., DNA hypomethylation at repetitive elements). Moreover, alterations of epigenetic profiles per se might serve as decisive factor in cellular reprogramming during malignant transformation. Indeed, it has been proposed to cause tumorigenesis especially in those cancer contexts where

the driver genetic aberrations are lacking[198]. Since epigenetics is relatively dynamic because of the functions of writers, erasers, readers and remodelers and its link to cell metabolism, investigators have envisioned cancer therapeutics by targeting epigenetic enzymes and interacting proteins to restore the disrupted epigenetic profiles, and to break the resultant oncogenic transcriptional circuitry.

Herein, I'll summarize the cancer-related altered epigenetic profiles. I will also give a brief overview of the currently-identified aberrations of epigenetic players and their possible roles in cancer. Finally, I will summarize the current therapeutic approached to impact the cancer epigenome and their clinical efficacy. Since noncoding RNA, DNA methylation and chromatin remodelers are not the main topics in this thesis, I will leave out most of the details relating to them and will focus on histone modifications.

2.1 Disrupted epigenetic mechanisms contribute to oncogenesis

2.1.1 Altered epigenetic signatures in cancer

Cancer cell epigenome displays distinct patterns compared to their normal counterparts. Alterations of cancer epigenomic signatures are typically exemplified by the well-characterized DNA methylation, which shows global hypomethylation (including intergenic regions and repetitive elements) and regional hypermethylation (e.g., CpG islands) in cancer. These alterations contribute to cancer establishment and development. For instance, the hypermethylation at CpG islands, which are present in most gene promoters, can repress gene transcription including that of tumor suppressors. In special cases such as colorectal cancer, CpG islands methylator phenotype (CIMP) can be observed, where a set of tumor suppressor genes could be repressed simultaneously. Additionally, hypomethylation at repetitive elements might lead to genomic instability, which might disrupt normal self-constraint program and envision genetic aberrations leading to oncogenesis[199]. Finally, spontaneous deamination of 5-methylcytosine (5mC) to thymine is likely to be responsible for generating mutation hotspots in somatic cells, which might increase the risk of tumorigenesis.

Histone modifications alterations are extensively implicated in cancer, both at a global level of the whole genome and at specific loci. For instance, an overall loss of acetylated and trimethylated forms of H4 (predominantly H4K16ac and H4K20me3) was detected in several cancers. Loss of these histone marks co-occurs with DNA hypomethylation at repetitive regions[200]. Furthermore, changes in histone modification patterns have been reported in a variety of tumors and are associated with prognosis[201-203]. Similar to DNA methylation, histone modifications may repress or activate oncogenic transcriptional circuits and might act as epigenetic drivers of cancer[204]. Certain histone modifications are associated with chromatin

alterations and genetic mutations, suggesting the existence of a crosstalk between chromatin organization and genetic abnormalities[205, 206].

2.1.2 Epigenetic players in cancer

In addition to the general alterations of the epigenetic patterns, genetic studies and exosome sequencing projects have led to the discoveries of writers, erasers, and readers of histone PTMs among the frequently altered genes in cancers. Alterations of epigenetic modifiers in different cancer contexts can result from gene mutation (gain-of-function mutation or loss-of-function mutation), translocation, gene amplification, overexpression and silencing from non-genetic causes, etc.[207-209]. In many cases, epigenetic modifiers can be either oncogenic or tumor-suppressive depending on the cell contexts. An additional layer of histone modification signaling circuits is through reader proteins. Aberrations of readers proteins have been reported in cancer, exemplified by BRD4-NUT fusion protein that acts as the oncogenic driver in midline carcinoma[210]. It is worth noting that, although numerous aberrations concerning epigenetic players have been identified in cancer, many of their roles are not fully understood. Moreover, in many cases, the understanding of the precise role of epigenetic players in cancer can be complicated due to their direct involvement in many intracellular signaling networks (e.g., act on non-histone substrates) other than via histone modulation and gene transcription.

Table 2. Common HMTs and their regulatory contexts in cancer.

Name	Histone targets	Types of aberrations	Cancer types	Roles in cancer
EZH2	H3K27me	gain-of-function mutation (Y641 mutations[211-213], A677 mutaion[214]), loss-of-function mutation, amplification, dysregulation[207-209]	Melanoma, lymphoid malignancies[212, 215]	Generally associated with accelerated transformation and progression, can be tumor-suppressive in certain types of cancer[216, 217].
MLL/KMT2 family	H3K4me	Translocates with more than 70 partner genes (e.g., AF4, AF9, AF10, ENL family and p-TEFb)	Acute leukemias	Oncogenic in hematological malignancies through activating transcriptional factors that control hematopoietic stem cell program, including Hoxa9 and Meis1[218-220].
		Nonsense or frameshift mutations [221]	Colorectal cancer, glioblastoma, melanoma, pancreatic carcinoma, hepatocellular carcinoma	KMT2A/B cooperate with genuine oncogenes in transcription regulation[222, 223]. KMT2C/D/F might be either oncogenic or tumor suppressive in solid tumors[221].
NSD family	H3K36me	NSD1 mutation, NUP98-NSD1 fusion	Human papillomavirus (HPV)-negative head and neck squamous cell carcinoma (HNSCC), laryngeal, prostate, pancreatic ductal tumors, acute myeloid leukemia	Loss-of-function NSD1 mutations confer to decreased risk of death in HNSCC[224]. NSD1 expression is associated with cancer metastasis in various solid tumors[225-227]. NUP98-NSD1 binds gene elements adjacent to HoxA7/9[228] and predicts poor outcome in AML[229-231].
		NSD2 mutation (E1099K, activating mutation)	Acute lymphoblastic leukemia (ALL), mantle cell lymphoma, chronic lymphocytic leukemia[232]	Contribute to abnormal gene expression programs associated with oncogenesis and cancer aggressiveness[233, 234]. Correlated with clonal evoluation and drug resistance in ALL[235, 236].

		NSD2 overexpression	Neuroblastoma, breast, bladder, prostate tumor, and multiple myeloma	NSD2 overexpression in t(4;14)+ multiple myeloma lead to an altered epigenomic landscape featured by increased H3K36me2 and concomitantly decreased H3K27me3. Transcriptional profile demonstrated that genes in p53 pathway, cell cycle regulation and integrin signaling were affected[237]. Associated with poor outcome in neuroblastoma[238].
		NSD3 amplification and overexpression, translocation (NUP98-NSD3, NSD3-NUT)	Breast cancer, myelodysplastic syndrome, acute myeloid leukemia, midline carcinoma[239-241].	Play a role in maintaining the dynamics of H3K4 and H3K36 methylation[242], transcriptional regulation of BRD4 targeted genes[239, 243]. Amplification was correlated with tumor grade and poor prognosis in breast cancer[244].
SETD2	H3K36me3	Mutations (missense mutations, focal deletions, and bi-allelic loss)	Clear cell renal cell carcinoma, high grade gliomas, colorectal cancer, and hematopoietic malignancies[245-247].	Associated with DNA damage responses (e.g., DNA mismatch repair, double strand break repair etc.)[248-250], RNA splicing machineries[251-253]. Required for cancer proliferation, DNA damage response respectively[254-256]. In general, SETD2 has tumor-suppressive potentials across various cancer entities, whose inactivating mutations are associated with chemotherapy resistance[257].
DOT1L	H3K79me1/2/3	Aberrant activation, missense mutation,	Gastric cancer[258], MLL-rearranged leukemias	Aberrant activation of DOT1L has been implicated in MLL rearrange leukemia, where its recruitment by MLL fusion partners, such as AF4, AF9, AF10, and ENL causes transcriptional activation of genes required for leukemia development (e.g., HoxA9)[259].

SUV39/KMT1 family	H3K9me	SUV39H1 overexpression	Melanoma and gastric cancer[260]	Context-dependent roles in cancer. SUV39H1 overexpression is associated with cancer development and poor prognosis in melanoma and gastric cancer. However, in cervical cancer, metastatic tumor cells displayed the feature of SUV39H1-low chromatin state[261-263].
		SETDB2 mutation	Clear-cell renal cell carcinoma, ALL	Plays an oncogenic role in acute lymphoblastic leukemia. In contrast, its low expression is associated with poor prognosis in renal cell tumor[264, 265].
		G9a overexpression	Breast cancer, gastric cancer, leukemia	Promote cancer survival and tumorigenesis via repressing specific genes (e.g., hypoxic response associated genes), or activating oncogenes (e.g., mTOR), or activating metabolic pathways (e.g., serine-glycine biosynthetic pathway, iron metabolism) in various cancer cells[266-269]. Cooperates with transcriptional factor YY1 to prevent tumor progression in leukemic cells[270]. G9a depletion was shown to exhibit distinct roles as repressive in short-term tumor initiation but confers to more aggressive behaviors in long-term progression in skin tumors[271].
SMYD2/KMT3C	H3K36, non-histone substrates (e.g., STAT3, NF-κB, p53)	Overexpression	Breast tumor, chronic lymphocytic leukemia, pediatric acute lymphoblastic leukemia	Associated with cancer progression and poor prognosis in these entities[272-274].

SMYD3/KMT3E	Non-histone substrates	Amplification, overexpression	Liver cancer, colon tumor, chronic lymphocytic leukemia	Play an oncogenic role via methylating non-histone proteins[273, 275-278].
SETD8/KMT5A	H4K20me	Overexpression	*Papillary thyroid cancer, breast cancer*	Might regulate genes associated with metabolic reprogramming[279, 280].
SETD7/SET7/SET9/KMT7	H3K4me1, non-histone substrates	Dysregulation	Colorectal cancer, breast cancer, hepatocellular carcinoma	Either oncogenic or tumor-suppressive depending on different cancer models[281-283].
PRMT family	Arginine methylation of non-histone substrates	Amplification, overexpression, dysregulation	Breast cancer, melanoma, glioblastoma, leukemia	enhanced PRMT5 activity promotes leukemia growth in acute myeloid leukemia[284].

Table 3. Common KDMs and their implications in cancer.

Name	Histone targets	Implications in cancer
LSD1	H3K4me1/2, H3K9me1/2	Overexpression of LSD is associated with cancer aggressiveness in neuroblastoma, leukemias[285-287]. LSD1 is required to maintain oncogenic program controlled by driver oncogenes in acute lymphoblastic leukemias[288-290]. LSD1 dysregulation is directly involved in activating oncogenes such as p21, CCNA2, E2F1, E-cadherin etc. in solid tumors[286, 291]. LSD1 was also characterized as a tumor suppressor in breast cancer[292-294].
UTX/KDM6A	H3K27me2/3	UTX/KDM6A mutations (e.g., missense, truncating and indels mutations), gene amplifications, and gene fusions, dysregulation are found in various solid tumors and hematological malignancies[295]. Tumor suppressive or oncogenic in different types of cancers[296-300].
JMJD3/KDM6B		Loss of JMJD3 is associated with poor prognosis in colorectal cancer and is associated with aggressive pancreatic ductal adenocarcinoma[301, 302].

		JMJD3/KDM6B is oncogenic in leukemias[303]. Overexpression of JMJD3 is associated with poor prognosis in esophageal squamous cell carcinoma[304], clear renal cell carcinoma, glioma, non-small cell lung cancer[305-307], multiple myeloma[308].
KDM5A	H3K4me2/3	NUP98-KDM5A was detected in acute megakaryoblastic leukemia and is associated with worse outcome[309, 310]. Expression of KDM5A promotes cell proliferation in lung, ovarian cancer[311 312]. KDM5A is downregulated in metastatic glioma[313].
KDM5B		Oncogenic in various solid cancers whose expression is associated with poor prognosis[314-319] KDM5B promotes the drug tolerance of melanoma propagating cells[320].
KDM5C		KDM5C mutation has been discovered in clear cell renal carcinoma cells[245, 321]. KDM5C overexpression was identified in breast, gastric, and prostate cancer and is associated with metastasis and poor prognosis[322-324]. KDM5C point mutation was identified in acute myeloid leukemia and is associated with chemo-resistance[325]
KDM5D		KDM5D is frequently deleted in metastatic types and its low level is associated with drug resistance and poor prognosis in prostate tumors[326-328]. KDM5D can also play a role in metastasis of gastric cancer[329, 330].

Table 4. Common HATs and their implications in cancer.

Name	Targets	Implications in cancer
p300/CBP	Histones and non-histone substrates	Loss of heterozygosity (LOH) mutations concerning p300/CBP have been identified in gastric, colon, cervical cancers, leukemia and lymphomas and are markers for poor prognosis[331-334]. MLL-CBP, MLL-p300, MOZ-p300, MOZ-CBP translocations can be found in acute myeloid leukemia, chronic myelomonocytic leukemia and myelodysplastic syndrome[335-341]. Generally p300/CBP displays tumor-suppressive functions[342-345]. Mutation or translocation mediated oncogenic activities can be attributed by their regulation of non-histone proteins (e.g., BCL6, p53, AML1, NF-κB)[345-349].

GCN5/PCAF	Histones and non-histone substrates	Somatic mutations and deregulation were identified in many tumors[204, 350, 351]. The major oncogenic role of GCN5/PCAF is to cooperate with bona fide oncoproteins (e.g., Myc, E2F1 etc.) and promotes their activities[352-356]. PCAF/GCN5 are also suggested to exert tumor-suppressive functions[357, 358].
MOZ	Histones and non-histone substrates	The oncogenic roles of MYST family are mainly through transcriptional activation, DNA damage repair, DNA replication etc. dependent or independent of their acetyltransferase activity towards histones[61, 359]. MOZ-CBP, MOZ-p300, MOZ-TIF2, MORF-CBP can be found in acute leukemias[360].
HBO1	Histones and non-histone substrates	HBO1 can be oncogenic in cancer cells and its overexpression has been identified in many cancers due to gene amplification[361-364]. Can be tumor-suppressing through upregulation of tumor suppressor[365]. NUP98-HBO1 chimera could induce chronic myeloid monocytic leukemia[366].
TIP60	Histones and non-histone substrates	Has bivalent roles in human cancer[52]. TIP60 acetylates p53 and regulates cell cycle progression and apoptosis[367, 368]. TIP60 was also found to promote androgen receptor, c-Myc and NF-κB mediated gene transcription and cell transformation[369, 370].

HDACs

HDACs are involved in a variety of cancers including hematological and solid tumors[204]. A high level of HDACs is generally associated with aggressive disease and inferior outcomes of patients[371-373]. In fewer cases, HDACs have putative tumor-suppressive effects, as exemplified by the identification of HDAC2 loss of function mutation in epithelial cancers, where its re-expression causes a reduced tumor growth[374, 375]. Deregulated HDAC activity in cancer results mostly from overexpression, which has been detected in cohorts of primary samples and diverse cancer cell lines, presenting a specific application domain for HDAC inhibitors in cancer treatment[376, 377]. In many cases, aberrant enzymatic activity has also been identified and accounts for altered epigenomic profiles and the oncogenic roles of HDACs[378, 379]. Additionally, oncogenic effects of HDACs can be mediated by abnormal recruitment by key regulators. For example, in acute leukemia, HDAC-containing repressor complexes can be recruited by PML-RARα, AML1-ETO, which in turn contribute to the oncogenic chimera proteins-induced leukemogenesis[380, 381].

Mechanisms of HDAC contribution to tumorigenesis are diverse and to a large extent, context-dependent. This is partially due to the fact that HDACs can impact various key molecules and intracellular regulatory pathways by deacetylating histone and non-histone substrates. Hagelkruys and colleagues have reviewed studies of HDACs and cancer in 2011, where they highlighted various aspects of HDACs activities in cancer biology, predominantly including cell proliferation and cell cycle, apoptosis, differentiation, DNA damage response, metastasis, angiogenesis, autophagy, etc.[382].

Table 5. Histone deacetylases regulate various hallmarks of cancer.

Hallmark capabilities	HDACs members	Signaling networks
Proliferation and cell cycle progression	HDAC1 and HDAC2	Inhibition of HDAC1 and HDAC2 leads to increased p21, p57 and p27, causing cell cycle arrest at G1 phase[383, 384].
	HDAC3, 4, 5	Inhibits p21[385-387]. HDAC4 was also reported to act as corepressor on cyclin D1 promoter[388]. HDAC3 can induce G2/M arrest via impaired Aurora B activity [389]
	HDAC6	Deacetylate α-tubulin and impairing BCL3 translocation and cyclin D1 expression[77].
	HDAC10	cyclin A2 expression and regulate G2/M progression[390].
	SIRT1 and SIRT2	Inhibition of SIRT1 and SIRT2 induces decreased expression of cyclin D1/E, CDK2/4/6 and leads to G0/G1 arrest in colorectal cancer cells[391]. SIRT2deacetylates tubulin and regulates heterochromatin structure[392-394]
	SIRT3-5	SIRT3 could deacetylate p53 and is antiproliferative. In contrast, it could also regulates energy metabolism and promotes proliferation[395, 396].
	SIRT6	Activation of SIRT6 inhibits cell proliferation and induces cell cycle arrest in hepatocellular carcinoma[397].
Apoptosis	HDACs	Inhibition of HDACs promotes cell apoptosis by directly activating intrinsic and extrinsic pathways (e.g., caspase-8, 10 expression)[398, 399], or by sensitizing cells to apoptosis via downregulating antiapoptotic proteins (e.g., cFLIP, Bcl2, survivin, XIAP, Mcl-1 etc)[371, 400-403] [494-496].
	SIRTs	Inhibition of SIRT1/2 inhibition was found to activate caspase-3, -8 and -9[391]. Ectopic overexpression of SIRT6 could upregulate Bcl-2 expression and decrease cleaved caspase-3 and Bax[404]. Knocking out SIRT4 confer to 5-FU chemoresistance via inhibiting cell apoptosis[405].
Differentiation	HDAC1, 2, 3	AML1/ETO can bind with HDAC1, 2 and 3 and recruit them to promoters of AML1 targeted genes in acute leukemia[406].
	HDAC3	PML-RARα could recruit HDAC3 as component of nuclear receptor corepressor (NCoR) complexes and repress gene expression program associated with hematopoietic differentiation[407].

		HDAC3 deacetylase activity and NCoR/HDAC3 complex were shown critical in regulating differentiation in rhabdomyosarcoma via blocking myoblast determination protein 1 (MYOD1)-mediated myogenic differentiation[408].
	HDAC6	HDAC6 depletion was shown to decrease cancer stem cells pluripotency and promote differentiation in tetratocarcinoma[409].
DNA-Damage Response	HDAC1, 2	HDAC1 and HDAC2 promote nonhomologous end-joining (NHEJ)[410]. HDACs were also reported to regulate proteins in DNA damage response, such as ATM, ATR, FUS, KU70, Rad52 etc.[411, 412].
	Class IIb HDACs (HDAC6, 10)	HDAC6 and HDAC10 have been shown to deacetylate DNA mismatch repair protein 2 (MSH2), leading to MSH2 ubiquitination and degradation and therefore impair mismatch repair[413, 414].
	SIRT1	SIRT1 was reported to interact with several DDR proteins, including KU70, APE1, XPA, PARP-1 etc.[371].
	SIRT6	SIRT6 was found to regulate base excision DNA repair[415] and contribute to the activation of PARP1 and therefore promotes both HR and NHEJ[416, 417].
Metastasis	HDACs	HDACs were found to silence epithelial markers and promotes epithelial-mesenchymal transition (EMT)[418-420].
	SIRT1	SIRT1 could be recruited to CDH1 promoter and regulate cell migration in prostate cancer cells[421, 422]. SIRT1 was also reported to inhibit metastasis via deacetylating Smad4 in breast epithelial cells and in oral squamous cell carcinoma[423, 424].
	SIRT2	SIRT2 is required for gastric cancer metastasis. SIRT2 inhibitor, SirReal2 could inhibit SIRT2 activity and decrease cell migration, which is associated with impaired mitochondrial metabolism and RAS/ERK/JNK/MMP-9[425].
	SIRT6	SIRT6 could promote EMT via interacting with Snail and through suppressing TET1 transcription by removing H3K9ac at its promoter regions[426].
Angiogenesis	Class I HDACs	upregulated in hypoxia and could interact with HIF-1α[427, 428], promote HIF-1α protein stability[429-431]. HDAC2 and HDAC3 act as co-repressor of VEGF[432].
	Class IIa HDACs	Increase HIF-1α transcription and repress pro-angiogenic genes[433, 434]. HDAC7 could repress matrix metalloproteinase10 (MMP10), therefore promote blood vessel development and vascular integrity maintenance[435, 436].

	Class IIb HDACs	HDAC6 regulates HIF-1α and VEGF and positively[437, 438] or negatively regulate angiogenesis[439].
	SIRT1	Deacetylates HIF-1α and inhibits its activity[440]. SIRT1 activation could downregulate VEGF expression and suppress angiogenesis in human osteosarcoma[441]. SIRT1 was also reported to decrease VEGF biological activity through promoting PAR modification of VEGF[442].
	SIRT6	SIRT6 was reported to exert anti-angiogenic effect by repressing the expression of VEGF and FGF-2 in endothelia cells[443].
Autophagy	HDAC1	Induce autophagic cell death by promoting accumulation of LC3-II in liver cancer cells[444]. HDAC3 could promote the expression and the activity of proteasome and induce autophagy[445].
	HDAC6	An important regulator of basal autophagic flux as well as a central component for ubiquitin proteasome system[409, 446], mitophagy[447] etc.
	HDAC10	HDAC10 could ensure efficient autophagosome-lysosome fusion and protect cells against cytotoxic drug in neuroblastomas[448].
	SIRT1	Directly deacetylates autophagy-associated proteins, including Atg5, Atg7, Atg8, and LC3 and contributes to the induction of autophagy[449-451]. Directly upregulate transcriptional level of autophagy associated proteins (e.g., LC3-II, beclin-1)[452, 453].
	SIRT3, 5	Trigger autophagy in osteosarcoma, mesothelioma, breast cancer, colorectal cancer, and diffuse large B cell lymphomas[454-457].
	SIRT6	Regulate autophagy in melanoma, esophageal cancer, hepatocellular carcinoma[458-461]. Required for the activation of the AMPK-ULK1-mTOR signaling in ROS triggered autophagy. Pharmacological activation of SRIT6 could confer to autophagy-related cell death in cancer cell lines[462].

READERS

As discussed above, histone modifications, especially acetylation and acylation signaling largely relys on readers and their impact on chromatin structure and gene transcription. Indeed, numerous studies depicted histone PTM readers as key players in oncogenic transcription program, chromatin structure regulations, DNA damage response, genome integrity. For example, BRD4 is well-known for its oncogenic role in regulating Myc transcription in diverse cancers[463]. In addition, YEATS domain-containing protein ENL, links histone acetylation to cancer-driving genes' expression (e.g., MYC, HOX) in acute leukemia as well as in Wilms tumor[120, 464-466]. Indeed, acetylation readers, predominantly including BET family members, have been extensively studied and exploited as therapeutic targets in various cancers.

BET

BET family proteins comprise of BRDT, BRD2, BRD3 and BRD4. Of them BRDT is exclusively present in the male geminal tissue, while the other three members are ubiquitously expressed in all tissues. BET family members share two tandem BrDs and C-terminal extra-terminal (ET) domain. BrDs of BET specifically bind acetylated histones, while the C terminal extended domain is involved in recruiting chromatin regulator factors. BRD4 was firstly characterized as a scaffold for transcription machineries, predominantly in association with elongation factors P-TEFb. It therefore promotes RNA Pol II - dependent transcription. Furthermore, BRD4 might have an intrinsic kinase activity, which can directly phosphorylates CTD Ser2 of RNA Pol II [467]. Besides, BRD4 is found as a cofactor of Mediator complexes, which integrates information from transcription factors and coactivators at enhancer regions to promoters and RNA polymerases, therefore regulates transcription initiation[468]. BRD4 was also shown to possess intrinsic acetyltransferase activity. It can acetylate H3K122 and contributes to nucleosome eviction and chromatin decompaction, therefore promoting transcription[469]. However, these properties of BRD4 were not reported by any other group and should be taken into account with caution. Functionally, BRD4 is involved in cell identity determination via accumulating on hyper-acetylated regions (both promoters and enhancers) as well as by regulating lineage specific transcription factors during embryonic development and cell differentiation. While in transformed cells, oncogenic role of BRD4 is represented by its impact on 1) the expression of key oncogenic factors; 2) the expression of cell identity program.

Oncogenic role of BRD4 was firstly investigated in NUT midline cancer. BRD4 gene could be translocated to NUT gene, generating a driver oncoprotein BRD4-NUT that blocks differentiation. Mechanistically, BRD4-NUT forms discrete nuclear foci that are enriched with p300 and acetylated histones dependent the BrDs of BRD4, which binds acetylated histones, and AD1 domain of NUT, which binds and activates p300. The BRD4-NUT chromatin foci sequester p300, which becomes depleted from the differentiation-associated genes, leading to

a global hypoacetylation and silencing of differentiation program in BRD4-NUT midline carcinoma[210, 470, 471].

Most studies on BRD4 in cancers, prominently in hematological malignancies are focusing on its role in regulating of MYC in various cancers. Targeting BRD4 via bromodomain inhibitors or protein degradation, selectively down-regulates MYC and MYC-dependent target genes, prompting cell-cycle arrest and repressing cell proliferation in multiple myeloma, Burkitt's lymphoma, acute myeloid leukemia, colorectal cancer, gastric cancer, bladder cancer etc.[472-476]. Interestingly, BRD4 was shown to directly phosphorylate MYC at Thr58, leading to MYC protein ubiquitination and degradation[477]. In addition to MYC, BRD4 also regulates other key oncogenic pathways. For example, BET inhibition disrupts the key oncogenic driver, Forkhead box protein M1 (FoxM1) and its down-stream pathway and leads to antitumor effect in ovarian cancer[478]. In prostate cancer, BRD4 could promote the expression of HOXB13, which is a lineage-specific transcription factor and maintains pro-proliferative network in castration resistance cells[479]. Besides, genomic profiling identified that BRD4 binds to cell type-specific enhancer regions and can activate STAT5 pathway in AML cells[480].

The functional specificity of BRD4 in mediating oncogene expression in cancer has been partly explained by its specific action on the super-enhancers (SEs). SEs are large clusters of enhancers featured by enriched transcription machineries and chromatin remodelers, possibly compartmentalized by liquid-liquid phase separation[481, 482], often marked by H3K27ac and H3K4me1, and lineage-specific transcription factors and oncogenic factors. The involvement of BRD4 in SEs has been characterized in multiple myeloma, where BRD4, Mediator, and P-TEFb were found to be enriched on SEs. Inhibition of BRD4 using BETi leads to loss of BRD4 preferentially at SEs, thereby disrupting SE - mediated oncogene expression including c-MYC in multiple myeloma[483].

Apart from acting as master regulator of transcription, BRD4 has also been implicated in RNA splicing, DNA damage response and telomere regulation[463]. BRD4 was found to interact with splicing machinery and to regulate alternative splicing[484, 485]. Several studies reported that BRD4 is required for DNA damage repair (e.g., NHEJ, HR) in cancer cells[486-488]. Mechanistically, BRD4 can be recruited by increased H4 acetylation that occurs at DNA double strand breaks and serves as platform for DNA repair machineries. BRD4 was found to interact with 53BP1 and might stabilize its binding with DNA repair complex at break sites[487]. In addition, BRD4 as discussed above, might have intrinsic acetyltransferase and kinase activities, which might acetylate or phosphorylate DNA repair proteins and regulate their functions[467, 481]. BRD4 could also positively regulate DNA damage checkpoint activation by interacting with components including DNA pre-replication factor CDC6, chromatin condensing II complex (SMC2) or by transcriptional regulation of damage response protein TopBP1[489-492].

Recently, BRD4 has been also implicated in telomere maintenance in cancer cells[493]. BRD4 was found to be involved in regulation of telomerase complex component TERT in TERT promoter mutated cancers[494, 495]. Inhibition of BRD4 with BET-inhibitors or genetic depletion of BRD4 reduces TERT expression in TERT promoter mutated cancers[496].

Other readers

In addition to BRD4, other readers have also been implicated in cancers. For example, BRD3 was also identified as fusion partner of NUT, with the fusion protein functioning similar to BRD4-NUT. BRD7 has been characterized as a tumor-suppressive factor in nasopharyngeal carcinoma, breast cancer, prostate cancer, etc[497]. Mechanistically, BRD7 can act as a coactivator of p53 and its target genes, thereby promoting p53-dependent senescence and suppresses tumorigenicity[498]. In breast cancer, BRD7 interacts with BRCA1 and regulates estrogen receptor gene expression [499]. Besides, it could decrease the expression of transcriptional activator YB1, therefore blocks epithelial-mesenchymal transition and tumor metastasis[500]. BRD9 is the subunit of SWI-SNF chromatin-remodeling complex. BRD9 plays an oncogenic role in acute myeloid leukemia (AML) and squamous cell lung cancer by regulating MYC transcription[501, 502]. YEATS domain-containing protein ENL has been implicated in leukemia and Wilms tumor, where it regulates oncogene expression (e.g., MYC, HOX) and the mediated oncogenic program[120, 464-466]. Another member of YEATS protein, GAS41 was found to bind H3K27ac, H314ac and to promote H2A.Z deposition. GAS41 is necessary for cell growth and survival in non-small cell lung cancer[122]. YEATS4 was reported to promote cell proliferation by activating Wnt/β-catenin in gastric cancer cells[503].

p300/CBP possesses both bromodomains, transcription binding domains as well as a acetyltransferase module. p300/CBP has been implicated as a critical mediator of histone marks in actively transcribed regions. p300/CBP bromodomain is required for sustaining cell type-specific gene expression, inhibition of bromodomain of p300/CBP decreases H3K27ac and chromatin accessibility at target genes, thereby accelerating induced pluripotent stem cells (iPSCs) cellular reprogramming[105].

2.2 Histone PTMs' therapeutic implications in cancer

Epigenetic drugs have been developed to target DNA/histone-modifying enzymes, histone readers, or other chromatin-associated proteins. Some of these drugs have displayed promising efficacy in treating cancers in research and in clinical usage. For example, DNMTi (azacytidine and decitabine) has been approved by US Food and Drug Administration (FDA) for treatment of myelodysplastic syndrome (MDS) or AML, and has achieved 15% response rate in these patients[504, 505]. Following DNMTi, a variety of epigenic drugs were developed, some had been

approved by US FDA and entered clinical trials or are still under research (**Table 6**). In general, there are three major classes of epigenetic drugs according to the enzymes they target and the potential mechanisms they exploit: 1) those who impact deregulated epigenetic profiles, including HDACi, DNMTi; 2) those who disrupt specific key oncogenes and oncogenic programs, represented by BETi, HDACi, DNMTi; 3) those that are exploited in specific cancer types, including DOT1Li, LSD1i. Epigenetic drugs have been tested either as monotherapy or in combination with additional epigenetic drugs or traditional chemotherapies to achieve therapeutic efficacy[204].

Here, I describe the therapeutic strategies by targeting epigenetic players and their working mechanisms in cancers.

2.2.1 Impact of deregulated epigenetic profiles in cancer establishment and develoment

As introduced above, cancer cells tend to have altered epigenetic profiles including DNA methylation and histone modifications. These changes, could on one hand directly deregulate the expressions of key oncogenes or tumor suppressors, and on the other hand allow for oncogenic genome reprogramming. A permissive chromatin state is required for oncogenic transcription factor activity and for the occurrences of mutations [506, 507]. Therapeutic strategies targeting the cancer-specific altered epigenetic profiles are well documented by the use of DNMTi (e.g., azacytidine, decitabine)[507]. In the case of HDAC, an increasing body of studies has focussed on the development and characterization of various generalist or class-specific HDAC inhibitors.

Over last decades, dozens of HDAC inhibitors have been evaluated on tumors, among which pan-HDACi Vorinostat (SAHA), belinostat and romidepsin have been approved for treating T cell lymphomas, and another pan-HDACi panobinostat was approved for treating refractory/relapsed multiple myeloma. Lately, more selective HDACi, for example, class I HDACs inhibitor entinostate (MS-275), HDAC1, 2, 3, 10 inhibitor chidamide have been developed.

HDACi have been tested as monotherapy or in combination with hypomethylating agents azacytidine, histone demethylating agents (named as KMTi hereafter) as well as chemotherapeutic regimens in cancer treatment[508]. In general, HDACi displayed higher efficacy in hematological malignancies than in solid tumors, possibly in part due to the short half-life of the molecules that prevent these agents to reach therapeutic concentrations in solid tumors[509].

HDACi could act at multiple levels given that they increase global histone acetylation and enhance chromatin decompaction. Additionally, they also act on numerous non-histone proteins[510]. It is clear that several studies have indicated that HDACi treatment efficacy could at least in part be attributed to its impact on chromatin landscape. For example, using ATAC-

seq technology, Qu and colleagues reported that clinical response to HDACi in cutaneous T cell lymphoma is associated with a gain in DNA accessibility[511]. In addition, using high-grade gliomas, which possess a reshaped chromatin landscape (i.e., loss of H3K27me3 and gain of H3K27ac) as models, Krug and colleagues demonstrated that DNA methyltransferases and histone deacetylase inhibitors could exaggerate the increased H3K27ac at and repeat elements, leading to their induced activation and thereby conferring to therapeutic vulnerability[512].

2.2.2 Epigenetic drugs regulate crucial oncogenic or tumor-suppressive signaling

In addition to their impact on global epigenetic pattern, HDACi or DNMTi could also exert anti-tumor functions by bringing about changes on specific oncogenes/tumor suppressors or oncogenic programs[513]. For instance, DNMTi azacitidine and decitabine causes robust demethylation of specific tumor suppressor gene promoters such CDKN2B, or global gene-specific demethylation concomitant with genome-wide DNA hypomethylation[514-516]. HDACi treatment resulted in differential expression of many oncoproteins (e.g., PI3-kinase catalytic subunit PI3KCB) and tumor suppressors (e.g., programmed cell death protein 4 PDCD4) in malignant B- and T- cell lines[517]. In addition, HDACi was reported to directly increase the acetylated c-Myc at K323 and hence regulating c-Myc mediated oncogenic program[518].

Epigenetic drugs (HDACi, KMTi and DNMTi) have also been documented to impact cell differentiation, metabolic reprogramming, cell immunity etc. For instance, Combination of LSD1/HDAC inhibitors increase H3K27ac and H3K4me1 and control differentiation-associated genes expression in diffuse intrinsic pontine glioma[519]. Treatment with DNMTi/HDACi was also reported to downregulate IRF4 and MYC and induce a gene expression profile of mature plasma cells in myeloma cells[520]. In the case of immune response, DNMTi treatment was reported to upregulate the expression of tumor associated antigens (e.g., surface marker of MHC, cancer testis antigens, etc.). In addition, DNMTi combined with HDACi was reported to induce interferon-α/β based transcription program and enhanced antigen presentation, accompanied by altered host immunity, therefore contributing to tumor immune cell invasion of non-small-cell lung cancers[521]. Epigenetic drugs could also facilitate metabolic reprogramming and therefore make the cancer cells sensitive to the corresponding treatment. For example, in glioblastoma models, HDACi treatment triggered metabolic reprogramming of cells with impaired glycolysis and enhanced oxidative phosphorylation, by suppressing c-Myc and increasing transcriptional drivers of fatty acid oxidation, PGC1α and PPARD[522]. Other regulators targeted by epigenetic drugs that are involved in the cell cycle, proliferation, apoptosis, angiogenesis etc. had been discussed in section **2.1.2** and are reviewed in[204, 523].

The most prominent epigenetic drugs that control oncogene expression is exemplified by BET factors bromodomain inhibitors (BETi). I have already mentioned that BETi inhibiting BRD4 disrupts BRD4-mediated SEs. BETis (e.g., birabresib, venetoclax, molibresib) have been tested in several small cohorts in solid and hematological tumors, where they achieved some responses in clinical studies. Preclinical studies also indicated that a combined treatment of BETi with additional epidrugs/other therapies including HDACi, CDKi, bcl2 inhibitors, hormone therapy, standard chemotherapy etc,.. could be advatageous.[524-526]. Additionally, BETi resistance have been reported in several researches, which had prompted investigators searching for specific combinatorial strategies[527, 528].

2.2.3 Epigenetic drugs targeting specific types of cancers

Some types of cancers are known to be driven by specific aberrations of epigenetic modifying enzymes (e.g., MLL rearranged leukemia), making them the most promising targets for treating the corresponding cancers. Small molecules inhibitors targeting interaction between MLL and Menin has been developed and has displayed effective anti-tumor effects in MLL-rearranged leukemia cells and in mouse models[529]. DOT1L is aberrantly regulated in MLL-rearranged leukemia and is required for leukemogenesis of this cancer subtype, small molecules inhibitors targeting DOT1L were shown to be effective in MLL-rearranged leukemia [530-532].

In addition, inhibitors of LSD1 are active in a subset of small cell lung carcinoma with specific DNA methylation patterns[533]. In AML, LSD1i displayed antileukemic effect through enhancing PU.1- and C/EBPα - dependent differentiation program in MLL-AF9 leukemia cells[534]. IDH mutations have been identified and characterized as key oncogenic events in glioma, leukemia etc…. In these cases, IDH inhibitors could be used as a targeted therapy [535, 536]. EZH2 gain of function mutations have been identified in lymphoma, and the inhibition of EZH2 exerted cytotoxic effects in cancer cells carrying these mutations[208, 537, 538].

Of note, the situation could be very complex and it is not always easy to define a precise therapeutic strategy based on the use of epidrugs. For example, DOT1L inhibition could also lead to the deregulation of oncoproteins including Myc, which can be detrimental in a variety of cancers[539-542].

Table 6. Epigenetic drugs .

Compound	Target	Cancer type	Phase
Azacitidine	DNMT	MDS	EMA and FDA
Decitabine	DNMT	AML, MDS	EMA and FDA
Guadecitabine	DNMT	AML	Phase III
Belinostat	HDAC class I and II	Peripheral T cell lymphoma	FDA
Panobinostate	HDAC class I, II and IV	Multiple myeloma	FDA
Romidepsin	HDAC class I	Cutaneous T cell lymphoma	FDA

Vorinostat	HDAC class I, class II and class IV	Cutaneous T cell lymphoma	FDA
Abexinostat	HDAC class I, class II and class IV	Lymphoma (DLBCL, FL, MCL) , advanced solid tumor	Phase I and phase II
ACY-241	HDAC6	Multiple myeloma	Phase I
AR-42	HDAC class I, class II and class IV	Haematological malignancies	Phase I
CUDC-907	HDAC class I and class IIb	Solid tumours and haematological malignancies	Phase I
CXD101	HDAC class I	Solid tumours and haematological malignancies	Phase I
Entinostat	HDAC class I	Breast cancer	Phase III
Givinostat	HDAC class I and class II	Haematological malignancies	Phase II
Mocetinostat	HDAC class I	Solid tumours and haematological malignancies	Phase II
Resminostat	HDAC1, HDAC3 and HDAC6	Hepatocellular carcinoma	Phase II
Ricolinostat	HDAC6	Solid tumours and haematological malignancies	Phase II
CPI-0610	Pan-BET	R/R lymphoma	Phase I
TEN-010	Pan-BET	AML, MDS and solid tumours	Phase I
BAY1238097	Pan-BET	Solid tumours and lymphomas	Phase I
OTX015	Pan-BET	Acute luekemia, R/R lymphoma or MM, NSCLC, NMC, CRPC, recurrent glioblastoma	Phase I and phase II
INCB054329	Pan-BET	Leukaemias and solid tumours	Phase I and phase II
BMS-986158	Pan-BET	Solid tumours	Phase I and phase II
FT-1101	Pan-BET	AML and MDS	Phase I
GSK525762	Pan-BET	R/R AML	Phase I
PLX51107	Pan-BET	Advanced solid tumors	Phase I
ABBV-075	Pan-BET	R/R AML and R/R solid tumors	Phase I
AG-881	Pan-IDH1/2 mutant	Glioma with IDH mutations	Phase I
AG-120	IDH1 mutant	Advanced solid tumors with IDH1 mutations, including including cholangiocarcinoma, chondrosarcoma, and glioma	Phase I
IDH305	IDH1 mutant	Grade II or III gliomas with IDH1 mutations that have progressed after observation or radiation therapy.	Phase II
AG-221	IDH2 mutant	Advanced solid tumors with IDH2 mutations, including glioma, angioimmunoblastic T cell lymphoma,	Phase I and phase II

		intrahepatic cholangiocarcinoma, chondrosarcoma.	
BAY1436032	IDH1 mutant	Solid tumors with IDH1 mutations	Phase I
DS-3201b	EZH2	R/R NHL	Phase I
CPI-1205	EZH2	R/R B-cell lymphomas	Phase I
EPZ-6438 (Tazemetostat)	EZH2	Lymphomas	Phase I and phase II
GSK2816126	EZH2	R/R DLBCL, tFL, other NHL, solid tumors, and MM	Phase I
EPZ-6438 combined with prednisolone	EZH2	B-cell lymphoma, advanced solid tumors, DLBCL, FL, tFL, PMBL	Phase I and phase II
GSK2879552	LSD1	AML and small-cell lung cancer	Phase I and phase II
EPZ-5676	DOT1L	R/R MLL-rearranged leukaemias	Phase I
Abbrevations: AML: acute myeloid leukemia; MDS: myeodysplasic syndrome; MM:multiple myeloma; NHL: non-Hodgkin lymphoma; R/R relapsed/refractory; DLBCL: difuse large B cell lymphoma; MCL: mantle cell lymphoma; FL: follicular lymphoma; tFL: transformed FL; NSCLC: non small cell lung cancer; NMC: NUT-midline carcinoma; CRPC: castration-resistant prostate cancer; IDH: isocitrate dehydrogenase; PMBL: primary mediastinal large B-cell lymphoma.			

Note: This table is adapted from [507, 543].

3. Cell metabolism is a major driver of histone modifications

As noted above, histone PTMs are dynamic and are constantly regulated by counteracting enzymes designated as writers and erasers. Most of these enzymes utilize metabolic cofactors to exert their catalytic reactions. This situation hence creates a tight interplay between cell metabolism and histone modifications. For instance, KMTs, PRMTs and DNMTs utilize SAM, KATs utilize acetyl-CoA or acyl-CoA, and kinases utilize ATP respectively as co-substrates to transfer the chemical moieties to DNA or to the amino acid residues of histones. In contrast, JmjC family demethylases (JMJD or JHJM for short) require α-ketoglutarate, SIRT family deacetylases require NAD as cofactors to remove the modifications.

In this chapter, I will introduce the compartmentalization and maintenance of several key epimetabolites pools, as well as the biochemical pathways that generate or consume these molecules. I will also give examples of how these metabolites change in response to nutritional perturbations and how they impact histone modifications. Finally, I will briefly discuss how the resultant epigenetic alterations regulate nuclear gene transcription programmes, which in turn impact other biological processeses such as cell fate determination.

3.1 SAM

3.1.1 One-carbon metabolism

S-adenosylmethionine (SAM) is involved in the methionine cycle (**Figure 17**). SAM is synthesized from methionine and ATP, a reaction which is catalyzed by methionine adenosyltransferase (MAT). After the methyl group is transferred for methylation usage, SAM is converted to S-adenosyl homocysteine (SAH), which then is hydrolyzed to homocysteine (hCys) and adenosine by SAH hydrolase (SAHH). Homocysteine is then remethylated and converted back to methionine by vitamin B12-dependent methionine synthase (MS) using 5-methyl-tetrahydrofolate (5-mTHF, MTHF) as methyl group donor or alternatively, in the case of liver, by betaine homocysteine methyltransferase (BHMT) with the production of dimethylglycine (DMG).

Methionine cycle is fueled by the folate cycle. 5-mTHF in folate cycle donates its one-carbon methyl group to homocysteine. After transferring the methyl group, 5-mTHF is converted to THF. THF is then used to produce 5,10-meTHF by receiving methyl group from serine, which subsequently is converted to glycine by serine hydroxymethyltransferase (SHMT). This reaction that converts serine to glycine is reversible. The last step to complete folate cycle is to convert 5,10-meTHF back to 5-mTHF via NADPH-dependent catalysis acted by 5,10 methylenetetrahydrofolate reductase (MTHFR).

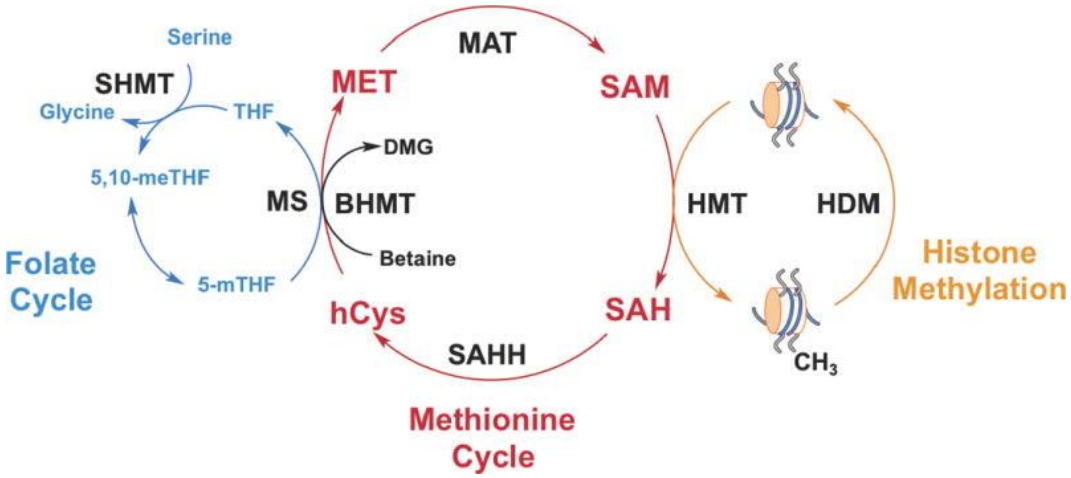

Figure 17. One carbon metabolism.

The methionine cycle (red, middle) can provide methyl group in the form of SAM to fuel biochemical reactions, such as histone methylation (yellow, right). The methyl group in the methionine cycle is provided by the folate cycle (blue, left). The main donor of the above one-carbon unit is serine. SAM: S-adenosylmethionine; MAT: Methionine adenosyltransferase; SAH: S-adenosyl homocysteine; SAHH: SAH hydrolase; hCys: homocysteine; MS: methionine synthase; MET: methionine; THF: tetrahydrofolate; 5-mTHF: 5-methyl-tetrahydrofolate; BHMT: betaine homocysteine methyltransferase; 5;10-meTHF: 5;10; methylenetetrahydrofolate. From[544].

3.1.2 SAM in histone methylation

SAM is the methyl donor for histone and DNA methylation processes. As co-product of methylation reaction, SAH is a potential inhibitor of methyltransferases. Thus, the level of SAM and the ratio of SAM/SAH tunes the methylation state of chromatin. Indeed, the modulation of SAM levels and SAM/SAH ratio through changes of methionine supplementation affects global DNA/histone methylation status, with H3K4me3 displaying the most prominent change. ChIP-seq analysis of H3K4me3 revealed that only the level of this mark but not the genomic distribution altered upon methionine restriction. This correlation between H3K4me3 level and methionine availability was observed both in cell line and in the mice liver[545]. SAM generation and SAM/SAH ratio maintained by glucose and serine metabolism were also suggested to support H3K36me3, which mediates IL-1β production for inflammation response in macrophages[546].

3.1.3 Methionine supplement

As an essential amino acid, *methionine* can be absorbed from the environment and not surprisingly, its intracellular level is affected by amino acid transporter (e.g., LAT1). Knockdown of LAT1 results in methionine as well as SAM reduction, which is concomitant with decreased H3K27me3, H3K4me and H4K20me marks[547]. In addition to the uptake of methionine, dietary intake of other nutrients that participate in SAM production and maintenance (e.g., SAM, folic acid, vitamin B12, Choline and its metabolite, betaine) might modulate histone methylation[548, 549].

3.1.4 Serine metabolism

Serine synthesis pathway (SSP) starts with the glycolytic intermediate 3-phosphoglycerate (3-PG) being converted to 3-hydroxypyruvate by phosphogycerate dehydrogenase (PHGDH). 3-hydroxypyruvate is then used to produce phosphoserine through a transamination reaction catalyzed by phosphoserine aminotransferase (PSAT1), phosphoserine is dephosphorylated by phosphoserine phosphatase (PSPH) and produces serine[550].

Since serine is a one-carbon source that contributes to folate cycle, serine metabolism can impact SAM production and might regulate histone methylation. In addition, serine can support de novo ATP synthesis, which is required for SAM production from methionine[551]. Indeed, elevated serine synthesis pathway mediated by loss of LKB1 leads to high SAM level through upregulation of PSAT1 and PSPH, which results in DNA hypermethylation[552, 553].

3.1.5 SAM compartmentalization

In addition to the global intracellular level, the subcellular compartmentalization of SAM also impacts histone methylation because of different accessibility to the chromatin-modifying enzymes. For example, SAM was found in the nuclear compartment in yeast and was suggested to control specific gene expression. Li and colleagues identified that, in yeast, SESAME (Serine-responsive SAM-containing Metabolic Enzyme complex) interacts with Set1 and is recruited to target genes[554].

3.2 Acetyl-CoA

3.2.1 Production and utilization of acetyl-CoA

Acetyl-CoA can be produced in mitochondrion, cytoplasm and nucleus and are generated from diverse nutrient sources, including pyruvate, fatty acid, amino acids, acetate, and citrate (**Figure 18**).

In mitochondrial compartment, pyruvate generated from glycolysis enters into mitochondrion and is converted to acetyl-CoA by pyruvate dehydrogenase complex (PDC). Acetate is ligated to CoA by acyl-CoA synthetase short-chain family members 1 and 3 (ACSS1/3). Fatty acids undergo β-oxidation through rounds of dehydrogenation, hydration, dehydrogenation and thiolase, producing one acetyl-CoA and one fatty acyl-CoA (with a reduction of 2C) during each round. Amino acids (e.g., tryptophan, lysine, phenylalanine, tyrosine etc.) can be converted to acetoacetyl-CoA and acetyl-CoA through multiple steps. Acetyl-CoA generated in mitochondrion enters into tricarboxylic acid (TCA) cycle and is completely oxidized, releasing ATP through coupling with oxidative phosphorylation.

For the moment there is no known acetyl-CoA carrier in the mitochondrial membrane, therefore acetyl-CoA must be converted to citrate before it shuttles to cytoplasm. Acetyl-CoA and oxaloacetate are then regenerated in cytosol by ATP citrate lyase (ACLY). Another source of acetyl-CoA outside of mitochondrion is through acetyl-CoA synthase (AceCS1/ACSS2), which is located in cytosol/nucleus and uses acetate as substrate. In addition, PDC can be translocated to nucleus, where it can produce acetyl-CoA for nuclear usage. Acetyl-CoA in cytoplasm and nucleus is used for histone and non-histone protein acetylation as well as *de novo* fatty acid and cholesterol biosynthesis.

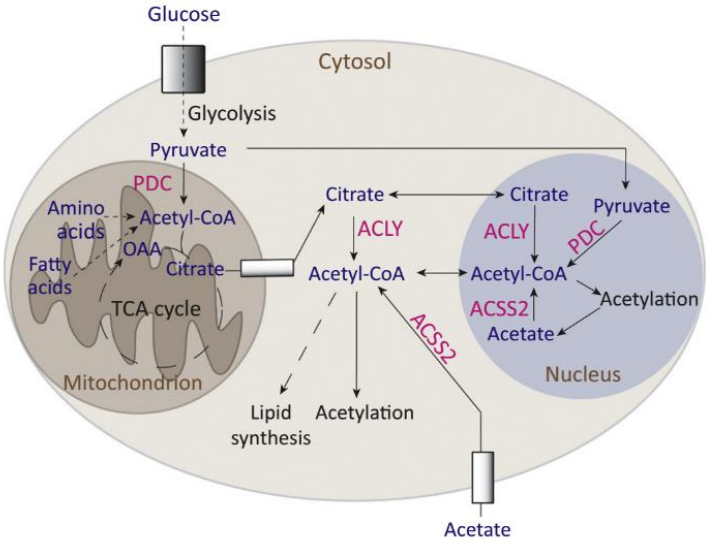

Figure 18. Production and utilization of acetyl-CoA.

Acetyl-CoA can be produced in mitochondrion, cytosol and nucleus. Acetyl-CoA produced in mitochondrion can be exported to cytosol in the form of citrate, where it is converted back to acetyl-CoA under the reaction of ACLY. In addition, ACSS2 can generate acetyl-CoA from acetate in cytosol and in nucleus. PDC can be translocated to nucleus, where it produces acetyl-CoA from pyryvate. ACLY: Acetyl-CoA lyase; ACSS2: Acetyl-CoA synthase; PDC: Pyruvate dehydrogenase complex. From[555].

3.2.2 Acetyl-CoA links cellular metabolism to histone acetylation

Undoubtedly, acetyl-CoA availability dictates histone acetylation level *in vitro*. It is well-documented that this also applies to intracellular situation. In mammals, concentration of acetyl-CoA ranges approximately 2-20 μM in cultured cells depending on nutrient availability[556]. The cellular acetyl-CoA is likely also available in the nucleus as it can be judged by the occurrence of nuclear histone/protein acetylation. Given that Michaelis constant (Km) of KATs for acetyl-CoA are micromolar [557, 558], fluctuation of acetyl-CoA might indeed impact the catalytic activity of KATs and the resultant histone acetylation under the physiological condition. Besides, the ratio of acetyl-CoA:CoA was suggested to modulate KATs activity and histone acetylation levels, as the reaction product of CoA can act as an inhibitor of KATs[556].

Acetyl-CoA pool for histone acetylation is replenished by various nutritional sources. Glucose is one of the major sources that fuels cell growth of tumor cells. A large body of evidence suggests that glucose derived acetyl-CoA is the major driver of histone acetylation during cell proliferation. Consistently, limitation of glucose or inhibition of glycolysis leads to decreased acetyl-CoA production and hence histone acetylation[559-561]. However, when supplied with medium-chain fatty acid, McDonnell and colleagues reported that lipid-derived acetyl-CoA contributes to 90% of certain sites of histone acetylation, even supplied with abundant glucose. Considering that fatty acid oxidation occurs in mitochondria, theoretically, the generated acetyl-CoA needs to be exported from mitochondria via citrate shuttle in order to be

used for histone modification in the nucleus. However, in the above-mentioned experimental setting, the knock down of ACLY and ACSS2, did not affect the increased histone acetylation by octanoate supplement, suggesting that the fatty acids derived acetyl-CoA might be exported through a yet unknown major pathway different from the citrate cycle[562]. In addition, in the case of ACLY deficiency, acetate was found to compensate for acetyl-CoA production through upregulation of ACSS2, which supported histone acetylation and lipid synthesis[563]. These studies, in addition to documenting metabolic adaptation, also implicate a delicate choice of priority for metabolites contributing to histone acetylation, and have raised the question of whether there are other undetermined possibilities for transporting acetyl-CoA across subcellular compartments (e.g., acetylcarnitine-carnitine system)[564, 565].

Acetyl-CoA pool homeostasis for histone acetylation is sustained by catabolic and anabolic metabolism. In addition to protein acetylation, intracellular acetyl-CoA can also be consumed in TCA cycle or serve as building blocks for lipid biosynthesis, therefore perturbation of mitochondrial respiration and lipid synthesis might in turn impact protein acetylation by competing with the usage of acetyl-CoA. Inhibition of acetyl-CoA carboxylase expression, which catalyzes the first and rate-limiting step of fatty acid synthesis, results in increased acetyl-CoA available for histone acetyltransferases and enhances histone acetylation[566, 567]. Yucel and colleagues reported that compared to proliferating muscle stem cell (MuSCs), quiescent and differentiated MuSCs have elevated utilization of glucose and acetyl-CoA for mitochondrial respiration, and therefore have decreased acetylation[568]. Conversely, using mitochondrial DNA mutated cell model, and inhibition of mitochondrial translation, Kopinski and colleagues identified that decrease of mitochondrially derived acetyl-CoA causes a reduction in histone H4 acetylation[569].

The signaling between metabolic state and histone acetylation via acetyl-CoA can rewire the transcriptional program in response to nutrient availability. For example, in adipocyte, expression of glucose transporter gene GLUT4 is dependent on glucose and ACLY, which fuels acetyl-CoA production and histone acetylation at Slc2a (encoding GLUT4) locus, suggesting a positive feedback between glucose metabolism and gene expression[570]. Under hypoxic stress, acetyl-CoA produced from acetate induces H3 hyperacetylation at the promoter regions of ACACA and FASN genes and therefore enhances lipid synthesis[571].

Of note, evidences began to flourish uncovering that acetyl-CoA concentration alterations can impact specific sets of genes and therefore could contribute to cell fate and cell functioning[560]. For example, toll-like receptor activation induces glycolytic flux and ACLY activation, which enhances acetyl-CoA production and histone acetylation, thereby facilitating the transcription of LPS (lipopolysaccharide) -inducible gene sets[572]. During the muscle regeneration process, glucose metabolism program determines histone acetylation profile, which dominates stem cell and cell-cycle genes transcription and cell functioning[568]. In

glioblastoma cells, ACSS2 is phosphorylated and translocated into nucleus, where it binds with transcription factor EB (TFEB) and enhances lysosomal and autophagy-related gene expression via recycling acetate and providing acetyl-CoA to TFEB targeted gene promoters[573]. The above examples demonstrate the crucial role of cellular metabolism in determining cellular phenotypes and point to epigenetic metabolites as potential targets for therapeutic usage. One key question arises as how the level of acetyl-CoA impacts histone acetylation at specific loci and regulates specific sets of genes. Campbell and Wellen summarized two possibilities that explain this issue[560]: **1)** spatiotemporal regulation of acetyl-CoA production (i.e., spatiotemporal control); and **2)** transcription factor ability to respond to acetyl-CoA concentrations.

2.2.3 Spatiotemporal control of acetyl-CoA

The cytoplasm and nucleus are likely to constitute a single compartment with respect to acetyl-CoA, because of the existence of nuclear pores that are large enough for small molecules to pass through. This supposition implies the occurrence of an interplay between nuclear and cytoplasmic acetyl-CoA pool. Recent evidences, however, suggest that acetyl-CoA may not exchange freely between nuclear and cytoplasmic compartments. Mammalian cells are filled with macromolecules (e.g., protein concentration range from 50 to 250g/L, nucleic acid 20-50g/L), and these molecules are not homogenously distributed and could cause macromolecular crowding, therefore the diffusion of molecules might be largely perturbed especially between sites that are spatially far away[574]. This principle points to the possibility of a local compartmentalization in nucleus where small metabolites are generated close enough to where they are consumed (onsite generation)[575]. To this end, PDC, ACLY and ACSS2 have been found to be present in nucleus. For example, under oxygen and serum limitation, nuclear ACSS2 can capture acetate released from histone deacetylation to maintain histone acetylation[576]. In neuronal cells model, Mews and colleagues have identified that ACSS2 increases in the nucleus of differentiating neurons and is recruited to chromatin, where it directly regulates histone acetylation and controls memory-related neuronal genes expression[577]. ACLY was found to be phosphorylated in response to DNA damage, whereby it orchestrates acetyl-CoA production and enables H4 acetylation near DNA double-strand breaks, therefore enhances BRCA1 mediated homologous recombination of DSB repair[578]. PDC was found to be translocated from mitochondrion to nucleus in response to serum, growth factor, or mitochondrial stress and in a cell-cycle-dependent manner, where it catalyzes synthesis of acetyl-CoA for acetylation of core histones[579]. In mammals, nuclear PDC accumulation was found to be crucial and indispensable for zygotic gene expression by maintaining histone acetylation[580]. The spatiotemporal control of epimetabolites has yielded an exciting perspective for metabolic signaling to epigenome and gene regulation specificity. More comprehensive studies are needed to address the current

questions, such as the existence of microcompartments for metabolites, the molecular mechanism of nuclear translocation of acetyl-CoA producing enzymes. It is also important to identify proteins that interact with metabolite-producing enzymes and understand how cells sense environmental cues and initiate the process of enzyme translocation etc.[555].

2.2.4 Transcription factors mediating specific sets of genes expression in response to acetyl-CoA concentration alteration

Increasing evidence indicate that acetyl-CoA abundance can impact gene transcription via the regulation of transcription factors.

Firstly, transcription factors per se can be acetylated, which might consequently impact its subcellular location, protein stability and trans-activating capacity. For example, elevated acetyl-CoA levels resulted from ACC1 inhibition induces Smad2 acetylation, which then translocates into the nucleus and activates Snail and Slug mediated epithelial-mesenchymal transition program and promotes cancer invasion[567].

Similarly, in chondrocyte, inhibition of ACLY reduces acetylation of p65, NF-κB and H3K27, which attenuate IL-1β induced gene transcription. Besides, under these conditions SOX9 acetylation is reduced, promoting its nuclear localization and increasing the mRNA level of aggrecan and Col2a1[581].

Secondly, transcription factors can be regulated by acetyl-CoA levels through an indirect mechanism. For example, a change of acetyl-CoA abundance regulates H3K27ac at specific loci correlated with integrin signaling and cell adhesion. This pathway participates to the modulation of calcium signalings, which trigger nuclear translocation of the transcription factor NFAT1 (nuclear factor of activated T cells), where it mediates acetyl-CoA dependent genes transcription[582].

Thirdly, acetyl-CoA can regulate specific sets of genes through transcriptional coregulators. For instance, BET family proteins which read acetylated lysine can recruit Mediator complex and regulate a set of genes which are dependent on locus control regions[463]. In leukemia cells, acetyl-CoA reduction mediated by AMPK depletion can reduce BET-dependent gene expression program by decreasing histone acetylation and therefore displacing BET protein from chromatin[583].

3.3 Acyl-CoAs

Similar to acetyl-CoA, acyl-CoAs are key factors linking cellular metabolism to chromatin regulations. Recent studies documented that many HATs (e.g., p300/CBP, GCN5) can also utilize acyl-CoAs to generate respective histone modifications, and that the concentrations of

acyl-CoAs are correlated with the level of respective histone acylations. However, while acetyl-CoA metabolism and compartmentalization are extensively studied, the process of acyl-CoA metabolism and their signaling to chromatin modifications remain poorly understood. From a biochemical point of view, non-acetyl acyl-CoAs are generated during lipid metabolism, amino acid catabolism, ketogenesis and can be directly converted from short chain fatty acids provided by intestinal microbiota fermentation. It is postulated that, since many of the biochemical processes generating acyl-CoAs occur in mitochondrion, the export of these metabolites is needed for nuclear usage, via yet unknown mechanisms. Similar to the compartmentalization of acetyl-CoA, the production and maintenance of acyl-CoAs in cytoplasmic and nuclear compartments could also exist, but this is in need of further studies.

Here I will introduce the metabolic pathways involving acyl-CoA generation. I will emphasize on the current evidences about their role in histone acylations. I will discuss the possible mechanisms contributing to compartmentalization and enabling their nuclear availability. Finally, I will also give examples of their functional output considering chromatin-based biological events.

3.3.1 Lipid metabolism

Many acyl-CoAs are present as intermediates in lipid metabolism, including β-oxidation, fatty acid and *cholesterol synthesi*s.

Fatty acid uptake is coupled with CoA esterification by acyl-CoA synthetases (ACSs) known as lipid activation. This reaction consumes energy leading to ATP breakdown to AMP and pyrophosphate (PPi). ACSs present several members, who have specificity for different lipids depending on the carbon-chain of lipids, namely, long chain specific acyl-CoA synthetases (ACSL), medium chain acyl-CoA synthetases (ACSM), and short chain acyl-CoA synthetases (ACSS). ACSL is associated with outer membrane of mitochondria, peroxisomes and endoplasmic reticulum, and ACSM are located in mitochondrial matrix while ACSS can be found both in mitochondrial matrix or cytosol.

In mammals, both peroxisome and mitochondria ensure lipid oxidation but with separate enzymatic systems and have distinct features. Some types of lipids such as very long chain fatty acids (VLCFA), branched-chain fatty acids, bile acid intermediates and long chain dicarboxylic acids are poorly taken up by mitochondrion and are mainly degraded in peroxisome. However, peroxisome β-oxidation only generates shortened fatty acids (i.e., medium chain acyl-CoA, C6-8), while mitochondrion can proceed complete oxidation of lipids[584].

Long chain fatty acyl-CoA cannot penetrate mitochondrial membrane and must be assisted by carnitine-acylcarnitine shuttle system. The acyl group of fatty acyl-CoA is transferred to carnitine at the outer membrane catalyzed by carnitine palmitoyl-transferase I (CPT I), acyl-

carnitine can then cross the membrane through carnitine translocation catalyzed by carnitine-acyl-cartnine translocase (CACT). Acyl-carnitine is then converted back to acyl-CoA and carnitine at the inner membrane by carnitine palmitoyl-transferase II (CPT II). In contrast, medium (C6-12) and short chain (C4-6) can directly enter mitochondrial and are then activated to the corresponding acyl-CoAs in mitochondrial matrix.

β-oxidation process proceeds as repetitive cycles of four reactions, namely 1) dehydrogenation, which introduced double bond between α and β carbon, 2) hydration which add water molecules and breaks the carbon double bond, 3) dehydrogenation, which dehydrogenate 3-hydroxyacyl-CoA to 3-ketoacyl-CoA, and 4) thiolation which cleaves the bond between α and β carbon in the presence of CoA, producing one acetyl-CoA and a shortened acyl-CoA (Figure 19). Acetyl-CoA produced here can then enter TCA cycle for complete oxidation. These reactions are catalyzed by acyl-CoA dehydrogenase, enoyl-CoA hydratase, 3 (β)-hydroxyacyl-CoA dehydrogenase, 3-ketoacyl-CoA thiolase (acyl-CoA acetyltransferase) respectively. In mammals, the first step of β-oxidation is catalyzed by several dehydrogenase, with (very) long chain acyl-CoA dehydrogenase ((V)LCAD) catalyzing C12-24, medium chain acyl-CoA dehydrogenase (MCAD) catalyzing C6-12, and short chain acyl-CoA dehydrogenase (SCAD) catalyzing C4-6. The last 3 steps of LCFAs and MCFAs are mainly catalyzed by mitochondrial trifunctional proteins (MTP, or TFP abbreviated), while SCFAs are catalyzed by ECHS, HADH and KAT respectively[585].

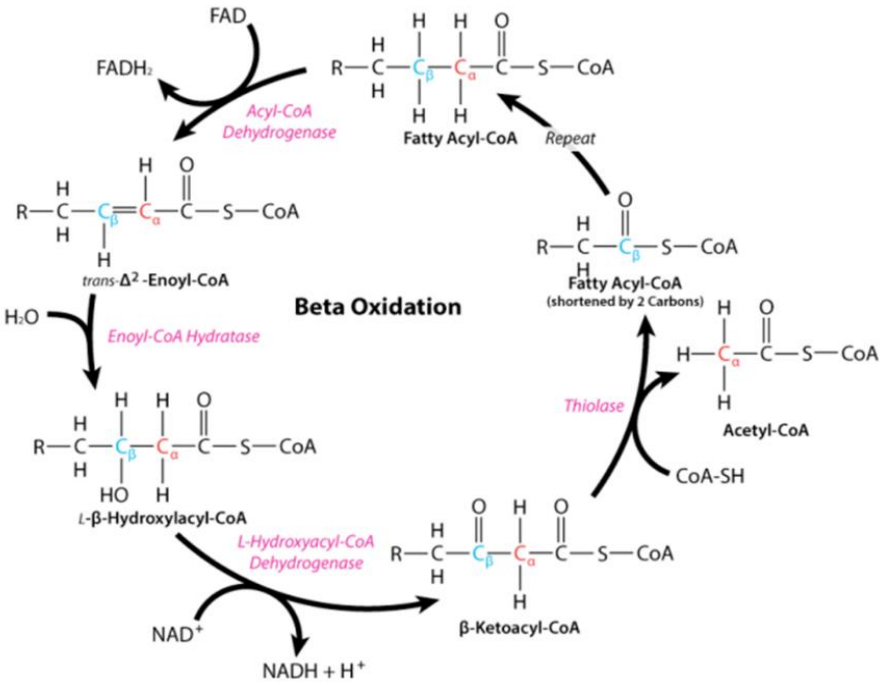

Figure 19. β-oxidation.

β-oxidation spiral contains dehydrogenation, hydration, dehydrogenation and thiolation. Through each round of β-oxidation, a acetyl-CoA and a shortened acyl-CoA (-2C) are produced.

From (bio.libretexts.org/Bookshelves/Biochemistry/Book%3A_Biochemistry_Free_and_Easy_(Ahern_and_Rajagopal)/06%3A_Metabolism_I_-_Oxidative_Reductive_Processes/6.11%3A_Fatty_Acid_Oxidation)

Even chain FA can produce butyryl-CoA while odd chain FA produces propionyl-CoA through β-oxidation. Propionyl-CoA can be further converted to methylmalonyl-CoA catalyzed by propionyl-CoA carboxylase (PCC), and then to succinyl-CoA through several reactions. Crotonyl-CoA can be produced from butyryl-CoA by SCAD, and the crotonyl-CoA could further be converted to L (S)-β-hydroxybutyryl-CoA through enoyl-CoA hydratase in β-oxidation.

Fatty acid synthesis (FAS) occurs in the cytoplasm or mitochondrion (mtFAS) and the chemical reactions are reversibly similar to β-oxidation except a few differences. Chemical reaction of *de* novo FAS starts with two acetyl-CoA forming malonyl-CoA catalyzed by acetyl-CoA carboxylase (ACC). Malonyl-CoA then forms malonyl-ACP (acyl-carrier protein), which then becomes fatty acyl-ACP, following the addition of two carbons to the growing chain of fatty acyl-ACP during each cycle of fatty acid synthesis. The carbon chains of fatty acyl-ACP keep growing by rounds of condensation, reduction, dehydration, and reduction until it reaches 16 or 18. The three differences between FAS and FAO are, 1) ACP is used for stabilizing acyl esters; 2) NADPH instead of NAD system is used; 2) D (R)-form rather than L (S) enantiomers are generated during the spiral. In mammals, cytoplasmic FAS is catalyzed by a single complex called fatty acid synthase (FASN), comprising of 6 catalytic subunits and an ACP. mtFAS was firstly characterized in yeasts where it mainly produces octanoate and then converted to lipoic acid, which is an important cofactor for a number of mitochondrial enzymes. In mammalian cells however, mtFAS is less characterized[586].

Evidences suggests that lipid metabolism might be an important source of acyl-CoA for histone acylations. For instance, crotonate supplementation can stimulate histone crotonylation, which is due to the increased conversion to acyl-CoA by ACSS2[144, 587]. Depletion of PCC, which consumes propionyl-CoA, causes an increase in propionyl-CoA and histone propionylation (H3K14pr) in mouse livers. However, SCAD knockout mice did not show increased H3K14bu, although an increase of butyryl-CoA and non-histone protein butyrylation were observed in liver cells[169]. Using highly synchronized yeast metabolic cycle, Gowans and colleagues reported that histone crotonylation coincides with expression of genes in β-oxidation in the metabolic cycle[170]. In mitochondrion, short chain acyl-CoA can be converted to acyl-carnitine by carnitine acetyltransferase (CrAT), indicating the possibility of acyl-CoA being exported out of mitochondrion and this could support its export and the subsequent histone propionylation[588]. Lately, Choi and colleagues identified that many FAO enzymes including ACSL1, HADHA and ACAA2 are located in the nucleus, implicating the generation of acyl-CoA in nuclear compartment[589]. Besides, the cytosolic FAS process and peroxisomal FAO are two other

possibilities to fuel cytocylic/nuclear compartment of acyl-CoA pools. For example, succinyl-CoA, succinate and glutarate might be produced through dicarboxylic metabolism in peroxisome[590]. Fang and colleagues observed that the expression of peroxisomal acyl-CoA oxidase ACOX3 is increased during endoderm differentiation of embryonic stem cells, which along with other crotonyl-CoA producing enzymes (e.g., ACSS2) enhances histone crotonylation and control the gene expression program of endodermal differentiation[587].

3.3.2 Ketogenesis, TCA cycle and amino acid catabolism

Ketogenesis occurs in the mitochondria of liver cells triggered by glucose depletion conditions such as fasting. The reaction starts with two molecules of acetyl-CoA being converted to acetoacetyl-CoA by thiolase, which is then modified by an additional acetyl-CoA molecule and generates hydroxylmethylglutrayl-CoA (HMG-CoA) by HMG-CoA synthase. HMG-CoA lyase then cleaves HMG-CoA and produces acetoacetate. Acetoacetate either makes acetone through non-enzymatic decarboxylation or D (R)-β-hydroxybutyrate catalyzed by β-hydroxybutyrate dehydrogenase.

The contribution of ketogenesis to histone acylations is documented in several studies. For example, mice liver cells exhibited higher intracellular acyl-CoA levels and increased histone butyrylation, β-hydroxybutryrylation after fasting[141, 591]. It is worth noting that ketone bodies might contribute to histone modifications through increased acyl-CoA generation or through directly inhibiting HDAC activity. β-hydroxybutyrate, as well as other short chain fatty acids (e.g., butyrate) which is predominantly produced by intestinal microbiota, are known as HDAC inhibitors[592, 593].

TCA cycle links acetyl-CoA oxidation with energy production, which is coordinated by several metabolic intermediates including oxaloacetate, citrate, isocitrate, α-KG, succinyl-CoA, succinate, fumarate, malate. Succinyl-CoA is generated from α-KG, which is catalyzed by α-ketoglutarate dehydrogenase (α-KGDH) and is hydrolyzed to succinate by succinyl-CoA synthetase. The resultant succinate can subsequently be converted to fumarate by succinate dehydrogenase (SDH).

Although succinylation occurs prominently on mitochondrial proteins through non-enzymatic reaction, recent studies revealed that histones and extramitochondrial non-histone proteins could also be succinylated. Indeed, TCA cycle enzymes have been suggested to impact histone succinylation. For example, it is documented that SDH depleted MEF cells, which have TCA cycle defect, displayed higher intracellular succinyl-CoA concentration and increased histone succinylation[594]. In addition, α-KGDH complex was found to be present in nucleus where it produces succinyl-CoA for chromatin succinylation[151, 589].

Succinyl-CoA is an abundant metabolite with its concentration ranging 0.1 - 0.6 mM inside mitochondria[595]. Succinyl-CoA might be exported through carnitine / succinyl-carnitine system

and produce a cytosol/nuclear succinyl-CoA pool, as suggested by the evidence that succinate can be exported from mitochondrion through dicarboxylate carrier SLC25A10 [596].

Amino acid catabolism might be another source for acyl-CoAs. Ketogenic amino acids such as lysine, leucine and tryptophan can be converted to acetoacetyl-CoA and participate in ketogenesis. Methionine and branched chain amino acids (BCAA, e.g., valine, isoleucine) can be converted to propionyl-CoA through multiple steps. The most abundant amino acid, glutamine is subjected to glutamate production catalyzed by glutaminase. Glutamate can then be converted to α-ketoglutarate (α-KG) through a reversible reaction catalyzed by glutamate dehydrogenase and therefore participates TCA cycle, which as described above, might impact acyl-CoAs pool.

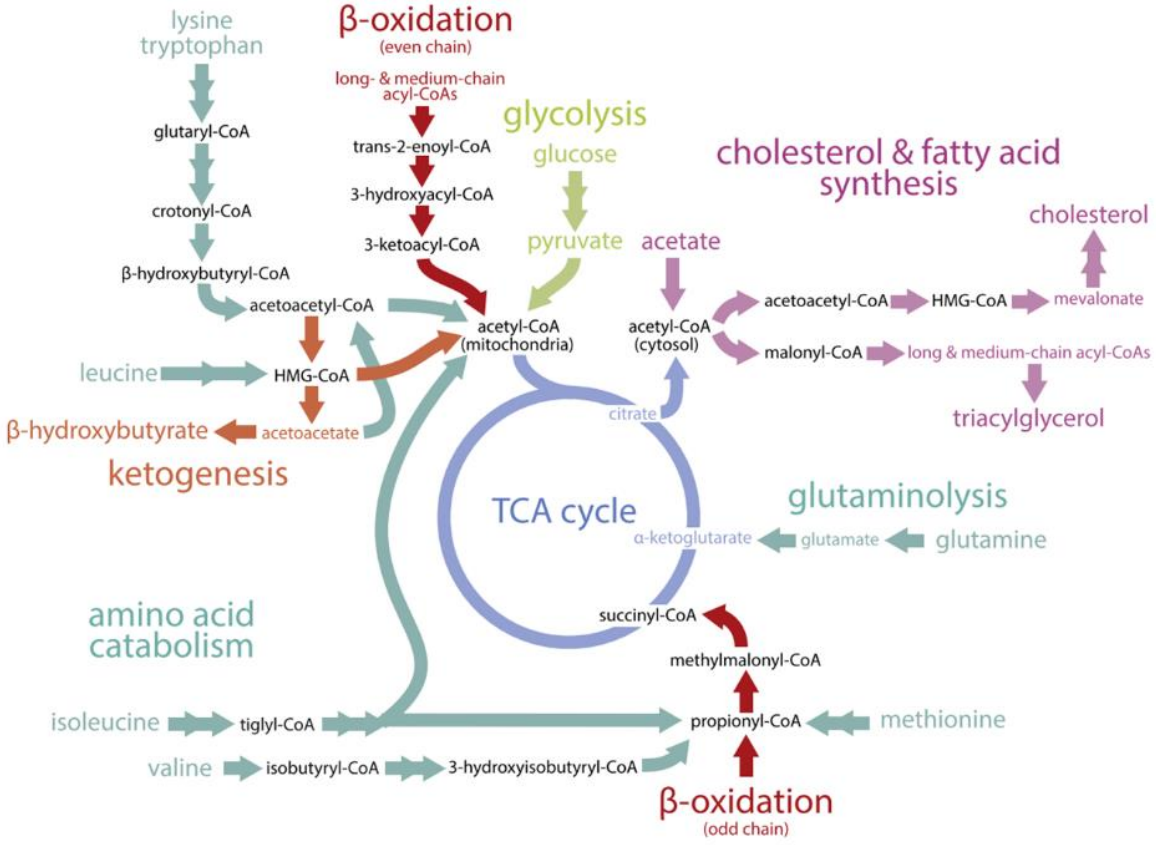

Figure 20. Acyl-CoAs metabolism

Acyl-CoAs can be produced and consumed in various catabolic and anabolic pathways including β-oxidation, glutaminolysis, glycolysis, ketogenesis and amino acid catabolism. The various pathways involved and the key corresponding metabolites are indicated in the figure and are highlighted in different color. β-oxidation is labeled in red, ketogenesis is labeled in orange, cholesterol and fatty acid synthesis are labeled in magenta, TCA cycle in blue, amino acid metabolism in cyan, glycolysis in olive green. From[597].

3.3.3 Glycolysis

Lactate is produced from pyruvate in the last step of glycolysis catalyzed by lactate dehydrogenase (LDH). In response to hypoxia or mitochondrial complex I inhibition, which

induces glycolysis and lactate production, macrophages displayed increased level of histone lactylation. Consistently, inhibition of glycolysis using 2-DG or inhibiting PDH (pyruvate dehydrogenase) and LDH by sodium dichloroacetate (DCA) and Oxamate respectively, reduce lysine lactylation[140].

3.4 Other metabolites (NAD, FAD, PKM2, IDH)

3.4.1 NAD

In mammals, nicotinamide adenine dinucleotide (NAD) is synthesized from tryptophan or vitamin B3 precursors, which are provided by diet. Tryptophan is degraded through kynurenine pathway, which produces quinolinic acid and then nicotinic acid mononucleotide (NAMN). Vitamin B3 includes nicotinamide (NAM, NM), nicotinic acid (NA), nicotinamide riboside (NR) and nicotinic acid riboside (NAR), which can either generate NAMN (e.g., NA is used) or nicotinamide mononucleoside (NMN) (e.g., NR, NAM as sources). NAMN and NMN are then converted to their corresponding dinucleotide (NAAD or NAD+) by NMN adenylyltransferases (NMNAT), of which NAAD is amidated to NAD+ by NAD synthetase (NADS)[598]. NAD exists as NAD+ and the reduced state NADH in cells which senses intracellular metabolic state.

NAD is a cofactor for SIRT family deacetylase. During deacetylation reaction, acetyl group cleaved from acetyl-lysine is transferred to ADP-ribose of NAD, generating O-acetyl-ADP ribose and unmodified lysine (See **Figure 11**). Therefore, NAD homeostasis can regulate histone acetylation in a SIRT-dependent manner. For example, knocking down NMNAT1 results in decreased intracellular NAD and increased levels of histone acetylation in retina[599]. Similarly, expression of nicotinamide phosphoribosyltransferase (NAMPT), which catalyzes the generation of NMN from NAM was shown to increase NAD levels and activate SIRT1, which consequently reduces histone acetylation and represses histone gene expression[599]. During the transition from quiescence to proliferation of muscle stem cell, decreased intracellular NAD level resulting from metabolism reprogramming leads to reduced SIRT1 activity, which promotes H4K16ac and transcriptional activation of muscle genes[600].

NAD also serves as co-substrates for ADP-ribosylation. ADP-ribose transferases use NAD and transfer single or several ADP-ribosyl moieties from NAD to acceptor proteins including histones, generating protein ADP-ribosylation (See **Figure 11**). Adding NAD to cell nuclei increased tremendously protein ADP-ribosylation[601]. Nuclear NAD+ synthase NMNAT-1 can promote histone H2B ADP-ribosylation via synthesizing NAD and directing poly (ADP-ribose) polymerase (PARP)-1 catalytic activity, which subsequently inhibits phosphorylation of adjacent residue and precludes adipocyte differentiation[129].

3.4.2 FAD

FAD is synthesized from riboflavin (vitamin B2). The reaction starts from generation of riboflavin mononucleotide from riboflavin catalyzed by riboflavin kinase, resultant riboflavin mononucleotide can then be converted to FAD by FAD synthase (FADS). FAD is a cofactor for numerous biochemical processes, including histone demethylation. Lysine demethylases LSD1/KDM1A and LSD2/KDM1B are FAD-dependent oxidase that remove methyl group with the conversion of FAD to FADH2[602]. FADS was found to be located in nucleus, although less abundant than its mitochondrial counterpart, which might contribute to nuclear pool of FAD[603].

3.4.3 α-KG

α-KG pool is maintained through several nutritional pathways. It is generated through the action of glutamate dehydrogenase (GDH, GLUD) from glutamate or from isocitrate by isocitrate dehydrogenase (IDH), and can be converted to succinyl-CoA by α-KGDH during TCA cycling. Therefore, metabolites such as fumarate and succinate are TCA products downstream of α-KG can competitively inhibit the generation of α-KG. As a cofactor for DNA demethylase TET and JmjC family of histone demethylases, α-KG has been widely studied for its role in histone methylation and gene expression regulation. For example, intracellular α-KG/succinate ratio was shown to regulate H3K27me3 and DNA methylation, which in turn impact pluripotency-associated gene expression[604]. Fumarate and succinate accumulation by dysfunctional fumarate hydratase (also known as fumarase) and succinate dehydrogenase leads to genome-wide increase of histone and DNA methylation by inhibiting α-KG dependent dioxygenases[605].

3.4.4 PKM2

Pyruvate kinase M2 (PKM2) is a tumor specific kinase and is well-established for aerobic glycolysis. PKM2 was found to bind to and phosphorylate histone H3, which promotes HDAC3 dissociation and CCND1, MYC gene expression[606]. PKM2 was also suggested to directly phosphorylate H2AX and promotes genomic instability in tumor cells[607].

3.4.5 IDH

Isocitrate dehydrogenase (IDH) catalyzes reversible conversion of isocitrate to α-KG in TCA cycle. IDH1 and IDH2 were found frequently mutated in glioblastoma and in myeloid leukemia patients. Mutated IDH1/2 could produce 2-hydroxyglutarate (2-HG) from α-KG, which competes with α-KG for the active site of demethylases and subsequently inhibits α-KG-

dependent dioxygenases, including histone demethylases and TET family of DNA methylcytosine hydroxylases[608]. Consistently, IDH1/2 mutated cancer cells have altered genome-wide histone and DNA methylation that contributes to oncogenic programs (e.g., suppression of differentiation associated genes)[609, 610].

In conclusion, metabolic state impacts the nuclear genome in many ways and hence tunes all chromatin-based biological activities in response to nutritional cues, adding a new layer of complexity to intracellular signaling. The metabolism-nucleus crosstalk is, to a large extent, mediated by metabolites, which act as cofactors for epigenomic modifications. Unraveling the regulation of nuclear accessibility to epigenomic metabolites is an important challenge in modern biology. For instance, it would be critical to know what are the nuclear compartments or sub-compartments of metabolites and how they are impacted by fluctuations of other non-nuclear pools and by nutrient signaling.

Additionally, the question of how metabolites specifically impact specific genomic outputs, is a very important one. Answer to these questions would undoubtedly help us to solve many issues in modern biology and to provide the community with a deep understanding of what we call epigenetics. Given the fact that alterations of the cellular metabolism have been observed in many diseases including cancer, understanding of the metabolism-nucleus signaling and the key players would also shed a new light on new therapeutical approaches.

4. Metabolism-driven histone modifications contribute to cancer biology

4.1 Cancer cells have reprogrammed metabolism

Cancer cells depend on their reprogrammed metabolism to maintain unrestricted proliferation and to survive environmental stress (e.g., hypoxia, nutrients restriction). This metabolic rewiring also allows to meet the demand for energy supply, macromolecules biosynthesis and redox homeostasis. Pavlova and Thompson summarized six metabolic hallmarks harbored by cancer cells, including deregulated glucose and amino acid uptake, increased demand for nitrogen, plastic modes for nutrient acquisition, increased biosynthesis using metabolites, metabolism driven gene regulation and cell signaling and metabolic interactions with microenvironment[611]. As described above, since chromatin signaling is impacted by cellular metabolism, the specific crosstalk between metabolism and chromatin should be commonly adopted in all cancers and hence this crosstalk should be considered as a pillar of cancer biology.

Herein I will firstly introduce metabolic characteristics of cancer cells, including the altered metabolism of glucose, amino acid and then the enhanced biosynthesis of intracellular biomass. In the second part of this chapter, I'll briefly introduce metabolic signaling to cell nucleus, give

examples of how metabolic alterations impact or even dominate cell behavior through epigenetic modulation.

4.1.1 Enhanced glucose uptake and glycolysis

Cancer cells require continuous supply of nutrients to build cytoskeleton and macromolecules for assembling new cells. In mammalian cells, glucose and glutamine are two important nutrients that are used for macromolecules biosynthesis. Indeed, increased glucose uptake was observed in cancer cells by Warburg more than a century ago. Compared with nonproliferating adult cells, cancer cells prefer to use glycolysis even when supplied with abundant oxygen (termed as aerobic glycolysis)[612]. Although carbon sources produce much less ATP (reducing equivalents) through glycolysis than coupled with the TCA cycle. Based on this, positron emission tomography (PET) imaging that determines glucose uptake of tissues using radioactive glucose has been used in the clinics for tumor staging and diagnosis.

Increased glucose uptake and utilization in glycolysis had been proposed to result from dysfunctional mitochondria following early studies. However, later researches identified that many cancer cells did have functional mitochondria and intact oxidative phosphorylation machineries. One hypothesis of such metabolic switch is to enhance glycolytic intermediates production which fuel various biosynthetic pathways, including nucleosides and amino acids. Indeed, such a metabolism is also adopted by rapidly dividing embryonic cells, demonstrating its role in support of cell proliferation. Moreover, elevated pentose phosphate pathway (PPP), which deviates from lactate production after the first rate-limiting step of glycolysis, has been observed in cancer cells. PPP supplies ribose for nucleotides synthesis as well as generates NADPH for fatty acid synthesis[613]. An additional glycolytic intermediate which is required for biomass production is dihydroxyacetone phosphate (DHAP). DHAP is produced from glyceraldehyde-3-phosphate, and is utilized in the biosynthesis of phospholipids when converted into glycerol-3-phosphate.

Besides biosynthesis, enhanced glucose uptake and glycolysis protects cancer cells from excessive oxidative damage. On one hand, reduced use of glucose to fuel the TCA cycle and hence the reduced coupled oxidative phosphorylation, restrict the production of reactive oxygen species (ROS) from mitochondrial respiration[614, 615]. On the other hand, increased production of NADPH from alternative pathway (e.g., PPP) helps to maintain the redox homeostasis in response to oxidative stress. Consistently, inhibition of glucose uptake and glycolytic enzymes have been considered as serious anti-cancer strategies[616, 617].

Enhanced glucose uptake and glycolysis are mediated by altered cell signaling. PI3K-Akt signaling pathway is a master regulator of glucose uptake. PI3K-Akt signaling promotes expression of the major glucose transporter GLUT-1 and its translocation to the cell surface[618,

[619]. In addition, Akt can activate hexokinase (HK) and phosphofructokinase (PFK), which catalyze rate-limiting steps in glycolysis[620, 621]. Other oncogenic pathways (e.g., RAS, MYC) and mutations of tumor suppressors (e.g., TP53) have also been reported to be associated with glycolysis[197]. Enhanced glycolysis is also coupled with changes in expression/activity of key metabolic enzymes. Cancer cells predominantly express M2 form of pyruvate kinase (PK), which depending on its homo-multimerizations PKM2 could possess limited catalytic activity compared to M1, expressed in most normal cells. PKM2 in its less active form induces the accumulation of glycolytic intermediates which could be used in synthetic processes, such as nucleic acid-, phospholipid-, and amino acid synthesis. Besides, the expression of pyruvate dehydrogenase kinase 1 (PDK1), which phosphorylates and inhibits pyruvate dehydrogenase, is also increased in cancer cells and hence further restricts the use of pyruvate into TCA cycle[615, 622].

The Warburg effect is likely to be triggered by limited supply of oxygen and nutrients in tumor microenvironment. Under hypoxic condition, hypoxia-inducible factor 1α (HIF-1α) is stabilized, which in turn induces the expression of metabolic enzymes involved in glycolysis, including GLUT, PKM2, PDK1 and LDHA, and leads to glycolytic reprogramming[623-625]. Furthermore, acidic environment resulted from glycolysis could stabilize HIF-1α and couid reinforce its function[626]. In addition, PKM2 is activated by metabolites (e.g., fructose bisphosphate, serine), therefore the nutrient-depleted tumor microenvironment disfavors glucose entry into TCA cycle[627, 628].

Interestingly, solid tumors have been described to contain metabolically distinct subpopulations, those who adopt glycolysis and produce lactate, and those who utilize lactate as major carbon source[629, 630]. The coexistence of both lactate producing and lactate consuming cells might somehow reflect the cooperation of tumor cells and the adaptation to intratumoral environment[197]. During last few decades, a subpopulation of slow cycling cells has been identified in many types of solid tumors as well as in hematological malignancies. Those slow-growing, stem-like cells might constitute a minor fraction of the cells. In contrast to bulk tumor cells, these cells could be more resilient to environmental stress (e.g., chemotherapies, nutrients limitation, etc.), therefore they could be responsible for replenishing bulk tumors after treatment and disease relapse[631, 632]. Interestingly, in contrast to rapidly dividing bulk tumor cells, quiescent cells display higher dependence on oxidative phosphorylation[633-635].

4.1.2 Increased demand for glutamine and elevated glutaminolysis (Glutamine addiction)

Increased demand for glutamine by proliferating cells was firstly described by Eagle in the 1950s, when he demonstrated that cultured HeLa cells require 10- to 100-fold excessive of glutamine in culture medium relative to other amino acids[636]. Later studies found that glutamine

is depleted from the environment in tumor samples compared to normal tissues[637, 638]. Indeed, deprivation of glutamine could lead to cell cycle arrest and cell death in certain cellular contexts[639, 640]. Such dependence of glutamine is known as glutamine addiction.

Glutamine addiction ensures glutamate-derived macromolecules biosynthesis. Glutamine is transported across cell membrane via amino acid transporters, ASCT2 (also known as SLC1A5) and SN2 (also known as SLC38A5). Once imported into cytoplasm, glutamine can be converted into substrates through multiple steps that fuel the TCA cycle. Glutamine is firstly converted to glutamate by glutaminase (GLS). Glutamate is then converted into α-KG either by glutamate dehydrogenase (GLUD), which generates ammonium and NADH/NADPH, or by transaminases (oxaloacetate transaminase, GOT; glutamate–pyruvate transaminase, GPT; phosphoserine transaminase, PSAT). In addition, glutamine is the important nitrogen donor for the biosynthesis of nitrogen-containing molecules (e.g., bases of nucleotides, nonessential amino acids, polyamines etc.). Transaminases in glutaminolysis promote the generation of nonessential amino acids (NEAAs) from glutamine, including aspartate, alanine, and phosphoserine. The deamination of glutamine into glutamate donates an amide group to enable nucleotides synthesis *de novo* and the synthesis of amino sugars and NAD+ cofactors[641]. Glutamine is also involved in oxidative stress by serving as substrate for glutathione (GSH) synthesis. L-glutamate and cysteine form γ-glutamylcysteine (GCL) catalyzed by glutamate-cysteine ligase (GCLC), which together with glycine, generates GSH by glutathione synthase (GSS). Glutathione is an important antioxidant used to deplete peroxide and is vital to multiple cellular processes.

Similar to glucose, positron emission tomography (PET) imaging has also exploited radio labeled glutamine (^{18}F or ^{11}C) to assess glutamine uptake and utilization by cancer cells, which has shown great potential in cancer diagnosis and therapeutic monitoring in some tumor contexts[642-644]. This is especially interesting for tumors that cannot be effectively distinguished by glucose uptake, for example, tumors in brain tissues where physiological heavy glucose utilization is found.

Glutamine metabolism is strictly controlled in cancer. C-Myc is the major driver of glutamine utilization by various cancer cells[645, 646]. It increases the expression of glutamine transporters ASCT2 and SN2, therefore enhances glutamine uptake. Furthermore, it can upregulate GLS1, phosphoribosyl pyrophosphate synthetase (PRPS2), carbamoyl-phosphate synthetase 2 (CAD) and promote the utilization of glutamine to glutamate[647-649]. Other factors that regulate glutamine metabolism include oncogenes KRAS, PI3K/Akt/mTOR, and tumor suppressors such p53, Rb, LKB1etc. LKB1 and Rb have been reported to inhibit ASCT2 expression and reduce glutamine uptake[650, 651]. KRAS decreases the expression of GLUD but enhances the expression of GOT and therefore increases NADPH production[652]. mTOR can repress SIRT4 expression, which is

responsible for inhibition of GDH[653]. PI3K/Akt and p53 were reported to promote the generation of GSH and therefore protect cells from ROS damage[654, 655].

4.1.3 Altered metabolism of other amino acids

4.1.3.1 Increased biosynthesis of serine

Mammalian cells can acquire serine from the environment via alanine/serine/cysteine/ threonine (ASCT) transporters (e.g., ASCT1, ASCT2), system A transporters (e.g., SAT1, SAT2) and alanine/serine/cysteine (ASC) transporter system[656]. Serine can be biosynthesized from glycolytic intermediate 3-phosphoglycerate (3-PG) via the phosphorylated pathway, which requires the action of several enzymes including phosphoglycerate dehydrogenase (PHGDH), phosphoserine aminotransferase (PSAT1), and phosphoserine phosphatase (PSPH). Additionally, serine can be generated from glutamate transaminase reaction by the catalysis of PSAT1 and PSPH.

Serine is consumed in folate cycle. The generation of 5,10-methylenetetrahydrofolate (CH2-THF) from tetrahydrofolate (THF) requires the donation of one carbon unit by serine accompanied by the production of glycine with the action of serine hydroxymethyltransferase (SHMT). The produced CH2-THF is needed for thymidine synthesis, and when converted to 10-formyl-tetrahydrofolate (CHO-THF) through folate cycle, is needed for purine synthesis. In addition, folate cycle provides carbon source for SAM pool through methionine cycle. Collectively, serine contributes to nucleoside biosynthesis as well as supports SAM production and protein methylation. As noted above, serine can be used for GSH production and thus plays an important role in redox homeostasis.

Increased serine metabolism has been observed in tumor cells[657]. Some tumors depend on the availability of serine supply, depletion of serine suppresses cell proliferation in those cancer contexts[658]. Elevated expression of enzymes involved in the serine metabolism, including PHGDH amplification and increased activity of SHMT1 (cytosolic SHMT) have been identified in a variety of cancers[659-661]. Furthermore, increased serine synthesis pathway (SSP) such as PHGDH overexpression is associated with higher tumor grade in gliomas[662]. The contributions of serine metabolism to tumor cells proliferation and survival could, at least partially, provide carbon for nucleotide synthesis and might involve other biological processes utilizing one carbon substrates including protein methylation and might also involve redox homeostasis[551].

Serine metabolism is regulated by various factors (e.g., p53, c-Myc, TAp73, ATF4, G9a, NRF2, PKCζ) in tumors[613]. Asparagine serves as amino acid exchange factor for serine and threonine transport. In human cervical cancer cell lines, inhibition of asparagine synthase or deprivation of asparagine supplement impair the uptake of serine, leading to an increased

expression of SSP enzymes to compensate for decreased serine uptake[663]. p53 is a critical regulator for cells to deal with extracellular depletion of serine. Upon serine starvation, p53 activates p21 to promote GSH production to limit ROS stress[664, 665]. In addition, the oncogene c-Myc has been found to regulate serine and glycine metabolism (e.g., increases PSPH expression and enhances SSP) under normal as well as starvation conditions[666].

4.1.3.2 Addiction to branched-chain amino acids

Branched-chain amino acids (BCAAs) including leucine, isoleucine and valine are essential amino acids that must be acquired from diet or from protein degradation. BCAAs are metabolized in cancer cells by branched-chain aminotransferase (BCAT1 in cytosol, BCAT2 in mitochondrion) into branched-chain α-keto acids (BCKAs). In this process α-KG is converted to glutamate by receiving the amide group. The produced glutamate could be used in nucleotide and nonessential amino acid synthesis as aforementioned. BCKAs can be further catabolized to produce acetyl-CoA or succinyl-CoA[613, 667]. To this end, BCAAs metabolism are enhanced in certain types of cancer and are required for cancer growth[668]. Furthermore, BCAT1 was found to be associated with wild-type IDH expression and balance α-KG with 2-HG oncometabolites in glioblastoma and ovarian cancer[669]. In addition, accumulated intracellular BCAAs levels, especially leucine, can activate mammalian target of rapamycin (mTOR) via cytosolic leucine sensor proteins and promote cancer progression[670].

Increased catabolism of tryptophan has also been observed in some types of cancer. Tryptophan-2,3-dioxygenase (TDO), which is responsible for the conversion of tryptophan to kynurenine was found to be overexpressed in various tumors[671, 672]. Tryptophan catabolism can modulate immune cell function including promoting Treg and inhibit effector T cell function, therefore contributes to tumor invasion[673, 674].

Asparagine metabolism plays a crucial role in tumor survival, although the mechanism has not been clearly elucidated. Asparagine is produced from aspartate by asparagine synthetase (ASNS) using glutamine as amide donor. Acute lymphoblastic leukemia cells lack ASNS and rely on exogenous asparagine. Based on this fact, L-Asparaginase that can deplete extracellular asparagine, has been used as an anticancer treatment in ALL[675, 676].

4.1.3.3 De novo lipid synthesis

While the de novo biosynthesis of fatty acids is low in normal adult tissues, tumor cells possess increased lipid synthesis[677, 678]. Lipid synthesis enzymes are upregulated in tumor samples and their inhibition reduces tumor growth[679-681]. The increased lipid synthesis might not only facilitate the formation of lipid bilayers but also enables the alteration of cell membrane composition with increased oxidative damage-resistant saturated fatty acids[682].

4.1.4 Utilization of acetate, ammonia, ketone bodies, lactate

Cancer cells face deficient nutrients supply. In addition to glucose and glutamine, tumor cells are able to take advantage of nonconventional nutritional sources including acetate, ammonia, ketone bodies and lactate.

Lactate:

As noted, cancer cells have increased aerobic glycolysis as well as lactate production. Lactate has been found to be absorbed by cancer cells and be oxidized in mitochondrial respiration for ATP production in several cancer cells[683]. Lactate might also be the carbon source for lipid synthesis in lung cancer cell lines (i.e., HeLa and H460)[684].

Acetate:

ACSS2 enzyme, which utilizes acetate for the production of acetyl-CoA, was found to be upregulated in breast, ovarian and lung tumor samples[613]. Acetate-deriven acetyl-CoA contributes to cancer growth through modulating histone acetylation as well as providing carbon for fatty acid and phospholipid.

Keton bodies:

Ketone bodies are mainly synthesized by liver cells (ketogenesis) and are transported and utilized by extrahepatic tissues such as brain and skeletal muscle (ketolysis). The normal hepatocytes per se are not able to perform ketolysis due to the lack of the key ketolytic enzyme OXCT1. However, the reactivation of ketolysis resulting from increased OXCT1 expression has been discovered in liver cancer cells in response to starvation[685].

Ammonium ions:

Free ammonium ions often accumulate in tumor environment. It has been found that ammonia can be used for glutamine production by cancer-associated fibroblasts and then transferred to and be used by cancer cells[686]. Ammonia might also be a source for proline, aspartate, glutamate and BCAA generation in breast cancer cells[687]. In addition, cancer cells have been reported to use exogenous proteins, including living cells, apoptotic bodies under nutritional stress[611].

4.2 Cell metabolism signals to nucleus via epigenetic modifications

Emerging evidences suggest that cellular metabolism is not merely the adapted outcome of extracellular nutrition, but can in turn transmit the information of nutritional availability to nucleus via metabolites and metabolic enzymes. Accordingly, they coordinate chromatin behavior and gene expression and the metabolic state. This coordination is highlighted in cancer, as cancer cells have metabolic reprogramming and display metabolic plasticity to survive nutritional perturbations. The crosstalk between cell metabolism and chromatin, and their contribution to cell biology have received much attention.

As described above, acetyl-CoA is the central metabolite bridging multiple biosynthetic and catabolic pathways, and is the substrate for protein acetylation. Various studies have documented that, the abundance of acetyl-CoA could link cellular metabolism to the cancer cell behavior via epigenetic modifications of histone and non-histone proteins.

Akt phosphorylates ACLY and enhances its activity[688]. Increased glucose availability as well as introduction of Akt increase acetyl-CoA abundance, thereby leading to increased global histone acetylation, which in turn promotes gene expression and tumor development[556]. AMPK was shown to be required for acetyl-CoA homeostasis and histone acetylation. Depletion of AMPK reduces histone acetylation and displaces BET protein, the combination of BET inhibitor and AMPK inhibitors suppresses the development of MLL-rearranged AML[583]. ACC1 catalyzes carboxylation of acetyl-CoA to malonyl-CoA for *de novo* fatty acid synthesis. TGFβ-activated kinase mediated phosphorylation of ACC1 inhibits its activity, leading to increased acetyl-CoA levels and the acetylation of transcription factor SMAD2, thereby conferring to increased metastasis in breast and lung cancer[567]. Similarly, metformin treatment results in AMPK-dependent ACC phosphorylation, leading to increased acetylation of histone and non-histone proteins (e.g., NF-kB p65 subunit) and enhanced expression of NF-kB target genes[689]. In addition to acetyl-CoA, a number of studies reported that DNA and histone methylation is sensitive to intracellular SAM levels[690-692].

Metabolic enzymes have been implicated in tumorigenesis as well. IDH1/2 mutations have been identified in glioblastoma and in leukemia cells. IDH1/2 mutants can produce oncometabolite 2-HG from α-KG, which competitively inhibit α-KG dependent demethylases and result in DNA and histone hypermethylation that contribute to tumorigenesis[693]. In addition, α-KGDH binds GCN5/KAT2A and produces succinyl-CoA at local sites, which promotes GCN5 dependent H3K79 succinylation and facilitates gene expression and tumor growth[151].

Collectively, these findings suggest that metabolic reprogramming might play an important role in cancer biology through epigenetic modulations.

5. Identification of a gene associated with poor prognosis in ALL

5.1 Overview of ALL

Acute lymphoblastic (lymphocytic) leukemia (ALL) is a hematological malignant disorder which derives from clonal lymphoid precursors. More than 75% of ALL patients are B cell type (B-ALL). ALL affects mostly children, with about 60% of the patients are below 20 years[694]. Typically, the clinical manifestations include hematopoietic failure, e.g., anemia, thrombopenia and leukopenia, and the resultant signs and symptoms, e.g., fatigue, dyspnea etc. Patients can also display splenomegaly, hepatomegaly, or lymphadenopathy when leukemic blasts infiltrate the corresponding organs. Diagnosis is defined by cell smear showing that leukemic blasts comprise > 25% of nucleated cells in bone marrow. The more precise diagnosis of ALL relies on the definition of characteristic molecular and cytogenetic alterations as well as on immunophenotyping, which not only provides information that is useful for diagnosis and risk stratification, but also contributes to treatments guidance.

Traditional treatment strategy corresponds to multiagents-based chemotherapy, with the conventional backbone consisting of cyclophosphamide, anthracyclines, and corticoids. Currently, the treatment strategy is strictly dependent on patients' risk stratification in order to orient intensive chemotherapy towards the high-risk patients and to save the low-risk patients from excessive toxicity of chemotherapy. Thanks to the adoption and development of risk-adapted treatment strategies, the last 5 decades have seen the improvement of patient managment so as ALL is now one of the most curable cancer, with long term survival of pediatric patients approaching 90%. However, around 10-15% of pediatric patients still undergo relapse. Traditionally, the salvage therapies are Allogenous hematopoietic stem cell transplantation (Allo-HCT) following second complete remission (CR). However, with the adoption of multiple agents-based chemotherapy during the initial treatment, the relapsed patients are often resistant to the chemotherapy, therefore it could be difficult to reach second CR. Besides, a small percentage of patients develop resistance at the early onset of treatment (designated as refractory cases). Indeed, relapse and refractory (r/r) are still the main cause for treatment failure in childhood patients.

Additionally, the treatment for adult patients is much more challenging, with nearly half of adult patients relapse and 5-year overall survival (OS) falls to less than 50%[695]. The main reasons of dismal outcome of adult patients are higher frequency of cytogenetic abnormalities (such as Ph-like, hypodiploidy, near-haploidy, complex karyotype etc.), less tolerance over childhood regimens (such as the usage of asparaginase), less treatment adhesion and obedience, higher relapse and resistance rate, etc.

Hematologists and researchers are trying to improve the adult patients' outcome. Inspired by the success of childhood ALL treatment, adolescents and young adults (AYA, 15-39 years) are also prescribed with pediatric ALL regimens now. However, older patients cannot tolerate childhood regimen especially the frequent applications of L-asparaginase. Another promising approach is the use of targeted therapy. Indeed, targeted therapy increases the response rate of older adults who cannot tolerate multi-agents based chemotherapy. Lately, new therapies, such as monoclonal antibodies (e.g., CD19, CD20, CD22 antibodies, etc.), bispecific anti-T receptor/CD19 antibody blinatumomab, and chimeric antigen receptor (CAR) T cell therapy (e.g., CD19 CAR) have brought additional choices for treating r/r patients[696-698]. However, there are limitations associated with these approaches such as immune escape, less persistence, the high expenses of antibodies, and the less experienced techniques etc.[699]

Prognostic factors are the main bases for risk stratification and treatment choices. Traditionally, prognostic factors include age, immunophenotype, WBC count at disease onset, the infiltration of central nervous system (CNS), morphological CR status etc. Adults (>35 years), T cell subtype, high WBC (>30×10^9 in B-ALL, >100×10^9 in T-ALL), delayed remission (>4 weeks) or not remission are poor prognostic factors. More recently, minimal residue diseases (MRD), which refers to the residual blasts after initial therapy has been incorporated to the evaluation for prognosis and used to monitor the relapse.

Cytogenetic and molecular abnormalities are important prognostic factors. In B-ALL, the Ph chromosome, MLL rearrangement, hypodiploidy, etc. are associated with poor outcome. In contrast, ETV6-RUNX1 fusion, hyperdiploidy, E2A-PBX1 translocation, triosmy (+4, +10, +17) etc., are associated with good prognosis. Notably, the novel Ph-like subtype whose transcriptional profile is much alike those seen in the Ph positive blasts, but lack of BCR-ABL1 oncoprotein, has been identified. Ph-like cases are featured by frequent mutations of B cell development and differentiation genes, activation of cytokine receptor genes and kinase pathways, and is associated with persistent MRD and higher relapse rate compare to non Ph-like counterparts[700]. Besides, MEF2D rearrangement, DUX4 rearrangement, ZNF384 rearrangement, PAX5 mutation, IKZF1deletion etc., have been reported to predict prognosis.

Prognostic factors involving genetic abnormalities might provide evidence for the development of targeted therapies. The most successful example is the exploitation of tyrosine kinase inhibitors (TKIs). Nowadays, TKIs combined with chemotherapy has been the standardized treatment strategy for BCR-ABL1 positive patients. In addition, the inhibitors targeting JAK-STAT have entered clinical trials.

In conclusion, the treatment of high-risk and r/r ALL cases remains challenging. Currently, risk-adapted chemotherapy remains the first-line treatment strategy. Identifying prognostic factors and understanding the corresponding pathophysiology could not only minimize relapse rate by early application of intensified chemotherapy but also could help to decide Allo-HCT

at CR1 for high-risk patients. In addition, this would guide the clinicians to prescribe the optimal treatment and to avoid the unnecessary toxicity of the intensified chemotherapy for standard risk patients. This would also point to new targeted therapies.

5.2 Ectopic activation of testis-specific genes is associated with cancer aggressiveness

Tissue development and differentiation is a programed process. Mature tissues composed of differentiated cells are generated by successive expression of specific genes. Under these conditions many tissue-specific genes remain silent. These genes' expression activation and silencing are precisely controlled by the cell-type specific epigenetic profile. Malignant transformed cells have a life-sustaining capability, which is facilitated by the activation of genes underlying the so-called cancer hallmarks.

The abnormal signaling in cancer cells is to some extent established and stabilized by an altered epigenetic landscape. One common feature displayed in multiple cancers is a genome-wide DNA hypomethylation and locus-specific hypermethylation (e.g., CpG islands). Methylation-mediated repression of critical tumor suppressor genes has been well documented to be oncogenic events[701]. Additionally, global DNA hypomethylation contributes to a higher genomic instability (e.g., chromosome rearrangements) which is a frequent cancer-associated event. However, an unexplored feature of cancer is the oncogenic activity of the many genes that are aberrantly activated due to DNA hypomethylation.

Most of the cancer-specific hypomethylated genes are testis-specific genes (termed as cancer-testis, C/T, also termed as cancer-germline, C/G), whose expression is restricted in normal adult tissues. Generally, testis-specific factors play a role in spermatogenesis. It is postulated that the ectopic activation of C/T genes might contribute to the signaling network required for cell transformation and/or malignancy maintenance[702, 703]. This theory has been documented by several studies. For instance, Janic and colleagues have identified a soma-to-germline transformation with an ectopic expression of germline genes during malignant brain tumorigenesis in Drosophila, while inhibition of these germline genes suppress tumor growth[704]. There are many examples of the functional studies of the C/T genes in cancer. One interesting example is the aberrantly activated PRAME gene, which was found to be an antagonist for retinoic acid receptor (RAR), inhibiting the RAR-dependent cell differentiation program[705].

The ectopic activation of C/T genes can be associated with cancer behavior and patients' prognosis. In most cases, the frequent activation of C/T genes indicate higher tumor grade and poor outcome[706]. For instance, in a cohort of 293 lung cancer cases, Rousseaux and colleagues have identified an ectopic gene expression signature associated with a subset of highly aggressive tumors, predictor of patient's outcome[707]. In addition, Emadali and colleagues discovered that an ectopically-expressed gene CYCLON, is associated with cancer

aggressiveness and resistance to anti-CD20 antibody in high-risk lymphoma. CYCLON gene expression is driven by MYC and could be sensitive to the BET inhibitor JQ1. The depletion of CYCLON could reverse drug resistance[708].

Higher expression of C/T genes could occur in cancer stem cells (CSCs) compared to the bulk cells. For example, MAGEA9 is highly expressed in CSCs in hepatocellular carcinoma. In addition, compared to the bulk of leukemic blasts, CD34+CD38- cells (known as leukemic stem cells) have higher expression of MAGEA1.

C/T genes are plausible candidates for immunotherapy since they could be immunogens. For instance, CD4+ T cell immunotherapy targeting MAGEA3 has achieved partial response in advanced esophageal cancer, urothelial carcinoma and osteoblastoma[709]. Anti-C/T tumor vaccines have been tested in multiple types of cancers, some of the corresponding clinical trials show the low-toxicity and promising efficacy of this approach[710].

Indeed, increasing evidence indicate that C/T genes can be important in cancer development, with demonstrated oncogenic roles in establishing/promoting multiple cancer hallmarks. Examples are C/T genes role in growth signaling, metabolism reprogramming, resisting apoptosis etc… Some of these mechanisms have been reviewed by Tongelen and colleaguess and are summarized in (**Figure 21**)[703]. What is fascinating about C/T genes is that, because of their limited expression in normal tissues, they could be promising therapeutic targets in cancer with minimized side effects[710].

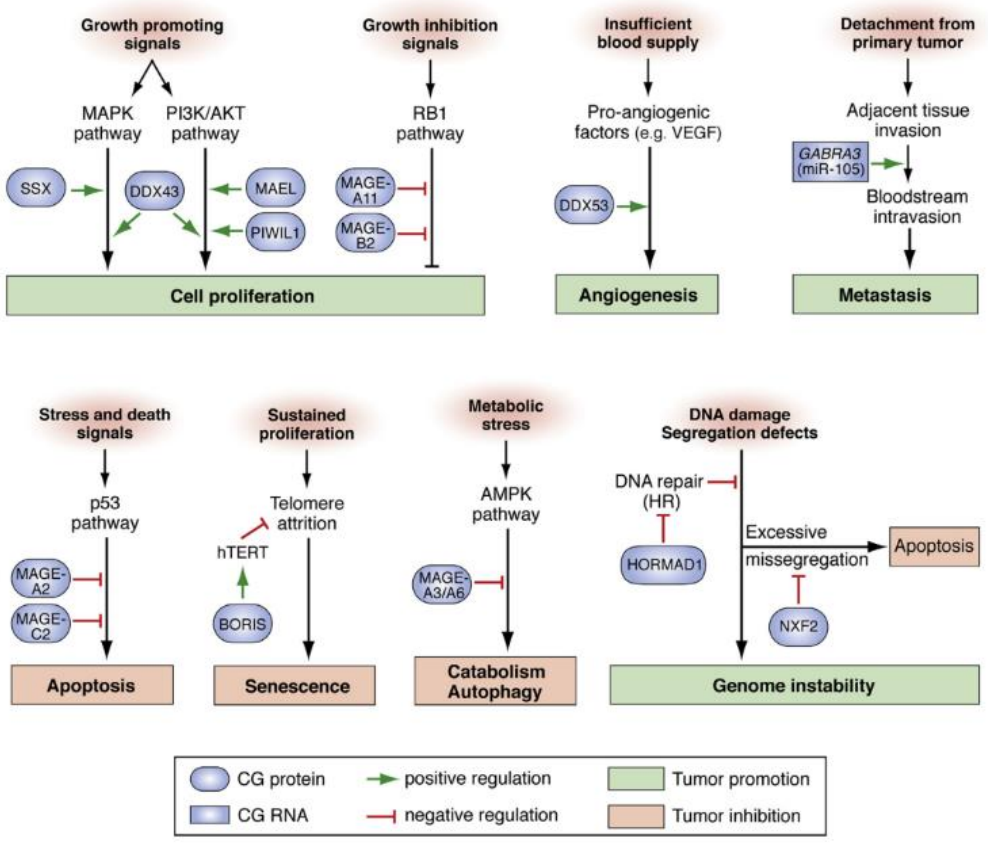

Figure 21. C/T genes contribute to various pro-tumoral processes.
Examples of C/T genes sustaining cancer hallmarks, including cell proliferation, angiogenesis, metastasis, apoptosis, senescence etc... For more details, please refer to[703]. From[703].

5.3 Identification of six genes' signature associated with patients' outcome in ALL

Previously, a work conducted in collaboration between the Grenoble team and the Shanghai Institute of Hematology identified six genes whose combined expression is associated with prognosis in ALL[711]. In this work, they firstly screened genes that are exclusively expressed in testis/placenta/embryonic stem (ES) cells but not in normal adult tissues. In the next step, genes that are sporadically expressed in normal bone marrow were filtered out. The rest of the remaining genes were subjected to screening for ectopically activated genes in ALL. Among the imposed criteria, was an expression above mean values + 3 standard deviations of 112 normal adult tissues and occurring in more than 10% of the ALL blasts. Finally, genes whose expression was associated with prognosis in ALL were screened out and were ranked by the p-value of their association with prognosis. This leads to the identification of 6 genes (AK022211, FASTKD1, STARD4, CAMSAP1, PCGF6 and SH3RF) (**Figure 22**).

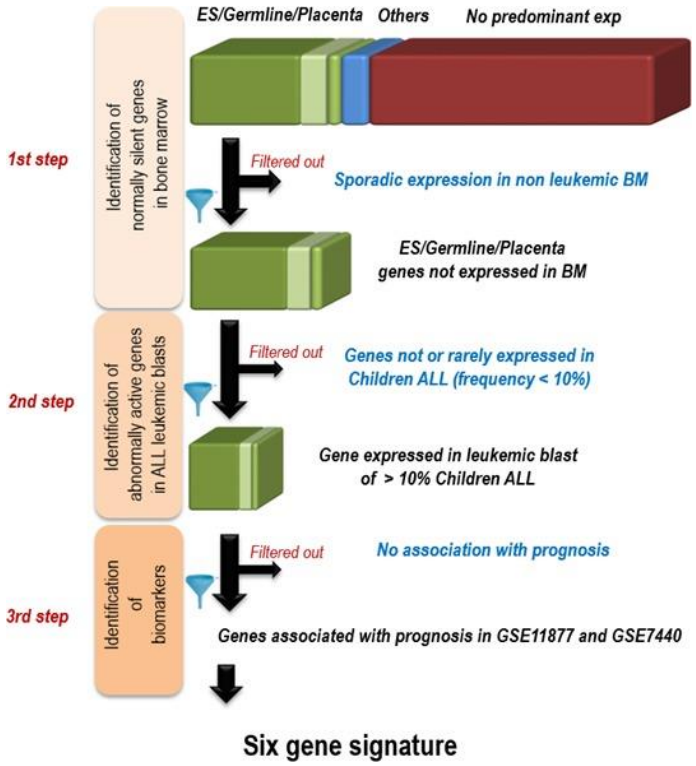

Figure 22. Identification of six gene signature in ALL.
The figure shows the workflow to screen genes ectopically expressed in ALL that are associated with prognosis in two ALL cohorts, GSE11877 and GSE7440. After ranking the p-value of the gene's association with prognosis, the top six genes were screened out and used for further study. ES: Embryonic stem cells; BM: Bone marrow. From[711]

Among these 6 genes, expression of AK022211, FASTKD1 and STARD4 is associated with poor prognosis, termed as "negative genes", while the expression of CAMSAP1, PCGF6 and SH3RF is associated with good prognosis, termed as "positive genes". Further, they designed an algorithm combining these 6 genes, which can stratify childhood ALL. Patients with blasts expressing one or more of the "negative genes" plus none or only one of the "positive genes" are assigned as group P3, while the others are assigned as P1 and P2 based on the expression state of "negative genes" plus at least two "positive genes". These assignments successfully stratified patients into relatively good (P1&P2) and poor (P3) outcomes.

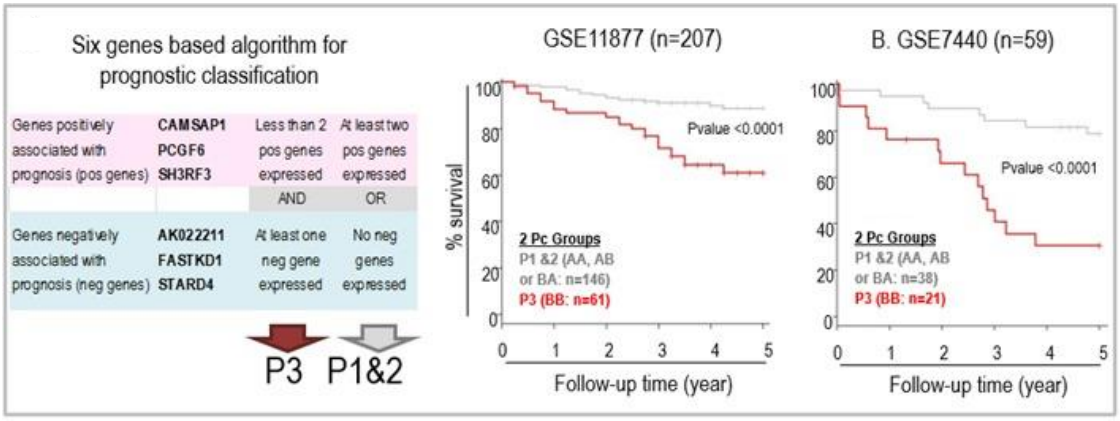

Figure 23. Six genes' signature stratify prognosis in two childhood ALL cohorts.
AK022211, FASTKD1 and STARD4 whose expression is associated with poor outcome are designated as negative genes. CAMSAP1, PCGF6 and SH3RF3, whose expression is associated with good outcome are designated as positive genes. Tumors expressing at least one of negative genes and less than 2 of the positive genes are defined as P3 group, while the rest are defined as P1&P2 group. This six genes-based algorithm stratifies patients' prognosis in GSE11877 (N=207) and GSE7440 (N=59) cohorts. Compared to P3 group (red line), P1&P2 group of patients (grey line) present a better outcome. From[711].

Furthermore, the six gene's algorithm was applied to another two adult cohorts and successfully predicted patients' outcome as well. Notably, compared with childhood patients, adult cases identified higher frequency of patients that have been assigned to P3 group, which is in accord with the overall worse prognosis of the adult patients observed in the clinics.

Following a supervised analysis of the global transcriptomic data, the gene expression profile of the aggressive P3 group was identified. The authors of this work found that in childhood and in the adult cohorts, P3 group exhibited similar expression pattern. One interesting feature of this gene expression profile is that a group of hematopoietic stem cell genes was activated, while genes involved in proliferation and cell cycle were inhibited. These data suggest that the aggressive leukemia might acquire non-dividing and stem-like properties. Indeed, standard treatments of ALL are based on cytotoxic agents, many of which target important steps in cell division (such as DOX inhibits DNA topoisomerase II) and metabolism (MTX inhibit dihydrofolate reductase and thus purine and pyrimidine synthesis), thereby cause severe effects

in rapidly proliferated cells, low-cycling cells are documented to be less sensitive to chemotherapies and are viewed as the leading causes for refraction/relapse[632].

These authors further checked ectopically activated genes individually with respect to their association with prognosis. Among which FASTKD1 alone was significantly associated with shorter survival in two ALL cohorts (GSE11855 and GSE7440) (Figure 24)[711].

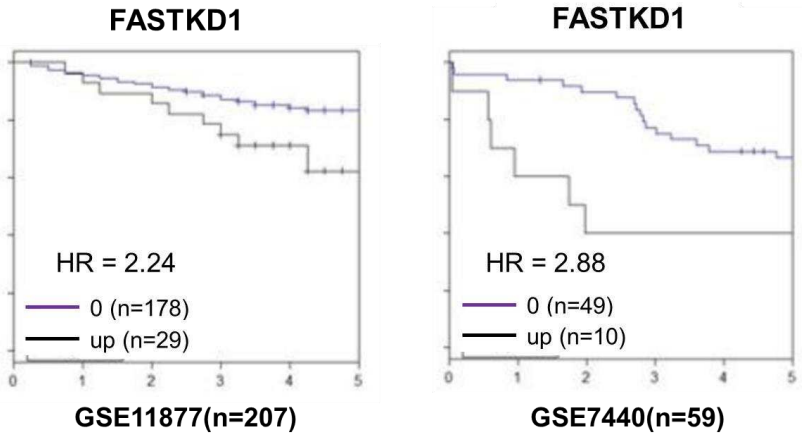

Figure 24. FASTKD1 is associated with poor prognosis.

FASTKD1 predicts outcome in two cohorts (GSE11877 N=207, GSE7440 N=59): expression of FASTKD1 (black line) is associated with poorer prognosis. HR: Hazard ratio. From[711].

5.4 FASTKD1 is a potential regulator of mitochondrial activity

5.4.1 Mitochondrial genome

Mitochondrial genome (mtDNA) is alike bacterial DNA in that it is compacted and organized into nucleoid structures. Mitochondrial nucleoids are genetic units of mtDNA segregation and allocation to the separate mitochondria during mitochondrial fission[712]. Each mitochondrial nucleoid contains 1-2 copies of mtDNA (1.4 on average in human cells and 1.1–1.5 on average in mouse cells)[713]. mtDNA is a double-strand circular DNA comprising of approximately 16.5 kb. mtDNA genes are encoded by the two strands named here chains: the heavy chain (H) encodes 2 rRNAs, 14 tRNAs and 12 mRNAs, and the light chain (L) that encodes *ND6* mRNA and 8 tRNAs (**Figure 25)**. All of the 13 polypeptides are enter the respiratory complexes, also known as oxidative phosphorylation (OXPHOS) complexes, including complex I, III, IV and V.

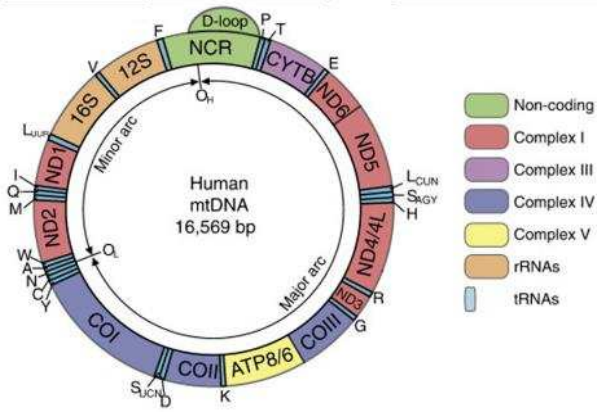

Figure 25. mtDNA.

mtDNA is double strand circular DNA that encodes 13 mRNAs: ND1-4, ND4L, ND5-6, CO I-III, CYTB, ATP6/8. This figure also shows the important structures of mtDNA. For instance, the D-loop is located at non-coding region (NCR). More details about D-loop are described in[714]. From[714].

5.4.2 mtDNA transcripts processing and maturation

mtDNA is transcribed from both strands, producing polycistronic transcripts corresponding to almost the entire length of mtDNA. mtDNA transcripts (mtRNAs hereafter) are subsequently processed and matured giving rise to functional mtRNAs. Primary mtRNAs are processed in dynamic protein structures called RNA granules (MRG), which are composed of mtRNAs and the associated RNA-binding proteins. Most of the mtRNAs are processed via tRNA punctuation, where tRNAs flanking most of the mt-mRNAs and mt-rRNAs coding regions are cleaved by RNase P and RNase Z at the 5' ends and 3'ends of ORFs, respectively. The resultant mRNAs will be polyadenylated with shorter poly-A tails than nuclear mRNAs, and are capped with NAD+. This cap influences mRNA stability and protein translation. The mtRNAs processing, maturation, degradation and translation are tightly regulated by a repertoire of factors associated with MRGs[712].

5.4.3 OXPHOS complexes

In mammalian cells, OXPHOS complexes are consisted of multiple subunits encoded by mtDNA and nuclear genome (nDNA). Complex I (also known as NADH dehydrogenase) is the largest enzyme of electron transport chain (ETC), it oxidizes NADH to NAD+ and transfers two electrons each cycle via flavin mononucleotide (FMN), iron–sulphur (Fe-S) clusters to ubiquinone (UbQ), namely NADH→FMN→Fe-S→Q, and produces ubiquinol (QH2). Complex I consists of ~44 subunits, of them ~37 subunits come from nDNA, while the other 7 subunits (ND1-6, ND4L) are encoded by mtDNA. Complex II (also known as succinate dehydrogenase, SDH or succinate-coenzyme Q reductase) forms the second entrance door for electrons. In complex II electrons transfer from succinate via FAD, Fe-S to UbQ, namely

succinate→FAD→Fe-S→Q and produce ubiquinol and fumarate. Complex II is composed of four subunits, SDHA, SDHB, SDHC, SDHD, which are all encoded by nDNA. Complex III (known as cytochrome C reductase) transfers electrons from ubiquinol (QH2) to cytochrome C. Complex III is a symmetric dimer, with each monomer composed of ~11 subunits, among them cytB is encoded by the mtDNA, while the rest of ~10 subunits are encoded by nDNA. Complex IV (known as cytochrome C oxidase) receives electrons from cytochrome C and reduces oxygen to water molecule. Complex IV contains 13 subunits, among them COX1-3 are encoded by mtDNA, while the other ~10 are encoded by the nDNA. Except complex II, all respiratory complexes pump protons across inner mitochondrial membrane. The created proton gradient drives the rotation of F1F0 ATP synthase (known as complex V), thereby, generating ATP. ATP synthase is formed by ~14 subunits, two of them (ATP6, ATP8) are encoded by mtDNA (**Figure 26**)[715].

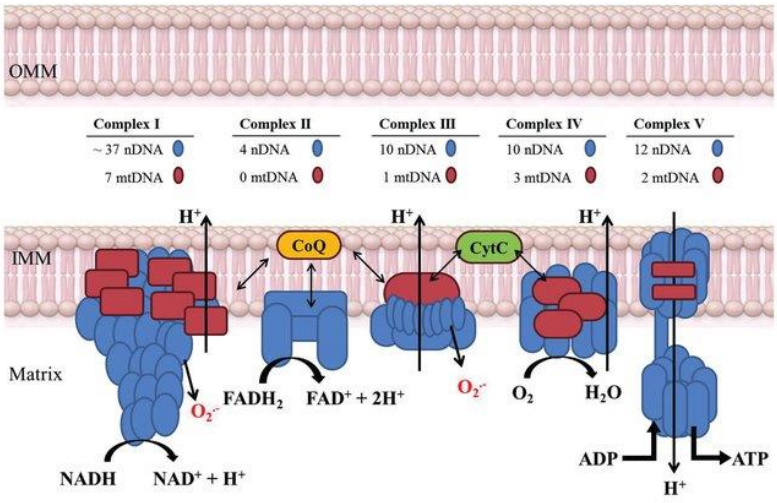

Figure 26. OXPHOS complexes.

OXPHOS complexes are composed of Complex I-V. Each Complex contains multiple subunits encoded by either mtDNA or nDNA. Complex I, III and IV pump proton across IMM. The resultant gradient is then used to generate ATP by complex V (also known as ATP synthase). OMM: Outer mitochondrial membrane; IMM: Inner mitochondrial membrane; coQ: Coenzyme Q, ubiquinone ; CytC: Cytochrome C. From[716].

In eukaryotes, OXPHOS is the major source of energy. OXPHOS complexes consume NADH, FADH2, which are mainly produced by the TCA cycle and β-oxidation of fatty acids and produce ATP. Besides ATP production, OXPHOS contributes to the generation of harmful superoxide ions prominently by complex I and III and therefore contributes to the cell oxidative stress. OXPHOS-mediated oxidative stress was traditionally proposed to be harmful to cancer cells survival. However, increasing evidence shows that some types of cancers rely on OXPHOS, leading to the OXPHOS as therapeutic targets in these cancer contexts[717, 718].

5.4.4 FASTKD1 regulates mtRNAs biology

FASTKD1 is one member of the FAS-induced serine/threonine kinase domain containing protein family (FASTK) which consists of five other members, FASTKD2-5 and FASTK. FASTK family protein were reported to localize in mitochondria[719]. These proteins share FAST_1, FAST_2 domains, which are of unknown function as well as RAP domain which is predicted to be a RNA binding module (**Figure 27**)[720, 721]. While FASTK has been documented to be a kinase, the other members do not appear to ensure any catalytic activity because of the lack of a conserved active site. Studies revealed that these proteins interact with the newly synthesized mitochondrial RNAs (mtRNAs) in mitochondrial RNA granules (MRGs), which are sites for posttranscriptional mtRNAs processing, maturation and mitochondrial ribosome biogenesis. Therefore they could regulate mitochondrial gene expression and the activity of respiratory complexes[719, 722, 723]. Indeed, FASTKD1 is documented as a negative regulator of ND3 gene[721].

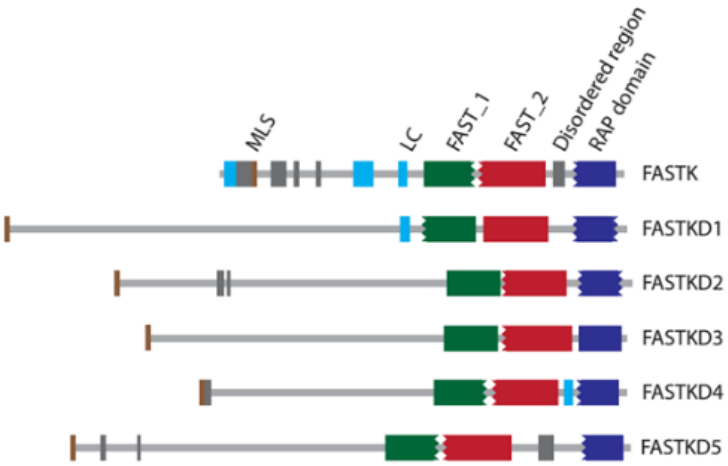

Figure 27. Domains of FASTK family proteins.

FASTK family encompasses five members, FASTK, FASTKD1-5. They share MLS (brown), FAST_1 (green), FAST_2 (red) and RAP (navy) domains. MLS (MTS), mitochondrial localization signal; LC, low complexity; FAST_1/FAST_2, FAST kinase like domains 1/2; RAP, putative RNA-binding domain particularly abundant in Apicomplexans. From[722].

A few studies uncovered the role of FASTK family proteins in cell biology and diseases. FASTK was found to be a survival protein, which is displaced from mitochondrion under stress and protect cells from UV-induced apoptosis. FASTKD2 is the only member that has been linked with mitochondrial encephalomyopathy[724]. In addition, FASTKD1 was reported to decrease complex I-dependent respiration and protect mouse embryonic fibroblasts (MEFs) from oxidative stress induced death[725].

THESIS OBJECTIVES

FASTKD1 is a potential regulator of mitochondrial activity and according to the team's previous study, is associated with poor prognosis in acute lymphoblastic leukemia. Based on this, my thesis project aims to characterize its oncogenic role in ALL. Since it is established that cell metabolism could regulate histone PTMs, this project was built on the link between mitochondrial metabolism and histone PTMs.

The preferential impact of FASTKD1 on mitochondrial activity and hence on histone non-acetyl acylations prompted us to investigate their roles in transcriptional regulations. A previous study from our laboratory suggested that the balance of histone acyl/acetyl marks impacts BET - chromatin interaction dynamics. Therefore, taking FASTKD1 as a tool, we also considered this hypothesis as well. Following this hypothesis, a role for acyl/acetyl-driven alteration of BRD4 dynamics and its impact on gene expression was considered.

Specifically, the main body of thesis project aims to:

1) characterize the function of FASTKD1 in regulating mitochondrial activity
2) document the correlation between mitochondrial activity and histone PTMs
3) substantiate the hypothesis that the relative levels of acyl/acetyl influence BET - chromatin interaction dynamics
4) address the role of mitochondrial metabolism-driven alteration of histone acyl/acetyl in transcriptional regulation

RESULTS

1. FASTKD1 represses mitochondrial activity in ALL

1.1 Exogenous expression and depletion of FASTKD1 in B-ALL cell lines

To study the function of FASTKD1 in ALL, we carried out the 'loss of function' and 'gain of function' experiments. I first tested several commercial antibodies from Abcam, Abclonal and Origine company, none of them displayed specific or stable signal in various ALL cell lines. We also generated our own antibody in house but still failed to get valid signal. Therefore, during all the following project, I either used flag-tag for exogenously expressed protein, or use qPCR to determine transcriptional level of this gene.

After introducing LeGO-FASTKD1-flag recombinant DNA into REH and NALM6, expression of the protein was checked with anti-flag antibody as well as with qPCR, the latter of which displayed 8 (NALM6) or 12 folds (REH) of mRNA upregulated than in empty vector (EV) transfected cells (**Figure 28A**). In the case of knockdown effect, 5 out of 10 shRNAs successfully knocked down the mRNA level to less than 1/2 in REH, as well as 3shRNAs in RS4;11, and NALM6 cell lines, which is shown in **Figure 28B.**

Two pieces of single guide RNAs targeting exon 4 and exon 7 respectively were used separately to generate knockout cell lines. After co-transfection of lenti-cas9 and lentiguide RNAs, multiplex cell populations were firstly genotyped with PCR amplification to check if gene-editing occurred. Multiple spikes were observed around sgRNA targeting sequence in sanger sequence map, indicating that a certain percentage of cells have been edited (**Figure 28C, left**). Genotype of both alleles of single clone was determined by PCR amplification followed by TA cloning. Knockout clones showing frame-shift indels were nominated as ko-1, ko-2 (**Figure 28C, right**) and were used for further experiments.

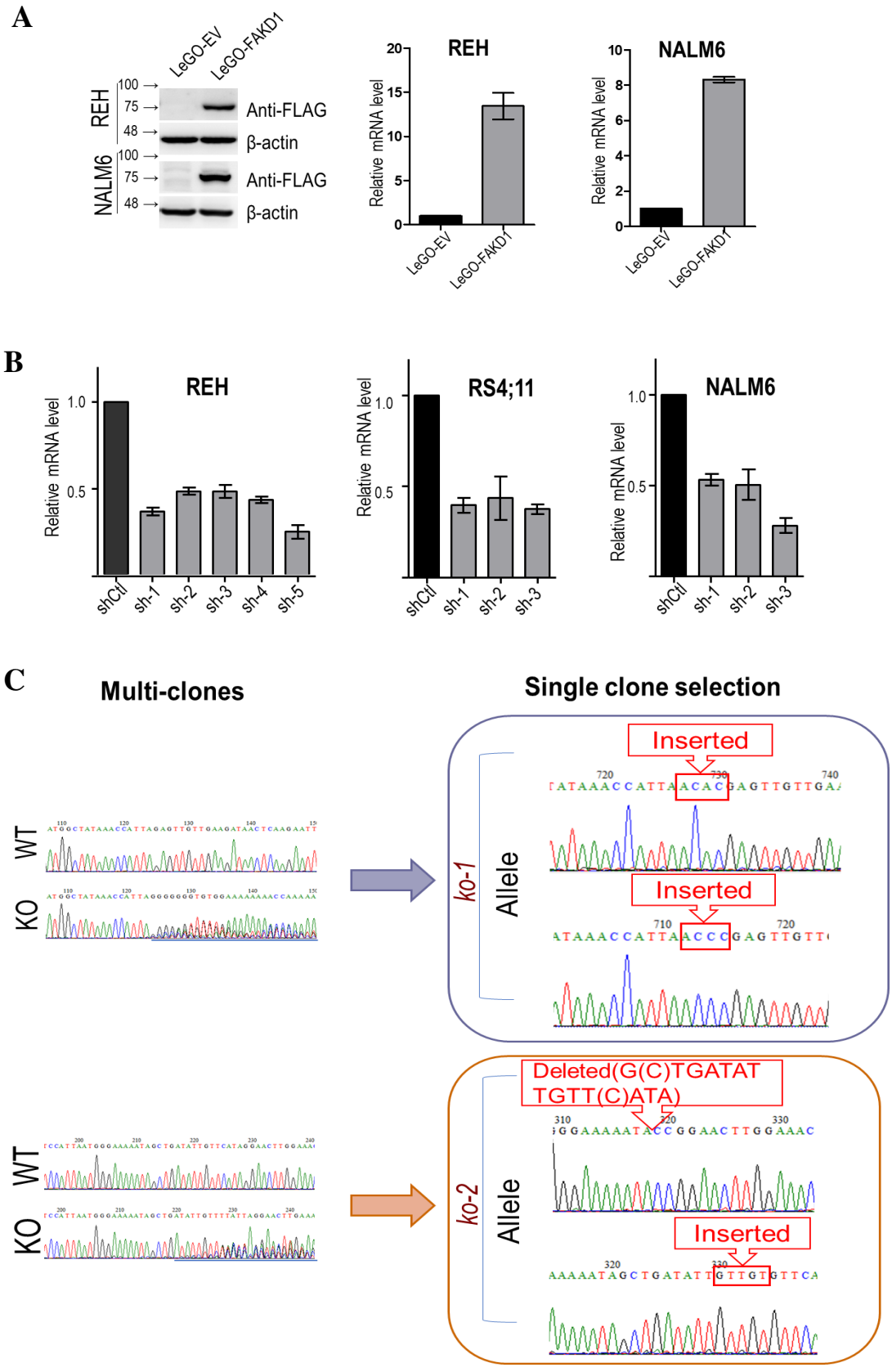

Figure 28. Exogenous expression and depletion of FASTKD1 in B-ALL cell lines.

A. Overexpression of FASTKD1 in REH and NALM6 cells. Flag tag is at the C terminus of FASTKD1 protein. Anti-flag antibody was used to probe the FASTKD1-flag protein (left panels). Relative FASTKD1 mRNA level was determined using RT-qPCR. Compared to the corresponding control cells (LeGO-EV), the expression of FASTKD1

was increased by more than 10 folds in gene overexpressing REH cells, and more than 8 folds in gene overexpressing NALM6 cells (right panels). Data shown are mean ± SEM based on at least three independent RNA extractions.

B. Knocking down FASTKD1 gene using shRNAs approach in REH (left), RS4;11 (middle) and NALM6 (right) cell lines. Relative mRNA level of FASTKD1 was measured using RT-qPCR and is shown in the figure. For each figure, control (shCtl) is labeled as black bar, and the shRNAs introduced cells are shown as grey bars. Data shown are mean ± SEM based on at least three independent RNA extractions.

C. Knocking out FASTKD1 gene with CRISPR/sgRNA in REH cells. Left panels show the genotypes of wild-type cells (WT) and the multiclones (KO) after co-introduced with cas9 and sgRNA. Right panels show the genotypes of two single clones that are depleted of FASTKD1, designated as ko-1 and ko-2 respectively.

1.2 FASTKD1 overexpression or depletion do not cause significant phenotypic alterations in ALL cell lines

Since FASTKD1 is associated with inferior outcome in ALL, and was reported to confer a protective role in MEF cells under oxidative stress conditions[725], we also tested if overexpression or depletion of FASTKD1 cause any changes in ALL cell lines. For this purpose, we counted the cells for cell proliferation, performed CCK-8 assay to measure cell viability after exposure to chemotherapy (DEX, Ara-C), PI staining to detect cell cycle. Unfortunately, none of these experiments gave stable or significant differences between control and gene-depleting or gene-overexpressing cells (**Figure 29**).

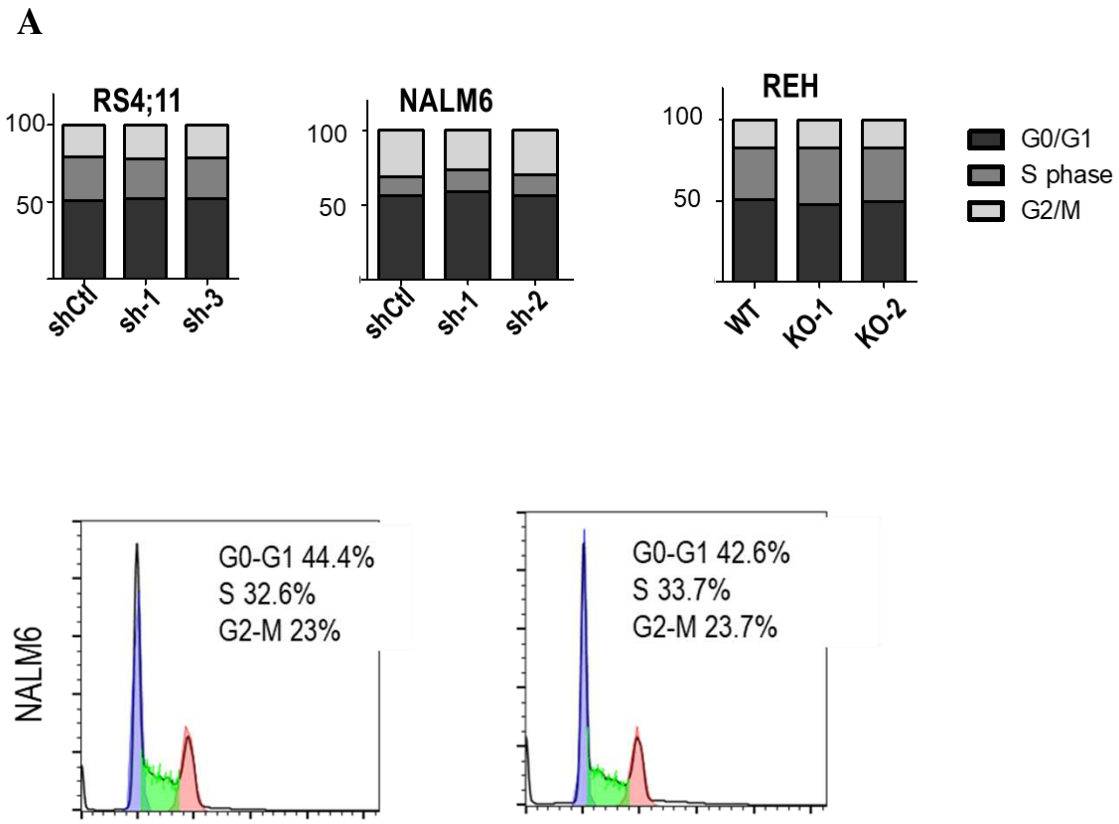

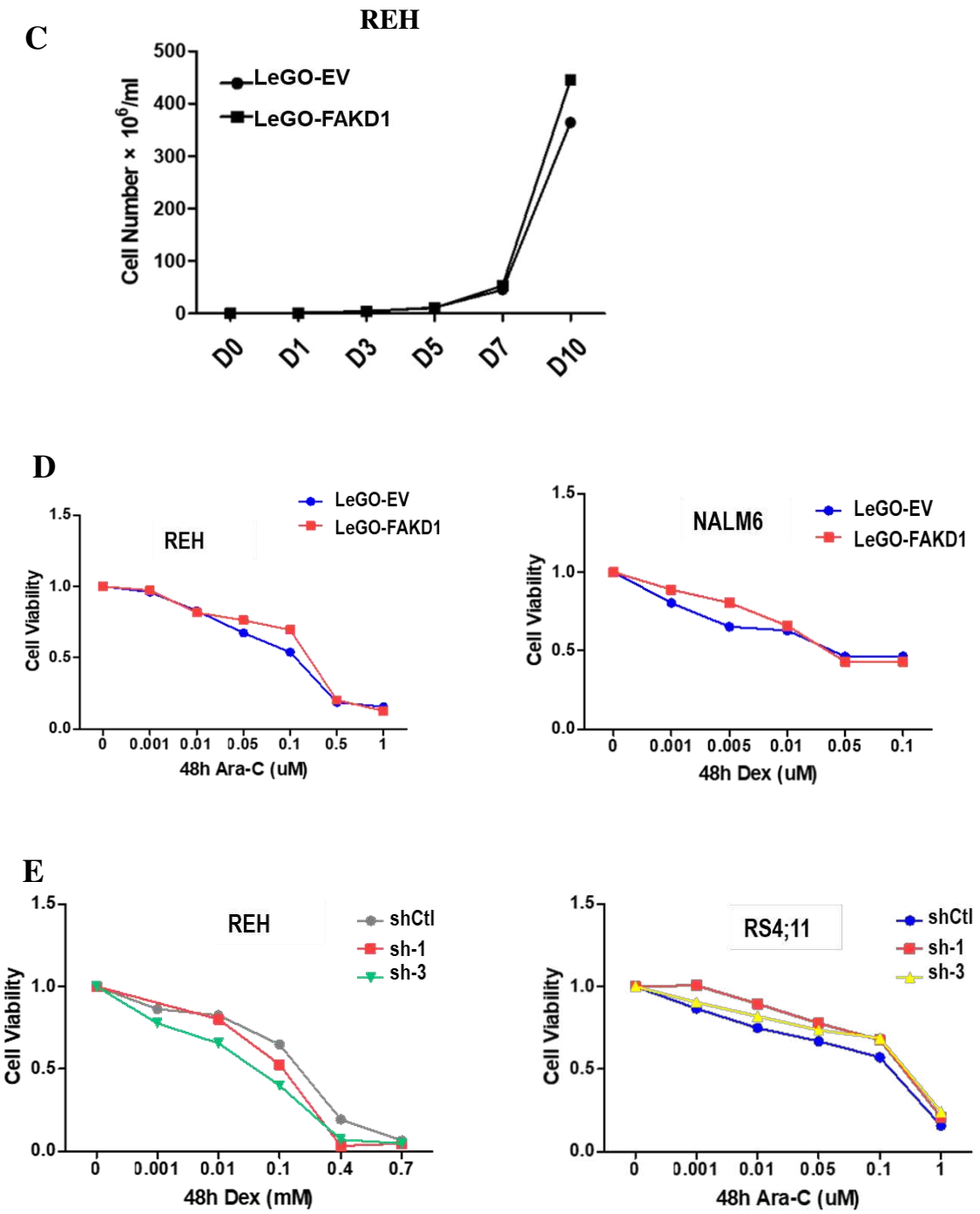

Figure 29. Deletion or overexpression of FASTKD1 do not impair cell proliferation, cell cycle or chemotherapy responses in ALL cell lines.

A. Cell cycle analysis of knockdown cells in RS4;11, NALM6 and REH knockout cells. Cells were harvested and fixated with 70% ethanol. After RNase treatment and PI staining, fluorescence signal was collected with flow cytometry and analysed with Flowjo.

B. Cell cycle analysis of FASTKD1 overexpressing REH (upper panel) and NALM6 (lower panel) cell lines. Compared with control (LeGO-EV) cells, the FASTKD1 expressing cells (LeGO-FAKD1) do not show significant changes in cell cycle.

C. Cell number of FASTKD1 control (LeGO-EV) and overexpressing (LeGO-FAKD1) cells was counted for 10 days.

D. Cell viability assay for overexpressed REH and NALM6 cells (left panels), and knockdown REH and RS4;11 cells (right panels). Cells were exposed to different concentrations of (dexamethasone, Dex) or cytarabine (Ara-C) as indicated in the figure for 48 h. Cells were then harvested and yielded to CCK8 analysis to determine the cell viability.

1.3 FASTKD1 represses mitochondrial activity

Following the previous studies uncovering that FASTKD1 plays a role in mitochondrial biology[721], its role in mitochondrion was also checked in our ALL cell lines. Firstly, with FASTKD1 overexpressing cell line, we confirmed that this protein is located in mitochondrion in ALL cell lines (**Figure 30A**). RNA-seq analysis on FASTKD1 knockdown and knockout cells revealed that depletion of FASTKD1 led to the upregulation of all mtRNAs encoded by mtDNA (**Figure 30B**). Repressive function of FASTKD1 in mitochondrial transcription (with ND2 and ND3 as the most affected genes) was also validated with qPCR (**Figure 30C**). Protein level of respiratory complexes were checked with cocktail OXPHOS antibody, demonstrating that FASTKD1 represses the expression of OXPHOS complexes, especially complex I in protein level (**Figure 30D**). Finally, we measured the oxygen consumption rate (OCR) using seahorse XFe96 analyzer and uncovered that both the basal level and maximal level of OCR increased in KO cells (**Figure 30E**).

To confirm that increased mitochondrial activity is mediated by depletion of FASTKD1, we re-expressed FASTKD1 in ko-1 cells, which in turn repressed the mitochondrial gene expression (**Figure 30F**). In addition, mtDNA copy number showed no significant difference between control and knockout cells, which is consistent with previous study uncovering that FASTKD1 regulates post-transcriptional processes of mitochondrial genes (**Figure 30H**).

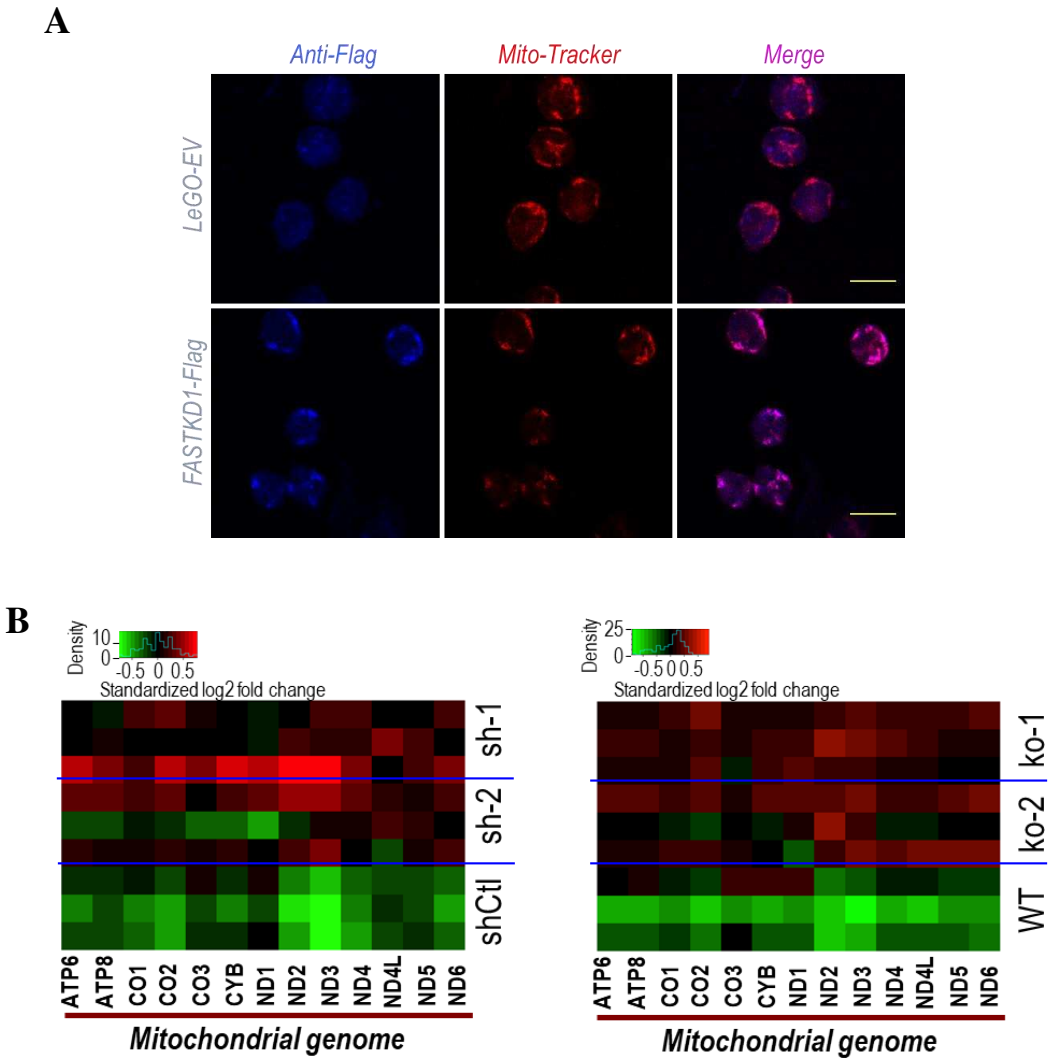
A
Anti-Flag
Mito-Tracker
Merge
LeGO-EV
FASTKD1-Flag
B
Density
Standardized log2 fold change
sh-1
sh-2
shCtl
ko-1
ko-2
WT
ATP6 ATP8 CO1 CO2 CO3 CYB ND1 ND2 ND3 ND4 ND4L ND5 ND6
Mitochondrial genome
C
Relative mRNA level
shCtl sh-1 sh-2 sh-3 sh-4 sh-5
WT ko-1 ko-2
ND2
ND3

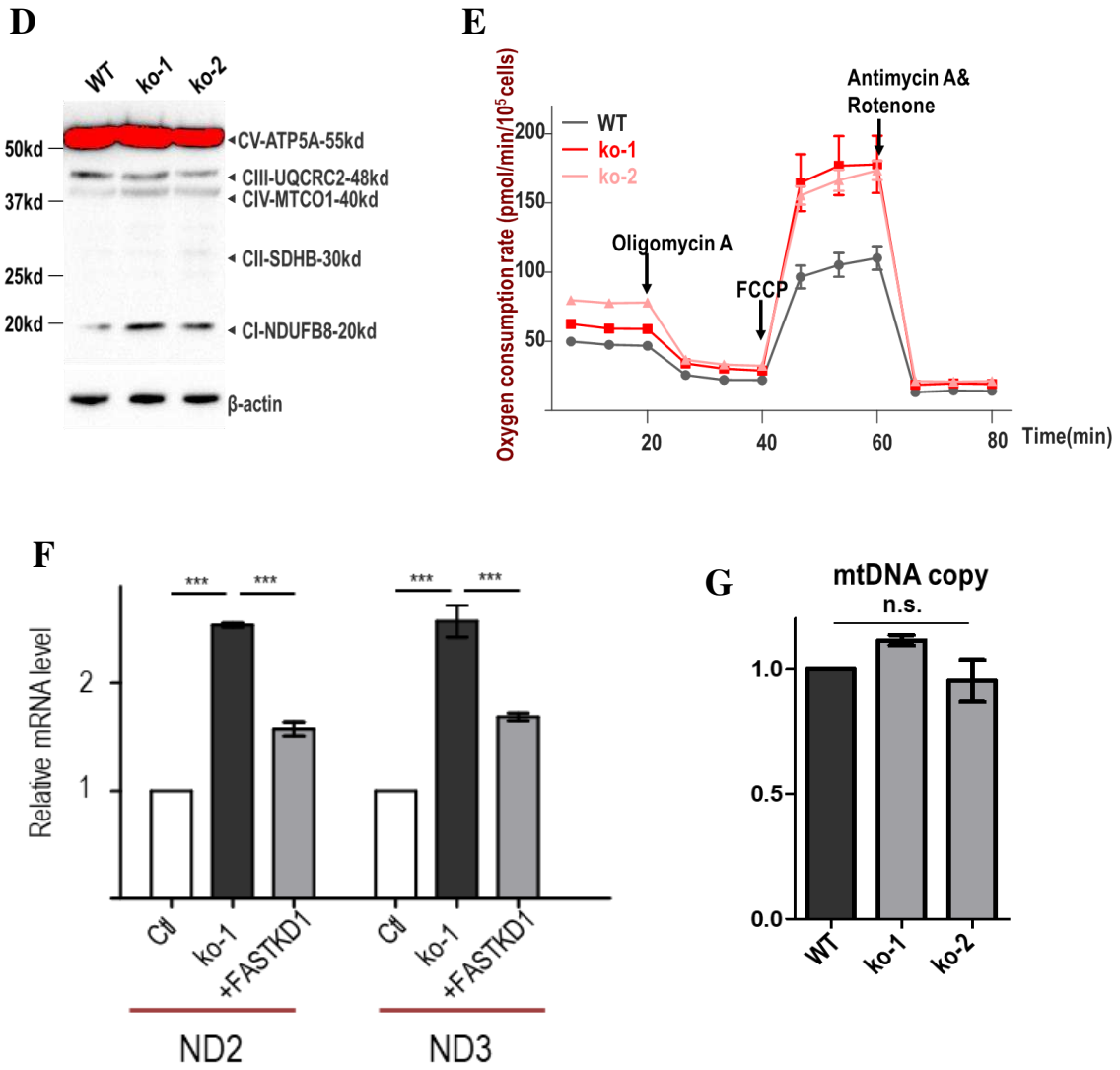

Figure 30. FASTKD1 is a negative regulator of mitochondrial respiration.

A. Immunofluorescence to detect the localization of FASTKD1-flag in overexpressing cell line. Anti-Flag signal overlaps Mitotracker dye. Scale bar = 50µM.

B. Heatmap of mitochondrial transcriptomic data of FASTKD1 knockdown (sh-1, sh-2) and knockout (ko-1, ko-2) cell lines (REH). Data shown are from three independent RNA extractions.

C. Relative level of ND2 and ND3 in FASTKD1 knockdown (left) and knockout (right); GAPDH was used as internal control. Fold changes of gene expression level were calculated via $2^{-\Delta\Delta Ct}$ and are represented by mean ± SEM based on at least three independent experiments. Statistical differences between WT and two knockout clones, or between shCtl and shRNAs groups were calculated with Fisher's LSD post one-way ANOVA test using SPSS v20. * p<0.05, ** p<0.01, ***p<0.001.

D. Protein level of OXPHOS complexes. OXPHOS cocktail antibodies were used to probe each respiratory complex. Complex I is represented by NDUFB8 subunit, Complex II is represented by SDHB, Complex III is represented by UQCRC2, Complex IV is represented by COX1, Complex V (ATP synthase) is represented by ATP5A subunit.

E. Mitochondrial activity assessed by seahorse XFe96 mito stress test. Oxygen consumption rate (OCR, pmol/min per 1×10^5 cells) was measured at basal level as well as after injection of Oligomycin A (1 µM), FCCP (1 µM), Rotenone (0.5 µM) and Antimycin A (1 µM) respectively. Data shown are Mean ± SEM based on 5 replicates of seeding cells.

F. Quantification of ND2 and ND3 relative level after FASTKD1 was re-expressed into ko-1 cell lines with qPCR. Data shown are mean ± SEM based on 3 RNA extractions. GAPDH was used as internal control. Statistical analysis was done as indicated in **C**.

G. mtDNA copy number was determined using qPCR. The relative quantity of mtCOX normalized by actin gene (DNA) in ko-1, ko-2 and WT cells was shown in the figure. Data are represented by mean ± SEM based on 3 DNA extractions. Statistical significance was determined using one-way ANOVA. n.s. not significant.

2. Mitochondrial activity and β-oxidation drive histone PTMs

2.1 Mitochondrial metabolism drives histone modifications

It is well established that cell metabolism could influence nuclear gene expression by regulating DNA methylation or histones acetylation. Indeed, as previously discussed, metabolites can act as substrates (SAM, acetyl-CoAs etc) or cofactors (FAD, α-KG etc) for enzymes capable of adding or removing histone post-translational modifications. More emerging evidences suggest that in cancer cells, metabolic alterations and subsequent changes in chromatin modifications could potentially modulate cellular characteristics and impact tumor establishment and growth.

Since our previous data demonstrated that FASTKD1 could regulate the mitochondrial activity, we postulated that depletion of FASTKD1 might also affect mitochondrial metabolic activities and hence affect histone PTMs, specially histone acylation. To this end, we performed MS analysis in an unbiased manner the change of histone acylation with a focus on propionylation and butyrylation. As shown in **Figure 31A**, there is an increased level of H4K5 and H4K8/12bu in two ko cells compared to WT cells. We performed western blot analysis to validate these findings by an independent approach. After the knockout of FASTKD1, we observed an overall change in various site-specific of histone modifications, especially affecting non-acetyl acylations: butyrylation, beta-hydroxybutyrylation, crotonylation, lactylation and succinylation (**Figure 31B**). Since many of the novel acylations are of unknown function, we focused our latter research on histone crotonylation and butyrylation, which have been reported to mark active transcription. Interestingly, our data showed that there was an increase in H4 lysine 5/8 butyrylation/crotonylation in FASTKD1 KO cells, while no significant change was observed in acetylation of the same sites (**Figure 31B**). We further treated the cells with OXPHOS inhibitors, rotenone, which is known to inhibit complex I, and discovered a decrease of histone acylation (**Figure 31C**).

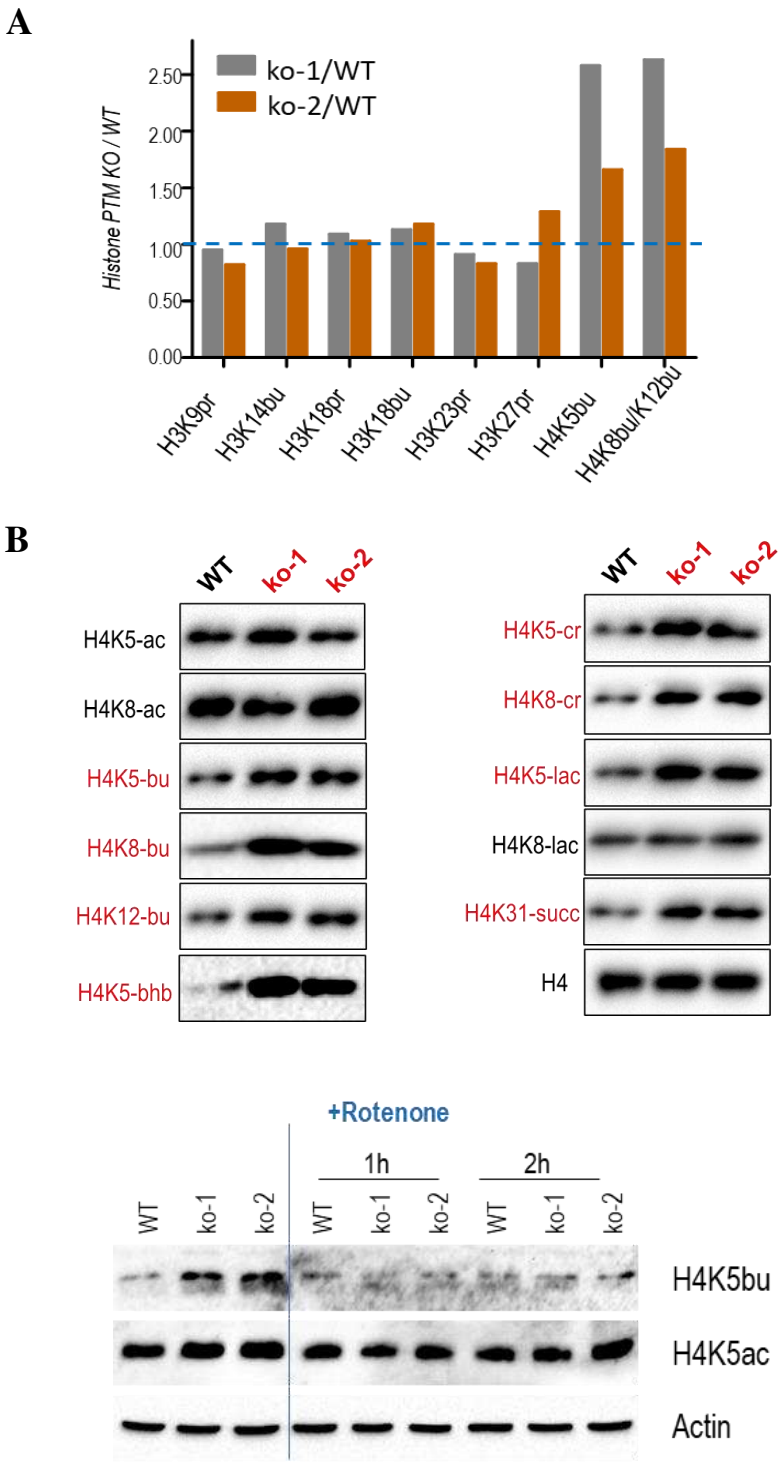

Figure 31. Mitochondrial activity drives histone modifications.

A. Histones acid extracts from WT and two knockout cell lines were subjected to HPLC/MS/MS to determine different H3 and H4 PTMs indicated in the figure. Column represents the relative amount in KO versus WT.

B. Western blot of the indicated histone PTMs using total cell protein extracts from WT and two ko cell lines. Histone acetylation (ac), butyrylation (bu), crotonylation (cr), β-hydroxybutyrylation (bhb), lactylation (lac), and succinylation were probed with indicated site-specific anti-PTM antibodies.

C. WT and knockout cells (ko-1, ko-2) were exposed to 0.5µM rotenone for the indicated time. Total protein was used for probing H4K5bu and H4K5ac.

2.2 Fatty acid metabolism (β-oxidation) is a major driver of histone acetylation-acylation

Acyl-CoAs are predominantly involved in lipid metabolism, including FA biosynthesis, degradation. They are also involved in ketogenesis, ketolysis and amino acid catabolism. Since in KO cells, several acylations marks (bu, cr, bhb) changed, from a biochemical point of view, we hypothesized that fatty acid metabolism could be involved. To study the role of fatty acid metabolism in histone acylation, we take advantage of some compounds that either fuels or inhibit fatty acid metabolism (Figure 32A). Octanoate is an 8-carbon fatty acid which is known to fuel beta-oxidation. Addition of octanoate to the cell culture medium drastically enhanced the overall level of histone modifications, including acetylation, butyrylation, and crotonylation (Figure 32B). Additionally, treatment of cells with crotonate (4 carbon non-saturated fatty acid) not only increased histone crotonylation but also acetylation (Figure 32

Figure 32**C**). Repressing acyl-CoA thiolase (KAT) involved in β-oxidation spiral with ranolazine attenuates the basal, as well as octanoate induced acetylation and acylation (Figure 32**D**). Furthermore, inhibition of long chain fatty acid-CoA synthetase (ACSL) enzymes with Triacsin C, or of acetyl-CoA carboxylase 1 (ACACA, producing malonyl-CoA from acety-CoA in lipid de novo synthesis) with ND-630 reduced histone acylation (Figure 32**E&F**). Finally, we also knocked down key enzymes in β-oxidation. These data suggest that β-oxidation indeed might be the important pathway in driving histone acylation and acetylation.

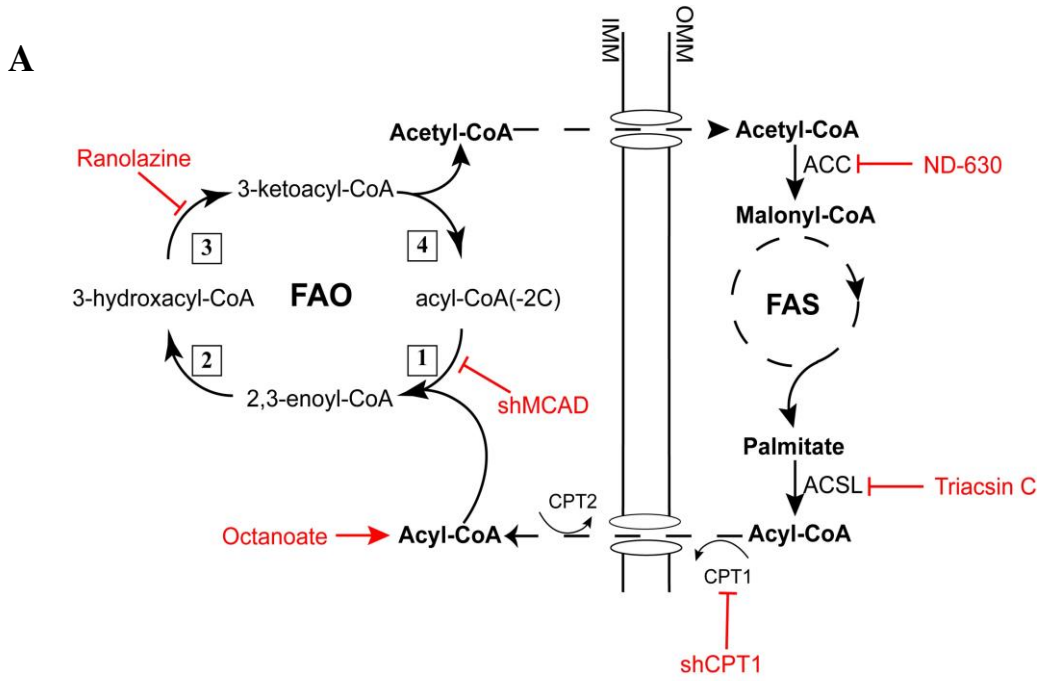
A
IMM
OMM
Acetyl-CoA
Acetyl-CoA
Ranolazine
3-ketoacyl-CoA
ACC
ND-630
Malonyl-CoA
3
4
3-hydroxacyl-CoA
FAO
acyl-CoA(-2C)
FAS
2
1
2,3-enoyl-CoA
shMCAD
Palmitate
ACSL
Triacsin C
CPT2
Octanoate
Acyl-CoA
Acyl-CoA
CPT1
shCPT1

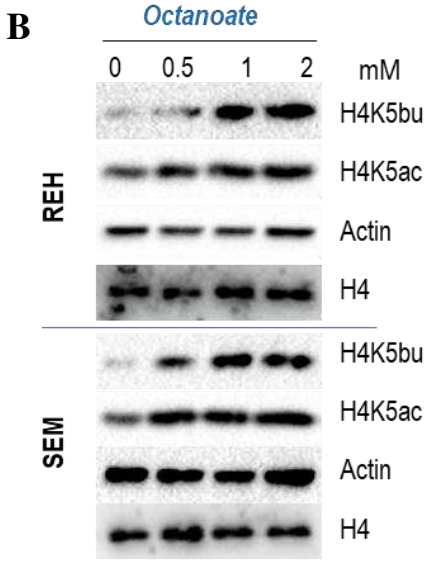
B
Octanoate
0 0.5 1 2 mM
REH
H4K5bu
H4K5ac
Actin
H4
SEM
H4K5bu
H4K5ac
Actin
H4

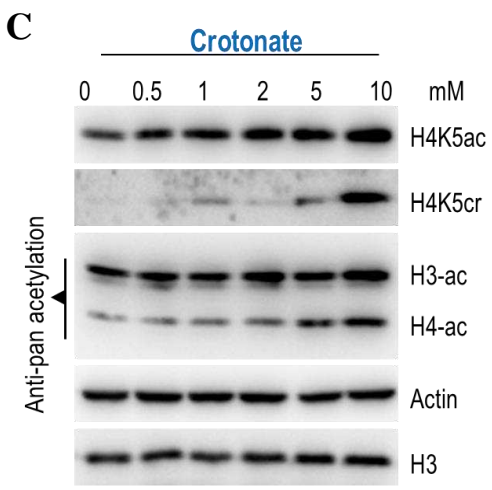
C
Crotonate
0 0.5 1 2 5 10 mM
H4K5ac
H4K5cr
Anti-pan acetylation
H3-ac
H4-ac
Actin
H3

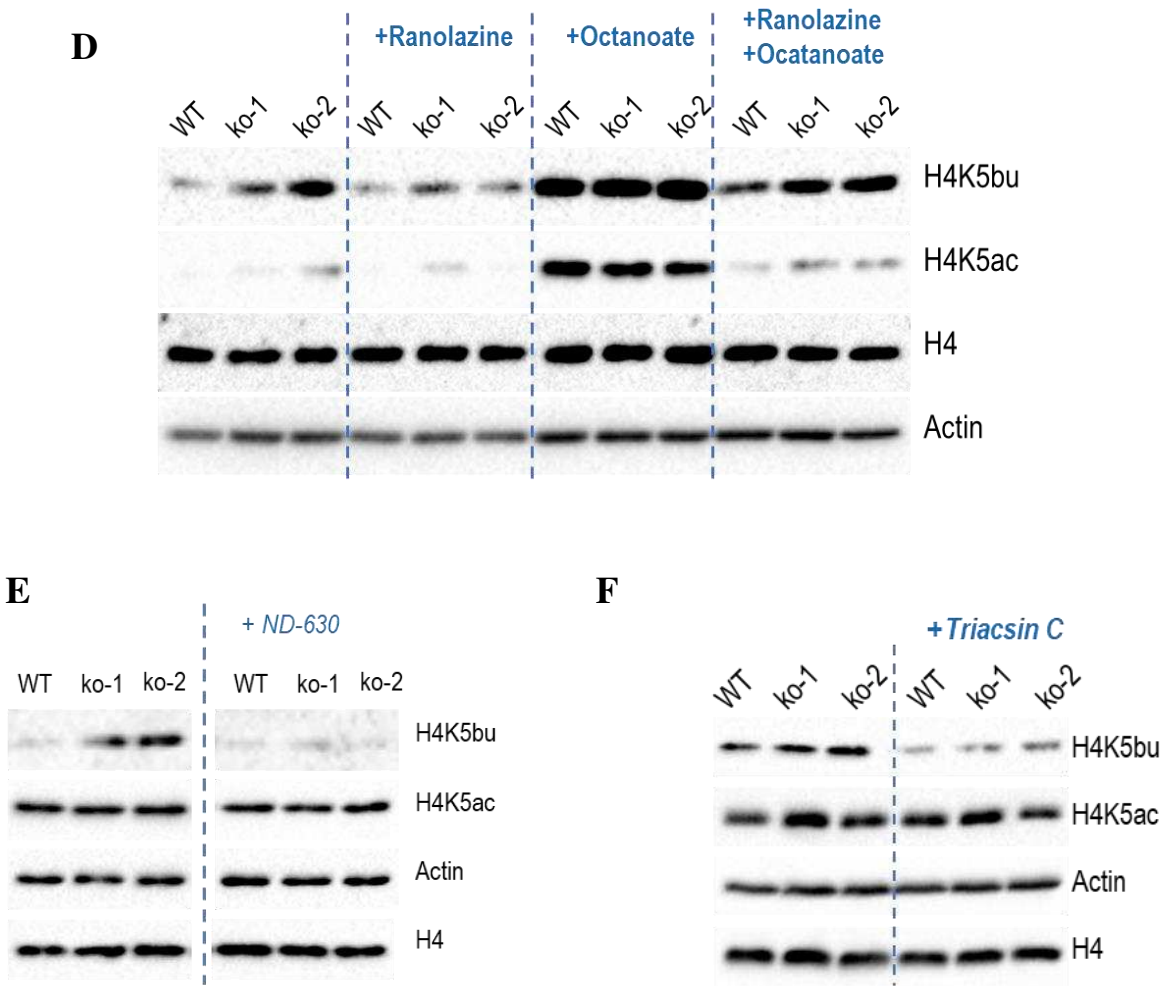

Figure 32. β-oxidation drives histone acylations.

A. Treatment strategy targeting fatty acid metabolism. ACC, Acetyl-CoA carboxylase; ACSL, long chain acyl-CoA ligase; CPT, carnitine palmitoyltransferase.

Western blot analysis of H4K5ac and H4K5bu were performed in urea cell extracts from cells pre-treated with the indicated chemical compounds. REH (upper panel) and SEM (lower panel) cells were treated with octanoate for 24 hours with the indicated concentrations (**B**). REH was treated with crotonate for 6 hours with the indicated concentrations before western blot analysis (**C**). REH WT and two ko cell lines were exposed to 0.3 mM ranolazine with and without 2 mM octanoate for 24 hours (**D**), or with100 nM ND-630 for 6 hours (**E**) , or with 3 µM Triacsin C for 16h (**F**).

2.3 Mitochondrial activity is associated with β-oxidation and histone acylation in B-ALL patients' samples

Inspired by our data one cell lines, we come back to ALL patients' samples. Bone marrow samples from a cohort of 31 B-ALL patients were acquired and protein and RNA were extracted in parallel and used to monitor specific gene expression by RT-qPCR and the occurrence of histone PTMs by ELISA. First, we found that CPT1A mRNA level is highly correlated with ND2 (rs = 0.531) and ND3 (rs = 0.508) (**Figure 33A, B**), implicating the correlation of mitochondrial activity and β-oxidation in patients. Besides, the positive correlation between

mitochondrial activity and histone acylation (H4K5cr/bu), and between CPT1A and H4K5cr/bu were determined in B-ALL patients (**Figure 33C, D**).

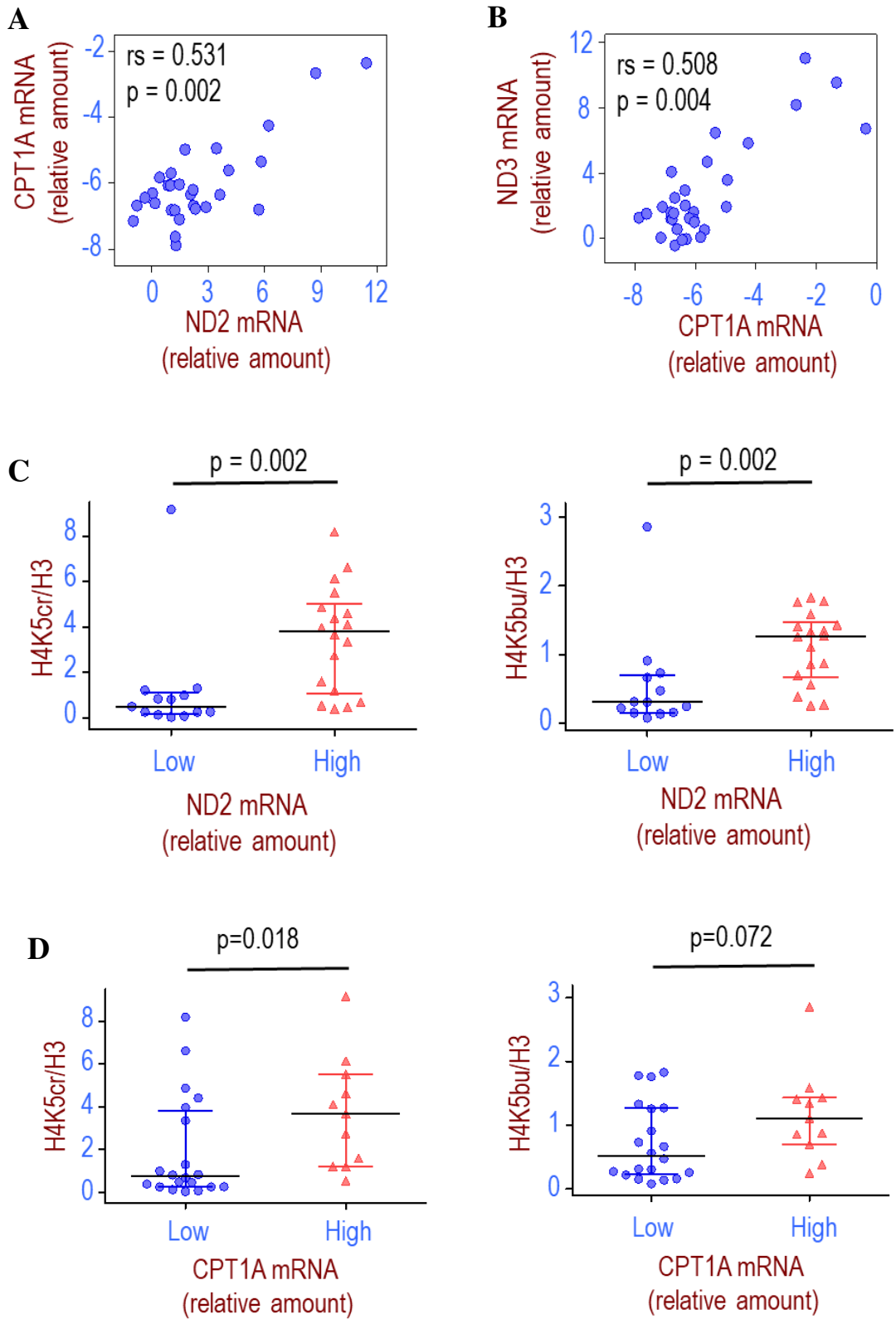

Figure 33. Mitochondrial activity is associated with β-oxidation and histone acylation in B-ALL patients.

RNAs and proteins were extracted from same batch of patients' bone marrow mononuclear cells samples (n=31) using AllPrep DNA/RNA/Protein Mini Kit (Qiagen). ND3 and CPT1A mRNA levels were determined by RT-qPCR and were represented by -ΔCt (subtracted from GAPDH). H4K5cr and H4K5bu were measured by ELISA normalized with respect to H3. Correlation of ND2 and CPT1 mRNA levels (**A**) and ND3 and CPT1A mRNA levels (**B**) were determined by spearman correlation. rs and P value are indicated at corresponding figures.
C. Patients were divided into two groups using ROC curve according to the contribution of ND2 (**C**) or CPT1A (**D**) value to H4K5cr/bu. Patients with low level of ND2 (n=13) have reduced level of H4K5cr/bu compared to high ND2 group (n=18). Similarly, patients with low level of CPT1A (n=20) have reduced level of H4K5cr/bu compared to high CPT1A group (n=11). Each dot or triangle represent one individual. Bar is median ± quartile range.

3. Acyl/acetyl determines the dynamic interaction of BET with chromatin

3.1 BRD4 binds acetylated but not K5 acylated histones

BET family proteins are important readers that link acetylation with transcriptional regulation. Previous study indicated that first bromodomain (BD1) of BRDT accommodates diacetylated lysine residue (H4K5acK8ac) but not when the K5 residue is butyrylated (i.e., H4K5buK8ac). Therefore the ratio of acyl/acetyl might impact BET-chromatin interaction dynamics: higher ratio disfavors BRDT-chromatin interaction, resulting in a loose and dynamic bound state, while a decreased ratio favors a tight binding and leads to a stable interaction[145]. We noticed that FASTKD1-mediated mitochondrial activity prominently impacts non-acetyl acylations but not acetylations, therefore we decided to take this cell model as a tool to test such hypothesis. In this setting, we considered BRD4, the ubiquitously expressed BET protein. We tested BRD4's ability to bind H4K5 and K8 ac/bu peptides following a pull down experiment. As expected, BRD4's binding to an acetylated H4 tail peptide can be inhibited by butyrylation, especially H4K5bu (**Figure 34**).

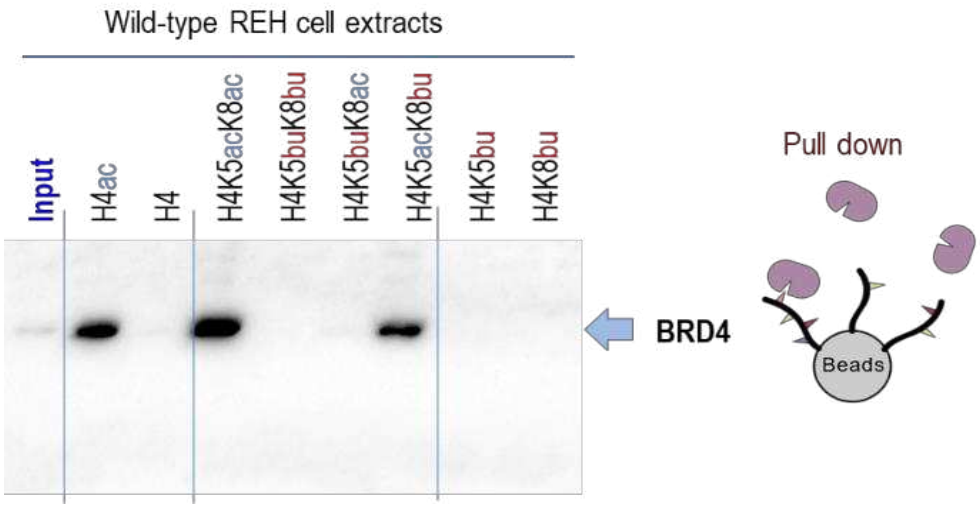

Figure 34. The binding of BRD4 to acetylated peptides are perturbed by K5bu.

Cell extracts were prepared from REH WT cells and was incubated with beads conjugated with the indicated modified peptides. BRD4 was visualized after the pull-down assays.

3.2 Acyl/acetyl ratio determines BRD4 binding affinity to chromatin in REH cells

As described in the introduction part, we proposed the hypothesis that BRD4 binds to chromatin in a dynamic manner, furthermore, such binding dynamics is determined by acyl/acetyl ratio. Since our previous data suggested that the depletion of FASTKD1 increases dramatically histone butyrylation and crotonylation but not significantly acetylation. This situation should in turn result in an increased acyl/acetyl ratio. We decided to take use of these cell line models to verify our hypothesis. Firstly, we confirmed that the altered acyl/acetyl did not change the amount of total BRD4, nor the ability of BRD4 binding with chromatin in control and KO cell lines (**Figure 35A**). To visualize the bound state of BRD4 to chromatin, we took advantage of salt elution assay and JQ1 dissociation assay. Indeed, we obtained more soluble BRD4 in KO cells using a lysis buffer containing 200 mM NaCl compared to WT cells, which suggest less tightly bound state of BRD4 to chromatin in KO cells (**Figure 35B**). Similarly, when treating cells with low dose of JQ1 to competitively dissociate BRD4 with chromatin, we obtained more soluble BRD4 in KO cells, which is in accord with a more dynamic binding in vivo (**Figure 35C**). Furthermore, we treated REH cell nuclei with butyryl-CoA to increase butyryl/acetyl ratio and performed salt elution assay to obtain BRD4. As shown in **Figure 35D**, we eluted more BRD4 in butyryl-CoA treated compared to control cell nuclei. Collectively, these data suggest that increased acyl/acetyl ratio contributes to loosely bound state between BRD4 and chromatin in REH cells.

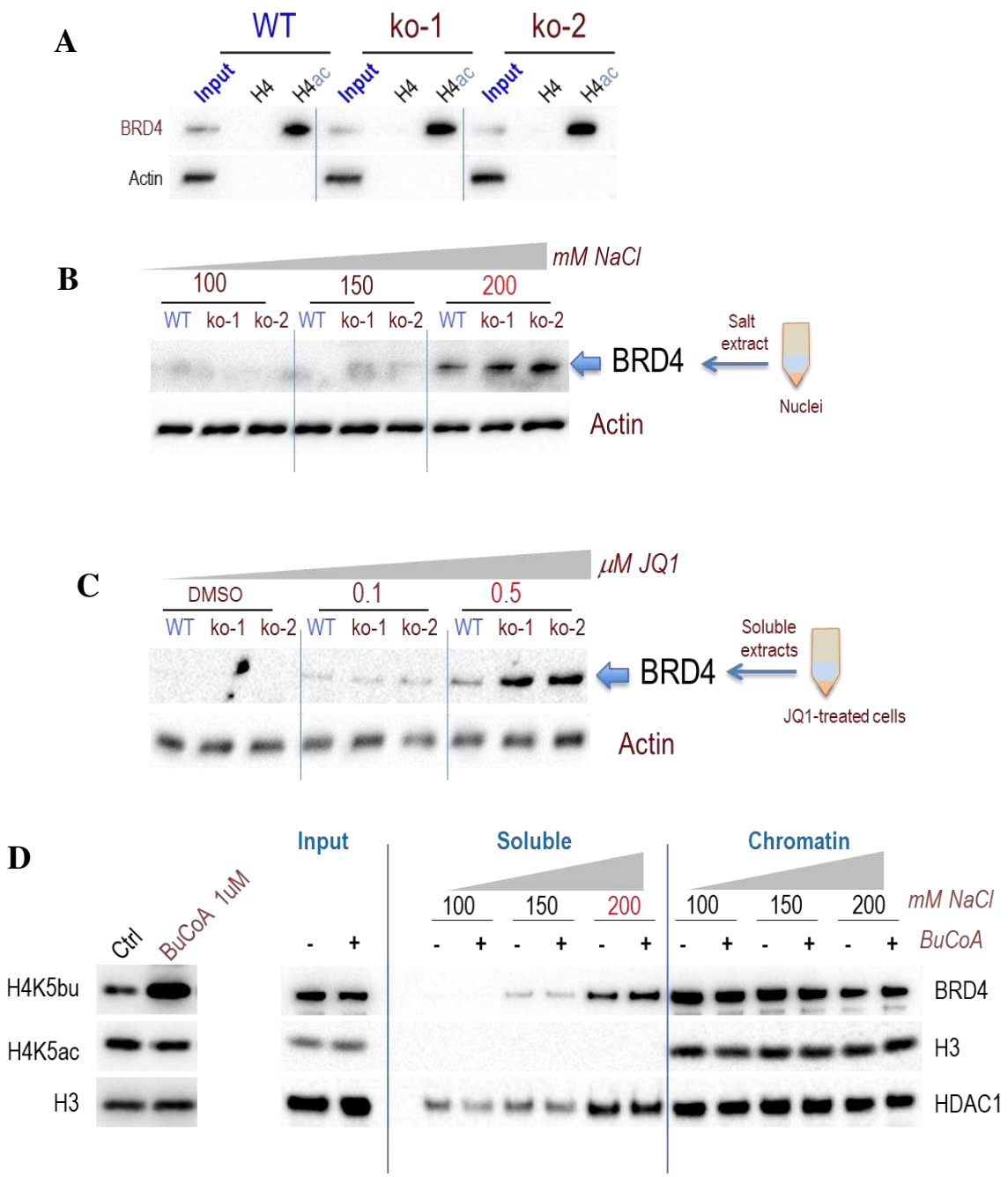

Figure 35. Acyl/acetyl ratio determines the BRD4 binding affinity to chromatin.

A. REH WT and two KO cell lines were extracted with lysis buffer containing 500 mM salt, the supernatants containing total BRD4 were then collected and diluted to reach a concentration of 250 mM, which used in a peptide pull-down assay with the indicated peptides. BRD4 was then eluted from beads and probed following a western blot analysis.

B. REH WT and two KO cells were used to extract proteins with lysis buffers containing increased concentrations of NaCl. After centrifugation to pellet nuclei, supernatants were used to detect soluble BRD4. In this figure BRD4 appeared to be less tightly bound to chromatin in KO cell groups when salt concentrations reached 200mM (red text).

C. Western blot of soluble BRD4 dissociated by JQ1. WT and two ko cell lines were pre-exposed to JQ1 (concentrations as indicated) before cell lysis in a buffer containing 100 mM NaCl. Less tightly bound BRD4 was dissociated from chromatin in KO cells when treated with 0.5 μM JQ1.
D. Nuclei from REH cells were used for acylation reaction. Left panel shows the H4K5bu and H4K5ac level after acylation reaction. Acylated nuclei were used in a salt elution assay similar to **B** (right panel).

3.3 Acyl/acetyl ratio determines BRD4-chromatin binding dynamics in COS-7 cells

Previously, Pr. Heinz Neumann and Dr. Martin Spinck constructed several mutants of CobB which displayed distinctive deacetylase, decrotonylase or debutyrylase activity[730]. We therefore transfected this protein and its mutants in order to change the balance of acylation/acetylation status. Unfortunately, we failed to establish stable changes of de-ac/bu/cr marks after transient transfection of either wild type or mutated CobB following different series of experiments (data not shown). We also established stable cell lines expressing wild type CobB and managed to obtain a stable increased acyl/acetyl ratio in CobB-expressing cells. The increased acyl/acetyl ratio was observed both with western blot analysis and ELISA (**Figure 36A&B**). Next, we performed salt elution assay in control and CobB-expressing cells. Similarly, we obtained more soluble BRD4 in CobB expressing cells, which is in accord with a more dynamic binding of BRD4 in this group of cells. To visualize the dynamics of BRD4 in live cells, we decided to perform FRAP experiment on BRD4. According to our previous experience, BRD4 was found to be very dynamic in COS cells. Therefore we reasoned that it might be difficult to record an even more dynamic movement by FARP on BRD4 in COS-CobB cells. To solve this problem, we performed FRAP experiment on BRD4-NUT, given that it forms stable foci on chromatin dependent on histone acetylation and BRD4 bromodomains[471]. Using this system, we observed faster recovery after photobleaching, with shorter t1/2 of recovery time in CobB transfected cells (6.26 ± 0.33s VS 8.94 ± 0.73s, and a higher mobile fraction in CobB expressing cells (0.84 ± 0.05 VS 0.76 ± 0.02), indicative of a more dynamic binding of BRD4 in CobB expressing group (**Figure 36C&D**). These data suggest that acyl/acetyl ratio determines binding dynamics between BRD4 and chromatin.

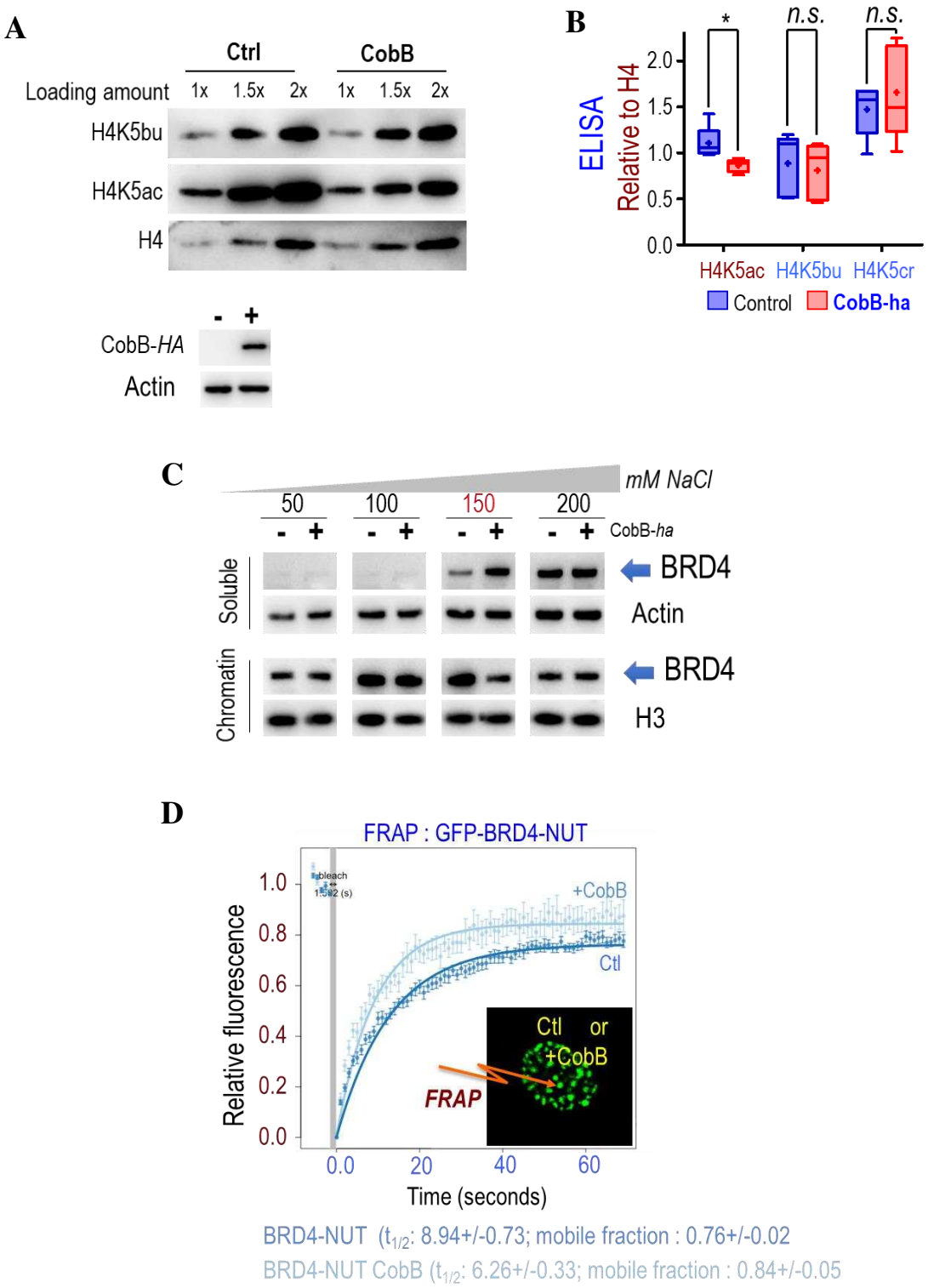

Figure 36. Acyl/acetyl ratio determines BRD4-chromatin binding dynamics in COS-7 cells.

A. COS-7 cells stably expressing CobB were used in this experiment. Left panels showed the levels of histones acetylation and butyrylation in control and CobB expressing cells. Left panel shows the expression of the exogenous CobB-HA.

B. H4K5ac, H4K5bu, H4K5cr levels were determined between control and CobB-expressing COS-7 cells. CobB expressing cells displayed a significant decreased H4K5ac but mildly decreased H4K5bu and H4K5cr. Median and interquartile range from 5 datasets are plotted in the boxplot and the Whiskers represent the top and bottom quartiles. Mean values were indicated as "+".

C. COS-7 control and CobB-expressing cells were extracted with lysis buffer containing increased concentrations of NaCl. After centrifugation to pellet nuclei, supernatants were used to detect soluble BRD4. In this figure BRD4 appeared less tightly bound to chromatin in CobB-expressing group when salt concentrations reached 150 mM (red text).

D. FRAP experiment on BRDR-NUT was performed in COS-7 control and in CobB-expressing cells and GFP florescence was recorded after photobleaching. Datasets for each cell group were individually fitted onto the single exponential model described in materials and methods. Data shown is mean± 2SEM based on 8 replicates. The t1/2 values were calculated from the FARP curve.

4. Acyl/acetyl drives BET redistribution across genome

4.1 H4K5cr is enriched on highly acetylated chromatin and is associated with active transcription

We performed ChIP-seq on H4K5cr, H4K5ac to visualize the distribution of these marks across the genome. RNA-seq analysis was also performed to determine the transcriptional output of these alterations. First, we confirmed the correlation between histone acylation (H4K5cr in our case) with transcriptional activation, as it has been characterized and reported in previous publications[142, 144, 167]. Furthermore, we identified that higher H4K5cr/ac ratio marks the most active genes (**Figure 37A**). Ever since the discovery of short chain histone acylations, these marks have been suggested to be redundant with acetylation, given that they overlap with acetylation and are relatively of low abundance. However, in our work, we uncovered that the correlation between histone acetylation and crotonylation does not always follow a linear correlation. Indeed, by comparing all the genes TSSs' coverage of these two marks, we identified that at low level of histone acetylation, there is a linear correlation between H4K5ac and H4K5cr, whereas, at high levels of acetylation, a 3rd degree polynomial correlation better fits their correlation (**Figure 37B, right panel**). Besides, we found that in FASTKD1 KO cells which harbor increased acyl/acetyl, such deviation between the fitted linear correlation and 3rd degree polynomial correlation is even more obvious (**Figure 37B, left panel**). Collectively, these data suggest that, H4K5cr preferentially occurs on highly acetylated area and covers the highly active genes.

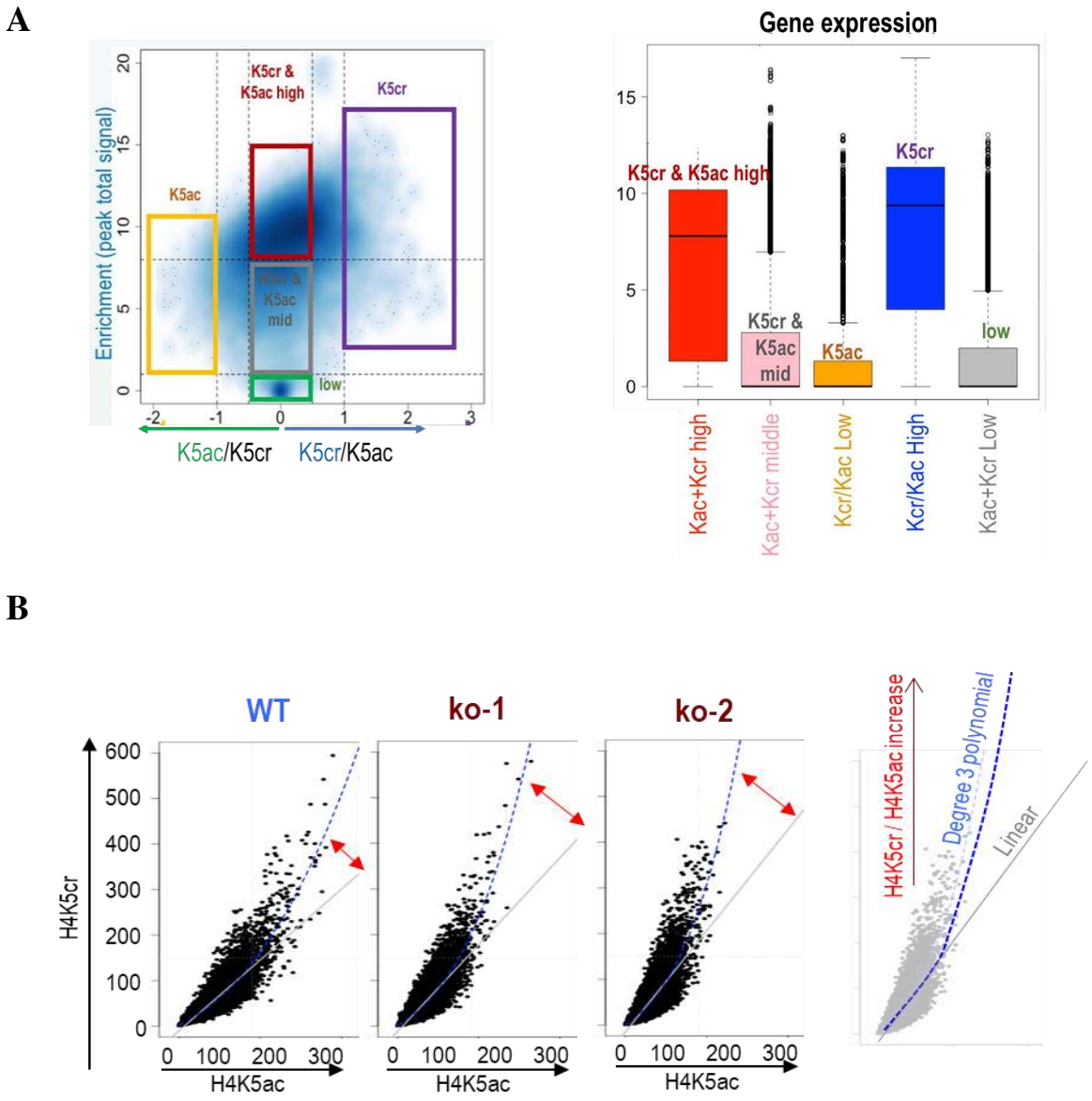

Figure 37. H4K5cr is enriched on the highly acetylated TSS regions and is associated with active transcription.

A. Heatmap of H4K5cr and H4K5ac distribution across genome from WT cells. According to the level of H4K5ac/cr ratio, genes are divided into 5 groups, as shown in the figure (left panel). Those which are covered by high H4K5cr/ac marks are most highly transcribed (right panel).

B. Total level of H4K5ac and H4K5cr on gene TSSs. As shown in the figure, most gene TSSs which are covered with low to median level of H4K5ac are also covered with modest level of H4K5cr, as shown by the linear correlation between H4K5ac and H4K5cr in the figure. However, genes that are covered by very high level of H4K5ac are covered with extremely high level of H4K5cr, as shown by the 3rd degree polynomial correlation between H4K5ac and H4K5cr. In ko-1 and ko-2 cells, the polynomial correlation is even more obvious than the control cells, as indicated by the red arrows in the figure.

4.2 Altered H4K5cr/ac drives a redistribution of BRD4 genomic localization

As described above, our previous results suggested that a higher acyl/acetyl ratio favors the dynamic movement of BRD4. Since the total amount of BRD4 does not increase in KO cells,

we hypothesized that the increasing acyl/acetyl ratio might result in a re-distribution of BRD4 on genomic regions. To characterize the genomic distribution of BRD4, we performed ChIP-seq analysis. We could identify that BRD4 is enriched over the nucleosome free region (NFR) surrounded by the +1 and -1 nucleosomes (**Figure 38A, left panel**). When grouping gene TSS regions (± 2000bp) according to their transcriptional activity, we better visualized that H4K5cr, H4K5ac and BRD4 preferentially cover active genes (**Figure 38A**). In the case of BRD4, the highly active genes are covered by high levels of BRD4 on the NFR-associated regions (**Figure 38B**). In addition, cells with an increased acyl/acetyl ratio (FASTKD1 KO), we observed an increased enrichment of BRD4 at the NFR regions. These data suggest that, upon increased acyl/acetyl marks, BRD4 can be released from various genomic regions towards the NFRs of active genes.

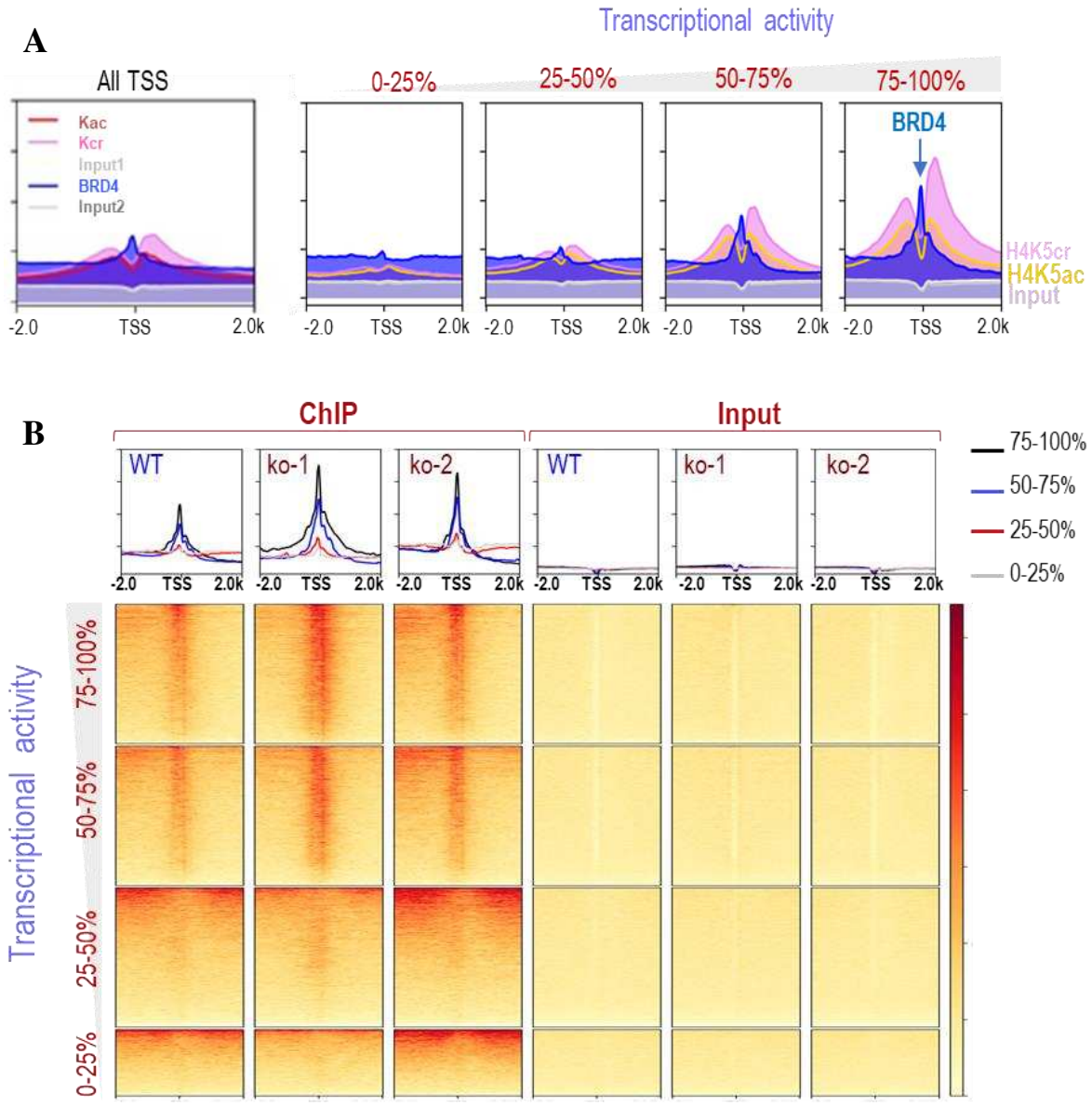

Figure 38. H4K5cr/ac ratio confers to BRD4 genomic re-distribution.

Anti-BRD4, H4K5ac and H4K5cr ChIP were performed in WT, ko-1 and ko-2 cells.

A. (Left panel) Distribution of BRD4 on all TSS regions (TSS ± 2000). A peak on nucleosome free regions (NFRs) other than -1/+1 nucleosome was identified at TSS (shown as blue). TSS regions were then divided into four groups according to their expression state (right panels). H4K5ac, H4K5cr and BRD4 distributions were indicated in each group of genes. As shown in the figure, the most highly expressed genes are associated with high H4K5cr and H4K5ac, and are mostly enriched with BRD4 at NFRs.
B. ChIP signals of BRD4 were mapped on TSS regions in different groups described in **A**. As shown in the figure, the most highly expressed genes are mostly enriched with BRD4 at NFRs, in ko-1 and ko-2, such enrichment is more obvious.

4.3 Genomic redistribution of BRD4 regulates the expression of sets of genes in REH cells and ALL patients

BRD4 is a master regulator of gene transcription, therefore the redistribution of BRD4 should result in an alteration of specific gene transcription. To uncover the transcriptional changes mediated by BRD4, we treated the WT cells with BRD4 bromodomain inhibitor, JQ1 and performed RNA-seq analysis. Using GSEA, we identified that a subset of genes upregulated in FASTKD1 KO cells are enriched in genes downregulated in JQ1 treated cells. Of note, we also identified a subset of genes upregulated in FASTKD1 KO cells enriched in downregulated genes in JQ1 treated cells (**Figure 39A, B**). This data demonstrate that these two sets of genes in FASTKD1 KO groups are JQ1 sensitive, and the differential expression of these genes in KO compared to WT group is likely attributed to the redistribution of BRD4 in KO cells. Furthermore, we also identified that genes downregulated and upregulated in FASTKD1 KO groups are also enriched in different groups of B-ALL patients samples with high or low acylation level respectively (**Figure 39C, D**). We further performed Gene Ontology analysis and identified that genes that encode mitochondrial membrane protein, cell cycle are upregulated, while genes that encode stemness are downregulated in FASKTD1 KO cells or in JQ1 treated cells (**Figure 39E**).

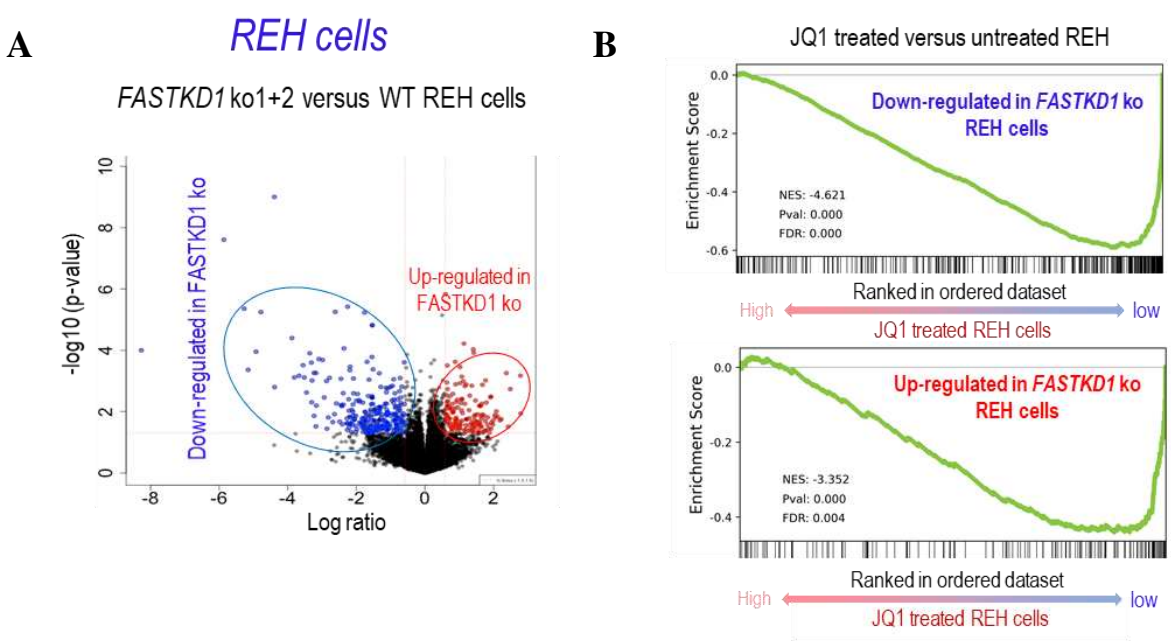
A
REH cells
FASTKD1 ko1+2 versus WT REH cells
-log10 (p-value)
Log ratio
Down-regulated in FASTKD1 ko
Up-regulated in FASTKD1 ko
B
JQ1 treated versus untreated REH
Enrichment Score
Down-regulated in FASTKD1 ko REH cells
NES: -4.621
Pval: 0.000
FDR: 0.000
Ranked in ordered dataset
High
low
JQ1 treated REH cells
Up-regulated in FASTKD1 ko REH cells
NES: -3.352
Pval: 0.000
FDR: 0.004
Ranked in ordered dataset
High
low
JQ1 treated REH cells

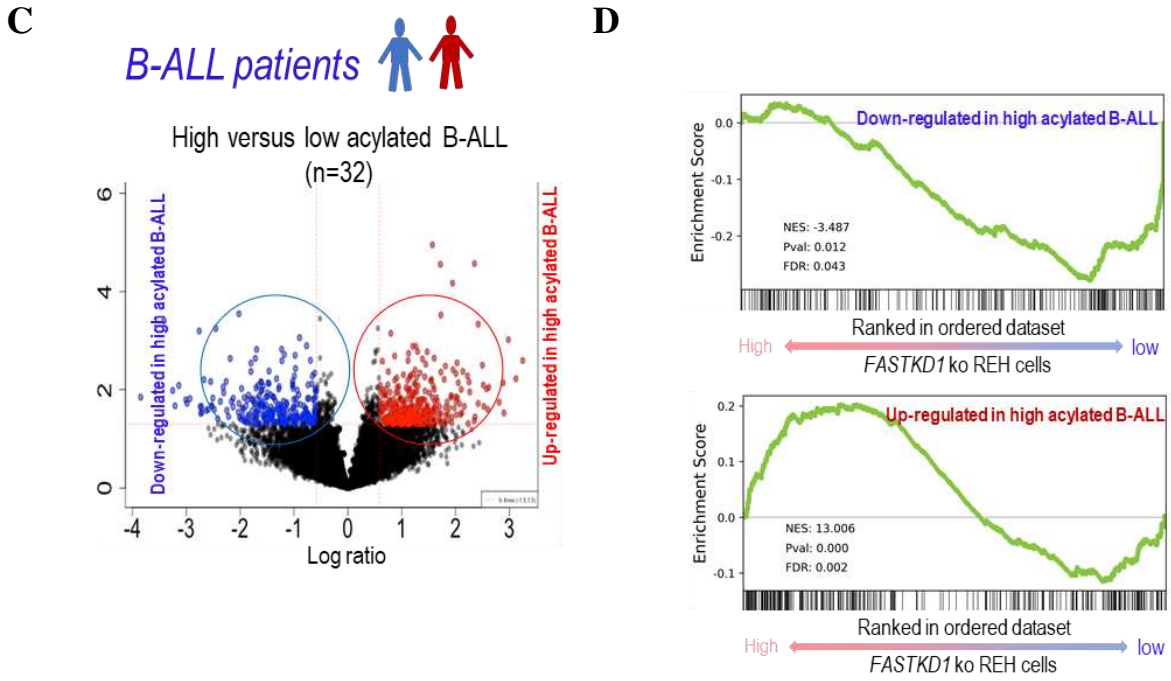
C
B-ALL patients
High versus low acylated B-ALL
(n=32)
Down-regulated in high acylated B-ALL
Up-regulated in high acylated B-ALL
Log ratio
D
Enrichment Score
Down-regulated in high acylated B-ALL
NES: -3.487
Pval: 0.012
FDR: 0.043
Ranked in ordered dataset
High
low
FASTKD1 ko REH cells
Up-regulated in high acylated B-ALL
NES: 13.006
Pval: 0.000
FDR: 0.002
Ranked in ordered dataset
High
low
FASTKD1 ko REH cells

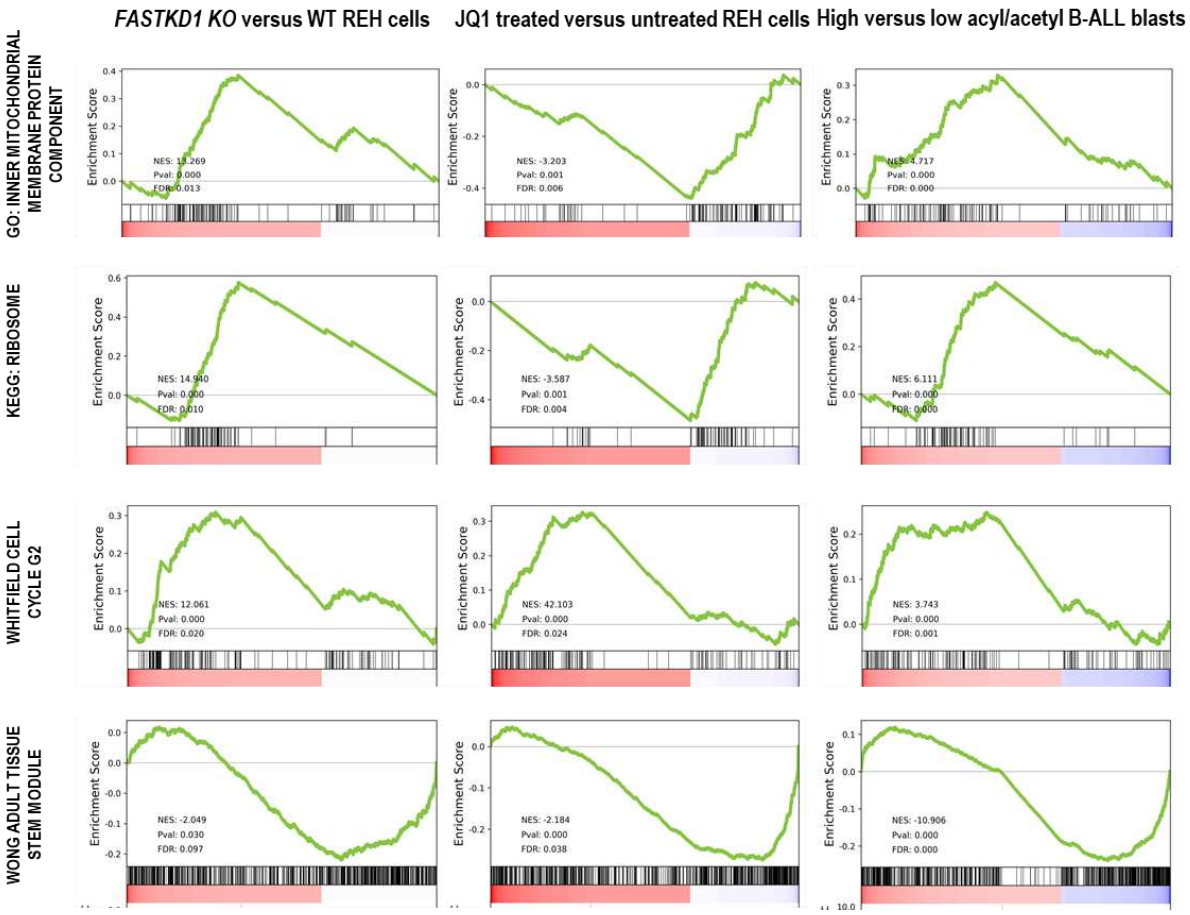

Figure 39. Genomic redistribution of BRD4 regulates specific sets of genes in REH cells and ALL patients.

Volcano plot demonstrating the differential gene expression signature between FASTKD1 KO (**A**) and control, and between B-ALL blasts with high H4K5 acylations (crotonylation and/or butyrylation, n = 15) and B-ALL blasts with low acylations (n = 10) (**C**). Y axis: -log10 (p-value); x-axis: log (ratio of normalized expression values between ko and WT cells) (**A**), log (ratio of normalized expression values between B-ALL with high and low acylation levels) (**C**). The genes down-regulated or up-regulated with a fold change >1.5 and a Student t-test p-value < 0.05 are respectively represented in blue and red.

B. The two gene groups defined in **A** were respectively used as genesets for GSEA plots to test for their enrichment/depletion in the JQ1-treated REH cells. These plots show a significant depletion of genes up or down regulated in FASTKD1 KO cells. These genes are therefore JQ1 sensitive.

D. The two gene groups defined in **C** were respectively used as genesets for GSEA plots to test for their enrichment/depletion in the FASTKD1 KO cells. These plots show significant depletion or enrichment of genes respectively down or up regulated in FASTKD1 KO cells suggesting that the transcriptional effect of high acylation in B-ALL blasts is similar to the effect of FASTKD1 ko- induced high acylation in REH cells.

E. GeneSet Enrichment Analysis (GSEA) plots representative of genesets enriched or depleted in the transcriptomic signature of KO versus WT cells (left panels), of JQ1 treated versus untreated (middle panels) REH cells and B-ALL with high versus low H4K5cr/bu levels (right panel). NES = normalized enrichment score; Pval =

nominal p-value, a p-value of 0 indicates a p-value < 1/2000 (since our analysis was performed with 2000 permutations); FDR = False discovery rate adjusted for gene set size and multiple hypotheses testing.

DISCUSSION

1. Oncogenic role of FASTKD1 in ALL

An increasing body of evidence established that reactivation of C/T genes initiates additional cell signaling required for cell transformation and tumor aggressiveness[702]. Based on this theory, my colleagues previously established specific data mining strategies to identify ectopically activated C/T genes, which are correlated with prognosis in ALL. Among the identified genes the expression of the single gene FASTKD1 predicts inferior outcome[711]. My PhD thesis project aimed to unravel the oncogenic role of this gene in ALL.

FASTKD1 belongs to the FASTK family, which are known to be involved in mitochondrial mtRNA biology, from RNA processing to translation. Among the six proteins of this family, FASTK, FASTKD2-5 have all been reported to be required for the proper expression of various mitochondrial mRNAs and are required for ETC stoichiometry and function[712]. In contrast, FASTKD1 appears to be the only member that negatively regulates mitochondrial mRNAs [721]. FASTK family proteins possess distinctive specificities over mitochondrial mRNAs. For instance, FASTK was reported to protect ND6 from mitochondrial degradosome-mediated degradation, while FASTKD1 specifically represses ND3 expression[719, 723, 738, 739]. FASTKD2 and FASTKD5 were characterized to profoundly regulate the overall biogenesis of mitochondrial proteins[722, 740].

In our previous experiment, we confirmed that FASTKD1 is a negative regulator in mtRNA biology. However, in our study, compared to Boehm and colleagues' study[721], depletion of FASTKD1 leads to an overall upregulation of mitochondrial mRNAs in addition of ND3. This discrepancy might be attributed to the different cell models used in our work. Besides, we uncovered that FASTKD1 does not influence mtDNA copy number of cells, implicating that it is the regulation of mitochondrial mRNAs. Indeed, our data indicate that FASTKD1 should act at transcriptional or post-transcriptional levels, such as RNA processing and degradation.

Previous studies indicate that OXPHOS activity is associated with cancer cell survival or tumor progression, although it remains enigmatic whether it is oncogenic or tumor-suppressive[741-743]. Traditionally, high OXPHOS activity generates high reactive oxygen species (ROS), which in turn damage the tumor cells. Indeed, this has been viewed as one of the major mechanisms underpinning dysfunctional mitochondrial activity in solid tumors. We also measured the ROS in FASTKD1-depleted cells but found no significant changes (data not shown), indicating that the redox balance could be well-maintained in our model system. As FASTKD1 represses mitochondrial respiration, we assumed that it might protect cells from stress. However, although we monitored various phenotypic changes after depletion or

overexpression of FASTKD1, no impact on the cell proliferation, chemotherapeutic responses and the cell cycle were observed. We also cultured FASTKD1-deleted and overexpressing cells to FBS starvation but still no significant difference was observed compare to control cells (data not shown). Such observations implicate that the oncogenic role of FASTKD1 in ALL is either modest or more delicate to detect.

Cancer aggressiveness relays on a series of pathological events that favor resilient cellular characteristics in cancer as well as the manifestation of refractory or relapsed diseases in the clinics. In general, aggressive cancers can be classified as: 1) cancer cells that are primarily resistant to therapies, i. e., the percentage of blasts barely reduces after the initial therapy; 2) the bulk of blasts is eliminated after initial therapy, but a small fraction of cells survive and induces the development of a tumor in a short term; 3) patients achieve morphological complete remission but develop relapse in the long run.

The primary resistance or short-term relapse might result from the enhanced ability of the cells to export chemotherapeutic drugs, or to acquired anti-apoptotic capabilities, etc. In contrast, long-term relapse is mediated by persistent cancer re-initiating cells. Such cancer re-initiating cells possess some common characteristics, such as dormancy and stemness[632]. Indeed, in the previous work leading to the identification of the six marker genes, thanks to their cell stratifying ability, we could uncovered that tumoral cells from patients who have poor outcome have acquired “stem-like” characteristics[711].

However, it is noteworthy that relapsed or refractory diseases are complex traits and could depend on may linked or independent oncogenic events. Indeed, we know that 1) the *in vivo* environment (e.g., bone marrow microenvironment) of tumoral cells is much more complicated than that of cell lines; 2) the relapse-inducing cells are minor clones; 3) the acquisition of cancer aggressiveness could be a multiple-step process. These considerations might partially explain why in our *in vitro* studies we did not detect any frank oncogenic activity associated with FASTKD1 expression.

In conclusion, this part of work addressed the repressive role of FASTKD1 on mitochondrial activity, and uncovered that FASTKD1 does not influence the proliferation nor the viability of REH cells in vitro. We also identified a correlation between the mitochondrial gene expression and prognosis by reviewing clinical data of B-ALL and T-ALL cohorts (not shown). Supporting the conclusion of our molecular studies. Collectively, this part of my work uncovered the correlation between mitochondrial activity and cancer prognosis in ALL.

2. Mitochondrial activity affects histone PTMs

It has long been established that cell metabolism affects histone modifications. Since more than two decades ago, the perturbation of acetyl-CoAs has been documented to impact the protein

acetylation, including histone acetylation[744, 745]. With the identification of novel types of modifications, including crotonylation, butyrylation, succinylation etc., more evidences have emerged concerning the process of cellular metabolism-driven histone modifications in physiology and diseases, including cancer.

For the last few decades, studies have revealed the spatiotemporal control of metabolite production. Indeed, metabolites, including acetyl-CoA, non-acetyl acyl-CoA have different subcellular compartments. Normally, cytosolic and nuclear compartments are believed to share the same metabolite pool because of the existence of permissive nuclear pores. Mitochondrion, however is a distinctive compartment because of its non-permissive membranes. Although transport systems have been characterized for the export of acetyl-CoA and import of fatty acids, there are still many obscure aspects of CoA derivatives' export that need to be understood.

Lately, more studies have described metabolite compartmentalization and the underlying mechanisms. Two new concepts have been introduced regarding the metabolism-driven histone modifications. Firstly, various metabolic enzymes, including the TCA enzymes have been to found to be located in the nucleus, whereby they produces the corresponding metabolites for histone modifcations[594]. Secondly, several studies indicate that other than the citrate shuttle, there might be unknown mechanisms regarding the metabolites cross-talk between mitochondrial and nuclear compartment. For instance, McDonnell and colleagues have reported that fatty acid is the major fuel of histone aceylation and the produced acetyl-CoA could impact histone acetylation in a manner that is independent of the citrate shuttle[562]. In addition, Murphy and colleagues have pointed out that sccinyl-CoA might be shuttled through carnitine-succinylcarnitine system, while succinate can be exported from mitochondrion through dicarboxylate carrier SLC25A10 and supplies the cytosol/nuclear succinyl-CoA pool[596]. With our cell model and in patients tumoral cells, we established the link between mitochondrial activity and histone PTMs, prominently non-acetyl acylations, where an increased mitochondrial activity drives a higher level of histone H4 acylations (e.g., crotonylation, butyrylation, β-hydroxybutyrylation, etc.).

As cancer cells have almost ubiquitously reprogrammed metabolism, metabolism-driven histone modifications could be a common mechanism underpinning tumor biology. Indeed, although only tested in a small patient samples cohort, our studies uncovered that mitochondrial metabolism-driven histone modifications (H4K5cr and H4K5bu) also occurs in tumoral samples. However, more precise models need to be established to address the functional roles of the interplay between cell metabolism and its epigenome and to precisely characterize the resultant changes (e.g., cell fate), as well as to demonstrate the specific epigenetic patterns underpinning the corresponding functions in cancer biology.

Collectively, metabolism-driven histone modifications have begun to emerge as one of the crucial oncogenic mechanisms. Our work on mitochondrial activity – fatty acid metabolism –

histone PMTs added one piece of evidence to these mechanisms. For the moment, the precise epimetabolic pathways active in cancer cells remain enigmatic. More specially there are many questions regarding metabolic enzymes translocation, metabolites shuttling etc. In the case of functional output of metabolism-driven epigenome programming, it would be important to define the types of epigenetic patterns that are required for specific aspects of cancer biology. Furthermore, the mechanisms underpinning specific epigenetic alterations and gene expression programs are to be understood. All these fields await further investigations and might shed light on novel mechanisms underlying cancer establishment and development.

3. The ratio of acyl/acetyl tunes BET-chromatin interaction dynamics

Previous studies showed that the first bromodomain (BD1) of BET family protein has very weak affinity over monoacetylated lysine. However, this binding is greatly enhanced by multiple acetylated sites, e.g., tetra-acetyllysine (H4K5acK8acK12acK16ac). In contrast, the second bromodomain (BD2) of BET can bind mono and multiple modified histones, including histone H3. Interestingly, the binding of BD2 to tetra-acetylated H4 has only 1/10 the affinity of the binding affinity of BD1 to tetra-acetylated H4[93]. Moreover, Morinière and colleagues have identified that BD1 binds simultaneously H4K5ac and H4K8ac and that the affinity of BD1 binding to diacetylated histone H4 tail is almost equal of its binding to tetra-acetylated histone H4 tail[100]. These data suggest that the interaction between BD1 and H4K5acK8ac is the major interaction underlaying the binding of BET to acetylated H4.

Furthermore, it has been suggested that the butyrylation at H4K5 can preclude the binding of acetylated H4 peptides by BD1. A structural model considering the interaction between BRDT BD1- H4K5buK8ac in comparison with BRD4 - H3K14bu revealed that the butyrylated lysine at H4K5 position results in a steric clash between the histone peptide and the ZA loop of BD1. Furthermore, the conformational adaptation of H4K5buK8ac into BD1-binding pocket might indeed disrupt many of the interactions between acetylated H4 peptides and BD1[100]. Our data was in accord with these findings, where the binding between BRD4 and acetylated H4 is abolished by the butyrylation at H4K5 site (**Figure 34**).

In the literature there are evidences indicating that H4 hyperacetylation is strictly ordered where histone H4 acetylation occurs from K16 and spreads over N terminal lysine residues (“zipper acetylation”). This theory is supported by the observations that only H4K16 acetylation, H4K16K12 di-acetylaion, K4K16K12K8 tri-acetylation and the tetra-acetylation of all four lysines (H4K5K8K12K16) were identified using mass spectrometry analysis of histone modifications. This situation was observed in a variety of organisms ranging from lower eukaryotes to human cells[746-748]. In this context, the presence of K5acK8ac is considered as a mark for H4 hyperacetylation and often indicates active transcription[749]. As demonstrated before,

in spermatocytes and round spermatids, there is a co-occurrence of H4 acetylation and H4 butyrylation marks (H4K5K8 ac/bu) around the TSS regions (TSS±5000), of the most active genes. Furthermore, the BRDT bound regions are enriched with a higher degree of the co-coverage of these four marks, even though H4K5bu perturbs BRDT - H4 interaction. Considering that histone acetylation and butyrylation are dynamic marks which undergo rapid turnover, the authors from my host laboratory proposed the hypothesis that explains such a paradox: BET (BRDT) binds with acetylated chromatin in a dynamic manner. Based on this hypothesis, the dynamics of BET-chromatin is tuned by the relative level of histone butyrylation over acetylation : increased butyrylation disfavors BRDT – H4 interaction and thus contributes to a more dynamic interaction. In contrast, increased acetylation favors a tight binding[145].

In our work, we brought additional arguments in favor of the above theory which seems to be also valid in a completely different system. Firstly, the above theory applies not only to butyrylation, but also to all other histone acylations (more than 3 carbons, >3C abbreviated). This is based on the evidence that: 1) short chain acylations, for example crotonylation, β-hydroxybutyrylation etc. have similar to butyrylation and longer chain acyl groups and the corresponding histone acylations should be less likely to properly interact with BD1. 2) Similar to acetylation, all these newly identified histone acylations have a rapid turnover rate. 3) These acylations systematically co-occur with histone acetylation (this will be further discussed in the next section). Secondly, the relative level of histone acetylation over acylation is tuned by acetyl/acyl-CoA level, which are themselves controlled by cell metabolism. The point has been covered in the introduction part.

Based on our data, we proposed that the interaction between BET proteins (BRD4 in our case) and chromatin are determined by acyl/acetyl ratio. A higher acyl/acetyl ratio leads to a more dynamic BRD4-chromatin interaction, whereas a lower ratio contributes to a tighter chromatin binding by BRD4. Among different experiments we performed, BRD4 elution assay and FRAP experiments directly support this hypothesis (**Figure 35**, **Figure 36**).

In conclusion, we discovered that acyl/acetyl ratio controls BET - chromatin interaction dynamics. As acyl/acetyl marks can be regulated by metabolic state, factors such as FASTKD1 that control the mitochondrial activity, could in turn control the metabolism – chromatin signaling. Since cancer cells present a systematic altered metabolism and given that BRD4 is broadly involved in various cancer types, the mechanism we uncovered here might largely contribute to oncogenesis.

In the next section, I will discuss how this dynamic pattern impact the BRD4 mediated biological processes including gene transcription.

4. Acyl/acetyl ratio controls BRD4 genomic redistribution and gene transcription

Since their identification, functional studies on histone acylations revealed redundant activities. Although much less abundant than acetylation, histone acetylation co-occurs with histone acetylation on active genes. However, there are some evidences supporting a distinct role for non-acetyl histone acylation in gene transcription. Among these evidences we can enumerate the identification of specific readers and writers for these acylations. However, here also we are missing convincing arguments in favor of the distinctive roles of these factors compared to those known to control histone acetylation.

Herein, we found that histone acylation, H4K5cr for example, is associated with active transcription, as reported in previous studies. Furthermore, we uncovered that, high ratio of cr/ac marks the most actively transcribed genes. Indeed, the ChIP-seq analysis revealed that metabolism-driven H4K5cr preferentially occurs on highly acetylated chromatin. As described in chapter III, longer chain acylations (>3C) preclude BET-chromatin interaction. We therefore reasoned that chromatin loci presenting high acyl/acetyl ratio should favor the release of BET proteins from the corresponding regions. This observation allowed us to propose the reservoir theory for BET factors. This hypothesis was previously proposed for a transcription factor MIFF which is released from low-affinity regions and as a result of its acetylation. Acetylated MIFF becomes then available to bind its high affinity regulatory elements[750]. In our case, BRD4 is displaced from regions gaining a higher acyl/acetyl ratio and becomes available for binding to other genomic regions, i. e., the TSS of highly active genes.

Gene transcription initiates with PICs assembly at the promoter regions upstream of TSS. Nucleosome free regions (NFRs) were firstly identified on Pol II promoters in yeast upstream of TSS[751, 752] and were then found on active gene.TSSs in human cells[13, 753]. Since most of the transcription factors preferentially access free DNA, NFRs could theoretically allow transcription factors to assemble in order to initiate transcription. NFRs were also suggested to modulate enhancer-promoter communication[754]. In our work, using MNase ChIP-seq, we observed that the NFRs could interact with BRD4. Furthermore, the redistribution of BRD4 driven by acyl/acetyl ratio impacts the presence of BRD4 at NFRs, which in turn might control gene transcriptional alterations. Our results identified subsets of both upregulated and downregulated genes in high acyl/acetyl cell group (FASTKD1 KO) that are also among the JQ1 sensitive genes. This observation also comes in support of our model on the regulation of BRD4 activity by the changing acyl/acetyl ratio.

It is noteworthy that we also monitored the acylation-tuned transcriptional output in patients' samples. Indeed, the gene set enrichment analysis showed that tumors with higher histone

acylation groups have enhanced expression of genes involved in mitochondrial component, cell cycle and ribosome synthesis. They also present decreased expression of stemness associated genes in cell lines and in primary blasts. These are in accord with less aggressive tumors, and a relatively favorable outcome in this group of patients.

Collectively, our work highlights the importance of these relatively low abundant histone marks in regulating gene transcription. More specifically, these acylations preferentially regulate highly transcribed genes where in combination with acetylation, they tune BRD4 availability across various genomic regions. Therefore, our work also proposes a new hypothesis on the functional importance of histone PTM combination, in addition to their individual role.

ANNEXES

1. A manuscript submitted

1.1 Manuscript text

Metabolically controlled histone H4K5 acylation/acetylation ratio drives BRD4 genomic distribution

Mengqing Gao[1, 2, 3 +], Jin Wang[1, 3 +], Sophie Rousseaux[2, 3], Minjia Tan[4], Lulu Pan[4], Lijun Peng[1, 3], Sisi Wang[1, 3], Wenqian Xu[1, 3], Jiayi Ren[1, 3], Yuanfang Liu[1], Martin Spinck[5], Sophie Barral[2, 3], Tao Wang[2, 3], Florent Chuffart[2, 3], Ekaterina Bourova-Flin[2, 3], Denis Puthier[6], Sandrine Curtet[2, 3], Lisa Bargier[6], Zhongyi Cheng[7], Heinz Neumann[5], Jian Li[8], Yingming Zhao[9], Jian-Qing Mi[1, 3*], Saadi Khochbin[2, 3, 10*]

1- Shanghai Institute of Hematology, State Key Laboratory of Medical Genomics, National Research Center for Translational Medicine at Shanghai, Ruijin Hospital Affiliated to Shanghai Jiao Tong University School of Medicine, 200025, Shanghai, China
2- CNRS UMR 5309/INSERM U1209/Université Grenoble-Alpes/Institute for Advanced Biosciences, 38706, La Tronche, France
3- Pôle Franco-Chinois de Recherche en Sciences du Vivant et Génomique, 200025, Shanghai, China
4- Shanghai Institute of Materia Medica, Chinese Academy of Sciences, 555 Zuchongzhi Road, 201203, Shanghai, China
5- Department of Structural Biochemistry Max-Planck-Institute of Molecular Physiology Otto-Hahn-Strasse 11, 44227, Dortmund, Germany
6- Aix Marseille Université, INSERM, TAGC, TGML, 13288, Marseille, France
7- Jingjie PTM Biolab (Hangzhou) Co., Ltd., 310018, Hangzhou, China
8- Clinical Research Center, Ruijin Hospital Affiliated to Shanghai Jiao Tong University School of Medicine, 200025, Shanghai, China
9- Ben May Department of Cancer Research, The University of Chicago, IL 60637, Chicago, USA

10- Lead Contact

+ equal contribution

* Correspondence:
Saadi Khochbin: saadi.khochbin@univ-grenoble-alpes.fr
Jian-Qing Mi: jianqingmi@shsmu.edu.cn

Abstract

In addition to acetylation, histones are modified by a series of competing longer chain acylations. Most of these acylation marks are enriched and co-exist with acetylation on active gene regulatory elements. Their seemingly redundant functions have hindered the understanding of histone acylations' specific roles. Here, by using an acute lymphoblastic leukaemia (ALL) cell model and blasts from B-ALL patients, we demonstrate a role for mitochondrial activity in controlling histone acylation/acetylation ratio, especially at H4K5. An increase of the ratio of non-acetyl acylations (crotonylation or butyrylation) over acetylation on H4K5 weakens BRD4 bromodomain-dependent chromatin interaction and enhances BRD4 nuclear mobility and availability for binding transcription start site regions of active genes. Our data suggest that the metabolism-driven control of the histone acetylation/longer chain acylation(s) ratio could constitute a common mechanism regulating the bromodomain factors' functional genomic distribution.

Introduction

Since the discovery of histone lysine propionylation and butyrylation in 2007 (Chen et al., 2007), an increasing number of different histone acylations has been reported. The vast majority of these histone post-translational modifications (PTMs) occur at sites already known to be acetylated and hence overall these new histone PTMs could collectively be considered as acetylation competing marks. Functional studies carried out on these histone marks in different biological systems have shown that they are all associated with active genes and directly stimulate transcription, similar to histone acetylation (Kebede et al., 2017; Goudarzi et al., 2016; Dai et al., 2014; Sabari et al., 2015; Smestad et al., 2018; Xie et al., 2016; Bao et al., 2019; Huang et al., 2018; Zhang et al., 2019).

Comparative high-resolution genome mapping also revealed that, in the majority of active chromatin loci, these histone acylations co-exist with acetylation (Tan et al., 2011; Dai et al., 2014; Goudarzi et al., 2016; Sabari et al., 2015; Kebede et al., 2017; Crespo et al., 2020). Additionally, although these acylations are mostly mapped at gene transcriptional start site (TSS)- associated regions, as would be expected for active histone marks, their relative abundance corresponds to only a small fraction in comparison with acetylated histones (Simithy et al., 2017). Finally, although different acyl-donor groups may result from different metabolic pathways, their redundant functions do not leave much room for any metabolic-specific action. These observations therefore raise an important unsolved issue in modern biology, which is the specific functional significance of these histone acylations compared to acetylation.

An answer to this issue came from the discovery of specific domains in various proteins that show a better affinity for binding to longer chain acyl groups on histones compared to acetylation. For instance, YEATS and DPF domains present a better binding activity for crotonylated histones than for acetylated histones (Andrews et al., 2016a; Li et al., 2016; Xiong et al., 2016).

An unexplored possibility to solve this issue is coming from *in vitro* data showing that most bromodomains lose their affinity for chromatin regions bearing histones with acyl groups longer than three carbons (Flynn et al., 2015; Goudarzi et al., 2016; Olp et al., 2017).

The functional consequence of the differential effects of histone acylation on bromodomain–chromatin interaction was first considered in the context of the late stages of differentiation of male germinal cells, during which a large-scale histone hyperacetylation is coupled to a genome-wide histone removal involving the testis-specific BET factor, Brdt (Shiota et al., 2018). Using this specific system, we discovered that H4 bearing butyrylation at K5 and K8 escapes this wave of replacement and survives longer in late spermatogenic cells than histone H4 bearing the corresponding acetylation. This observation supports the hypothesis that, since Brdt's first bromodomain is unable to bind H4 when it is modified by butyrylation specifically at K5 (Goudarzi et al., 2016), the corresponding histones "escape" acetylation and the consequent Brdt-dependent removal.

However, these observations remained correlative and the hypothesis of the modulation of the action of BET factors by an interplay between histone acetylation and acylation, awaited confirmation.

Here, by taking advantage of ALL cell biology, we directly demonstrate that a modified histone acetyl/acyl ratio, specifically at H4K5, controls the dynamics of interaction between chromatin and the ubiquitously expressed member of BET double bromodomain factor, BRD4, whose expression and activity are frequently dysregulated in many unrelated cancers (Fujisawa and Filippakopoulos, 2017). The emerging general concept developed here is that a mixture of finely tuned competing histone acetylation and longer chain acylations defines bromodomain factors functional availability.

Results

Aberrant activation of *FASTKD1* is associated with a general shut-down of mitochondrial activity

We previously identified *FASTKD1* as an ectopically expressed gene in childhood and adult B-ALL (Wang et al., 2015). FASTKD1 presents a mitochondrial targeting signal and hence is expected to exert its function in mitochondria (Jourdain et al., 2017). To investigate its function, we first identified the established B-ALL cell line REH, expressing *FASTKD1* and then generated REH cell lines stably expressing two different anti-*FASTKD1* shRNAs (Fig. S1A) or used the CRISPR/Cas9 system to knock-out the gene (Fig. S1B). RNA-seq were generated from the two *FASTKD1* knock-down as well as two independent *FASTKD1* knock-out clones (Fig. S1A, S1B). Focusing on mitochondrial gene expression, we observed that the inactivation of *FASTKD1* leads to a significant enhancement of mitochondrial encoded gene expression (Fig. 1A).

This activation of mitochondrial gene expression was also independently confirmed by RT-qPCR, by evaluating the expression of *ND2* and *ND3* genes after treating cells with a series of five different anti-*FASTKD1* shRNAs as well as in the two *FASTKD1* ko cell lines (Fig. 1B, upper panels, Fig. S1C). Finally, FASTKD1-Flag re-expressed in the *FASTKD1* ko cells resulted in the mitochondrial localization of the ectopically expressed FASTKD1-Flag and the downregulation of mitochondrial gene expression (Fig. S2, Fig. 1B, lower panels).

All these data demonstrate that FASTKD1 should logically down-regulate mitochondrial activity.

To test this hypothesis, mitochondrial respiration was measured from control REH cells or from the two *FASTKD1* ko clones. The results show an enhancement of respiration in both *FASTKD1* ko clones compared to the control REH cells, in perfect agreement with a role for FASTKD1 in the decrease of mitochondrial activity, more specifically the respiration (Fig. 1C).

Mitochondrial activity is a driver of histone acylation

FASTKD1 appeared to us as an excellent factor to investigate the relationship between mitochondrial activity and histone acetylation/acylation (Matilainen et al., 2017; Lozoya et al., 2019; Haws et al., 2020; Trefely et al., 2020) in the specific context of ALL. We focussed on histone H3 and H4 propionylation and butyrylation, since, while all bromodomains bind acetyllysines and propionyllysines, many of them are unable to bind butyryllysine (Flynn et al., 2015).

Histone extracts from wild-type REH cells and the two derived *FASTKD1* ko cell lines were used in an unbiased approach to measure changes in histone butyrylation and propionylation. After trypsin-digestion of histones, the resulting peptides were directly quantified using a label free mass spectrometry method.

These analyses were performed without prior enrichment of modified histone peptides (with anti-PTM antibodies) to detect and visualize the most abundant modified peptides.
This analysis demonstrated that histone H4 K5, K8 and K12 butyrylation is the most responsive to FASTKD1 depletion (Fig. 2A, Table S1, S2 and S3). A more detailed analysis of the mass spectrometry data also highlighted the occurrence of unique peptides with a combination of acetylation and butyrylation-propionylation (data file S1). This observation is indicative of continuing exchange of acylations at a particular lysine site.
We then decided to focus on H4 K5 and K8 to confirm these findings. Immunodetection of histone PTMs in protein extracts showed a clear increase in both butyrylation and crotonylation of H4K5 and H4K8 in the two *FASTKD1* ko cell lines. The corresponding histone acetylation level did not show any noticeable change in *FASTKD1* ko cell lines (Fig. 2B).
These results suggest the existence of a direct relationship between the studied histone acylations and the extent of mitochondrial activity. To confirm this conclusion, we treated control and *FASTKD1* ko cell lines with the electron transport chain poison Rotenone and demonstrated that the impairment of mitochondrial activity severely affects the maintenance of histone H4K5 butyrylation and H4K5 crotonylation (Fig. 2C). This treatment with Rotenone had relatively little effects on acetylation, probably due to the considerably higher levels and more stable pools of acetyl-CoA and acetylated histones.
Overall, these data also suggest that histone butyrylation and crotonylation could be more sensitive to a change in mitochondrial activity than histone acetylation.

Fatty acid synthesis / β-oxidation is a major driver of histone butyrylation and crotonylation

Fatty acid synthesis and β-oxidation particularly involve the generation of acyl-CoA derivatives that could potentially be used to add the corresponding acyl groups on histones (Pougovkina et al., 2014 ; McDonnell et al., 2016; Gowans, 2019; Tarazona et al., 2020). We therefore first used a competitive inhibitor of acyl-CoA synthetase, Triascin C, to prevent the synthesis of fatty acids and monitored the effect on H4K5K8 aceylation and butyrylation (Fig. 2H, scheme). The treatment of cells with Triascin C abolished the increase of H4 butyrylation at H4K5 observed in *FASTKD1* ko lines, with no remarkable effect on the acetylation of this residue (Fig. 2D). Additionally, we decided to target the enzyme that catalyses the first step of fatty acid synthesis, acetyl-CoA carboxylase (ACC1, Fig. 2H, scheme), by using the ACC1 inhibitor ND-630. The inhibition of acetyl-CoA carboxylase also abolished the increased level of H4K5bu compared to the parental cells, with no remarkable effect on H4K5ac (Fig. 2E).
In order to also test the role of fatty acid oxidation (FAO) in histone acylations, we sought an approach based on treating the cells with octanoate, a molecule directly usable in FAO (McDonnell et al., 2016). The octanoate treatment increases the levels of H4K5 acetylation, butyrylation and crotonylation in REH cells (Fig.2F and S3). However, compared to acetylation, the increase in H4K5bu-cr is more remarkable (Fig. S3).

In order to further test the role of FAO in histone acylation, we also used Ranolazine, an inhibitor of FAO, and showed that the treatment of cells with this inhibitor abolishes the increase in H4K5bu observed in the *FASTKD1* ko clones (Fig. 2G).

β-oxidation and mitochondrial activity are major sources of histone acylation in ALL malignancies

To generalize our conclusions on the relationship between mitochondrial activity and histone acylations, we quantitatively measured H4K5cr and H4K5bu by ELISA in 31 B-ALL patient malignant cells samples (Table S4). Using RT-qPCR, we quantified in the same samples, Carnitine Palmitoyltransferase 1A (*CPT1A*) mRNA, encoding a protein involved in the transport of long chain acyl groups into mitochondria controlling the fatty acids β-oxidation potential of the cells, and the mitochondrial gene *ND2* mRNA, as an indicator of mitochondrial activity.

Figure 3A shows that there is a tendency for coregulation between the expression of *CPT1A* mRNA, as a measure of β-oxidation potential, and the expression level of *ND2*, as a measure of mitochondrial activity ($rs = 0.531$).

From our functional data obtained in REH cells (Fig. 1 and 2), we expected to find a relationship between the level of mitochondrial transcription (*ND2* mRNA) and the intensity of H4K5 crotonylation and butyrylation. To test this hypothesis, ALL samples were divided into two groups as a function of the expression of *ND2*. A ROC curve of the RT-qPCR output values was used to define a cut-off value at -dCt=1.2782, which we used to stratify the ALL into two groups of 13 (42%) low *ND2* expressing and 18 (58%) high *ND2* expressing samples. The results showed that, similarly to REH cells, patients' ALL cells with higher mitochondrial activity are associated with higher levels of H4K5 crotonylation and butyrylation (Fig. 3B and 3C).

All these data support and extend our conclusions on the major role of mitochondrial activity and β-oxidation in driving histone acylation.

The H4K5 acyl/acetyl ratio is a major determinant of BRD4 - chromatin interactions

In a previous work, by analysing the function of histone H4K5K8 butyrylation in spermatogenic cells and its impact on the function of the testis-specific BET factor Brdt, we observed that, during late spermatogenesis, H4K5bu-containing nucleosomes escape the acetylation- and Brdt-dependent histone removal (Goudarzi et al., 2016).

Our present data suggest that similarly, in the case of ALL cells, a change in the ratio of H4K5 acetyl/butyryl-crotonyl could also affect the interaction between BRD4 and chromatin.

Using a peptide pull-down assay with a H4 N-terminal tail peptide bearing all combinations of acetylation and butyrylation at K5 and K8, we demonstrate the inability of BRD4 to bind H4, when the peptide is modified by a butyryl group at K5 (Fig. 4A). A depletion of FASTKD1 and a change of mitochondrial activity did not affect the total level of BRD4 in a high salt nuclear extract (Fig. 4B, input, also see Fig. 4C) nor its ability to bind to an acetylated H4 tail peptide (Fig. 4B, pull down).

These data suggest that H4 butyrylation at H4K5 should affect the ability of BRD4 to interact with chromatin. Accordingly, an increase in H4K5bu-cr, as observed in our *FASTKD1* ko cells, should to some extent loosen the interaction of BRD4 with chromatin compared to the wild-type cells.

In order to test this hypothesis, we used wild-type and *FASTKD1* ko REH cells to compare the strength of BRD4-chromatin binding, with the prediction that, in *FASTKD1* ko cells, a loose BRD4 – chromatin interaction should be observed due to the increase in the H4K5 acyl/acetyl ratio. Accordingly, wild-type and *FASTKD1* ko cells were lysed in a buffer containing increasing salt concentrations and, after centrifugation, the respective amounts of BRD4 released in the supernatant or remaining bound to chromatin were visualized by immunoblotting. Figure 4C (upper panels) shows that, in the presence of 200 mM NaCl, both *FASTKD1* ko clones released higher amounts of BRD4 compared to wild-type cells, suggesting a weaker binding of BRD4 to chromatin.

In order to further support our observation, we also treated our cells with increasing concentrations of the BRD4 small molecule inhibitor, JQ1. We reasoned that a more dynamic BRD4-chromatin interaction should make BRD4 bromodomains more sensitive to an inhibition by JQ1. After treating cells with the solvent, or 0.1, 0.5 or 5 µM of JQ1, the respective amounts of BRD4 in soluble protein extracts and in the chromatin-bound fractions were analysed. Figure 4C (lower panels) shows that, at 0.5 µM concentration, the JQ1 treatment leads to an increase in the soluble pool of BRD4 in *FASTKD1* ko cell, compared to wild-type cells.

Finally, in order to directly test the effect of a change in the histone acetylation/butyrylation-crotonylation ratio on the efficiency of BRD4 binding, we sought another approach to demonstrate a change in the dynamics of BRD4 in live cells. For this purpose, we used a previously characterized COS-7 cell-based system and induced a change in the ratio of histone acetylation/butyrylation-crotonylation in these cells. We had previously shown that the expression of the oncogenic fusion protein, BRD4-NUT, in COS-7 cells creates well-defined nuclear foci, which depend on chromatin acetylation and BRD4 bromodomains (Reynoird et al., 2010). In addition, these BRD4-NUT induced foci are large and stable enough to allow *in vivo* approaches such as Fluorescent Recovery After Photobleaching (FRAP) assays.

First, we stably expressed CobB, a bacterial NAD^+ deacetylase appropriately modified for expression in mammalian cells (Spinck et al, 2020), in COS-7 cells and visualized the effect of this deacetylase on the acetyl/butyryl-crotonyl ratio. Figures 4D and S4A show that the ectopic expression of CobB, while preferentially decreasing the level of H4K5ac, has no noticeable

effect on H4K5bu and H4K5cr *in vivo* in these cells. Therefore, our prediction was that, in the CobB-expressing cells, this increase in the H4K5acyl/acetyl ratio should be associated with an increased dynamic of the BRD4 – chromatin interaction. We also performed the salt extraction assay described above, in the control and in CobB-expressing COS-7 cells and observed that, similar to REH cells, an increase in the H4K5acyl/acetyl ratio enhances the salt elution of BRD4 from chromatin (Fig. S4B).
Finally, FRAP was used to precisely measure the dynamics of GFP-BRD4-NUT chromatin interactions in these cells. Figure 4E shows that the ectopic expression of CobB and an increased H4K5acyl/acetyl ratio clearly increases the dynamics of BRD4 - chromatin interaction.

A metabolically driven increase in H4K5 acylations preferentially occurs on highly acetylated chromatin regions

The distribution of H4K5cr-bu/H4K5ac ratio was the investigated at high resolution in a genome-wide manner. The H4K5cr, H4K5bu and H4K5ac ChIP-mapping allowed us to visualize the relationship between H4K5cr and H4K5bu with H4K5ac in each of the cell lines considered. To this end, we plotted the ChIP-seq read counts corresponding to H4K5cr and H4K5bu as a function of the read counts corresponding to H4K5ac on gene TSSs. This representation shows a linear correlation between H4K5cr-bu and H4K5ac on TSSs associated with relatively low levels of H4K5ac. However, at higher levels of H4K5ac, this linear relationship between the considered histone modifications is distorted with an increasing H4K5cr-bu/ H4K5ac ratio, and this part of the correlation plot best fits a non-linear (exponential regression) model (Fig. 5A).

The H4K5cr-bu/H4K5ac ratio controls BRD4 genomic distribution

Two independent anti-BRD4 ChIP-seq were performed to evaluate the impact of the change in H4K5cr-bu/ac ratio on the binding of BRD4 to chromatin at high resolution. Focussing on gene TSS, we found that BRD4 accumulates on the TSS of highly active genes.
By comparing the levels of these TSS region-bound BRD4 between wild-type and *FASTKD1* ko cells, in both anti-BRD4 ChIP-seq experiments we found significantly higher levels of BRD4 present on the highly active TSSs in the two ko cell lines (see Fig. 5B and C, showing heatmap and metagene profiles for all genes in the first experiment, also see Fig S5A showing heatmaps and profiles for a selection of genes with the highest BRD4 peaks in both anti-BRD4 ChIP-seq experiments). Since there was no change either in the total level of BRD4 (Fig. 4B, input and Fig. 4C) nor in its ability to bind acetylated H4 tail (Fig. 4B, pull down) in our *FASTKD1* ko cells compared to wild-type cells, we concluded that the observed increase in BRD4 on active gene TSSs in *FASTKD1* ko cells, should be due to a redistribution of BRD4. Therefore, the increased BRD4 binding to the TSS of highly active genes is very likely a

consequence of the genome-wide increase in BRD4 mobility making BRD4 more available for binding active gene TSS regions.

Functional significance of the genomic redistribution of BRD4 in REH cells and in ALL malignancies

We reasoned that the genes that show a change in expression in *FASTKD1* ko cells compared to wild-type cells, should to some extent, also be sensitive to the BET bromodomain inhibitor JQ1. To this end, we generated RNA-seq from wild-type REH cells treated with different doses of JQ1 and compared the differentially regulated genes (JQ1-responsive genes) with the genes that are differentially expressed between wild-type and *FASTKD1* ko REH cells. Interestingly, a significant number of genes differentially expressed in *FASTKD1* ko cells compared to wild-type cells are found among the JQ1-responsive genes (Fig. 6A and 6B). Indeed, a subset of genes that are down-regulated in FASTKD1 ko REH cells are also down-regulated in wild-type REH cells treated with JQ1 (Fig. 6B, upper panel). Additionally, a significant subset of genes among those that are upregulated in *FASTKD1* ko cells are also down regulated in wild-type JQ1 treated cells (Fig. 6B, lower panel).
The observation that both *FASTKD1* ko down- and up- regulated genes are significantly enriched among JQ1-sensitive genes suggests that both up- and down- regulated genes have a BRD4 dependent expression.
This is also illustrated by Figure S5 which shows that genes associated with BRD4 peaks are JQ1 sensitive. Indeed, to demonstrate the relationship between the redistribution of BRD4 between wild-type and *FASTKD1* ko cells, genes whose TSS regions were associated with high BRD4 peaks and increasing BRD4 binding in ko cells were selected (Fig. S5A). This group of genes was used as a geneset for a GSEA analysis to test for its enrichment/depletion in the transcriptomes of JQ1 treated REH cells. Figure S5B shows a significant depletion of this group of genes, visualizing their down regulation in JQ1 treated cells, which demonstrates that their expression is BRD4 dependent.

In order to show that this H4K5 acylation- and BRD4- dependent regulatory circuit could also be involved in B-ALL tumour cells, we analysed the transcriptomes of a subset of B-ALL tumours (Table S4) for which we had measurements of H4K5bu and H4K5cr levels (Fig. 3).
We generated RNA-seq from 25 B-ALL samples and identified the genes differentially expressed between the two groups of H4K5cr-bu high (n=15) and H4K5cr-bu low (n=10) B-ALL (Fig. S6). We then compared the list of differentially expressed genes between these two categories of ALL cells (Fig. 6C), with the list of differentially expressed genes between REH wild-type and *FASTKD1* ko REH cells (Fig. 6A), which also showed higher levels of H4K5cr-bu compared to wild-type cells (Fig. 2). Interestingly, the two transcriptional signatures share similarities since a significant number of genes are regulated in the same manner in *FASTKD1*

ko REH and in H4K5cr-bu high B-ALL (Fig. 6D). It is worthy to recall that the common point between these two systems is the comparison between the state of H4K5 acylations.

Accordingly, the Gene Set Enrichment Pathway Analysis (GSEA) shows that, in both REH *FASTKD1* ko cells and patients' H4K5cr-bu high B-ALL cells, the genes encoding for mitochondrial functions are significantly upregulated, confirming the presence of active mitochondria in these cells (Fig. S7 top panels). Other common features are shared by the expression signatures of both these cells, including high translational and proliferation/cell cycle related activities, and a significant depletion in hematopoietic stem cells genes (Fig. S7).

Discussion

Fatty acid β-oxidation has recently been shown to be a major source of acetyl-CoA driving histone acetylation (McDonnel et al., 2016). Our present investigations reveal that mitochondrial activity and fatty acid β-oxidation in particular, is also the main source of histone acylations. Interestingly, this conclusion is in full agreement with the recent finding identifying fatty acid β-oxidation, which in yeast takes place in the peroxisomes, as a driver of histone crotonylation in *S. cerevisiae*, particularly during Yeast Metabolic Cycles (Gowans et al., 2019). As demonstrated here, histone acylations preferentially occur, and hence concentrate, on regions with high levels of histone acetylations. The functional meaning of this observation is that the sum of a series of low abundance histone acylations and their local concentration on specific regions could make a significant contribution to non-acetyl histone modifications, in terms of stoichiometry and in terms of gene expression regulation, by competing with histone acetylation. This situation should have a direct effect on the stability of the interaction of bromodomains with chromatin. Indeed, structural studies have demonstrated why most of the bromodomains are unable to bind longer acyllysine modifications and how these modifications could attract other types of binder factors (Andrews et al., 2016b). Consequently, an increase in histone acylations/acetylation ratio, while destabilising chromatin binding by bromodomains, could in contrast stabilise the interaction of factors bearing YEATS and DPF domains, which could in turn enhance the displacement of bromodomain factors and their increased availability.

Another important concept developed here is that of a bromodomain factor “reservoir”. The pool of BRD4 bound to the genome-wide bulk of acetylated nucleosomes could be considered as a reservoir of BRD4. As shown here, a general increase of >3C acylations on H4K5 leads to a global increase in the solubility of BRD4. This “mobile” fraction of BRD4 would be released from numerous genomic sites and concentrate on a limited number of “hyperdynamic” chromatin loci, such as active gene TSSs. This explains the increase in BRD4 binding observed upon *FASTKD1* inactivation at highly active gene TSSs in our ChIP-seq mappings. This mechanism also makes BRD4 available for interactions with TSS-bound non-histone factors, including the acetylated cyclin T1 subunit of pTEF-b, in a bromodomain-dependent (Schroder et al., 2012) and independent (Lambert et al., 2019) manner.

We also took advantage of the quantitative measurements of H4K5bu and H4K5cr in B-ALL samples to investigate the relationship between gene expression and the level of H4K5 acylations.

The correlation between the level of expression of the mitochondrial gene *ND2* and the level of H4K5bu-cr in these patients’ samples suggests that our observation made in REH cells can be extended to patients’ B-ALL blast cells, where high mitochondrial transcriptional activity is also associated with an increased H4K5 acylation / acetylation ratio.

Based on all these data we propose that the activation of mitochondrial activity leads to an increase in the H4K5 acylation (butyrylation, crotonylation, etc..), loosening the binding of the genome-wide bulk of acetylated nucleosomes by BRD4 (BRD4 reservoir), making it available for recruitment and binding at active gene regulatory sites (Fig. 7). In the frame of ALL, we also propose that a decrease of mitochondrial activity in blasts due to aberrant *FASTKD1* expression or for any other reasons, could favour a gene expression pattern associated with aggressive forms of this pathology (Wang et al., 2015).

Overall, this work highlights several important concepts in the biology of chromatin and transcription. We propose that there is a systematic co-existence of histone acetylation and histone acylations at chromatin dynamic spots. With respect to bromodomain factors' function, histone acylations should be considered collectively and not individually. Namely, in terms of stoichiometry relative to acetylation, >3C histone acylations, including butyrylation, crotonylation, etc., are permanently exchanged and hence should be considered as one functional entity. Histone acylations occur and concentrate on regions of high histone acetylation. The ratio of histone acyl/acetyl is a critical functional parameter, which is tuned by upstream cell metabolic reactions. Mitochondrial activity and β-oxidation in particular, are important drivers of histone acylations. Histone acyl/acetyl ratio fine tunes the availability of BRD4 for recruitment at its sites of action and could represent a general mean of controlling bromodomain-containing factors availability and function.

ACKNOWLEDGEMENTS

This program was supported by Fondation ARC program N° RF20190208471, by ANR Episperm4 program and by the "Université Grenoble Alpes" ANR-15-IDEX-02 LIFE and SYMER programs, by INCa and IreSP, by Plan Cancer Pitcher and from MSD Avenir ERICAN programs. JM's lab is supported by National Natural Science Foundation of China (81670147), clinical research plan of Shanghai Hospital Development Center (16CR3008A), International Cooperation Projects of Shanghai Science and Technology Committee (15410710200) and Innovation Program of Shanghai Municipal Education Commission (8201001096). MG follows a Shanghai Jiao Tong University - Grenoble Alpes University joint PhD program of Cai Yuanpei - Campus de France supported by China Scholarship Council. This work was supported by the University of Chicago, Nancy and Leonard Florsheim family fund (YZ), NIH grants GM135504, DK118266 (YZ). MT's group acknowledges funding from "the Natural Science Foundation of China (91753203)". The TGML Platform is supported by grants from Inserm, GIS IBiSA, Aix-Marseille Université, and ANR-10-INBS-0009-10. NH and SM's work was funded by the Max-Planck Institute of Molecular Physiology.

AUTHORS' CONTRIBUTIONS

MG generated model cell lines and performed most of the experiments. MT performed H3 and H4 PTMs measurements. LB prepared all the libraries and performed the sequencing under the supervision of DP. SR performed and supervised all the bio-informatic analyses involving also FC and EFB. MS and HN produced the CobB expression vector and discussed the results. SC performed the FRAP experiments and analysed the data with the help of FC. SB performed anti-H4K5ac-cr ChIP experiments and TW, SW, WX helped with the RT-qPCR experiments. ZC produced and characterized the anti-histone PTM antibodies. JL helped with and discussed about the statistical analysis. JW recruited the B-ALL patients and took care of bio-bank setup and the formalities including the acquisition of the ethic committee approval. LP, JR, YL helped with the collection and disposition of patients' samples. JQM supervised the clinical part of the experiments and co-supervised MG work. YZ supervised the work on histone PTM and provided access to antibodies and helped with data interpretation. SK designed and coordinated the whole project and wrote the manuscript. All the authors read and commented the manuscript.

DECLARATION OF INTERESTS

All the authors declare no conflict of interest except ZC and YZ. Y.Z. is a founder, board member, advisor to, and inventor on patents licensed to PTM Biolabs Inc (Hangzhou, China and Chicago, IL) and Maponos Therapeutics Inc. (Chicago, IL). Zhongyi Cheng is an employee and equity holder of PTM BioLabs Inc.

Figure Legends

Figure 1: FASTKD1 controls mitochondrial genome expression and mitochondrial activity.

A- Total RNAs from REH cells stably expressing two independent anti-*FASTKD1* shRNAs (sh-1 and sh-2) or bearing CRISPR/Cas9-directed inactivation of *FASTKD1* gene (ko-1 and ko-2) were sequenced and the standardized and normalized read counts representing mitochondrial gene expression in the different conditions are shown on a heatmap.
B- The expression of *ND2* and *ND3* genes encoded by the mitochondrial genome was monitored by RT-qPCR in REH cells stably expressing empty vector (shCtl) or five independent anti-*FASTKD1* shRNAs (upper left panel). The expression of *ND2* and *ND*3 was also monitored by RT-qPCR in wild-type and the two *FASTKD1* ko REH cells (upper right panel). *FASTKD1* ko-1 cells were used to re-express *FASTKD1-Flag* and the expression of *ND*2 and *ND3* was monitored by RT-qPCR in the wild-type, ko-1 and the *FASTKD1* rescued cells (lower panel). Fold changes of gene expression level were calculated via 2^-ddCt and are represented by mean ± SEM based on at least three independent experiments. Statistical differences between wild-type and two *ko*, or between shCtl and shRNAs groups were calculated with Fisher's Least Significant Difference (LSD) post one-way ANOVA test. * $p<0.05$, ** $p<0.01$, ***$p<0.001$.
C- Wild-type and the two *FASTKD1* ko REH clones were assayed for the respiration capacity using the standard Seahorse Mito Stress assay. The data shown are the mean value ± SEM of 5 biological replicates' measurements.

See Figure S1 for information on the generation of REH knock-down and knock-out cells.
See Figure S2 for the mitochondrial targeting of FASTKD1 (related to Fig. 1B)

Figure 2: *FASTKD1* gene inactivation, mitochondrial activation and β-oxidation lead to an increase of H4K5K8 acylations.

A- Histone extracts from wild-type and *FASTKD1* ko cells were analysed by label free mass spectrometry method. The relative abundance of the indicated identified site-specific modifications was determined and expressed as the ratio *FASTKD1* ko to *wild-type*. The corresponding core histone peptides were used to normalize the considered modified peptides. Please note that K8bu and K12bu containing peptides could not be distinguished following these analyses. Consequently, the quantification regarding these two modification sites were plotted as H4K8bu-K12bu.
B- Total extracts from wild-type and *FASTKD1* ko cells were used to detect the indicated H4K5 and H4K8 modifications as well as actin in two parallel immunoblots using the corresponding specific antibodies as indicated. The specificities of these antibodies were confirmed by dot blot analyses on peptides bearing the target H4K5 acylations as well as unrelated acylations (data file S1).

C- *Wild-type* and *FASTKD1* ko cells were treated with Rotenone (0.5 µM) for one or two hours. Protein extracts were prepared, and the corresponding immunoblots were probed as in B.
D- *Wild-type* and *FASTKD1* ko cells were treated with Triacsin (3 µM) for 16 hours and protein extracts were prepared and analysed as in B.
E- *Wild-type* and *FASTKD1* ko cells were treated with ND-630 (100 nM) for 6 hours, extracts were prepared and analysed as in B.
F- *Wild-type* REH cells were treated with the indicated concentrations of octanoate for 24 hours and the indicated histone PTMs were analysed as in B.
G- *Wild-type* and *FASTKD1* ko cells were treated with Ranolazine (0.5 mM) for 6 hours and protein extracts were analysed as in B.
H- The scheme represents the metabolic pathways and the key enzymes targeted by the indicated inhibitors in this series of experiments (D to G). FAO stands for Fatty Acids Oxidation.

See Figure S3 for accumulation of H4K5 acetylation and various acylations in *FASTKD1* wild-type and ko cells after octanoate treatment (related to Fig. 2F).
See Tables S1, S2 and S3 for details on the unbiased determination of histone H3 and H4 propionylation and butyrylation (related to Fig. 2A).

Figure 3: β-oxidation and mitochondrial activity correlate with histone acylations in B-ALL tumour cells

A- Total RNAs and proteins were extracted from 31 adult B-ALL patients' primary cells and the relative levels of *Carnitine Palmitate Transferase 1A* (*CPT1A*), *ND3* and *GAPDH* mRNAs were measured by RT-qPCR and plotted as shown.
B and **C-** In the same samples the relative amounts of H4K5cr, H4K5bu and H3, were measured by ELISA. ALL samples were divided into two groups as a function of normalized *ND2* expression, low (in blue) and high (in red) based on the ROC curve of the RT-qPCR values, as described in the text. In each group the normalized ELISA values H4K5cr/H3 ratio (B) and H4K5bu/H3 ratio (C) are plotted. For each group, the median value (black line) and interquartile range (coloured horizontal lines) are shown. Statistical significance of histone acylations between *ND2* high and low group was analysed with Mann-Whitney U test.
See Table S4 for the Characteristics of B-ALL patients samples.

Figure 4: H4K5 acyl/acetyl ratio controls the dynamics of BRD4-chromatin interaction

A- Total wild-type REH cell extracts were used in pull-down experiments with the indicated peptides. After pull-down the peptide-bound proteins were recovered in SDS-PAGE loading buffer, submitted to PAGE and BRD4 was visualized using the corresponding antibody.
B- High salt extracts (total BRD4) from wild-type and *FASTKD1* ko cells were prepared and a peptide pull-down experiment was performed using unmodified H4 tail peptide or the corresponding acetylated peptide.

C- Wild-type and *FASTKD1* ko cells were lysed in a buffer containing the indicated concentrations of NaCl. After centrifugation, the corresponding supernatants and pellets (salt extracts and nuclei, respectively) were analysed by immunoblotting for the presence of BRD4. Actin was also visualized as a loading control for the soluble extracts and H3 for the nuclei fraction (upper panels).
Wild-type and *FASTKD1* ko cells were treated with the indicated concentrations of JQ1 for 3 hours, cells were lysed, and the nuclei pelleted by centrifugation. The soluble extracts and the nuclei fractions ("soluble" and "nuclei", respectively) were analysed as above (lower panels).
D- Protein extracts were prepared from COS-7 cells stably expressing the Ha-tagged bacterial deacetylase *CobB* or from control cells and used to visualize of CobB-ha and actin (upper panel), or H4 and its indicated modified forms using cell extracts (middle panel). 1X to 3X indicate increasing amounts for extracts loadings: one-fold to three-folds.
The relative amounts of H4, H4K5ac, H4K5bu and H4K5cr were measured by ELISA in COS-7 cells or in cells expressing CobB-ha in biological triplicates and were repeated for at least three times and the values presented in the lower panel (see also Fig. S4).
E- COS-7 cells described in "D", expressing *CobB-ha* or not, were transfected with a GFP-BRD4-NUT expression vector, and for each condition, 8 GFP-BRD4-NUT foci (one in each of 8 different cells) were bleached and the recovery of GFP fluorescence (FRAP) was monitored as a function of time. The 16 datasets corresponding to each FRAP experiment were individually fitted allowing for the determination of the half-life (t1/2) of fluorescence recovery and the mobile fractions (values indicated below the figure). The mean ± 2 SEM are shown for each time point. Scale bar represents 10µm.

See Figure S4A for the selective action of CobB on H4K5 acetylation compared to butyrylation and crotonylation in COS-7 cells (related to Fig. 4D).

See Figure S4B for the effect of CobB expression in COS-7 cells on BRD4 - chromatin interaction stability (related to Fig. 4E).

Figure 5: Characterization of H4K5cr-bu/H4K5ac ratio and BDR4 redistribution between wild-type and *FASTKD1* ko cells

A- Chromatin from wild-type and *FASTKD1* ko REH cells (one sample for each genotype wild-type, ko-1 and ko-2) was extensively digested by micrococcal nuclease (MNase) and the resulting nucleosomes were respectively immunoprecipitated with anti-H4K5ac, anti-H4K5cr and anti-H4K5bu antibodies and sequenced. The reads were aligned and the RPKM normalized read counts values were converted into a 10 bp bin matrix of the signal 2Kb upstream and downstream TSS regions (TSS +/-2000 bp), using deepTools2 as described in STAR methods. For all TSS, the mean normalized read counts/TSS were calculated for each genotype (wild-type, ko-1 and ko-2) and each experiment H4K5cr, H4K5bu and H4K5ac. Considering each genotype, the TSS regions were then plotted according to their mean normalized read counts

for H4K5cr (upper panels) or H4K5bu (lower panels) ChIP-seq (y-axis) as a function of their mean normalized read counts for H4K5ac ChIP-seq (x-axis). In order to evaluate the relationship between the measured parameters, the non-acetyl acylation (H4K5cr or H4K5bu) and the acetylation of H4 lysine 5 (H4K5ac), in wild-type cell and in the two FASTKD1 ko cells, a linear regression model (grey lines) and an exponential regression model (red lines) were fitted.

B and **C**- Anti-BRD4 ChIP-seqs were performed on the MNase digested chromatin of wild-type and *FASTKD1* ko cell lines. The heatmap (B) and profiles (C) show BRD4 ChIP-seq normalized read counts in wild-type as well as in *FASTKD1* ko REH cells over all gene TSS centred regions (TSSs +/- 2000 bp). The TSS were ranked as a function of their transcriptional activity in wild-type REH cells and grouped into quartiles, Q1, Q2, Q3 and Q4, the first quartile (Q1: 75-100%) corresponding to the 25% genes with highest expression and the fourth quartile to the lowest 25% (Q4: 0-25%); (B) These gene groups are shown on the heatmap from top to bottom: highest (Q1: 75-100%) to lowest (Q4: 0-25%) gene expression levels; (C) The profiles corresponding to the different quartile groups are shown in different colours as indicated.

Figure 6: Mitochondrial activity drives H4K5 acylation and directs BRD4 – dependent gene expression in REH cell line and in B-ALL patients blasts

A- Volcano plot illustrating the differential gene expression signature between *FASTKD1* ko (ko-1 and ko-2) and wild-type REH cells. Y axis: -log10 (p-value); x-axis: log (ratio of normalized expression values between *ko* and wild-type cells). The genes down-regulated or up-regulated with a fold change >1.5 and a Student t-test *p*-value < 0.05 are respectively represented in blue and red.

B- The two gene groups defined in A were respectively used as genesets for GSEA plots to test for their enrichment/depletion in the JQ1-treated REH cells. These plots show a significant depletion of genes up or down regulated in *FASTKD1* ko cells. Both these genes' categories are therefore JQ1 sensitive.

C- Volcano plot illustrating the differential gene expression signature between B-ALL blasts with high H4K5 acylations (crotonylation and/or butyrylation, n = 15) and B-ALL blasts with low acylations (n = 10). Y axis: -log10 (p-value); x-axis: log (ratio of normalized expression values between B-ALL with high and low acylation levels). The genes down-regulated or up-regulated with an absolute fold change >1.5 and a Student t-test *p*-value < 0.05 are respectively represented in blue and red.

D- The two gene groups defined in C were respectively used as genesets for GSEA plots to test for their enrichment/depletion in the *FASTKD1* ko REH cells. These plots show significant depletion or enrichment of genes respectively down or up regulated in *FASTKD1* ko cells suggesting that the transcriptional effect of high acylation in B-ALL blasts is similar to the effect of *FASTKD1* ko - induced high acylation in REH cells.

See Figure S6 showing differential expression between B-ALL blasts with high compared to low acylation levels.

See Figure S7 for the GSEA of the transcriptomic signatures of REH cells (*FASTKD1* ko versus wild-type, or JQ1 treated versus untreated) and B-ALL with high versus low H4K5cr/bu levels.

Figure 7: Control of BRD4 reservoir by mitochondrial activity and cell metabolism: a working model

Enhanced mitochondrial activity leads to a global increase of histone H4K5 acylation/acetylation ratio. Bromodomain containing factors, such as BRD4, lose their tight binding to the genome-wide acetylated nucleosomes (reservoir pool) and therefore become available to be redistributed from this reservoir pool towards specific and localized genome regions including active genes' TSSs (functional pool).

1.2 Key resource table

KEY RESOURCES TABLE

REAGENT or RESOURCE	SOURCE	IDENTIFIER
Antibodies		
Rabbit monoclonal anti-BRD4 (WB and ChIP)	Bethyl Lab	Cat# A301-985A100, RRID: AB_2620184
Rabbit polyclonal anti-H4K5bu (WB and ELISA)	PTM biolabs	Cat#PTM-313
Rabbit polyclonal anti-H4K5bu (ChIP)	PTM biolabs	Cat#PTM-310
Rabbit polyclonal anti-H4K8bu (WB)	PTM biolabs	Cat#PTM-311
Rabbit polyclonal anti-H4K5cr (WB, ChIP and ELISA)	PTM biolabs	Cat#PTM-521
Rabbit polyclonal anti-H4K8cr (WB)	PTM biolabs	Cat#PTM-522
Rabbit polyclonal anti-H4K5ac (WB)	PTM biolabs	Cat#PTM-119
Rabbit polyclonal anti-H4K8ac (WB)	PTM biolabs	Cat#PTM-120
Rabbit polyclonal anti-H4K5bhb (WB)	PTM biolabs	Cat#PTM-1205
Rabbit polyclonal anti-H4K5lac (WB)	PTM biolabs	Cat#PTM-1407
Rabbit monoclonal anti-H4K5ac (ChIP)	Abcam	Cat#ab51997; RRID: AB_2264109
Rabbit polyclonal anti-HA (WB and ELISA)	Abcam	Cat#ab9110; RRID: AB_307019
Rabbit polyclonal anti-H4 (WB and ELISA)	Abcam	Cat#ab10158; RRID: AB_296888
Mouse monoclonal anti-Flag M2 (IF)	Sigma-Aldrich	Cat#F1804; RRID: AB_262044
Mouse monoclonal Anti-β-Actin (WB)	Sigma-Aldrich	Cat#A5441; RRID: AB_476744
Rabbit polyclonal H3 antibody (ELISA)	Abcam	Cat#ab1791; RRID: AB_302613
Goat anti-Rabbit IgG (H+L)-HRP (WB and ELISA)	Bio-rad	Cat#1706515, RRID: AB_2617112
Goat anti-Mouse IgG (H+L)-HRP (WB)	Bio-rad	Cat#170-6516; RRID: AB_11125547
Goat anti-Rabbit IgG, HRP linked antibody (ELISA)	Cell Signaling Technology	Cat#7074; RRID: AB_2099233
Goat anti-Mouse IgG (H+L), DyLight 405 (IF)	Invitrogen	Cat# 35501BID; RRID: AB_2533209
Bacterial and Virus Strains		
One shot Stbl3 Competent E. coli	Invitrogen	Cat#C737303
Biological Samples		
B-ALL patients' bone marrow samples, see Table S4	This paper	N/A
Chemicals, Peptides, and Recombinant Proteins		
JQ-1	(Emadali et al., 2013)	N/A
Rotenone	Sigma-Aldrich	Cat#R8875
Oligomycin A	Sigma-Aldrich	Cat#75351

Antimycin A	Sigma-Aldrich	Cat#A8674
FCCP	Sigma-Aldrich	Cat#C2920
Sodium octanoate	Sigma-Aldrich	Cat#C5038
Ranolazine	Sigma-Aldrich	Cat#R6152
Triacsin C	Sigma-Aldrich	Cat#T4540
ND-630 (Firsocostat)	MedChemExpress	Cat#HY-16901
Puromycin	Sigma-Aldrich	Cat#P8833
Mitotracker Red	Invitrogen	Cat#M7512
Micrococcal nuclease S7	Sigma-Aldrich	Cat#10107921001
Lipofectamine 2000	Invitrogen	Cat#11668019
Complete Mini protease inhibitors	Sigma-Aldrich	Cat #11836153001
All histone peptides used in this study (H4 /H4K5acK8ac /H4K5buK8bu /H4K5acK8bu /H4K5buK8ac /H4K5bu /H4K8bu)	(Goudarzi et al., 2016)	N/A
LymphoPrep™ Solution	Axis Shield PoC	Cat#1114547
Gelatin solution	Sigma-Aldrich	Cat#G1393
TRIzol reagent	Invitrogen	Cat#15596018
Trichostatin A (TSA)	Sigma-Aldrich	Cat#T8852
Trichloroacetic Acid (TCA)	Sigma-Aldrich	Cat#T-0699
n-Butryric acid	Sigma-Aldrich	Cat#B-2503
Dynabeads protein G	Thermo Fisher	Cat#10007D
Streptavidin Sepharose beads	GE Healthcare	Cat#17-5113-01
Seahorse XF base medium	Agilent	Cat#103334-100
Seahorse XFe96 FluxPak	Agilent	Cat#102601-100
pMD19 T-vector	TAKARA	Cat#3270
3,3',5,5'-Tetramethylbenzidine (TMB) substrate	Abcam	Cat#ab171523
Stop solution for TMB Substrate	Abcam	Cat#ab171529
Critical Commercial Assays		
SuperScript III First-Strand Sythesis	Invitrogen	REF#18080-051
HieffTM qPCR SYBR® Green Master Mix (Low Rox Plus)	Yeasen	Cat#11202ES08
AllPrep DNA/RNA/Protein Mini Kit	QIAGEN	Cat#80004
NextSeq® 500/550 High Output v2.5(150 Cycles)	Illumina	Cat#20024907
MicroPlex Library Preparation Kit v2	Diagenode	Cat#C05010012
TruSeq Stranded Total RNA (RiboZero Human/Mouse/Rat) Library Prep	Illumina	Cat#RS-122-2201
Deposited Data		
All deposited data superseries	This study	GSE164072
ChIP-seq H4K5ac and H4K5cr (REH WT and KO)	This study	GSE164016
ChIP-seq BRD4 (REH WT and KO)	This study	GSE164031
RNA-seq REH WT and *FASTKD1* KO	This study	GSE164043
RNA-seq REH WT ctrl and JQ1	This study	GSE164045
RNA-seq B-ALL (25 patients)	This study	GSE164060
RNA-seq REH control and *FASTKD1* sh (knock down)	This study	GSE164071
Original western blot images	This study	Mendeley DOI: https://data.mendele

		y.com/drafts/2hk6dhmcbr
Experimental Models: Cell Lines		
Human: acute lymphoblastic leukemia cell line REH	ATCC	CRL-8286; RRID: CVCL_1650
Human: acute lymphoblastic leukemia cell line REH depleted of *FASTKD1 (ko-1)*	This study	N/A
Human: acute lymphoblastic leukemia cell line REH depleted of *FASTKD1 (ko-2)*	This study	N/A
Cercopithecus aethiops: SV40 transformed kidney fibroblast cell line COS-7	ATCC	CRL-1651; RRID: CVCL_0224
Oligonucleotides		
sgRNA targeting sequences: *FASTKD1* #1: GTTATCTTCAACAACTCTAA	(Sanjana et al., 2014)	N/A
sgRNA targeting sequences: *FASTKD1* #2: AAATAGCTGATATTGTTCAT	(Sanjana et al., 2014)	N/A
shRNA targeting sequences: *FASTKD1* #1: ACTTGCGTGCAACATCTTAAT	This study	N/A
shRNA targeting sequences: *FASTKD1* #2: GTCGGTTCTTACGCCTTATTAC	This study	N/A
shRNA targeting sequences: *FASTKD1* #3: GCCAGTTTGAATGGAACTCTAT	This study	N/A
shRNA targeting sequences: *FASTKD1* #4: GCTTCGTCTAAGAGCTATTTG	This study	N/A
shRNA targeting sequences: *FASTKD1* #5: ATTCGTCCATTCAGCGTATTG	This study	N/A
Primers see table S5	This study	N/A
Recombinant DNA		
Plasmid: lentiGuide-Puro	Kind gift from Feng Zhang(Sanjana et al., 2014)	Addgene plasmid # 52963; RRID: Addgene_52963
Plasmid: lentiCas9-Blast	Kind gift from Feng Zhang(Sanjana et al., 2014)	Addgene plasmid # 52962; RRID: Addgene_529 62
Plasmid: LeGO-iG2	Kind gift from Boris Fehse(Weber et al., 2008)	Addgene plasmid # 27341; RRID: Addgene_27341
Plasmid: LeGO-FASTKD1-3xflag	This study	N/A
Plasmid: Co1491-IRES-RFP	This study, kindly provided by Corinne Albiges-Rizo	N/A
Plasmid: Co1491-NLS-CobB-HA	This study, primary CMV-NLS-CobB construct is a kind gift from Heinz	N/A

	Neumann(Spinck et al., 2020)	
Plasmid: pLVX-shRNA1	Clontech	Cat#632177
Plasmid: BRD4-NUT-GFP	(Reynoird et al., 2010)	N/A
Plasmid: pMD2.G	Kind gift from Didier Trono	Addgene plasmid #12259; RRID: Addgene_12259
Plasmid: psPAX2	Kind gift from Didier Trono	Addgene plasmid #12260; RRID: Addgene_12260
Plasmid: pRSV-Rev	Kind gift from Didier Trono (Dull et al., 1998)	Addgene plasmid # 12253; RRID: Addgene_12253
Software and Algorithms		
STAR v2.5.2b	(Dobin et al., 2013)	https://github.com/alexdobin/STAR
Bowtie2 aligner	(Langmead and Salzberg, 2012)	http://bowtie-bio.sourceforge.net/bowtie2/index.shtml
DeepTools2	(Ramírez et al., 2016)	https://deeptools.readthedocs.io/en/develop/
R package DEseq2	Bioconductor	http://bioconductor.org/packages/3.12/bioc/html/DESeq2.html
HTseq v0.9.1	(Anders et al., 2015)	https://htseq.readthedocs.io
Mascot v2.3.01	Matrix Science	http://www.matrixscience.com
Qual Browser v3.0.63	Thermo Fisher	N/A
ImageJ	(Schneider et al., 2012)	https://imagej.nih.gov/ij/
GraphPad Prism 5	Graphpad	http://bowtie-bio.sourceforge.net/bowtie2/index.shtml
ZEISS ZEN lite	ZEISS	https://www.zeiss.com/microscopy/int/products/microscope-software/zen-lite.html
SPSS Statistics v20	IBM	https://www.ibm.com/support/pages/downloading-ibm-spss-statistics-20

1.3 STAR* Methods

RESOURCE AVAILABILITY

Lead contact

Further information and requests for resources and reagents should be directed to and will be fulfilled by the Lead Contact, Saadi Khochbin (saadi.khochbin@univ-grenoble-alpes.fr).

Materials Availability

Plasmids and cell lines generated in this study are available upon request.

Data and Code Availability

- The ChIP-seq data and RNA-seq data generated during this study haven been deposited at GEO and are publicly available as of the date of publication. Accession numbers are listed in the key resources table. Original western blot images have been deposited at Mendeley and are publicly available as of the date of publication. The DOI is listed in the key resources table. Microscopy data reported in this paper will be shared by the lead contact upon request.
- This study does not report original code.
- Any additional information required to reanalyze the data reported in this paper is available from the lead contact upon request.

EXPERIMENTAL MODEL AND SUBJECT DETAILS

Cell lines and cell cultures

Human lymphoblastic leukemia cell line REH (Female, CVCL_1650) was obtained from National Collection of Authenticated Cell Cultures and was authenticated by STR analysis prior to use. REH and the derivative cells were maintained in RPMI-1640 (Gibco) supplemented with 10% FBS (Dominique DUTSCHER), 4mM L-glutamine (Gibco) and 1% Penicillin-Streptomycin (Gibco). COS-7 (Male, CVCL_0224) were purchased from ATCC, and were cultured in DMEM (Low glucose, 1g/L, Gibco) supplemented with 10% FBS, 4mM L-glutamine and 1% Penicillin-Streptomycin. All cells were incubated at 37°C with 5% CO_2.

CRISPR/Cas9 mediated knockout cell line

REH cells were co-introduced with lenti-Cas9 and lenti-sgRNAs plasmids (targeting sequences indicated in Key Resource Table) using the lentivirus infection approach described in the method details. 3 days after infection, positive cells with sgRNAs were enriched using 1.0μg/ml puromycin (Sigma-Aldrich, Cat# P8833). Genotypes of the resultant cell populations were analysed by PCR amplification (primers shown in Table S5) and sanger sequencing. Successful genome-editing of cell populations was documented by multi-spikes in the sequence map of PCR products. After being seeded into 96-well plates for 2-3 weeks, single cell clones were obtained and genotypes of each allele of single cell clones was analysed through sanger sequencing following TA cloning of PCR products. Knockout clones with frameshift indels within the exons were used for further experiments.

B-ALL patients' bone marrow samples

All the patients (n = 31) enrolled in this study were newly diagnosed in Ruijin hospital (See Table S4). Bone marrow aspiration was conducted at diagnosis. Mononuclear cells were enriched from BM samples by density gradient centrifugation with LymphoPrep™ Solution (Axis Shield PoC, Cat#1114547) and were stored at -80°C as dry pellets for further experimental analysis. This study was approved by the ethical board of Shanghai Institute of Hematology. All patients and their guardians were provided with informed consent for sample collection and research in agreement with the Declaration of Helsinki.

METHOD DETAILS

Drug treatment and sample preparations

For sodium octanoate (Sigma-Aldrich, Cat#C5038) treatment, 5 x10^5/ml REH cells were seeded into 6-well plates, treated with or without indicated concentrations of sodium octanoate for 24 hours. For other compounds, REH wild-type, ko-1 and ko-2 cells were seeded at the density of 7.5 x10^5/ml in 6-well plates. Treatment strategy was as following: 100 nM ND-630 (MedChemExpress, Cat#HY-16901) for 6 hours, 0.5 μM Rotenone (Sigma-Aldrich, Cat#R8875) for 1 and 2 hours respectively, 0.5 mM Ranolazine (Sigma-Aldrich, Cat#R6152) for 6 hours, 3 μM Triacsin C (Sigma-Aldrich, Cat#T4540) for 16 hours. After exposition to the different compounds, these cells were lysed with 8 M urea and subjected to sonication (Biorupter, High, 30s ON/OFF, total 10min) to obtain total protein. Protein solutions were quantified using Bradford assay (Bio-rad) before being added with SDS-PAGE loading buffer for western blot analysis.

For JQ1 treatment, REH wild-type cells were exposed to 0.1 μM or 0.5 μM JQ1 or DMSO as control respectively for 24 hours. 5x10^6 cells were then harvested and yielded to RNA extraction with 500 μl TRIzol reagent (Invitrogen, Cat#15596018) according to the provider's protocol. Precipitated RNA was dissolved in DEPC-treated water and used for RNA-sequencing.

For salt elution experiments around 1x107 REH wild-type, ko-1 and ko-2 or 4x106 COS-7 control and CobB-ha expressing cells were harvested, washed twice with ice cold PBS, and split into equal aliquots. Each aliquot of cells was lysed in LSDB lysis buffer (50mM HEPES pH7.0, 3mM MgCl2, 20% glycerol, 0.1% NP-40, 1mM DTT, 1xprotease cocktail inhibitors) containing different concentrations of salts and 10mM sodium butyrate for 30 min on ice. For REH cells, the KCl concentrations of 100, 150, 200 or 250 mM were respectively used and for COS-7 cells, the KCl concentrations of 100, 150, 200 mM KCl were respectively added to the lysis buffer. After centrifugation at 12000g 4°C for 10min, the supernatants were saved to detect soluble BRD4, while the nuclei pellets were subjected to SDS-PAGE loading buffer to detect chromatin tightly bound BRD4.

For JQ1 treatment assay correlated with Figure 4C, lower panel, 1x10^6 /ml REH wild-type, ko-1 and ko-2 cells were exposed to 0.1 μM, 0.5 μM or 5 μM JQ1 or DMSO as control in 6-well plates. After 3 hours, cells were collected and lysed in LSDB lysis buffer with 100 mM KCl and 10 mM sodium butyrate for 30 min on ice. After centrifugation at 12000g for 10 min at 4°C, supernatants were collected to detect soluble BRD4, while the nuclei pellets were subjected to SDS-PAGE loading buffer to detect chromatin tightly bound BRD4.

Plasmids, shRNA and sgRNA

FASTKD1 (NM_024622) was chemically synthesized and was cloned into LeGO-iG2 (Addegene #27341) vector to generate LeGO-*FASTKD1-3x Flag* construct. Co1491-IRES-RFP modified from pSicoR PGK (Addgene #12084) was kindly provided by Corinne Albiges-Rizo. Co1491-NLS-CobB-HA was subcloned from CMV-NLS-CobB, which was kindly provided by Heinz Neumann (Spinck et al., 2020). shRNAs and sgRNAs were designed using GPP Web Portal(https://portals.broadinstitute.org) or referring to GeCKO v2 library (Sanjana et al., 2014) with the corresponding targeting sequences indicated in the Key Resource Table, and were cloned into pLVX-shRNA1 (Clontech, Cat#632177) and LentiGuide-Puro plasmid (Addgene

plasmid#52963) respectively. All plasmids were confirmed by sanger sequencing before being used in this study.

Lentivirus production and infection

5µg lentiviral transfer and package plasmids were co-transfected into 293T cells in each well of 6-well plates using lipofectamine 2000 (Invitrogen, Cat#11668019) according to the manufacturer's instructions. For pLVX-shRNA1, lentiCas9-blast, lentiGuide-Puro and the derivative plasmids, second generation packaging plasmids (psPAX2 and pMD2G) were used for generating viral particles, and an additional pRSV-Rev plasmid was used for transferring LeGO-iG2 and Co1491-IRES-RFP backbone as well as the subcloned plasmids. Virus supernatants were collected at 24 and 48 hours after plasmid transfection and precleared with 0.45 µm filter (Millipore). Amicon Ultra-15 fiters (Millipore) were used to concentrate virus supernatants by centrifugation at 4000 rpm 4°C for 30 min. Concentrated virus was diluted with complete growth medium and immediately used to infect the cells of interests. Infection was performed in 12-well plates, with each well containing 1ml diluted virus medium and $2x10^5$ REH cells, or at 20% confluency in the case of COS-7 cells. 24 hours after infection, virus medium was washed out and replaced with fresh culture medium. Cells were then maintained regularly before further selection. For shRNA knockdown, positive cells were enriched 3 days after virus infection by 1.0 µg/ml puromycin treatment and were maintained for an average of 1 week before experimental analysis. For CobB and FASTKD1 re-expressing cells, RFP and GFP positive cells were respectively sorted with FacsAria IIu- cell sorter (BD Biosciences) 1-2 weeks after infection.

Histone preparation

Histone samples were prepared by acid extraction protocol as previously described with minor modifications (Buchou et al., 2017). In brief, $1x10^7$ REH wild-type, ko-1 and ko-2 cells, or $1x10^7$ COS-7 control and CobB expressing cells were lysed in 1 ml lysis buffer (0.06% NP-40, 10 mM HEPES pH 7.0, 10 mM KCl, 1.5 mM $MgCl_2$, 0.34 M sucrose, 1xprotease cocktail inhibitor) with 10 mM sodium butyrate for 10 min on ice. Cell nuclei were pelleted by centrifugation at 250g 4°C for 5 min, and subjected to histones extraction using 0.2 M H_2SO_4 for 16 hours at 4°C. After centrifugation at 16000 g for 10 min at 4°C, solubilized histones were collected and then precipitated by adding TCA drop by drop to the final volume of 20%. Histone pellets were then washed once with cold acetone + 0.1%HCl, twice with cold acetone and were dried completely in air.

MS quantification of histone acylations

5 µg of each histone sample from REH wild-type, ko-1 and ko-2 cells were separated by SDS-PAGE and each spliced histone band was in-gel digested with trypsin. The tryptic peptides were analyzed by Orbitrap Fusion following an EASY-nLC 1000 HPLC system (Thermo Fisher Scientific, San Jose, CA). Mass spectrometry data were analyzed by Mascot software (version 2.3.01, Matrix Science Ltd., London, UK) against an in-house human histone sequence database (83 sequences; 13,870 residues) generated from the UniProt database (updated on 01/27/2015). All identified MS/MS spectra were manually verified. Peptides containing modifications were manually quantified using the Qual Browser (version 3.0.63, Thermo Fisher

Scientific, San Jose, CA) by the area under the curve (AUC) of the extracted precursor ion of each peptide. Acylated histone peptides were normalized to the corresponding histone peptides. The relative abundance of indicated histone acylations in two *ko* clones versus wild-type cells was plotted in the column chart.

Peptide pull-down assay

Peptides pull-down assay was performed using a protocol described previously (Goudarzi et al., 2016). Briefly, peptides (H4 /H4K5acK8ac /H4K5buK8bu /H4K5acK8bu /H4K5buK8ac /H4K5bu /H4K8bu) were first bound to beads by incubating equal amount of each type of peptide with Streptavidin Sepharose beads (GE Healthcare, Cat#17-5113-01) in PBS supplemented with 100ng/ml TSA for 20min. Bound beads were then washed with PBS and LSDB lysis buffer (50 mM HEPES pH 7.0, 3 mM $MgCl_2$, 20% glycerol, 0.1% NP-40, 1 mM DTT, 1xprotease cocktail inhibitors) with 25mM KCl and 10mM sodium butyrate.

Around $1x10^7$ *FASTKD1 ko* or wild-type cells were harvested and lysed in 500 µl LSDB lysis buffer with 500 mM KCl and 10 mM sodium butyrate for 20 min on ice. After centrifugation at 12000g for 10 min at 4 °C, protein supernatants were collected and diluted with LSDB lysis buffer with 10 mM sodium butyrate to achieve the salt concentration of 250 mM. A small volume of diluted protein supernatants was saved for input, and the rest was split into equal aliquots, each incubated with the corresponding conjugated beads for 2 hours at 4 °C. Beads then were pelleted and washed twice with LSDB lysis buffer with 250mM KCl and 10 mM sodium butyrate and once with PBS with 10 mM sodium butyrate. After incubating with 1x SDS-PAGE loading buffer at 100°C for 5min, pulled-down complexes were eluted from beads and preserved for western blotting analysis.

Western blotting

Western blotting with SDS-PAGE were carried out according to standard procedures using the antibodies listed in Key Resource Table. After adding ECL substrates (Bio-rad), revelation was performed with Chemidoc (Bio-rad) or Vilber Chemiluminescence system (Vilber). The dilutions of antibodies used in this study are as follows: anti-BRD4 (Bethyl Lab, 1:2000), anti-H4K5bu (PTM biolabs, 1:1000), anti-H4K8bu (PTM biolabs, 1:1000), anti-H4K5cr (PTM biolabs, 1:1000), anti-H4K8cr (PTM biolabs, 1:1000), anti-H4K5ac (PTM biolabs, 1:1000), anti-H4K8ac (PTM biolabs, 1:1000), anti-H4K5bhb (PTM biolabs, 1:1000), anti-H4K5lac (PTM biolabs, 1:1000), anti-HA (Abcam, 1:2000), anti-H4 (Abcam 1:1000), Anti-β-Actin (Sigma-Aldrich, 1:5000), Goat anti Rabbit IgG(H + L)-HRP (Bio-rad, 1:5000), Goat anti-Mouse IgG (H + L)-HRP (Bio-rad, 1:10000).

Relative quantification of histone acylations with ELISA

Indirect ELISA was set up according to a protocol described previously (Dai et al., 2011). Total protein was obtained from $5x10^6$ mononuclear cells of each patient in parallel with RNA extraction using AllPrep DNA/RNA/Protein Mini Kit (Qiagen) following the manufacturer's instructions. In the case of COS-7 control and CobB expressing cells, histones prepared through acid extraction protocol were used for ELISA assay. These precipitated proteins were dissolved in a small volume of 8 M urea and quantified by Bradford reagent (Bio-rad). Protein solution was diluted with PBS and coated into triplicate wells of 96-well flat-bottom plates (Nunc-Immuno products, Thermo Fisher) at 4°C for 16 hours. The amount of protein being coated was optimized according to the histone marks being detected and the protein samples being used.

In the case of total protein of B-ALL patients' samples, the protein amount for each well was as follows: 2.5µg for H4K5cr and H4K5bu detection, 0.0125 µg for H3 detection. In the case of protein from COS-7 control and CobB expressing cells, the amount of protein for each well was as follows: 0.15µg for H4K5bu and H4K5ac detection, 0.3 µg for H4K5cr detection, 0.015 µg for H4 detection. Coated plates were then blocked with 5% BSA for 1 hour at room temperature and sequentially incubated with primary antibodies accordingly and secondary antibodies. Dilutions of the antibodies used in this assay were: H4K5cr (PTM biolabs, 1:500), H4K5bu (PTM biolabs, 1:500), H3 (Abcam,1:5000), H4K5ac (Abcam, 1:2000), H4 (Abcam, 1:1000), HRP linked Goat anti Rabbit IgG (Bio-rad or CST, 1:4000). After the addition of TMB substrate (Abcam, Cat#ab171523) and acid stop solution (Abcam, Cat#ab171529), the signal intensity was recorded at OD 450 nm. Relative quantity of histone marks was calculated based on the value of signal intensity.

Immunofluorescence

Empty vector and FASTKD1-Flag expressing cells were treated with 250 nM Mitotracker Red (Invitrogen, Cat#M7512) dye for 20 min at 37 ℃ in CO2 incubator. Approximately $8x10^4$ cells were then collected, washed once with PBS and spined onto glass slide at 800 rpm for 5 min. Fixation was performed using 4% paraformaldehyde for 15 min, followed by permeabilization with 0.3% Triton-X100 for 10 min at room temperature. After being blocked with 10% BSA for 1 hour at room temperature, slides were sequentially incubated with anti-Flag antibody (Sigma-Aldrich, 1:500 dilution) and anti-Mouse IgG DyLight 405 (Invitrogen, 1:500 dilution). Fluorescent images were captured by confocal laser scanning microscope (TCS SP8, Leica) under a 63x 1.40 numeric aperture oil-immersion lens and were processed with ImageJ.

Fluorescence recovery after photobleaching (FRAP)

$2x10^5$ COS-7 control and CobB expressing cells were seeded in 1-well Chambered Coverglass (LAB-TEK brand products, Thermo Fisher) respectively the day before being transfected with 1µg BRD4-NUT-GFP plasmid using lipofectamine 2000 (Invitrogen). 24 hours after transfection, FRAP was performed on 8 independent cells of each group using fluorescent microscope (LSM710 NLO-LIVE7-Confocor3, Zeiss) equipped with a 488 nm laser and a LP505 filter. A circular region on GFP foci was bleached for 1.592 seconds and the recovery of fluorescence was recorded each second for a duration of 75 seconds after photobleaching by software ZEN lite. Immunofluorescence photos of BRD4-NUT-GFP foci from control and CobB expressing cells were captured before FRAP.

For the data analysis and plotting, fluorescence intensity was normalized and rescaled to a reference axis from 0 to 1. 8 datasets from each cell group were individually fitted using the single exponential model: $I(t) = \alpha(1 - 2^{-\frac{t}{\kappa}})$. The 8 biological replicates giving the best fitting statistics were used to calculate the average half-life ($t_{1/2}$) of fluorescence recovery (κ) and average mobile fractions (α). Values of mean ± 2 SEM are shown in the figure. FRAP curve was plotted on the mean of the 8 biological replicates ± 2 SEM at each time point.

Metabolic assay

Metabolic assay was performed according to the Seahorse XF Cell Mito Stress Test user manuals. Briefly, 1×10^5 REH wild-type, ko-1 and ko-2 cells were resuspended in 180 µl assay medium formulated as pH 7.4 ± 0.1 bicarbonate-free Seahorse XF base medium (Agilent,

Cat#103334-100), with 10 mM glucose (Gibco), 1 mM sodium pyruvate (Gibco) and 4 mM L-glutamine (Gibco). Resuspended cells were then seeded in XF96 cell culture plates (Agilent, Cat#102601-100), which had previously been coated with 0.1% gelatin (Sigma-Aldrich, Cat#G1393) for at least 1 hour at room temperature. The seeded plates were then incubated at 37 °C for 1 hour in a non-CO2 incubator before being loaded onto Seahorse XFe96 Analyzer (Agilent). Oxygen consumption rate (OCR) was measured at basal level as well as after injection of 1 µM oligomycin A (Sigma-Aldrich, Cat#75351), 1 µM FCCP (Sigma-Aldrich, Cat#C2920), 0.5 µM rotenone (Sigma-Aldrich, Cat#R8875) and 1 µM antimycin A (Sigma-Aldrich, Cat#A8674). OCR values (pmol/min) were normalized to cell number. Mean ± SEM based on 5 replicates were plotted in the figure.

RT-qPCR

$5x10^6$ cells from *FASTKD1* wild-type and two *ko* clones, or from shCtl and two shRNAs knockdown cell lines were collected and lysed in 500 µl TRIzol reagent (Invitrogen, Cat#15596018). Total RNA was obtained by phenol-chloroform extraction and isopropanol precipitation using standard procedure. For B-ALL patients' samples, total RNA was extracted from $5x10^6$ mononuclear cells of each patient using AllPrep DNA/RNA/Protein Mini Kit (Qiagen, Cat# 80004) following the manufacturer's instructions.

cDNA was produced from 1µg RNA with superscript III transcriptase (Invitrogen, Cat#18080-051) using random hexamers according to the manufacturer's instructions. Quantitative PCR (qPCR) was performed with SYBR green reagent (Yeasen, Cat#11202ES08) on ViiA 7(The Applied Biosystem) using primers described in Table S5. *CPT1A* and *ND2* with patients' samples were calculated via -dCt against GAPDH. The correlation between *CPT1A* and *ND2* was analysed with Spearman correlation. Mean values of triplicates were plotted with scatterplot using GraphPad Prism 5. Fold changes of gene expression levels were calculated via 2^-ddCt and are represented by mean ± SEM based on at least three independent experiments. Statistical differences between wild-type and two *ko*, or between shCtl and shRNAs groups were calculated with Fisher's Least Significant Difference (LSD) post one-way ANOVA test. * $p<0.05$, ** $p<0.01$, ***$p<0.001$.

RNA-seq

Three independent RNA extractions from *FASTKD1* wild-type and two *ko* clones (ko-1, ko-2), or from control and two knockdown cell lines (sh-1, sh-2), or from solvent and JQ1 treated wild-type cells, or from 25 B-ALL patients' bone marrow samples were sequenced. For each sample, 1 µg RNA samples (RIN = 10) were used for libraries preparations with TruSeq Stranded Total RNA (RiboZero Human/Mouse/Rat) Library Prep (Illumina, Cat#RS-122-2201) according to manufacturer's instructions. Each library was quantified on Qubit with Qubit® dsDNA HS Assay Kit (Life Technologies) and the size distribution was examined on the Fragment Analyzer with High Sensitivity NGS Fragment Analysis kit (Agilent). Libraries prepared from solvent and JQ1 treated cells samples were sequenced on Illumina NS500 (PE75) at the TGML Platform of Aix-Marseille Université, and those prepared from *FASTKD1* control and knockdown, wild-type and knockout cells samples, and B-ALL patients' samples were sequenced on Hiseq 4000 (PE150) platform in Novagene company.

The sequenced reads were aligned from raw sequence fastq data using STAR v2.5.2b software on UCSC hg19 reference genome. The aligned reads were normalized, and log transformed

using the R bioconductor package DEseq2 (http://bioconductor.org/packages/3.12/bioc/html/DESeq2.html).
The standardized and normalized read counts of mitochondrial genes were used to generate a heatmap in Figure 1A. Supervised transcriptomic analyses were performed to identify genes significantly up-and down regulated between two conditions using thresholds of Student t-test p-value <0.05 and fold change absolute value of 1.5.

ChIP-seq

ChIP assays for H4K5cr, H4K5ac and BRD4 were carried out as previously described with minor modifications (Buchou et al., 2017, Barral et al. 2017). Around 5 -10 x10^7 REH wild-type, ko-1 and ko-2 cells were harvested and lysed in 1.5 ml lysis buffer (0.05% Triton-X 100, 15 mM Tris-HCl pH 7.4, 60 mM KCl, 15 mM NaCl, 0.34 M sucrose, 2 mM EDTA, 0.5 mM EGTA, 1 mM DTT, 0.65 mM spermidine, 1x protease cocktail inhibitors) with 10 mM sodium butyrate and incubated for 5 minutes at 4°C. Cell nuclei were pelleted by centrifugation at 250 g for 5 min at 4°C and resuspended in MNase buffer (10 mM Tris-HCl pH 7.5, 10 mM KCl, 2 mM $CaCl_2$) with10 mM sodium butyrate. Then the cell nuclei solution was subjected to micrococcal nuclease S7 (Sigma-Aldrich, Cat#10107921001) digestion (5U MNase per 100µg nuclei) at 37°C for 20 min to obtain mononucleosomes. Small aliquots of mononucleosomes solutions were collected for input and used to check the efficiency of digestion before immunoprecipitation.

Immunoprecipitations were carried out as follows: 5 µg anti-H4K5cr (PTM biolabs, Cat#PTM-521), anti-H4K5bu (PTM biolabs, Cat#PTM-310), anti-H4K5ac (abcam, Cat#ab51997), anti-BRD4 (Bethyl lab, Cat#A301-985A100) antibodies were coupled with 50 µl Dynabeads protein G (Thermo Fisher, Cat#10007D) respectively according to the manufacturer's instructions. Digested mononucleosomes solutions were diluted with LSDB500 buffer (50 mM HEPES pH 7.0, 3mM MgCl2, 500 mM KCl, 20% glycerol, protease cocktail inhibitors) with 10 mM sodium butyrate to achieve the final KCl concentration of 350 mM. For each reaction, around 100 µg chromatin was incubated with antibody-coupled beads at 4°C for 16 hours. Immunoprecipitated beads were then washed three times with LSDB350 buffer (50 mM HEPES pH 7.0, 3 mM $MgCl_2$, 350 mM KCl, 20% glycerol, protease cocktail inhibitors) with 10 mM sodium butyrate and one time with elution buffer (10 mM Tris-HCl pH 8.5, 1 mM EDTA). ChIP samples were eluted from beads with elution buffer containing 1%SDS at 65°C for 15 min and were purified by phenol-chloroform extraction and ethanol precipitation in parallel with input samples.
For sequencing, ChIP libraries were prepared using MicroPlex Library Preparation Kit v2 (Diagenode) according to manufacturer's instructions. Each library was quantified on Qubit with Qubit® dsDNA HS Assay Kit (Life Technologies) and size distribution was examined on the Fragment Analyzer with High Sensitivity NGS Fragment Analysis kit (Agilent).
ChIP libraries against H4K5cr, H4K5ac and BRD4 (1st experiment) were sequenced on a High-output flow cell (400M clusters) using the NextSeq® 500/550 High Output v2.5 150 cycles kit (Illumina), in paired-end 75/75nt mode, according to manufacturer's instructions at the TGML Platform of Aix-Marseille University.
ChIP libraries against H4K5bu and BRD4 (2nd experiment) were sequenced using the NovaSeq 6000 in PE150 mode according to manufacturer's instructions at the Novogene company.

Raw fastq files were processed by 5 prime trimming, keeping 30 bp-length fragments, using `fastx_trimmer` (with options -l 30 -Q33). The trimmed fastq files were aligned on the USCS human hg38 genome using the Bowtie2 aligner (Langmead and Salzberg, 2012), with options –end-to-end, –no-mixed, –no-discordant. The aligned reads were filtered according to alignment quality (mapping quality score > 30) and normalized using bamCoverage by Reads Per Kilobase per Million mapped reads (RPKM) for the anti K5ac, K5cr and Kbu ChIP-seq and scaling factors for the anti-BRD4 ChIP-seq.
For the anti-BRD4 ChIP-seq, scaling factors were computed according to the Spike in free method (Jin et al., 2020). Accordingly, for the first experiment, the respective scaling factors 4.25, 3.58 and 5.81 were applied when calculating the BRD4 ChIP-seq read coverage in wild-type, ko1 and ko2 cells. For the second experiment the corresponding scaling factors of 4.85, 4.6 and 5.72 were respectively applied.
The aligned read counts were converted into a 10 bp bin matrix of the signal 2Kb upstream and downstream genes TSS, using computeMatrix (from the package deepTools2, Ramírez et al., 2016), heatmaps and profiles were generated using the respective deepTools2 packages, plotHeatmap and plotProfile.

Script for bamCoverage normalizing with RPKM:
bamCoverage -b myfile_notrim.srt.bam --extendReads --binSize 4 --minMappingQuality 30 --normalizeUsing RPKM -o myfile_notrim.bw
Script for bamCoverage with scaling factors:
bamCoverage -b my_file.bam --extendReads --numberOfProcessors 4 --binSize 4 --minMappingQuality 30 --normalizeUsing None --scaleFactor my_value -o my_file.bw

Scripts for computeMatrix and plotHeatmap
computeMatrix reference-point -R tss_grch38.bed -S \
  file1.bw \
  file2.bw \
  …
  --outFileName matrix_tss_grch38.txt.gz --referencePoint TSS --binSize 10 --beforeRegionStartLength 2000 --afterRegionStartLength 2000 --numberOfProcessors 32 --sortRegions keep
plotHeatmap --matrixFile matrix_tss_grch38.txt.gz --outFileName hm_tss_grch38.png --colorMap YlOrRd --sortRegions descend

QUANTIFICATION AND STATISTICAL ANALYSIS

Statistical analysis was performed with SPSS v20. Details of the number and type of replication for each experiment were described in method details or figure legends where appropriate. Each dot represents one individual in patients' experiment. Data were presented as median with interquartile range for non-normally distributed populations of patients' samples or mean ± 2 standard error of the mean (SEM) for FRAP experiment. All other data were presented as mean ± SEM. When comparing normally distributed two groups, statistical significance was determined by Student t-test. When comparing multiple groups, Fisher's LSD post one-way ANOVA test was used to determine the significance between groups. When comparing non-normally distributed data, Mann-Whitney U test was used to determine the significance, and

Spearman correlation was used to determine the correlation. $p < 0.05$ were considered statistically significant. Statistics are $*p < 0.05$, $**p < 0.01$, $***p < 0.001$.

1.4 References
REFERENCES

Anders, S., Pyl, P.T., and Huber, W. (2015). HTSeq--a Python framework to work with high-throughput sequencing data. Bioinformatics *31*, 166-169.

Andrews, F.H., Shinsky, S.A., Shanle, E.K., Bridgers, J.B., Gest, A., Tsun, I.K., Krajewski, K., Shi, X., Strahl, B.D., and Kutateladze, T.G. (2016a). The Taf14 YEATS domain is a reader of histone crotonylation. Nat. Chem. Biol. *12*, 396-398.

Andrews, F.H., Strahl, B.D., and Kutateladze, T.G. (2016b). Insights into newly discovered marks and readers of epigenetic information. Nat. Chem. Biol. *12*, 662-668.

Bao, X., Liu, Z., Zhang, W., Gladysz, K., Fung, Y.M.E., Tian, G., Xiong, Y., Wong, J.W.H., Yuen, K.W.Y., and Li, X.D. (2019). Glutarylation of Histone H4 Lysine 91 Regulates Chromatin Dynamics. Mol. Cell *76*, 660-675.e669.

Barral, S., Morozumi, Y., Tanaka, H., Montellier, E., Govin, J., de Dieuleveult, M., Charbonnier, G., Couté, Y., Puthier, D., Buchou, T., et al. (2017). Histone Variant H2A.L.2 Guides Transition Protein-Dependent Protamine Assembly in Male Germ Cells. Mol. Cell *66*, 89-101.e108.

Buchou, T., Tan, M., Barral, S., Vitte, A.L., Rousseaux, S., Arechaga, J., and Khochbin, S. (2017). Purification and Analysis of Male Germ Cells from Adult Mouse Testis. Methods Mol. Biol. *1510*, 159-168.

Chen, Y., Sprung, R., Tang, Y., Ball, H., Sangras, B., Kim, S.C., Falck, J.R., Peng, J., Gu, W., and Zhao, Y. (2007). Lysine propionylation and butyrylation are novel post-translational modifications in histones. Mol. Cell. Proteomics *6*, 812-819.

Crespo, M., Damont, A., Blanco, M., Lastrucci, E., Kennani, S.E., Ialy-Radio, C., Khattabi, L.E., Terrier, S., Louwagie, M., Kieffer-Jaquinod, S., et al. (2020). Multi-omic analysis of gametogenesis reveals a novel signature at the promoters and distal enhancers of active genes. Nucleic Acids Res. *48*, 4115-4138.

Dai, B., Dahmani, F., Cichocki, J.A., Swanson, L.C., and Rasmussen, T.P. (2011). Detection of post-translational modifications on native intact nucleosomes by ELISA. J. Vis. Exp., 2593.

Dai, L., Peng, C., Montellier, E., Lu, Z., Chen, Y., Ishii, H., Debernardi, A., Buchou, T., Rousseaux, S., Jin, F., et al. (2014). Lysine 2-hydroxyisobutyrylation is a widely distributed active histone mark. Nat. Chem. Biol. *10*, 365-370.

Dobin, A., Davis, C.A., Schlesinger, F., Drenkow, J., Zaleski, C., Jha, S., Batut, P., Chaisson, M., and Gingeras, T.R. (2013). STAR: ultrafast universal RNA-seq aligner. Bioinformatics *29*, 15-21.

Dull, T., Zufferey, R., Kelly, M., Mandel, R.J., Nguyen, M., Trono, D., and Naldini, L. (1998). A third-generation lentivirus vector with a conditional packaging system. J. Virol. *72*, 8463-8471.

Emadali, A., Rousseaux, S., Bruder-Costa, J., Rome, C., Duley, S., Hamaidia, S., Betton, P., Debernardi, A., Leroux, D., Bernay, B., et al. (2013). Identification of a novel BET bromodomain inhibitor-sensitive, gene regulatory circuit that controls Rituximab response and tumour growth in aggressive lymphoid cancers. EMBO Mol. Med. *5*, 1180-1195.

Flynn, E.M., Huang, O.W., Poy, F., Oppikofer, M., Bellon, S.F., Tang, Y., and Cochran, A.G. (2015). A Subset of Human Bromodomains Recognizes Butyryllysine and Crotonyllysine Histone Peptide Modifications. Structure *23*, 1801-1814.

Fujisawa, T., and Filippakopoulos, P. (2017). Functions of bromodomain-containing proteins and their roles in homeostasis and cancer. Nat. Rev. Mol. Cell. Biol. *18*, 246-262.

Goudarzi, A., Zhang, D., Huang, H., Barral, S., Kwon, O.K., Qi, S., Tang, Z., Buchou, T., Vitte, A.L., He, T., et al. (2016). Dynamic Competing Histone H4 K5K8 Acetylation and Butyrylation Are Hallmarks of Highly Active Gene Promoters. Mol. Cell *62*, 169-180.

Gowans, G.J., Bridgers, J.B., Zhang, J., Dronamraju, R., Burnetti, A., King, D.A., Thiengmany, A.V., Shinsky, S.A., Bhanu, N.V., Garcia, B.A., et al. (2019). Recognition of Histone Crotonylation by Taf14 Links Metabolic State to Gene Expression. Mol. Cell *76*, 909-921 e903.

Haws, S.A., Leech, C.M., and Denu, J.M. (2020). Metabolism and the Epigenome: A Dynamic Relationship. Trends Biochem. Sci. *45*, 731-747.

Huang, H., Zhang, D., Wang, Y., Perez-Neut, M., Han, Z., Zheng, Y.G., Hao, Q., and Zhao, Y. (2018). Lysine benzoylation is a histone mark regulated by SIRT2. Nat. Commun. *9*, 3374.

Jin, H., Kasper, L.H., Larson, J.D., Wu, G., Baker, S.J., Zhang, J., and Fan, Y. (2020). ChIPseqSpikeInFree: a ChIP-seq normalization approach to reveal global changes in histone modifications without spike-in. Bioinformatics *36*, 1270-1272.

Jourdain, A.A., Popow, J., de la Fuente, M.A., Martinou, J.C., Anderson, P., and Simarro, M. (2017). The FASTK family of proteins: emerging regulators of mitochondrial RNA biology. Nucleic Acids Res. *45*, 10941-10947.

Kebede, A.F., Nieborak, A., Shahidian, L.Z., Le Gras, S., Richter, F., Gomez, D.A., Baltissen, M.P., Meszaros, G., Magliarelli, H.F., Taudt, A., et al. (2017). Histone propionylation is a mark of active chromatin. Nat. Struct. Mol. Biol. *24*, 1048-1056.

Lambert, J.P., Picaud, S., Fujisawa, T., Hou, H., Savitsky, P., Uusküla-Reimand, L., Gupta, G.D., Abdouni, H., Lin, Z.Y., Tucholska, M., et al. (2019). Interactome Rewiring Following Pharmacological Targeting of BET Bromodomains. Mol. Cell *73*, 621-638.e617.

Langmead, B., and Salzberg, S.L. (2012). Fast gapped-read alignment with Bowtie 2. Nat. Methods *9*, 357-359.

Li, Y., Sabari, B.R., Panchenko, T., Wen, H., Zhao, D., Guan, H., Wan, L., Huang, H., Tang, Z., Zhao, Y., et al. (2016). Molecular Coupling of Histone Crotonylation and Active Transcription by AF9 YEATS Domain. Mol. Cell *62*, 181-193.

Lozoya, O.A., Wang, T., Grenet, D., Wolfgang, T.C., Sobhany, M., Ganini da Silva, D., Riadi, G., Chandel, N., Woychik, R.P., and Santos, J.H. (2019). Mitochondrial acetyl-CoA reversibly regulates locus-specific histone acetylation and gene expression. Life Sci. Alliance *2*.

Matilainen, O., Quirós, P.M., and Auwerx, J. (2017). Mitochondria and Epigenetics - Crosstalk in Homeostasis and Stress. Trends Cell Biol. *27*, 453-463.

McDonnell, E., Crown, S.B., Fox, D.B., Kitir, B., Ilkayeva, O.R., Olsen, C.A., Grimsrud, P.A., and Hirschey, M.D. (2016). Lipids Reprogram Metabolism to Become a Major Carbon Source for Histone Acetylation. Cell Rep. *17*, 1463-1472.

Olp, M.D., Zhu, N., and Smith, B.C. (2017). Metabolically Derived Lysine Acylations and Neighboring Modifications Tune the Binding of the BET Bromodomains to Histone H4. Biochemistry *56*, 5485-5495.

Popow, J., Alleaume, A.M., Curk, T., Schwarzl, T., Sauer, S., and Hentze, M.W. (2015). FASTKD2 is an RNA-binding protein required for mitochondrial RNA processing and translation. RNA. *21*, 1873-1884.

Pougovkina, O., te Brinke, H., Ofman, R., van Cruchten, A.G., Kulik, W., Wanders, R.J., Houten, S.M., and de Boer, V.C. (2014). Mitochondrial protein acetylation is driven by acetyl-CoA from fatty acid oxidation. Hum. Mol. Genet. *23*, 3513-3522.

Ramírez, F., Ryan, D.P., Grüning, B., Bhardwaj, V., Kilpert, F., Richter, A.S., Heyne, S., Dündar, F., and Manke, T. (2016). deepTools2: a next generation web server for deep-sequencing data analysis. Nucleic Acids Res. *44*, W160-165.

Reynoird, N., Schwartz, B.E., Delvecchio, M., Sadoul, K., Meyers, D., Mukherjee, C., Caron, C., Kimura, H., Rousseaux, S., Cole, P.A., et al. (2010). Oncogenesis by sequestration of CBP/p300 in transcriptionally inactive hyperacetylated chromatin domains. EMBO J. *29*, 2943-2952.

Sabari, B.R., Tang, Z., Huang, H., Yong-Gonzalez, V., Molina, H., Kong, H.E., Dai, L., Shimada, M., Cross, J.R., Zhao, Y., et al. (2015). Intracellular crotonyl-CoA stimulates transcription through p300-catalyzed histone crotonylation. Mol. Cell *58*, 203-215.

Sanjana, N.E., Shalem, O., and Zhang, F. (2014). Improved vectors and genome-wide libraries for CRISPR screening. Nat. Methods *11*, 783-784.

Schneider, C.A., Rasband, W.S., and Eliceiri, K.W. (2012). NIH Image to ImageJ: 25 years of image analysis. Nat. Methods *9*, 671-675.

Schroder, S., Cho, S., Zeng, L., Zhang, Q., Kaehlcke, K., Mak, L., Lau, J., Bisgrove, D., Schnolzer, M., Verdin, E., et al. (2012). Two-pronged binding with bromodomain-containing protein 4 liberates positive transcription elongation factor b from inactive ribonucleoprotein complexes. J. Biol. Chem. *287*, 1090-1099.

Shiota, H., Barral, S., Buchou, T., Tan, M., Couté, Y., Charbonnier, G., Reynoird, N., Boussouar, F., Gérard, M., Zhu, M., et al. (2018). Nut Directs p300-Dependent, Genome-Wide H4 Hyperacetylation in Male Germ Cells. Cell Rep. *24*, 3477-3487.e3476.

Simithy, J., Sidoli, S., Yuan, Z.F., Coradin, M., Bhanu, N.V., Marchione, D.M., Klein, B.J., Bazilevsky, G.A., McCullough, C.E., Magin, R.S., et al. (2017). Characterization of histone acylations links chromatin modifications with metabolism. Nat. Commun. *8*, 1141.

Smestad, J., Erber, L., Chen, Y., and Maher, L.J., 3rd (2018). Chromatin Succinylation Correlates with Active Gene Expression and Is Perturbed by Defective TCA Cycle Metabolism. iScience 2, 63-75.

Spinck, M., Neumann-Staubitz, P., Ecke, M., Gasper, R., and Neumann, H. (2020). Evolved, Selective Erasers of Distinct Lysine Acylations. Chem. Int. Ed. Engl. *59*, 11142-11149.

Tan, M., Luo, H., Lee, S., Jin, F., Yang, Jeong S., Montellier, E., Buchou, T., Cheng, Z., Rousseaux, S., Rajagopal, N., et al. (2011). Identification of 67 Histone Marks and Histone Lysine Crotonylation as a New Type of Histone Modification. Cell *146*, 1016-1028.

Tarazona, O.A., and Pourquié, O. (2020). Exploring the Influence of Cell Metabolism on Cell Fate through Protein Post-translational Modifications. Dev. Cell *54*, 282-292.

Trefely, S., Lovell, C.D., Snyder, N.W., and Wellen, K.E. (2020). Compartmentalised acyl-CoA metabolism and roles in chromatin regulation. Mol. Metab. *38*, 100941.

Wang, J., Mi, J.Q., Debernardi, A., Vitte, A.L., Emadali, A., Meyer, J.A., Charmpi, K., Ycart, B., Callanan, M.B., Carroll, W.L., et al. (2015). A six gene expression signature defines aggressive subtypes and predicts outcome in childhood and adult acute lymphoblastic leukemia. Oncotarget *6*, 16527-16542.

Weber, K., Bartsch, U., Stocking, C., and Fehse, B. (2008). A multicolor panel of novel lentiviral "gene ontology" (LeGO) vectors for functional gene analysis. Mol. Ther. *16*, 698-706.

Xie, Z., Zhang, D., Chung, D., Tang, Z., Huang, H., Dai, L., Qi, S., Li, J., Colak, G., Chen, Y., et al. (2016). Metabolic Regulation of Gene Expression by Histone Lysine β-Hydroxybutyrylation. Mol. Cell *62*, 194-206.

Xiong, X., Panchenko, T., Yang, S., Zhao, S., Yan, P., Zhang, W., Xie, W., Li, Y., Zhao, Y., Allis, C.D., et al. (2016). Selective recognition of histone crotonylation by double PHD fingers of MOZ and DPF2. Nat. Chem. Biol. *12*, 1111-1118.

Zhang, D., Tang, Z., Huang, H., Zhou, G., Cui, C., Weng, Y., Liu, W., Kim, S., Lee, S., Perez-Neut, M., et al. (2019). Metabolic regulation of gene expression by histone lactylation. Nature *574*, 575-580.

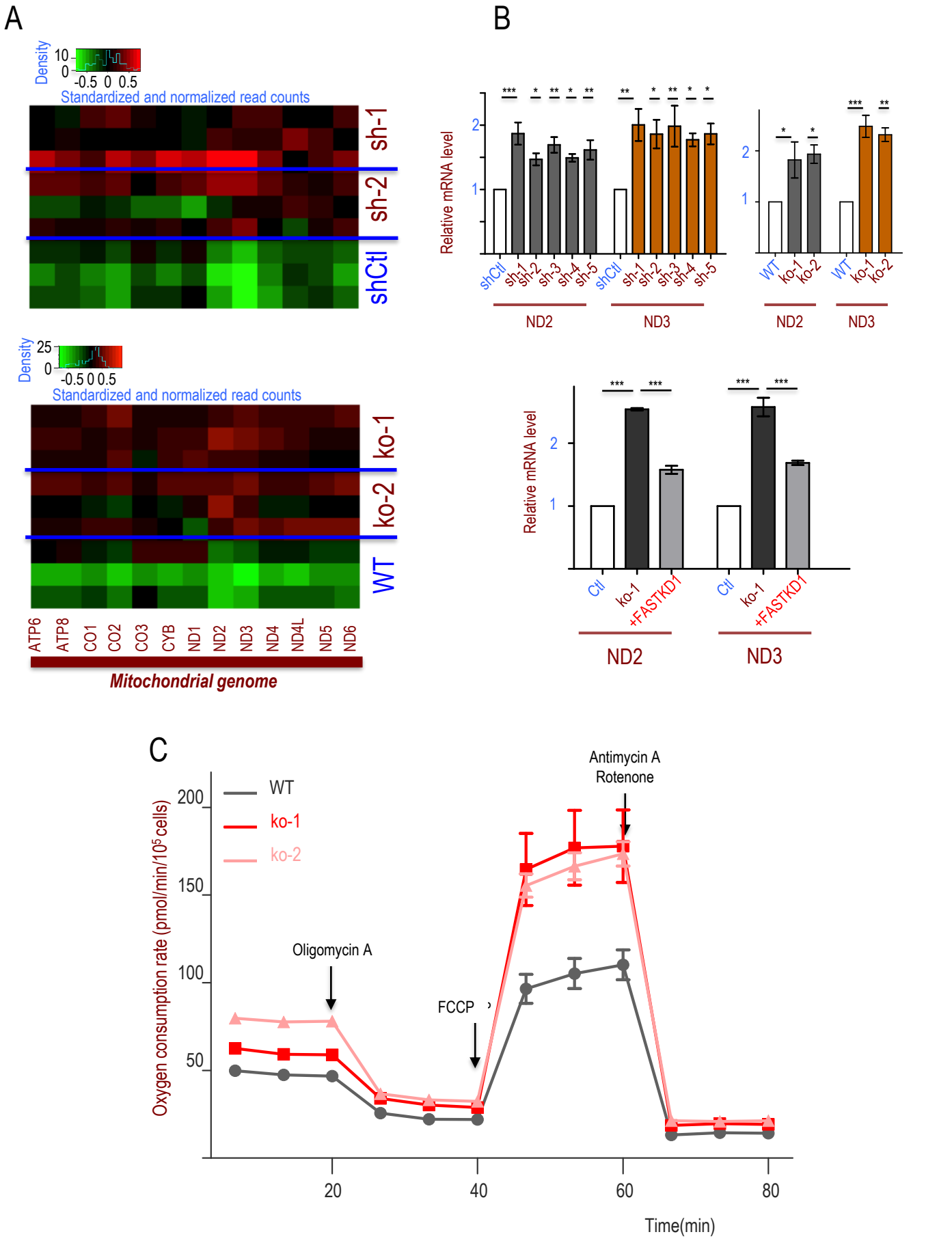
A
Density
10
0
-0.5 0 0.5
Standardized and normalized read counts
sh-1
sh-2
shCtl
Density
25
0
-0.5 0 0.5
Standardized and normalized read counts
ko-1
ko-2
WT
ATP6
ATP8
CO1
CO2
CO3
CYB
ND1
ND2
ND3
ND4
ND4L
ND5
ND6
Mitochondrial genome
B
Relative mRNA level
shCtl
sh-1
sh-2
sh-3
sh-4
sh-5
ND2
ND3
WT
ko-1
ko-2
Relative mRNA level
Ctl
ko-1
+FASTKD1
ND2
ND3
C
WT
ko-1
ko-2
Oligomycin A
FCCP
Antimycin A
Rotenone
Oxygen consumption rate (pmol/min/10^5 cells)
Time(min)

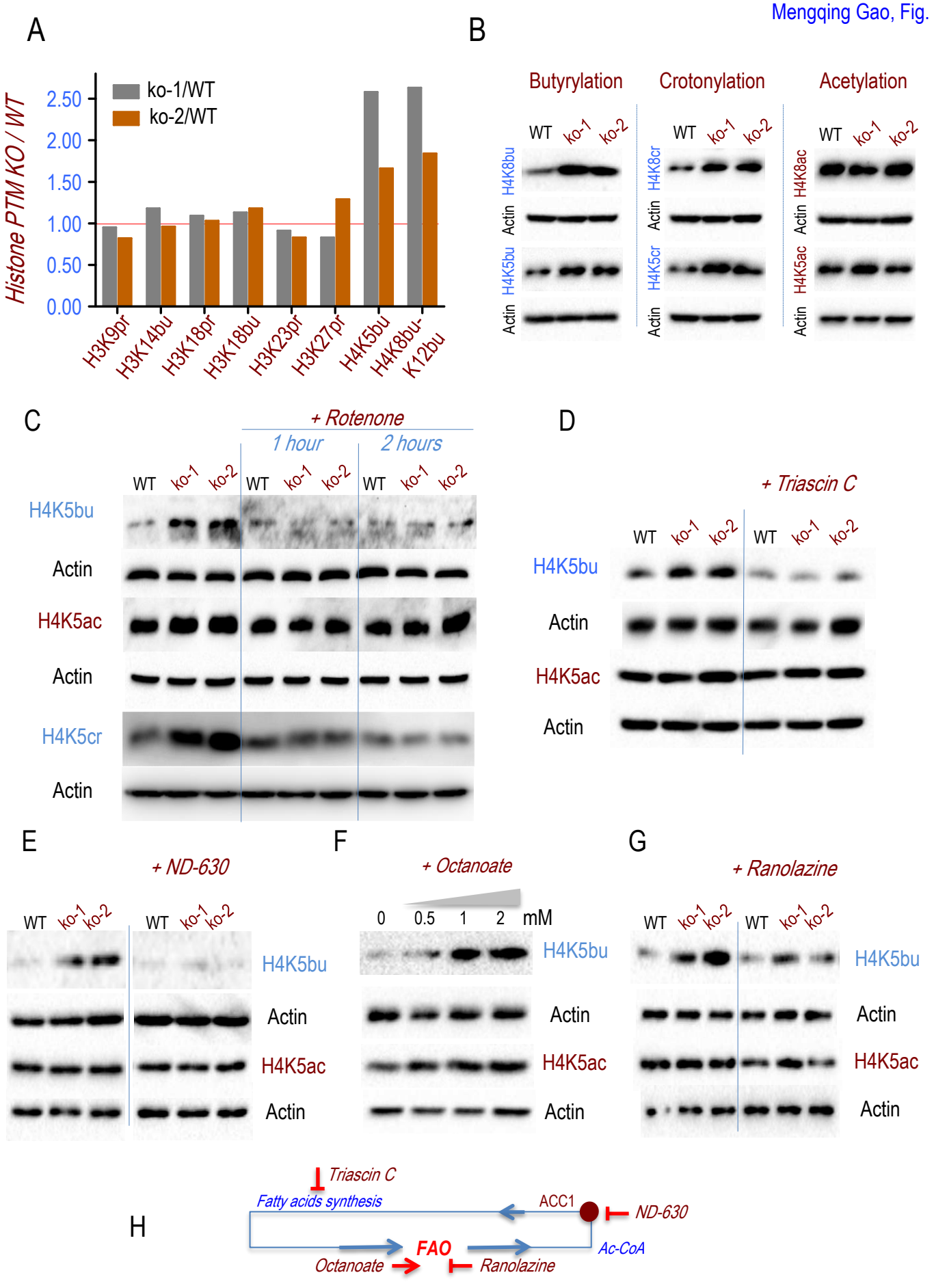
A
Histone PTM KO / WT
ko-1/WT
ko-2/WT
2.50
2.00
1.50
1.00
0.50
0.00
H3K9pr
H3K14bu
H3K18pr
H3K18bu
H3K23pr
H3K27pr
H4K5bu
H4K8bu-K12bu
B
Butyrylation
Crotonylation
Acetylation
WT
ko-1
ko-2
H4K8bu
H4K8cr
H4K8ac
H4K5bu
H4K5cr
H4K5ac
Actin
C
+ Rotenone
1 hour
2 hours
H4K5bu
H4K5ac
H4K5cr
Actin
D
+ Triascin C
E
+ ND-630
F
+ Octanoate
0
0.5
1
2
mM
G
+ Ranolazine
H
Triascin C
Fatty acids synthesis
ACC1
ND-630
FAO
Ac-CoA
Octanoate
Ranolazine

A

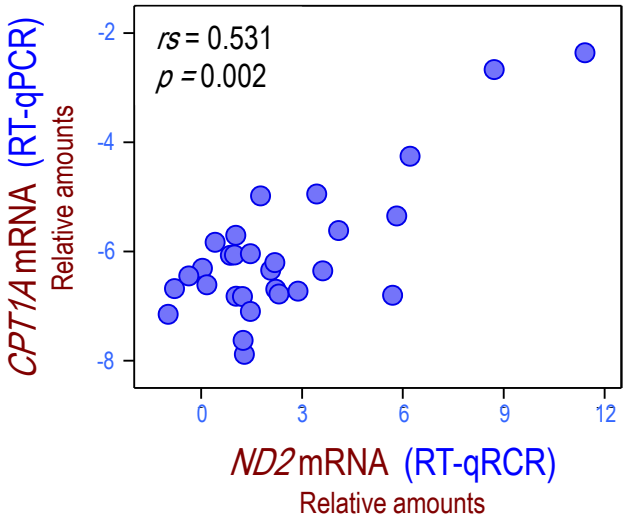
rs = 0.531
p = 0.002
CPT1A mRNA (RT-qPCR)
Relative amounts
-2
-4
-6
-8
0
3
6
9
12
ND2 mRNA (RT-qRCR)
Relative amounts

B

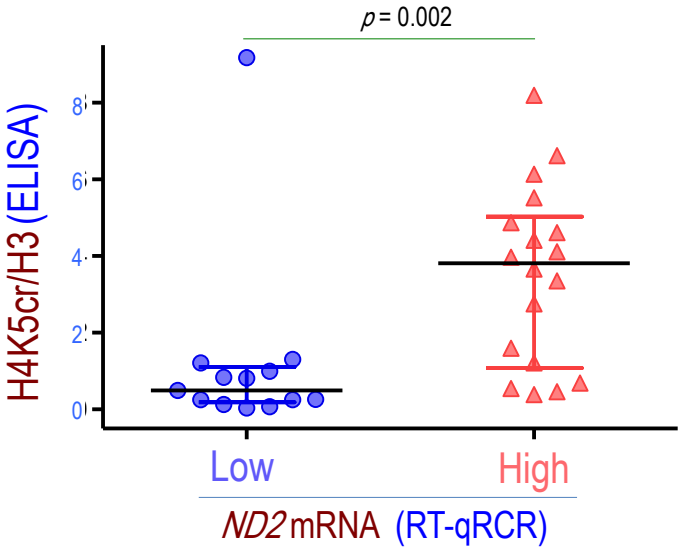
p = 0.002
H4K5cr/H3 (ELISA)
Low
High
ND2 mRNA (RT-qRCR)

C

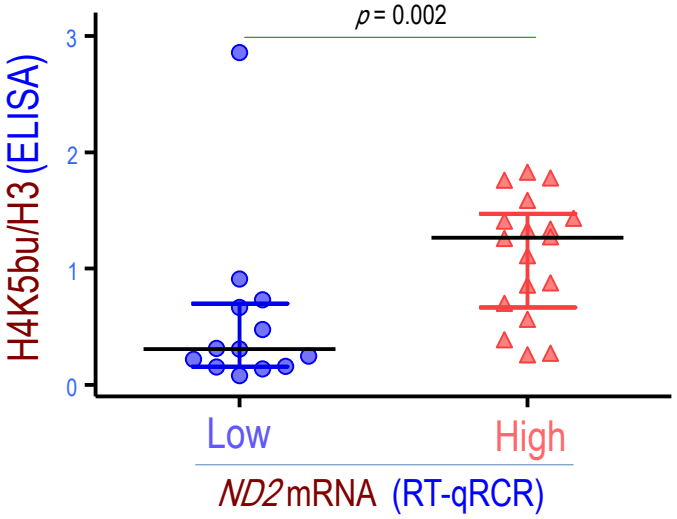
p = 0.002
H4K5bu/H3 (ELISA)
3
2
1
0
Low
High
ND2 mRNA (RT-qRCR)

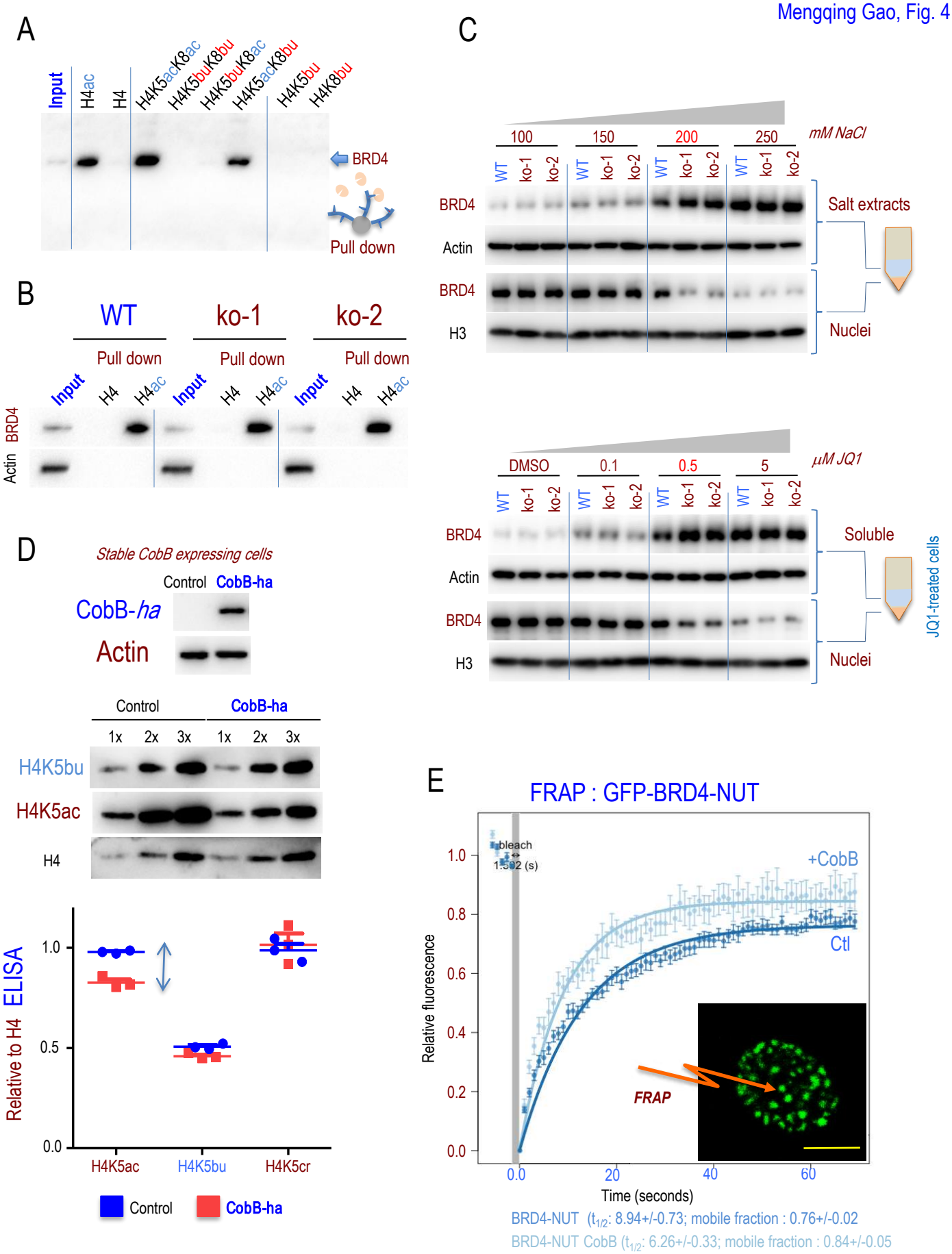
A
Input
H4ac
H4
H4K5acK8ac
H4K5buK8bu
H4K5buK8ac
H4K5acK8bu
H4K5bu
H4K8bu
BRD4
Pull down
B
WT
ko-1
ko-2
Pull down
Input
H4
H4ac
BRD4
Actin
C
100
150
200
250
mM NaCl
WT
ko-1
ko-2
BRD4
Actin
H3
Salt extracts
Nuclei
DMSO
0.1
0.5
5
μM JQ1
Soluble
JQ1-treated cells
D
Stable CobB expressing cells
Control
CobB-ha
CobB-ha
Actin
1x
2x
3x
H4K5bu
H4K5ac
H4
Relative to H4 ELISA
H4K5ac
H4K5bu
H4K5cr
E
FRAP : GFP-BRD4-NUT
bleach
+CobB
Ctl
FRAP
Relative fluorescence
Time (seconds)
BRD4-NUT (t1/2: 8.94+/-0.73; mobile fraction : 0.76+/-0.02
BRD4-NUT CobB (t1/2: 6.26+/-0.33; mobile fraction : 0.84+/-0.05

Mengqing Gao, Fig. 5

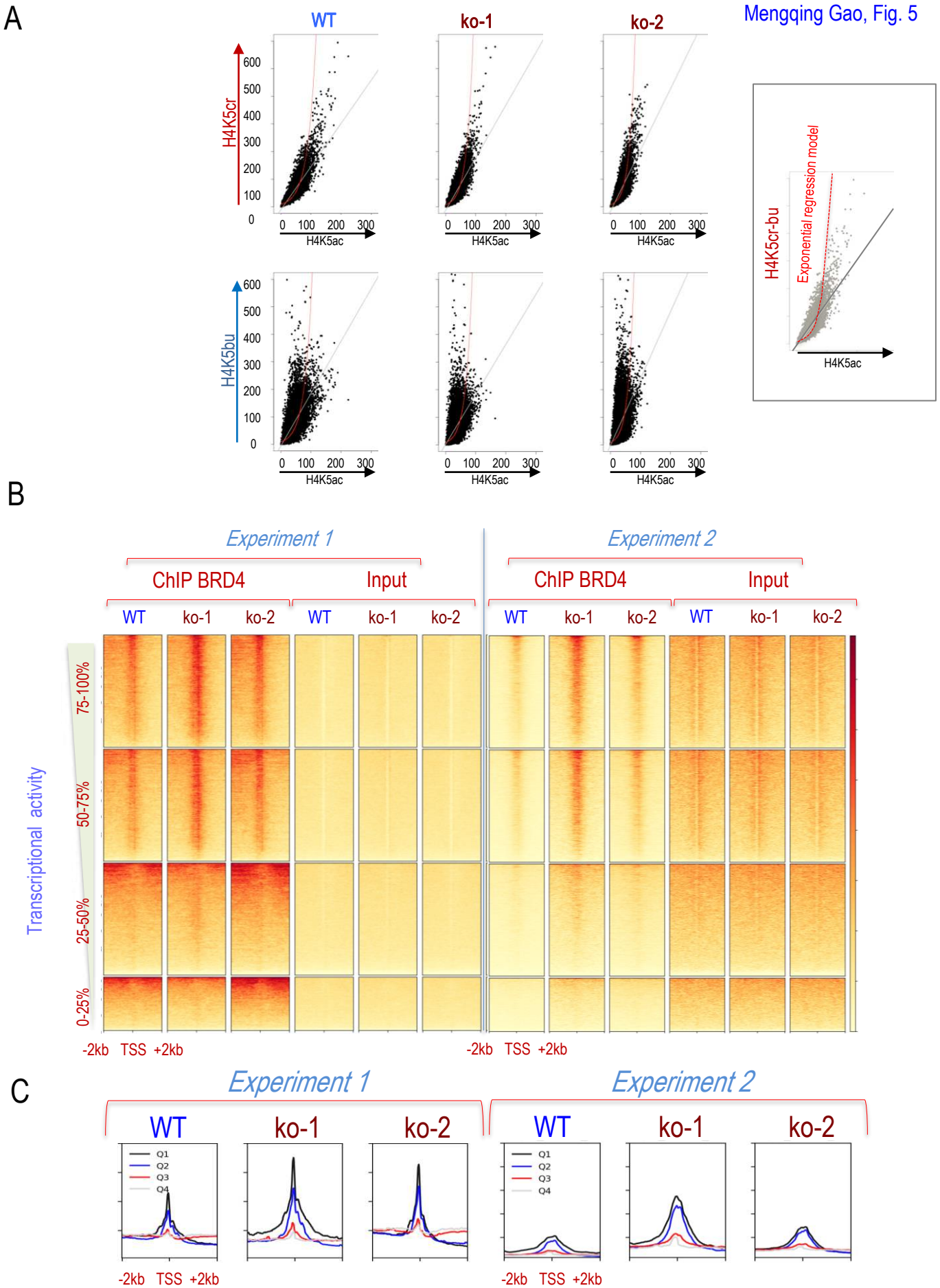

Mengqing Gao, Fig. 6

A

REH cells

FASTKD1 ko1+2 versus WT REH cells

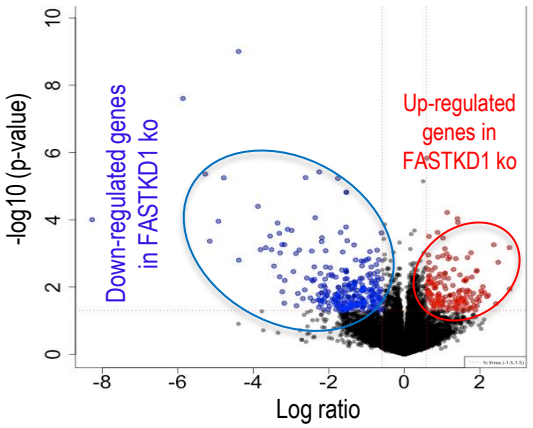

B

JQ1 treated versus untreated REH

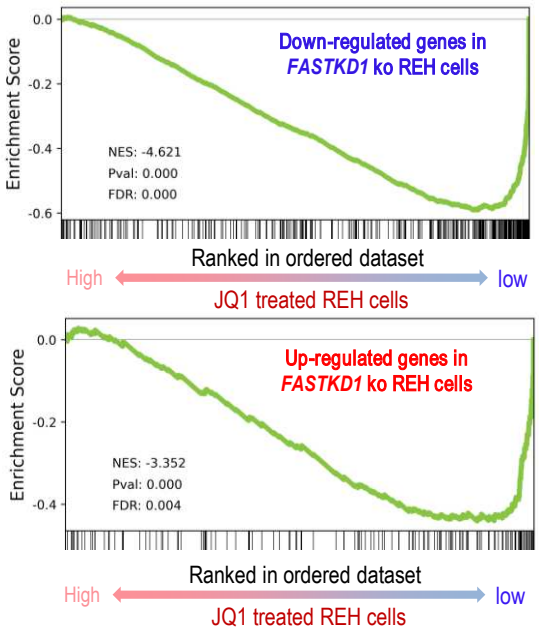

C

B-ALL patients

High versus low acylated B-ALL (n=25)

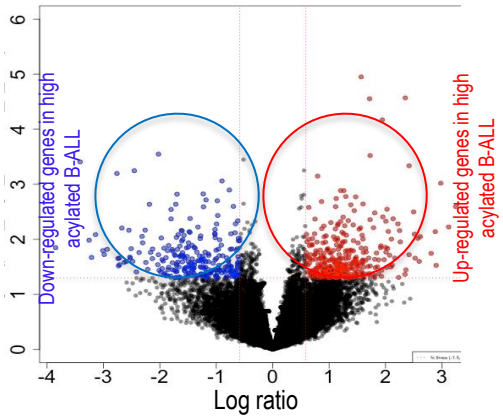

D

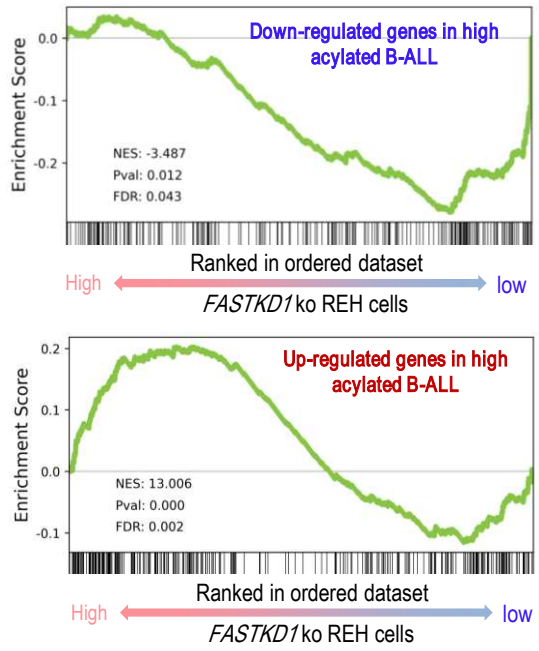

Mengqing Gao, Fig. 7

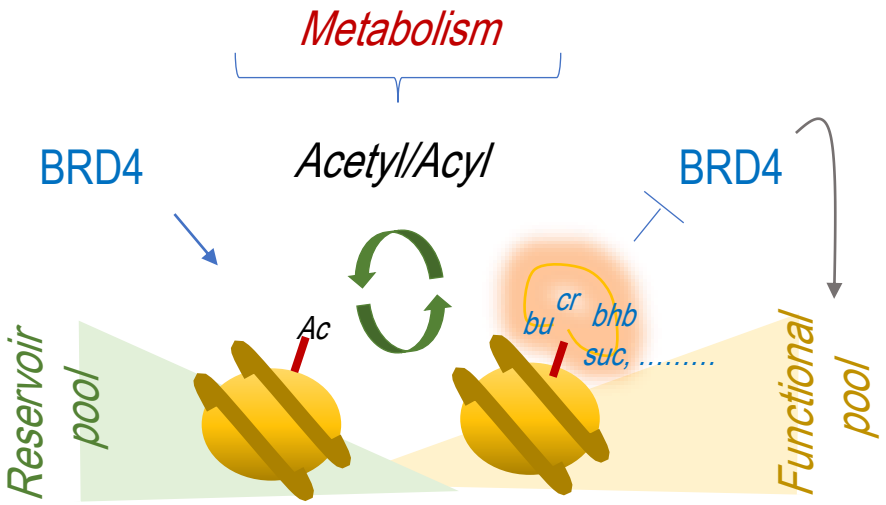

1.6 Supplementary data

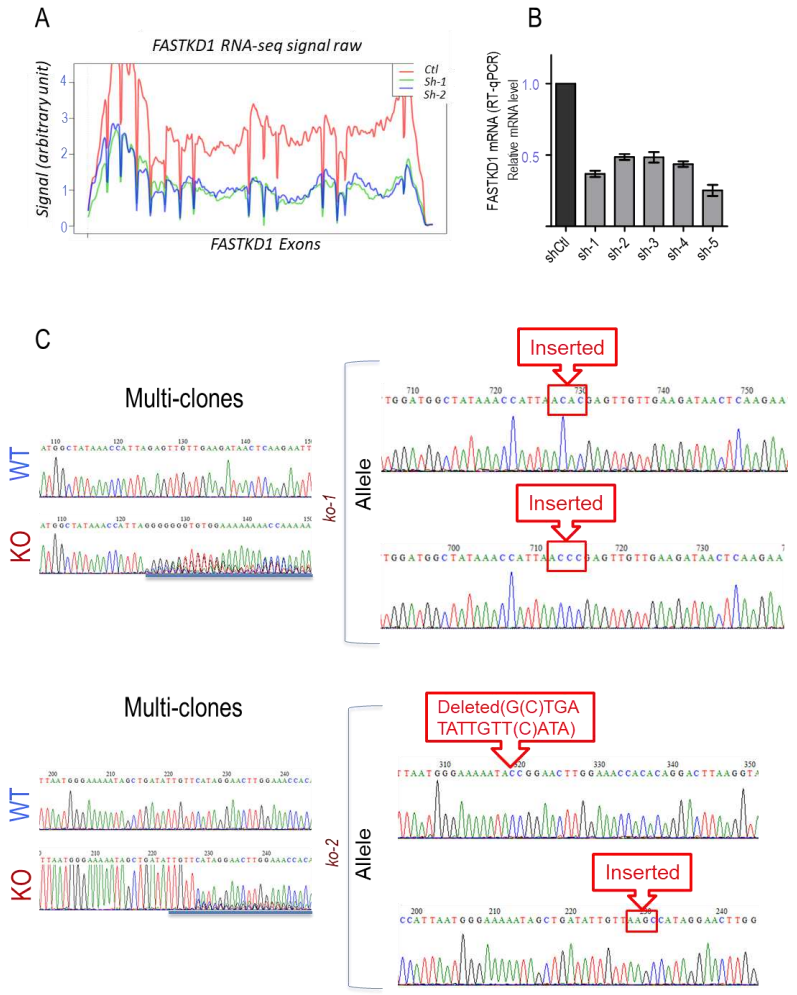

Supplementary Figure S1: Generation of stable FASTKD1 knock-down and knock out REH cell lines (related to Figure 1A).

A- Viral expression vectors expressing two independent anti-*FASTKD*1 shRNAs or an empty vector were established and used to generate RNA-seq data (Fig. 1A). The raw reads corresponding to the *FASTKD1* gene were aligned on *FASTKD1* gene exons and shown on the same diagram.

B- The CRISPR/Cas9 system was used to knock-out *FASTKD1* gene in REH cells using two different guide RNAs. The genomic DNAs of a pool of cells after CRISPR/Cas9 genome modification were sequenced around the targeted regions (indicated as multi-clones). Limit dilution of the two resulting multi-clone cells allowed for the isolation of single cell clones called ko-1 and ko-2. The sequence of the two isolated FASTKD1 clones and the corresponding sequence alterations are shown.

C- The level of *FASTKD1* expression was monitored by RT-qPCR in REH cells stably expressing an empty vector (shCtl) or five independent anti-*FASTKD1* shRNAs as indicated. Fold changes of gene expression level were calculated via 2^-ddCt and are represented by mean ± SEM based on at least three independent experiments.

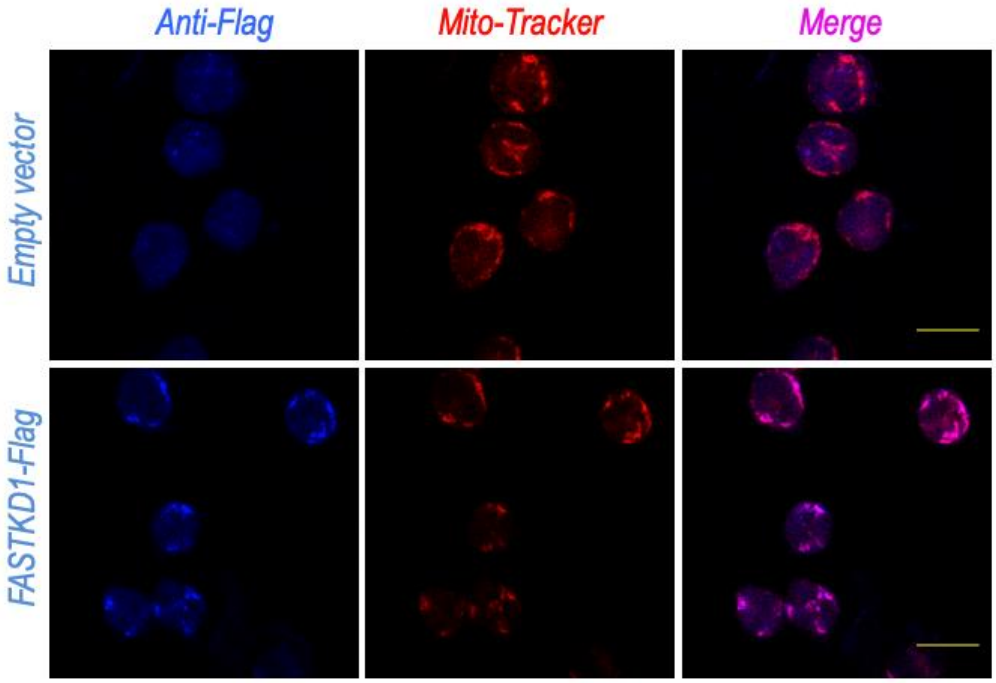

Supplementary Figure S2: Ectopically expressed FASTKD1 targets mitochondria (related to Figure 1B).

FASTKD1-Flag was expressed in REH cells and its intracellular localization was visualized using an anti-Flag immunodetection. In parallel mitochondria were visualised by mito-tracker as indicated. Scale bars represent 20 µm.

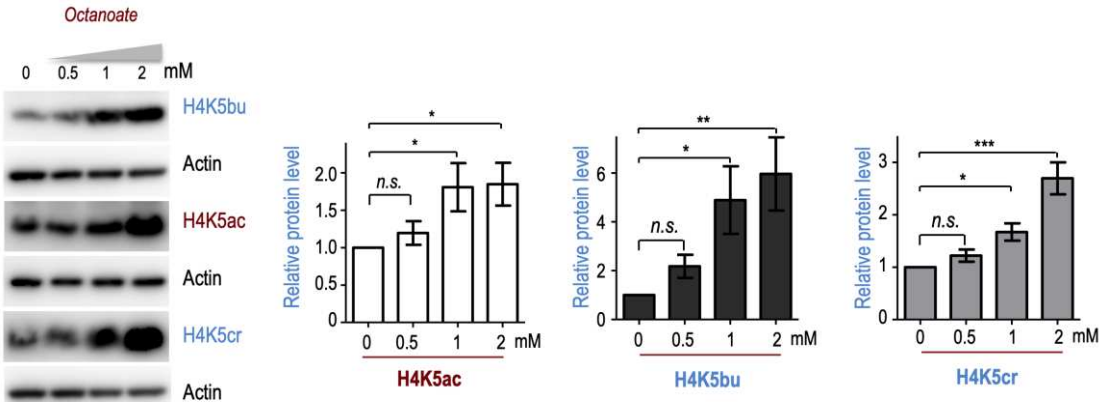

Supplementary Figure S3: Treatment of cells with octanoate leads to the accumulation of histone acetylation, butyrylation and crotonylation (related to Figure 2F).

The experiment shown in Fig. 2F was repeated three more times and the corresponding blots were used to detect the indicated proteins. The results of one of these experiments are shown on the left. The relative protein levels were quantified from the corresponding immunoblots using the Image J software. The data are represented by mean ± SEM based on 4 independent experiments. Statistical significance was determined using LSD post one-way ANOVA. * $p<0.05$, ** $p<0.01$, *** $p<0.001$.

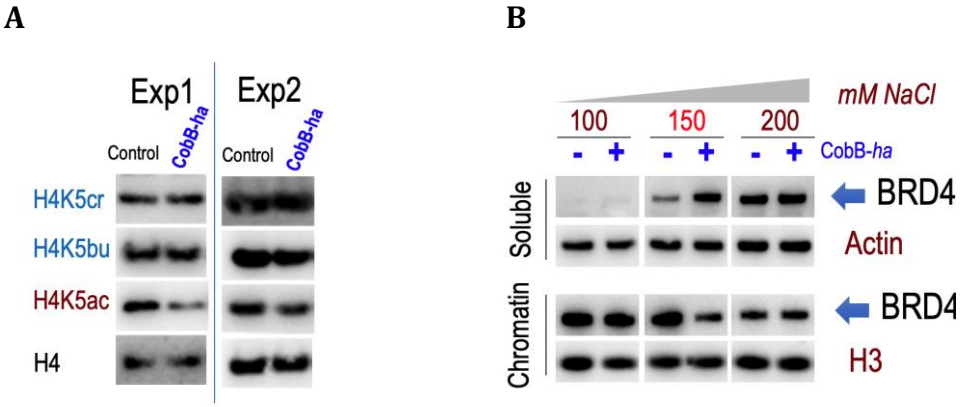

Supplementary Figure S4: H4K5 acyl/acetyl ratio controls the dynamics of BRD4-chromatin interaction (related to Figure 4D and E).

A – The experiment shown in Figure 4D was repeated twice again independently (Exp1 and Exp2, respectively) and the extracts were probed with different antibodies to visualize the indicated H4K5 modifications.

B - The salt elution approach used in the experiments shown in Figure 4C (upper panel), was applied to COS-7 cells control or expressing CobB-ha. After salt elution, nuclei were pelleted and BRD4 and actin were visualized in the soluble fraction (upper rows). BRD4 and histone H3 were also visualized in the pellet fraction (named "chromatin").

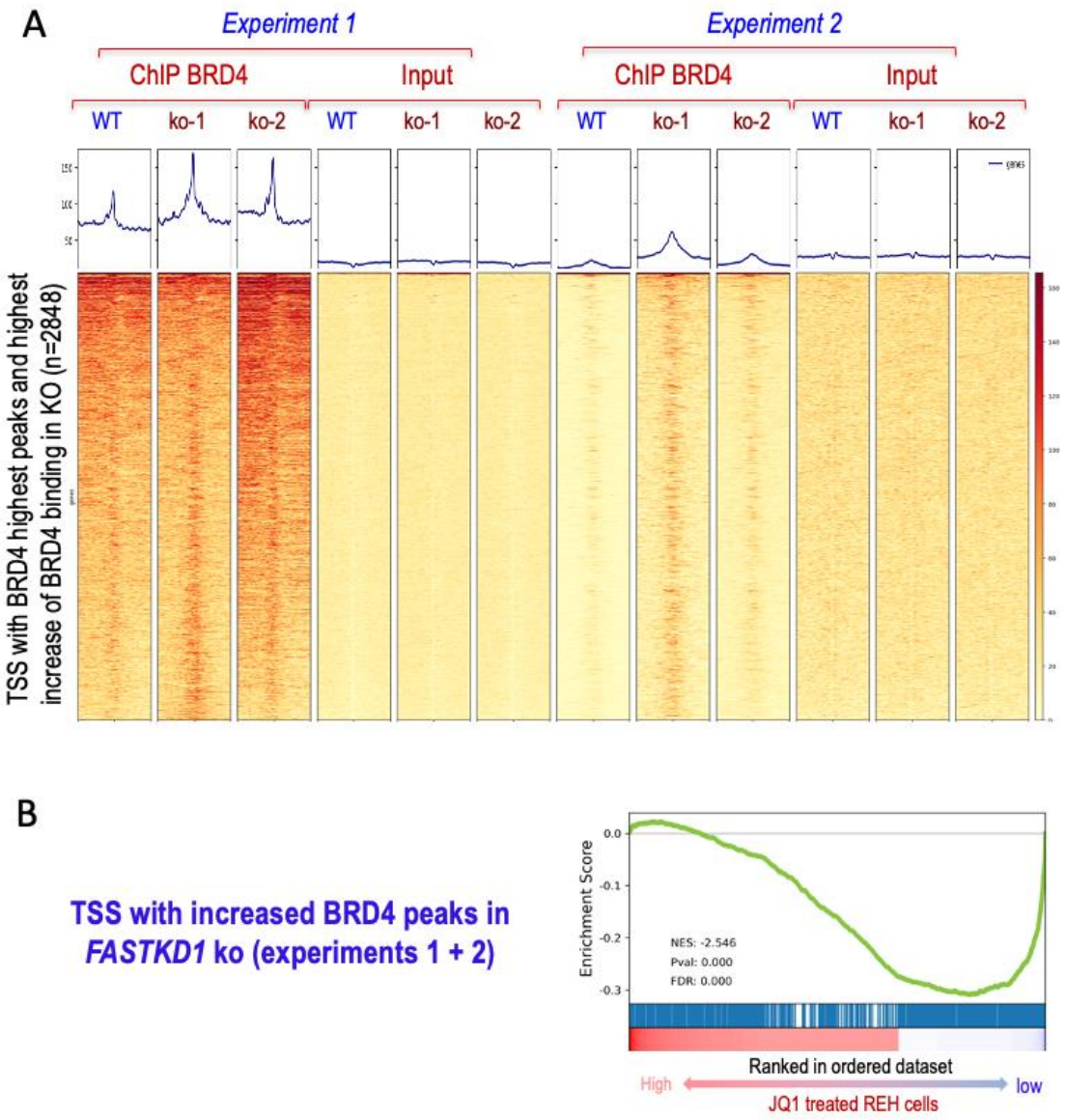

Supplementary Figure S5. Genes with increased BRD4 peaks in *FASTKD1* ko cells are sensitive to a JQ1 treatment (related to Figure 5B and 6B).

A. The heatmap shows BRD4 ChIP-seq normalized read counts in wild-type as well as in *FASTKD1* ko REH cells over the TSS centred regions of genes whose BRD4 binding increases in ko (TSSs +/- 2000 bp), in two independent experiments. Genes associated with high BRD4 peaks which increased in FASTKD1 ko were selected according to the following criteria. Their TSS+/- 2000bp was associated with i/ the highest BRD4 signals (top 5% in one or both BRD4 ChIP experiments) and ii/ a high (top 5%) signal ratio ko/wild-type (between at least one ko and wild-type REH cells). This list encompasses 2848 genes.

B. The gene group defined in A was used as a geneset for a GSEA plot to test for its enrichment/depletion in JQ1 treated REH cells. This plot shows a significant depletion of this group of genes, visualizing their down regulation in JQ1 treated cells, which demonstrates that their expression is BRD4 dependent.

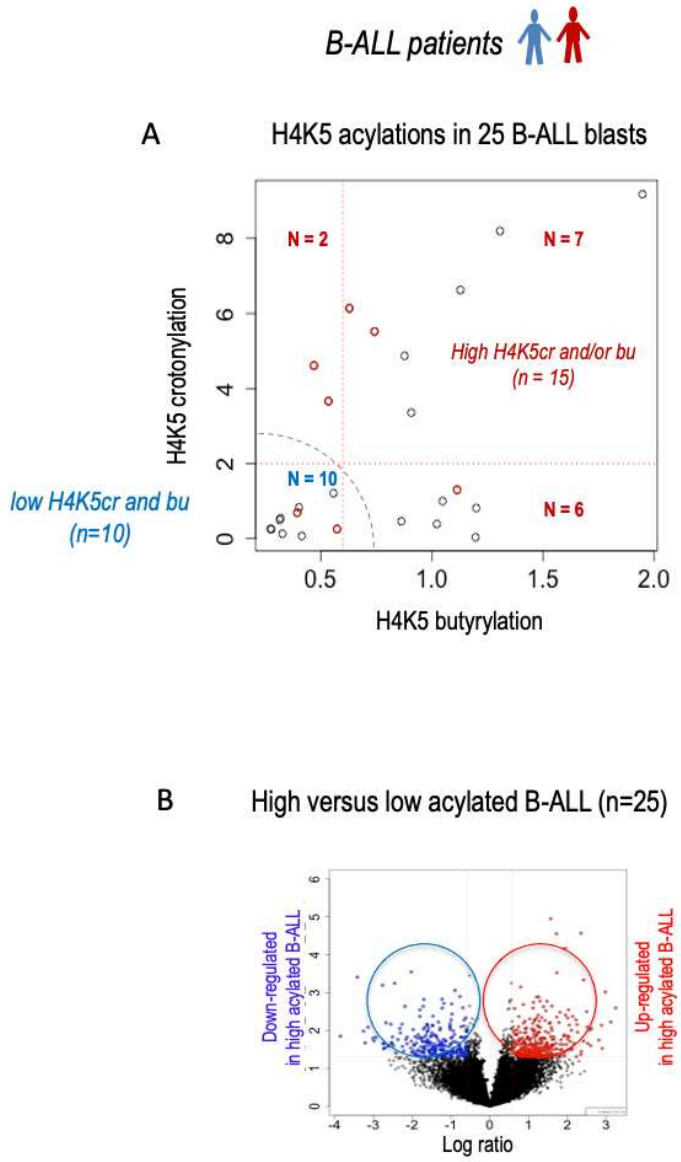

Supplementary Figure S6: Differential gene expression between B-ALL blasts with high and low H4K5 acylation levels (related to Figure 6C).

A- Plot showing H4K5 crotonylation (y-axis) as a function of butyrylation (x-axis) as detected by ELISA in B-ALL blasts samples selected for RNA-seq. The red dotted lines show the thresholds of butyrylation (value = 0.6) and crotonylation (value = 2) used to define the high and low acylation groups for each acylation. The red circles correspond to samples for which RNA-seq was performed in duplicates following two independent experiments.

B- Supervised transcriptomic analysis comparing B-ALL blasts with high H4K5 butyrylation and/or high crotonylation (n = 15) with B-ALL blasts with low H4K5 acylation (n = 10).

Volcano plot illustrating the differential gene expression signature between B-ALL blasts with high H4K5 acylations (crotonylation and/or butyrylation, n = 15) and B-ALL blasts with low acylations (n = 10). Y axis: -log10 (p-value); x-axis: log (ratio of normalized expression values between B-ALL with high and low acylation levels). The genes down-regulated or up-regulated with a fold change >1.5 and a Student t-test *p*-value < 0.05 are respectively represented in blue and red.

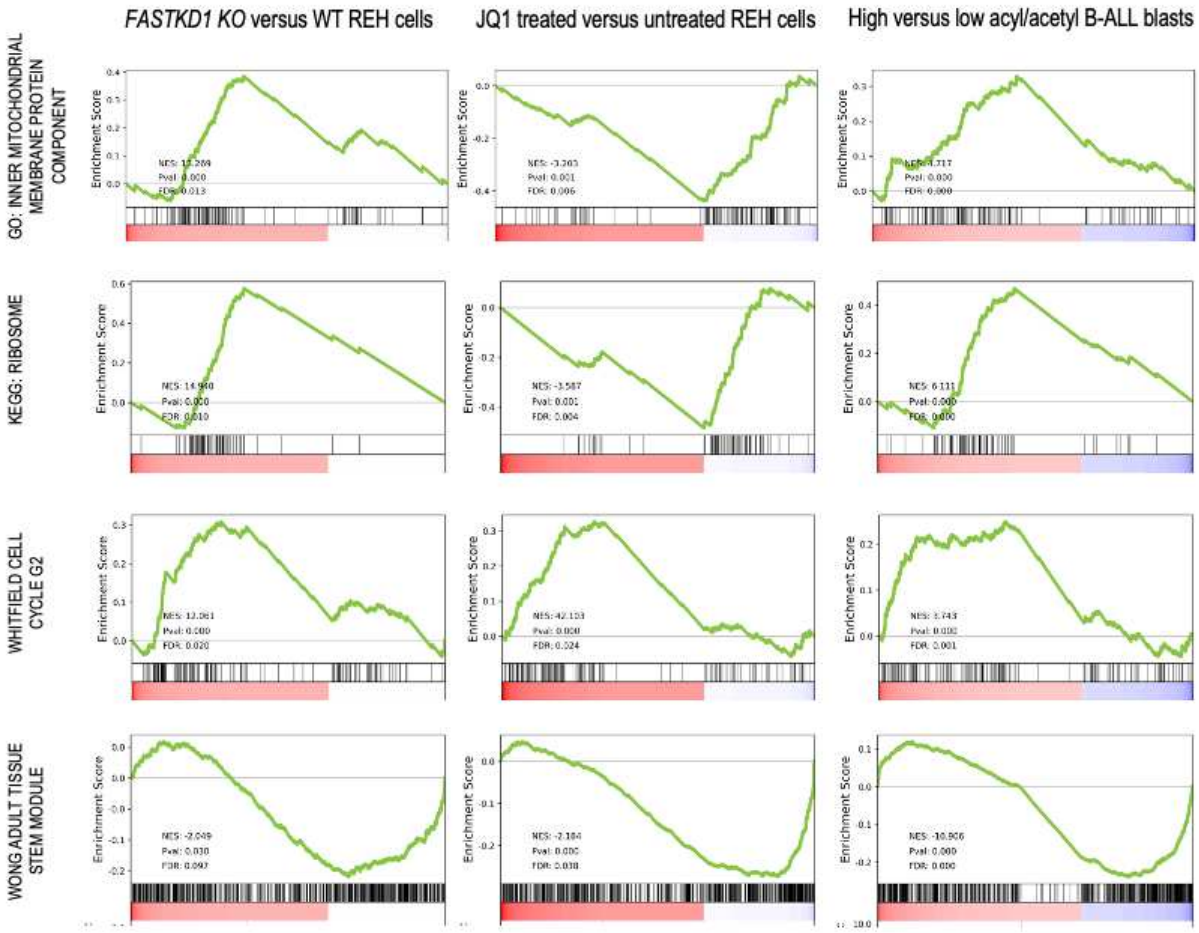

Supplementary Figure S7: GeneSet Enrichment Analysis (GSEA) of the transcriptomic signature of REH cells wild-type or *FASTKD1* ko or treated with JQ1 and B-ALL with high H4K5cr/bu levels (related to Figure 6).

GeneSet Enrichment Analysis (GSEA) plots representative of genesets enriched or depleted in the transcriptomic signature of REH *FASTKD1* - ko versus wild-type cells (left panels), of JQ1 treated versus untreated (middle panels) REH cells and B-ALL with high versus low H4K5cr/bu levels (right panel). GSEA preranked analysis and plots were generated using the python GSEA script and MsigDB genesets available on the Broad Institute website (described https://www.gsea-msigdb.org/gsea/doc/GSEAUserGuideFrame.html, genesets from http://www.gsea-msigdb.org/gsea/downloads.jsp). NES = normalized enrichment score; Pval = nominal *p*-value, a *p*-value of 0 indicates a *p*-value < 1/2000 (since our analysis was performed with 2000 permutations); FDR = False discovery rate adjusted for gene set size and multiple hypotheses testing.

Site	Ratio (Peak area) Normalized	
	ko1/ctrl	ko2/ctrl
H3K9pr	0.95	0.82
H3K14bu	1.18	0.96
H3K18pr	1.09	1.03
H3K18bu	1.13	1.18
H3K23pr	0.91	0.83
H3K27pr	0.83	1.29
H4K5bu	2.58	1.66
H4K8bu / H4K12bu	2.63	1.84
H2BK20bu	1.14	1.09

Table S1: Relative quantitative analysis of site-specific histone H3 and H4 propionylation and butyrylation in wild-type and two *FASTKD1* ko clones (**related to Figure 2A**). All the identified peptides with Mascot score above 20 were manually verified. The relative ratios of abundance of histone peptides in wild type and *FASTKD1* ko REH cells histone samples were calculated by the peak area of the corresponding peaks. The PTM with more than 1.5 times variations are highlighted (see Table S2 for details).

Histone	Site	Peptide	Peak area			Ratio (Peak area)		Ratio (Peak area)	
			ctrl	ko1	ko2	ko1/ctrl	ko2/ctrl	ko1/ctrl	ko2/ctrl
H3	H3K9pr	K(pr)STGGK(ac)APR	2.46E+07	1.73E+07	2.02E+07				
		SUM	2.46E+07	1.73E+07	2.02E+07	0.70	0.82	**0.95**	**0.82**
	H3K14bu	K(me1)STGGK(bu)APR	5.63E+07	4.92E+07	5.42E+07				
		SUM	5.63E+07	4.92E+07	5.42E+07	0.87	0.96	**1.18**	**0.96**
	H3K18pr	K(pr)QLATK	3.19E+08	2.59E+08	3.30E+08				
		K(pr)QLATK(ac)AAR	6.19E+06	3.85E+06	4.67E+06				
		SUM	3.25E+08	2.63E+08	3.34E+08	0.81	1.03	**1.09**	**1.03**
	H3K18bu	K(bu)QLATK	1.11E+08	9.13E+07	1.33E+08				
		K(bu)QLATK(ac)AAR	3.38E+07	2.96E+07	3.89E+07				
		SUM	1.45E+08	1.21E+08	1.71E+08	0.83	1.18	**1.13**	**1.18**
	H3K23pr	KQLATK(pr)AAR	1.07E+07	7.23E+06	8.84E+06				
		SUM	1.07E+07	7.23E+06	8.84E+06	0.68	0.83	**0.91**	**0.83**
	H3K27pr	K(pr)SAPATGGVK	4.06E+06	2.49E+06	5.23E+06				
		SUM	4.06E+06	2.49E+06	5.23E+06	0.61	1.29	**0.83**	**1.29**
H4	H4K5bu	GK(bu)GGK(ac)GLGK(ac)GGAK(ac)R	1.64E+06	2.83E+06	2.34E+06				
		SUM	1.64E+06	2.83E+06	2.34E+06	1.72	1.42	**2.58**	**1.66**
	H4K8bu / H4K12bu	GGK(bu)GLGK(ac)GGAK(ac)R / GGK(ac)GLGK(bu)GGAK(ac)R	2.47E+06	4.34E+06	3.89E+06				
		SUM	2.47E+06	4.34E+06	3.89E+06	1.76	1.58	**2.63**	**1.84**
H2B	H2BK20bu	AVTK(bu)AQK	9.29E+08	1.09E+09	1.22E+09				
		K(ac)GSK(ac)K(ac)AVTK(bu)AQK	5.01E+07	5.53E+07	8.52E+07				
		SUM	9.79E+08	1.14E+09	1.30E+09	1.17	1.33	**1.14**	**1.09**

Table S2: Relative quantitative analysis of site-specific histone H3 and H4 propionylation and butyrylation in wild-type and two *FASTKD1* ko clones (**related to Figure 2A**). Detailed quantitative analyses of site-specific histone propionylation and butyrylation used to generate Table S1 is shown.

Normalization information

Histone	Peptide	Peak area			Ratio (Peak area)	
		ctrl	ko1	ko2	ko1/ctrl	ko2/ctrl
H3	DIQLAR	8,92E+10	7,56E+10	1,01E+11	0,85	1,13
	STELLIR	2,72E+11	1,91E+11	2,61E+11	0,70	0,96
	YRPGTVALR	1,18E+11	8,47E+10	1,13E+11	0,72	0,96
	KLPFQR	1,35E+11	9,37E+10	1,29E+11	0,69	0,96
	Average				**0,74**	**1,00**
H4	ISGLIYEETR	2,89E+11	2,19E+11	2,34E+11	0,76	0,81
	VFLENVIR	2,77E+11	1,32E+11	1,96E+11	0,48	0,71
	TLYGFGG	9,59E+07	7,37E+07	1,01E+08	0,77	1,05
	Average				**0,67**	**0,86**
H2B	ESYSIYVYK	6,98E+10	6,94E+10	8,16E+10	0,99	1,17
	LLLPGELAK	4,22E+11	4,09E+11	5,29E+11	0,97	1,25
	EIQTAVR	1,51E+11	1,65E+11	1,88E+11	1,10	1,25
	Average				**1,02**	**1,22**

Sample	Protein sequence coverage (%)			
	H4	H3	H2B	H2A
Ctrl	84	60	93	49
ko1	80	58	86	49
ko2	81	58	88	46

Table S3: Relative quantitative analysis of site-specific histone H3 and H4 propionylation and butyrylation in wild-type and two *FASTKD1* ko clones (**related to Figure 2A**).

Normalization information (upper Table): values of the precursor ion AUC used to normalize the amount of each histone in label-free quantification.

Coverage information (lower Table): values of histone coverage for each experiment.

Patient No.	Gender	Age (Year)	Disease status	WBC at diagnosis ($x10^9/L$)	Ph chromosome	RNA-seq
1	Female	53	Newly diagnosed	303.1	Neg.	Yes
2	Female	18	Newly diagnosed	39.5	Neg.	Yes
3	Female	26	Newly diagnosed	36.93	Neg.	Yes
4	Female	36	Newly diagnosed	4.21	Neg.	Yes
5	Female	43	Newly diagnosed	34.2	Neg.	Yes
6	Female	35	Newly diagnosed	45.3	Neg.	Yes
7	Male	18	Newly diagnosed	123.05	Neg.	Yes
8	Male	53	Newly diagnosed	225.2	Neg.	Yes
9	Female	48	Newly diagnosed	8.55	Neg.	Yes
10	Male	21	Newly diagnosed	205	Neg.	Yes
11	Male	62	Newly diagnosed	36.62	Pos.	Yes
12	Male	36	Newly diagnosed	403.4	Neg.	Yes
13	Female	52	Newly diagnosed	15.92	Pos.	Yes
14	Female	33	Newly diagnosed	83.2	Pos.	Yes
15	Male	54	Newly diagnosed	3.3	Neg.	No
16	Male	26	Newly diagnosed	81.7	Pos.	No
17	Female	18	Newly diagnosed	27.32	Neg.	Yes
18	Female	33	Newly diagnosed	100.65	Neg.	No
19	Male	39	Newly diagnosed	58.86	Pos.	Yes
20	Female	27	Newly diagnosed	8.73	Neg.	Yes
21	Female	33	Newly diagnosed	13.2	Neg.	No
22	Female	58	Newly diagnosed	27.4	Neg.	Yes
23	Female	17	Newly diagnosed	103.84	Neg.	Yes
24	Female	15	Newly diagnosed	97.45	Neg.	Yes
25	Female	17	Newly diagnosed	5.6	Neg.	Yes
26	Female	14	Newly diagnosed	26.89	Neg.	Yes
27	Male	15	Newly diagnosed	26.69	Neg.	Yes
28	Female	14	Newly diagnosed	118.37	Neg.	No
29	Male	16	Newly diagnosed	3.1	Neg.	No
30	Female	14	Newly diagnosed	4.93	Neg.	Yes
31	Female	56	Newly diagnosed	27.5	Neg.	Yes

Table S4: Characteristics of B-ALL patients samples (**related to Figure 3, 6C&D, S6, S7**).

Name	Sequence	Reference
ko-1 genotyping forward	ATTCATTGCCGTTTCTCCA	N/A
ko-1 genotyping reverse	TCATCAGTTTATTGCCATTCC	N/A
ko-2 genotyping forward	TCTGACTTTTTAACTGTTGCCATGT	N/A
ko-2 genotyping reverse	CTCTTTTGCAGATGAGGATAACGA	N/A
RT-qPCR: FASTDK1 forward	AAGAATTAACTTTTCTGCATTTCCA	(Wang et al., 2015)
RT-qPCR: FASTDK1 reverse	CAGAACAGACACCTCAGTTGG	
RT-qPCR: ND2 forward	CTTAAACTCCAGCACCACGAC	(Popow et al., 2015)
RT-qPCR: ND2 reverse	AGCTTGTTTCAGGTGCGAGA	
RT-qPCR: ND3 forward	CCGCGTCCCTTTCTCCATAA	
RT-qPCR: ND3 reverse	AGGGCTCATGGTAGGGGTAA	
RT-qPCR: CPT1A forward	TTTCCATTCCTTCCCATTCG	N/A
RT-qPCR: CPT1A reverse	AACTTCAGCCTCTGTTCCACC	N/A
RT-qPCR: GAPDH forward	GAAGGTGAAGGTCGGAGTC	N/A
RT-qPCR: GAPDH reverse	GAAGATGGTGATGGGATTTC	N/A

Table S5: Primers used in this study (**related to STAR Methods**).

REFERNCE

1. Simonis, M., et al., *Nuclear organization of active and inactive chromatin domains uncovered by chromosome conformation capture-on-chip (4C).* Nat Genet, 2006. **38**(11): p. 1348-54.
2. Lieberman-Aiden, E., et al., *Comprehensive mapping of long-range interactions reveals folding principles of the human genome.* Science, 2009. **326**(5950): p. 289-93.
3. Magana-Acosta, M. and V. Valadez-Graham, *Chromatin Remodelers in the 3D Nuclear Compartment.* Front Genet, 2020. **11**: p. 600615.
4. Shoaib, M., N. Nair, and C.S. Sorensen, *Chromatin Landscaping At Mitotic Exit Orchestrates Genome Function.* Front Genet, 2020. **11**: p. 103.
5. Dixon, J.R., et al., *Chromatin architecture reorganization during stem cell differentiation.* Nature, 2015. **518**(7539): p. 331-6.
6. Rao, S.S., et al., *A 3D map of the human genome at kilobase resolution reveals principles of chromatin looping.* Cell, 2014. **159**(7): p. 1665-80.
7. Pombo, A. and N. Dillon, *Three-dimensional genome architecture: players and mechanisms.* Nat Rev Mol Cell Biol, 2015. **16**(4): p. 245-57.
8. Ramírez, F., et al., *High-resolution TADs reveal DNA sequences underlying genome organization in flies.* bioRxiv, 2017: p. 115063.
9. Jerkovic, I., et al., *Higher-Order Chromosomal Structures Mediate Genome Function.* J Mol Biol, 2020. **432**(3): p. 676-681.
10. Chereji, R.V. and A.V. Morozov, *Ubiquitous nucleosome crowding in the yeast genome.* Proceedings of the National Academy of Sciences of the United States of America, 2014. **111**(14): p. 5236-5241.
11. Nozaki, T., et al., *Dynamic Organization of Chromatin Domains Revealed by Super-Resolution Live-Cell Imaging.* Mol Cell, 2017. **67**(2): p. 282-293.e7.
12. Ricci, M.A., et al., *Chromatin fibers are formed by heterogeneous groups of nucleosomes in vivo.* Cell, 2015. **160**(6): p. 1145-58.
13. Baldi, S., P. Korber, and P.B. Becker, *Beads on a string-nucleosome array arrangements and folding of the chromatin fiber.* Nat Struct Mol Biol, 2020. **27**(2): p. 109-118.
14. Luger, K., et al., *Crystal structure of the nucleosome core particle at 2.8 A resolution.* Nature, 1997. **389**(6648): p. 251-60.
15. Davey, C.A., et al., *Solvent Mediated Interactions in the Structure of the Nucleosome Core Particle at 1.9Å Resolution.* Journal of Molecular Biology, 2002. **319**(5): p. 1097-1113.
16. Fyodorov, D.V., et al., *Emerging roles of linker histones in regulating chromatin structure and function.* Nat Rev Mol Cell Biol, 2018. **19**(3): p. 192-206.
17. Davey, C.A., et al., *Solvent mediated interactions in the structure of the nucleosome core particle at 1.9 a resolution.* J Mol Biol, 2002. **319**(5): p. 1097-113.
18. Segal, E., et al., *A genomic code for nucleosome positioning.* Nature, 2006. **442**(7104): p. 772-8.
19. Onufriev, A.V. and H. Schiessel, *The nucleosome: from structure to function through physics.* Curr Opin Struct Biol, 2019. **56**: p. 119-130.
20. Haberle, V. and A. Stark, *Eukaryotic core promoters and the functional basis of transcription initiation.* Nat Rev Mol Cell Biol, 2018. **19**(10): p. 621-637.
21. Raisner, R., et al., *Enhancer Activity Requires CBP/P300 Bromodomain-Dependent Histone H3K27 Acetylation.* Cell Rep, 2018. **24**(7): p. 1722-1729.
22. Andersson, R. and A. Sandelin, *Determinants of enhancer and promoter activities of regulatory elements.* Nat Rev Genet, 2020. **21**(2): p. 71-87.

23. Smith, E. and A. Shilatifard, *Enhancer biology and enhanceropathies.* Nat Struct Mol Biol, 2014. **21**(3): p. 210-9.
24. Lewis, M.W., S. Li, and H.L. Franco, *Transcriptional control by enhancers and enhancer RNAs.* Transcription, 2019. **10**(4-5): p. 171-186.
25. Zabidi, M.A. and A. Stark, *Regulatory Enhancer-Core-Promoter Communication via Transcription Factors and Cofactors.* Trends Genet, 2016. **32**(12): p. 801-814.
26. Dressler, G.R., *Epigenetics, development, and the kidney.* Journal of the American Society of Nephrology, 2008. **19**(11): p. 2060-2067.
27. Rea, S., et al., *Regulation of chromatin structure by site-specific histone H3 methyltransferases.* Nature, 2000. **406**(6796): p. 593-9.
28. Black, J.C., C. Van Rechem, and J.R. Whetstine, *Histone lysine methylation dynamics: establishment, regulation, and biological impact.* Mol Cell, 2012. **48**(4): p. 491-507.
29. Hu, S., L. Cheng, and B. Wen, *Large chromatin domains in pluripotent and differentiated cells.* Acta Biochim Biophys Sin (Shanghai), 2012. **44**(1): p. 48-53.
30. Ernst, P. and C.R. Vakoc, *WRAD: enabler of the SET1-family of H3K4 methyltransferases.* Brief Funct Genomics, 2012. **11**(3): p. 217-26.
31. Holoch, D. and R. Margueron, *Mechanisms Regulating PRC2 Recruitment and Enzymatic Activity.* Trends Biochem Sci, 2017. **42**(7): p. 531-542.
32. Healy, E., et al., *PRC2.1 and PRC2.2 Synergize to Coordinate H3K27 Trimethylation.* Mol Cell, 2019. **76**(3): p. 437-452.e6.
33. Cornett, E.M., et al., *Lysine Methylation Regulators Moonlighting outside the Epigenome.* Mol Cell, 2019. **75**(6): p. 1092-1101.
34. van Ingen, H., et al., *Structural insight into the recognition of the H3K4me3 mark by the TFIID subunit TAF3.* Structure, 2008. **16**(8): p. 1245-56.
35. Wiles, E.T. and E.U. Selker, *H3K27 methylation: a promiscuous repressive chromatin mark.* Curr Opin Genet Dev, 2017. **43**: p. 31-37.
36. Hyun, K., et al., *Writing, erasing and reading histone lysine methylations.* Exp Mol Med, 2017. **49**(4): p. e324.
37. Laugesen, A., J.W. Hojfeldt, and K. Helin, *Molecular Mechanisms Directing PRC2 Recruitment and H3K27 Methylation.* Mol Cell, 2019. **74**(1): p. 8-18.
38. Worden, E.J. and C. Wolberger, *Activation and regulation of H2B-Ubiquitin-dependent histone methyltransferases.* Curr Opin Struct Biol, 2019. **59**: p. 98-106.
39. Sharma, A., K. Singh, and A. Almasan, *Histone H2AX phosphorylation: a marker for DNA damage.* Methods Mol Biol, 2012. **920**: p. 613-26.
40. Millan-Zambrano, G., et al., *Phosphorylation of Histone H4T80 Triggers DNA Damage Checkpoint Recovery.* Mol Cell, 2018. **72**(4): p. 625-635 e4.
41. North, J.A., et al., *Histone H3 phosphorylation near the nucleosome dyad alters chromatin structure.* Nucleic Acids Res, 2014. **42**(8): p. 4922-33.
42. Izzo, A. and R. Schneider, *The role of linker histone H1 modifications in the regulation of gene expression and chromatin dynamics.* Biochim Biophys Acta, 2016. **1859**(3): p. 486-95.
43. Li, Y., et al., *The histone modifications governing TFF1 transcription mediated by estrogen receptor.* J Biol Chem, 2011. **286**(16): p. 13925-36.
44. Martire, S., et al., *Phosphorylation of histone H3.3 at serine 31 promotes p300 activity and enhancer acetylation.* Nat Genet, 2019. **51**(6): p. 941-946.
45. Mahajan, K., et al., *ACK1/TNK2 Regulates Histone H4 Tyr88-phosphorylation and AR Gene Expression in Castration-Resistant Prostate Cancer.* Cancer Cell, 2017. **31**(6): p. 790-803 e8.
46. Banerjee, T. and D. Chakravarti, *A peek into the complex realm of histone phosphorylation.* Mol Cell Biol,

2011. **31**(24): p. 4858-73.

47. Jackson, V., et al., *Studies on highly metabolically active acetylation and phosphorylation of histones.* J Biol Chem, 1975. **250**(13): p. 4856-63.
48. Duncan, M.R., M.J. Robinson, and R.T. Dell'Orco, *Kinetics of histone hyperacetylation and deacetylation in human diploid fibroblasts.* Biochim Biophys Acta, 1983. **762**(2): p. 221-6.
49. Agudelo Garcia, P.A., et al., *Identification of multiple roles for histone acetyltransferase 1 in replication-coupled chromatin assembly.* Nucleic Acids Res, 2017. **45**(16): p. 9319-9335.
50. Shang, W.H., et al., *Acetylation of histone H4 lysine 5 and 12 is required for CENP-A deposition into centromeres.* Nat Commun, 2016. **7**: p. 13465.
51. Nagy, Z. and L. Tora, *Distinct GCN5/PCAF-containing complexes function as co-activators and are involved in transcription factor and global histone acetylation.* Oncogene, 2007. **26**(37): p. 5341-57.
52. Judes, G., et al., *A bivalent role of TIP60 histone acetyl transferase in human cancer.* Epigenomics, 2015. **7**(8): p. 1351-61.
53. Thomas, T. and A.K. Voss, *The diverse biological roles of MYST histone acetyltransferase family proteins.* Cell Cycle, 2007. **6**(6): p. 696-704.
54. Su, J., et al., *The Functional Analysis of Histone Acetyltransferase MOF in Tumorigenesis.* Int J Mol Sci, 2016. **17**(1).
55. Voss, A.K. and T. Thomas, *Histone Lysine and Genomic Targets of Histone Acetyltransferases in Mammals.* Bioessays, 2018. **40**(10): p. e1800078.
56. Huang, F., S.M. Abmayr, and J.L. Workman, *Regulation of KAT6 Acetyltransferases and Their Roles in Cell Cycle Progression, Stem Cell Maintenance, and Human Disease.* Molecular and Cellular Biology, 2016. **36**(14): p. 1900-1907.
57. Doyon, Y., et al., *ING tumor suppressor proteins are critical regulators of chromatin acetylation required for genome expression and perpetuation.* Mol Cell, 2006. **21**(1): p. 51-64.
58. Tao, Y., et al., *Structural and mechanistic insights into regulation of HBO1 histone acetyltransferase activity by BRPF2.* Nucleic Acids Res, 2017. **45**(10): p. 5707-5719.
59. Lalonde, M.E., et al., *Exchange of associated factors directs a switch in HBO1 acetyltransferase histone tail specificity.* Genes Dev, 2013. **27**(18): p. 2009-24.
60. MacPherson, L., et al., *HBO1 is required for the maintenance of leukaemia stem cells.* Nature, 2020. **577**(7789): p. 266-270.
61. Lan, R. and Q. Wang, *Deciphering structure, function and mechanism of lysine acetyltransferase HBO1 in protein acetylation, transcription regulation, DNA replication and its oncogenic properties in cancer.* Cell Mol Life Sci, 2020. **77**(4): p. 637-649.
62. Weinert, B.T., et al., *Time-Resolved Analysis Reveals Rapid Dynamics and Broad Scope of the CBP/p300 Acetylome.* Cell, 2018. **174**(1): p. 231-244 e12.
63. Wang, F., et al., *Structures of KIX domain of CBP in complex with two FOXO3a transactivation domains reveal promiscuity and plasticity in coactivator recruitment.* Proc Natl Acad Sci U S A, 2012. **109**(16): p. 6078-83.
64. Zhang, Y., et al., *The ZZ domain of p300 mediates specificity of the adjacent HAT domain for histone H3.* Nat Struct Mol Biol, 2018. **25**(9): p. 841-849.
65. Holmqvist, P.H. and M. Mannervik, *Genomic occupancy of the transcriptional co-activators p300 and CBP.* Transcription, 2013. **4**(1): p. 18-23.
66. Dancy, B.M. and P.A. Cole, *Protein lysine acetylation by p300/CBP.* Chem Rev, 2015. **115**(6): p. 2419-52.
67. Chini, C.C., et al., *HDAC3 is negatively regulated by the nuclear protein DBC1.* J Biol Chem, 2010. **285**(52): p. 40830-7.
68. Yang, W.M., et al., *Functional domains of histone deacetylase-3.* J Biol Chem, 2002. **277**(11): p. 9447-54.
69. You, S.H., et al., *Nuclear receptor co-repressors are required for the histone-deacetylase activity of HDAC3 in*

vivo. Nat Struct Mol Biol, 2013. **20**(2): p. 182-7.

70. Brunmeir, R., S. Lagger, and C. Seiser, *Histone deacetylase HDAC1/HDAC2-controlled embryonic development and cell differentiation.* Int J Dev Biol, 2009. **53**(2-3): p. 275-89.
71. Chakrabarti, A., et al., *HDAC8: a multifaceted target for therapeutic interventions.* Trends Pharmacol Sci, 2015. **36**(7): p. 481-92.
72. Nechay, M.R., et al., *Histone Deacetylase 8: Characterization of Physiological Divalent Metal Catalysis.* J Phys Chem B, 2016. **120**(26): p. 5884-95.
73. Clocchiatti, A., C. Florean, and C. Brancolini, *Class IIa HDACs: from important roles in differentiation to possible implications in tumourigenesis.* Journal of Cellular and Molecular Medicine, 2011. **15**(9): p. 1833-1846.
74. Asfaha, Y., et al., *Recent advances in class IIa histone deacetylases research.* Bioorg Med Chem, 2019. **27**(22): p. 115087.
75. Yang, X.-J. and S. Grégoire, *Class II Histone Deacetylases: from Sequence to Function, Regulation, and Clinical Implication.* Molecular and Cellular Biology, 2005. **25**(8): p. 2873-2884.
76. Hai, Y. and D.W. Christianson, *Histone deacetylase 6 structure and molecular basis of catalysis and inhibition.* Nat Chem Biol, 2016. **12**(9): p. 741-7.
77. Li, T., et al., *Histone deacetylase 6 in cancer.* Journal of Hematology & Oncology, 2018. **11**(1).
78. Hai, Y., et al., *Histone deacetylase 10 structure and molecular function as a polyamine deacetylase.* Nat Commun, 2017. **8**: p. 15368.
79. Kumar, S. and D.B. Lombard, *For Certain, SIRT4 Activities!* Trends Biochem Sci, 2017. **42**(7): p. 499-501.
80. Dang, W., *The controversial world of sirtuins.* Drug Discov Today Technol, 2014. **12**: p. e9-e17.
81. Vaquero, A., et al., *Human SirT1 interacts with histone H1 and promotes formation of facultative heterochromatin.* Mol Cell, 2004. **16**(1): p. 93-105.
82. Chen, C., et al., *SIRT1 and aging related signaling pathways.* Mech Ageing Dev, 2020. **187**: p. 111215.
83. North, B.J., et al., *The Human Sir2 Ortholog, SIRT2, Is an NAD+-Dependent Tubulin Deacetylase.* Molecular Cell, 2003. **11**(2): p. 437-444.
84. Vaquero, A., et al., *SirT2 is a histone deacetylase with preference for histone H4 Lys 16 during mitosis.* Genes Dev, 2006. **20**(10): p. 1256-61.
85. Chang, A.R., C.M. Ferrer, and R. Mostoslavsky, *SIRT6, a Mammalian Deacylase with Multitasking Abilities.* Physiol Rev, 2020. **100**(1): p. 145-169.
86. Tasselli, L., W. Zheng, and K.F. Chua, *SIRT6: Novel Mechanisms and Links to Aging and Disease.* Trends Endocrinol Metab, 2017. **28**(3): p. 168-185.
87. Wu, D., et al., *Advances in Cellular Characterization of the Sirtuin Isoform, SIRT7.* Front Endocrinol (Lausanne), 2018. **9**: p. 652.
88. Liu, S.S., et al., *HDAC11: a rising star in epigenetics.* Biomed Pharmacother, 2020. **131**: p. 110607.
89. Gao, L., et al., *Cloning and functional characterization of HDAC11, a novel member of the human histone deacetylase family.* J Biol Chem, 2002. **277**(28): p. 25748-55.
90. Yanginlar, C. and C. Logie, *HDAC11 is a regulator of diverse immune functions.* Biochim Biophys Acta Gene Regul Mech, 2018. **1861**(1): p. 54-59.
91. Gong, F., L.Y. Chiu, and K.M. Miller, *Acetylation Reader Proteins: Linking Acetylation Signaling to Genome Maintenance and Cancer.* PLoS Genet, 2016. **12**(9): p. e1006272.
92. Dhalluin, C., et al., *Structure and ligand of a histone acetyltransferase bromodomain.* Nature, 1999. **399**: p. 491-496.
93. Filippakopoulos, P., et al., *Histone recognition and large-scale structural analysis of the human bromodomain family.* Cell, 2012. **149**(1): p. 214-31.
94. David J. Owen, P.O., Ji-Chun Yang, Nicholas Lowe, Philip R. Evans, Paola Ballario, David Neuhaus, Patrizia

Filetici, and Andrew A. Travers, *The structural basis for the recognition of acetylated histone H4 by the bromodomain of histone acetyltransferase Gcn5p.* EMBO J, 2000. **19**(22).

95. Zaware, N. and M.M. Zhou, *Bromodomain biology and drug discovery.* Nat Struct Mol Biol, 2019. **26**(10): p. 870-879.
96. Mujtaba, S., L. Zeng, and M.M. Zhou, *Structure and acetyl-lysine recognition of the bromodomain.* Oncogene, 2007. **26**(37): p. 5521-7.
97. Jacobson, R.H., et al., *Structure and function of human TAFII250 double bromodomain.* SCIENCE, 2000. **288**(5470): p. 1422-1425.
98. LeRoy, G., B. Rickards, and S.J. Flint, *The double bromodomain proteins Brd2 and Brd3 couple histone acetylation to transcription.* Mol Cell, 2008. **30**(1): p. 51-60.
99. Schroder, S., et al., *Two-pronged binding with bromodomain-containing protein 4 liberates positive transcription elongation factor b from inactive ribonucleoprotein complexes.* J Biol Chem, 2012. **287**(2): p. 1090-9.
100. Moriniere, J., et al., *Cooperative binding of two acetylation marks on a histone tail by a single bromodomain.* Nature, 2009. **461**(7264): p. 664-8.
101. Ruthenburg, A.J., et al., *Recognition of a mononucleosomal histone modification pattern by BPTF via multivalent interactions.* Cell, 2011. **145**(5): p. 692-706.
102. Tsai, W.W., et al., *TRIM24 links a non-canonical histone signature to breast cancer.* Nature, 2010. **468**(7326): p. 927-32.
103. Savitsky, P., et al., *Multivalent Histone and DNA Engagement by a PHD/BRD/PWWP Triple Reader Cassette Recruits ZMYND8 to K14ac-Rich Chromatin.* Cell Rep, 2016. **17**(10): p. 2724-2737.
104. Colino-Sanguino, Y., et al., *A Read/Write Mechanism Connects p300 Bromodomain Function to H2A.Z Acetylation.* iScience, 2019. **21**: p. 773-788.
105. Ebrahimi, A., et al., *Bromodomain inhibition of the coactivators CBP/EP300 facilitate cellular reprogramming.* Nat Chem Biol, 2019. **15**(5): p. 519-528.
106. Cieniewicz, A.M., et al., *The Bromodomain of Gcn5 Regulates Site Specificity of Lysine Acetylation on Histone H3.* Molecular & Cellular Proteomics, 2014. **13**(11): p. 2896-2910.
107. Poplawski, A., et al., *Molecular insights into the recognition of N-terminal histone modifications by the BRPF1 bromodomain.* J Mol Biol, 2014. **426**(8): p. 1661-76.
108. Awad, S. and A.H. Hassan, *The Swi2/Snf2 bromodomain is important for the full binding and remodeling activity of the SWI/SNF complex on H3- and H4-acetylated nucleosomes.* Ann N Y Acad Sci, 2008. **1138**: p. 366-75.
109. SJ, K., et al., *ATAD2 is an epigenetic reader of newly synthesized histone marks during DNA replication.* oncotarget, 2016. **7**(43): p. 70323-70335.
110. Cho, C., et al., *Structural basis of nucleosome assembly by the Abo1 AAA+ ATPase histone chaperone.* Nat Commun, 2019. **10**(1): p. 5764.
111. Sahu, R.K., S. Singh, and R.S. Tomar, *The mechanisms of action of chromatin remodelers and implications in development and disease.* Biochem Pharmacol, 2020. **180**: p. 114200.
112. Sanchez, R. and M.M. Zhou, *The PHD finger: a versatile epigenome reader.* Trends Biochem Sci, 2011. **36**(7): p. 364-72.
113. Lange, M., et al., *Regulation of muscle development by DPF3, a novel histone acetylation and methylation reader of the BAF chromatin remodeling complex.* Genes Dev, 2008. **22**(17): p. 2370-84.
114. Zeng, L., et al., *Mechanism and regulation of acetylated histone binding by the tandem PHD finger of DPF3b.* Nature, 2010. **466**(7303): p. 258-62.
115. Ali, M., et al., *Tandem PHD fingers of MORF/MOZ acetyltransferases display selectivity for acetylated histone H3 and are required for the association with chromatin.* J Mol Biol, 2012. **424**(5): p. 328-38.

116. Qiu, Y., et al., *Combinatorial readout of unmodified H3R2 and acetylated H3K14 by the tandem PHD finger of MOZ reveals a regulatory mechanism for HOXA9 transcription.* Genes Dev, 2012. **26**(12): p. 1376-91.
117. Zhang, Y., et al., *Selective binding of the PHD6 finger of MLL4 to histone H4K16ac links MLL4 and MOF.* Nat Commun, 2019. **10**(1): p. 2314.
118. Wang, A.Y., et al., *Asf1-like structure of the conserved Yaf9 YEATS domain and role in H2A.Z deposition and acetylation.* Proc Natl Acad Sci U S A, 2009. **106**(51): p. 21573-8.
119. Li, Y., et al., *AF9 YEATS domain links histone acetylation to DOT1L-mediated H3K79 methylation.* Cell, 2014. **159**(3): p. 558-71.
120. Wan, L., et al., *ENL links histone acetylation to oncogenic gene expression in acute myeloid leukaemia.* Nature, 2017. **543**(7644): p. 265-269.
121. Mi, W., et al., *YEATS2 links histone acetylation to tumorigenesis of non-small cell lung cancer.* Nat Commun, 2017. **8**(1): p. 1088.
122. Hsu, C.C., et al., *Recognition of histone acetylation by the GAS41 YEATS domain promotes H2A.Z deposition in non-small cell lung cancer.* Genes Dev, 2018. **32**(1): p. 58-69.
123. Cho, H.J., et al., *GAS41 Recognizes Diacetylated Histone H3 through a Bivalent Binding Mode.* ACS Chem Biol, 2018. **13**(9): p. 2739-2746.
124. Tessarz, P. and T. Kouzarides, *Histone core modifications regulating nucleosome structure and dynamics.* Nat Rev Mol Cell Biol, 2014. **15**(11): p. 703-8.
125. Bascom, G.D. and T. Schlick, *Chromatin Fiber Folding Directed by Cooperative Histone Tail Acetylation and Linker Histone Binding.* Biophys J, 2018. **114**(10): p. 2376-2385.
126. Dhar, S., et al., *The tale of a tail: histone H4 acetylation and the repair of DNA breaks.* Philos Trans R Soc Lond B Biol Sci, 2017. **372**(1731).
127. Shogren-Knaak, M., et al., *Histone H4-K16 Acetylation Controls Chromatin Structure and Protein Interactions.* Science, 2006. **311**(5762): p. 844-847.
128. Lee, J. and T.H. Lee, *How Protein Binding Sensitizes the Nucleosome to Histone H3K56 Acetylation.* ACS Chem Biol, 2019. **14**(3): p. 506-515.
129. Chatterjee, N., et al., *Histone Acetylation near the Nucleosome Dyad Axis Enhances Nucleosome Disassembly by RSC and SWI/SNF.* Mol Cell Biol, 2015. **35**(23): p. 4083-92.
130. Hayashi-Takanaka, Y., et al., *Distribution of histone H4 modifications as revealed by a panel of specific monoclonal antibodies.* Chromosome Res, 2015. **23**(4): p. 753-66.
131. Winter, G.E., et al., *BET Bromodomain Proteins Function as Master Transcription Elongation Factors Independent of CDK9 Recruitment.* Mol Cell, 2017. **67**(1): p. 5-18 e19.
132. Jang, M.K., et al., *The bromodomain protein Brd4 is a positive regulatory component of P-TEFb and stimulates RNA polymerase II-dependent transcription.* Mol Cell, 2005. **19**(4): p. 523-34.
133. Gates, L.A., et al., *Acetylation on histone H3 lysine 9 mediates a switch from transcription initiation to elongation.* J Biol Chem, 2017. **292**(35): p. 14456-14472.
134. Y, C.-S., C. SJ2, and V.-M. F, *H2A.Z acetylation and transcription: ready, steady, go!* Epigenomics, 2016. **8**(5): p. 583-586.
135. Clayton, A.L., C.A. Hazzalin, and L.C. Mahadevan, *Enhanced histone acetylation and transcription: a dynamic perspective.* Mol Cell, 2006. **23**(3): p. 289-96.
136. Ferrari, P. and M. Strubin, *Uncoupling histone turnover from transcription-associated histone H3 modifications.* Nucleic Acids Res, 2015. **43**(8): p. 3972-85.
137. Wang, Z., et al., *Genome-wide mapping of HATs and HDACs reveals distinct functions in active and inactive genes.* Cell, 2009. **138**(5): p. 1019-31.
138. Gryder, B.E., et al., *Histone hyperacetylation disrupts core gene regulatory architecture in rhabdomyosarcoma.* Nature Genetics, 2019. **51**(12): p. 1714-1722.

139. Tan, M., et al., *Identification of 67 Histone Marks and Histone Lysine Crotonylation as a New Type of Histone Modification.* Cell, 2011. **146**(6): p. 1016-1028.
140. Zhang, D., et al., *Metabolic regulation of gene expression by histone lactylation.* Nature, 2019. **574**(7779): p. 575-580.
141. Xie, Z., et al., *Metabolic Regulation of Gene Expression by Histone Lysine beta-Hydroxybutyrylation.* Mol Cell, 2016. **62**(2): p. 194-206.
142. Dai, L., et al., *Lysine 2-hydroxyisobutyrylation is a widely distributed active histone mark.* Nat Chem Biol, 2014. **10**(5): p. 365-70.
143. Simithy, J., et al., *Characterization of histone acylations links chromatin modifications with metabolism.* Nature Communications, 2017. **8**(1).
144. Sabari, Benjamin R., et al., *Intracellular Crotonyl-CoA Stimulates Transcription through p300-Catalyzed Histone Crotonylation.* Molecular Cell, 2015. **58**(2): p. 203-215.
145. Goudarzi, A., et al., *Dynamic Competing Histone H4 K5K8 Acetylation and Butyrylation Are Hallmarks of Highly Active Gene Promoters.* Molecular Cell, 2016. **62**(2): p. 169-180.
146. Zhao, S., X. Zhang, and H. Li, *Beyond histone acetylation-writing and erasing histone acylations.* Curr Opin Struct Biol, 2018. **53**: p. 169-177.
147. Huang, H., et al., *Landscape of the regulatory elements for lysine 2-hydroxyisobutyrylation pathway.* Cell Research, 2017. **28**(1): p. 111-125.
148. Kaczmarska, Z., et al., *Structure of p300 in complex with acyl-CoA variants.* Nat Chem Biol, 2017. **13**(1): p. 21-29.
149. Kollenstart, L., et al., *Gcn5 and Esa1 function as histone crotonyltransferases to regulate crotonylation-dependent transcription.* J Biol Chem, 2019. **294**(52): p. 20122-20134.
150. Ringel, A.E. and C. Wolberger, *Structural basis for acyl-group discrimination by human Gcn5L2.* Acta Crystallogr D Struct Biol, 2016. **72**(Pt 7): p. 841-8.
151. Wang, Y., et al., *KAT2A coupled with the alpha-KGDH complex acts as a histone H3 succinyltransferase.* Nature, 2017. **552**(7684): p. 273-277.
152. Liu, X., et al., *MOF as an evolutionarily conserved histone crotonyltransferase and transcriptional activation by histone acetyltransferase-deficient and crotonyltransferase-competent CBP/p300.* Cell discovery, 2017. **3**(17016).
153. Han, Z., et al., *Revealing the protein propionylation activity of the histone acetyltransferase MOF (males absent on the first).* J Biol Chem, 2018. **293**(9): p. 3410-3420.
154. Wei, W., et al., *Class I histone deacetylases are major histone decrotonylases: evidence for critical and broad function of histone crotonylation in transcription.* Cell Research, 2017. **27**(7): p. 898-915.
155. Zhang, X., et al., *Molecular basis for hierarchical histone de-beta-hydroxybutyrylation by SIRT3.* Cell Discov, 2019. **5**: p. 35.
156. Aramsangtienchai, P., et al., *HDAC8 Catalyzes the Hydrolysis of Long Chain Fatty Acyl Lysine.* ACS Chem Biol, 2016. **11**(10): p. 2685-2692.
157. Bao, X., et al., *Identification of 'erasers' for lysine crotonylated histone marks using a chemical proteomics approach.* Elife, 2014. **3**.
158. Tan, M., et al., *Lysine glutarylation is a protein posttranslational modification regulated by SIRT5.* Cell Metab, 2014. **19**(4): p. 605-17.
159. Du, J., et al., *Sirt5 is a NAD-dependent protein lysine demalonylase and desuccinylase.* Science, 2011. **334**(6057): p. 806-9.
160. Jiang, H., et al., *SIRT6 regulates TNF-alpha secretion through hydrolysis of long-chain fatty acyl lysine.* Nature, 2013. **496**(7443): p. 110-3.
161. Pannek, M., et al., *Crystal structures of the mitochondrial deacylase Sirtuin 4 reveal isoform-specific acyl*

recognition and regulation features. Nat Commun, 2017. **8**(1): p. 1513.
162. Zhao, D., et al., *YEATS2 is a selective histone crotonylation reader.* Cell Research, 2016. **26**(5): p. 629-632.
163. Li, Y., et al., *Molecular Coupling of Histone Crotonylation and Active Transcription by AF9 YEATS Domain.* Molecular Cell, 2016. **62**(2): p. 181-193.
164. Xiong, X., et al., *Selective recognition of histone crotonylation by double PHD fingers of MOZ and DPF2.* Nat Chem Biol, 2016. **12**(12): p. 1111-1118.
165. Klein, B.J., et al., *Recognition of Histone H3K14 Acylation by MORF.* Structure, 2017. **25**(4): p. 650-654 e2.
166. Flynn, E.M., et al., *A Subset of Human Bromodomains Recognizes Butyryllysine and Crotonyllysine Histone Peptide Modifications.* Structure, 2015. **23**(10): p. 1801-1814.
167. Barnes, C.E., D.M. English, and S.M. Cowley, *Acetylation & Co: an expanding repertoire of histone acylations regulates chromatin and transcription.* Essays Biochem, 2019. **63**(1): p. 97-107.
168. Dutta, A., S.M. Abmayr, and J.L. Workman, *Diverse Activities of Histone Acylations Connect Metabolism to Chromatin Function.* Mol Cell, 2016. **63**(4): p. 547-552.
169. Kebede, A.F., et al., *Histone propionylation is a mark of active chromatin.* Nat Struct Mol Biol, 2017. **24**(12): p. 1048-1056.
170. Gowans, G.J., et al., *Recognition of Histone Crotonylation by Taf14 Links Metabolic State to Gene Expression.* Mol Cell, 2019. **76**(6): p. 909-921 e3.
171. Uckelmann, M. and T.K. Sixma, *Histone ubiquitination in the DNA damage response.* DNA Repair (Amst), 2017. **56**: p. 92-101.
172. Du, H.N., *Transcription, DNA damage and beyond: the roles of histone ubiquitination and deubiquitination.* Curr Protein Pept Sci, 2012. **13**(5): p. 447-66.
173. Shiio, Y. and R.N. Eisenman, *Histone sumoylation is associated with transcriptional repression.* Proc Natl Acad Sci U S A, 2003. **100**(23): p. 13225-30.
174. Nathan, D., et al., *Histone sumoylation is a negative regulator in Saccharomyces cerevisiae and shows dynamic interplay with positive-acting histone modifications.* Genes Dev, 2006. **20**(8): p. 966-76.
175. Ryu, H.Y., et al., *The Ulp2 SUMO protease promotes transcription elongation through regulation of histone sumoylation.* EMBO J, 2019. **38**(16): p. e102003.
176. Wotton, D., L.F. Pemberton, and J. Merrill-Schools, *SUMO and Chromatin Remodeling*, in *SUMO Regulation of Cellular Processes*, V.G. Wilson, Editor. 2017, Springer International Publishing: Cham. p. 35-50.
177. Maison, C., et al., *SUMOylation promotes de novo targeting of HP1α to pericentric heterochromatin.* Nature Genetics, 2011. **43**(3): p. 220-227.
178. Farrelly, L.A., et al., *Histone serotonylation is a permissive modification that enhances TFIID binding to H3K4me3.* Nature, 2019. **567**(7749): p. 535-539.
179. Zlotorynski, E., *Histone serotonylation boosts neuronal transcription.* Nat Rev Mol Cell Biol, 2019. **20**(6): p. 323.
180. Anastas, J.N. and Y. Shi, *Histone Serotonylation: Can the Brain Have "Happy" Chromatin?* Mol Cell, 2019. **74**(3): p. 418-420.
181.Abplanalp, J. and M.O. Hottiger, *Cell fate regulation by chromatin ADP-ribosylation.* Semin Cell Dev Biol, 2017. **63**: p. 114-122.
182. Bartlett, E., et al., *Interplay of Histone Marks with Serine ADP-Ribosylation.* Cell Rep, 2018. **24**(13): p. 3488-3502 e5.
183. Hottiger, M.O., *ADP-ribosylation of histones by ARTD1: an additional module of the histone code?* FEBS Lett, 2011. **585**(11): p. 1595-9.
184. Thompson, P.R. and W. Fast, *Histone citrullination by protein arginine deiminase: is arginine methylation a green light or a roadblock?* ACS Chem Biol, 2006. **1**(7): p. 433-41.
185. Zhai, Q., et al., *Role of citrullination modification catalyzed by peptidylarginine deiminase 4 in gene*

transcriptional regulation. Acta Biochim Biophys Sin (Shanghai), 2017. **49**(7): p. 567-572.

186. Maksimovic, I., et al., *An Azidoribose Probe to Track Ketoamine Adducts in Histone Ribose Glycation.* J Am Chem Soc, 2020. **142**(22): p. 9999-10007.
187. Talasz, H., S. Wasserer, and B. Puschendorf, *Nonenzymatic glycation of histones in vitro and in vivo.* J Cell Biochem, 2002. **85**(1): p. 24-34.
188. Zheng, Q., et al., *Reversible histone glycation is associated with disease-related changes in chromatin architecture.* Nat Commun, 2019. **10**(1): p. 1289.
189. Zheng, Q., A. Osunsade, and Y. David, *Protein arginine deiminase 4 antagonizes methylglyoxal-induced histone glycation.* Nat Commun, 2020. **11**(1): p. 3241.
190. Spinelli, M., S. Fusco, and C. Grassi, *Nutrient-Dependent Changes of Protein Palmitoylation: Impact on Nuclear Enzymes and Regulation of Gene Expression.* Int J Mol Sci, 2018. **19**(12).
191. Wilson, J.P., et al., *Proteomic analysis of fatty-acylated proteins in mammalian cells with chemical reporters reveals S-acylation of histone H3 variants.* Mol Cell Proteomics, 2011. **10**(3): p. M110 001198.
192. Zou, C., et al., *Acyl-CoA:lysophosphatidylcholine acyltransferase I (Lpcat1) catalyzes histone protein O-palmitoylation to regulate mRNA synthesis.* J Biol Chem, 2011. **286**(32): p. 28019-25.
193. Wang, Z., et al., *Combinatorial patterns of histone acetylations and methylations in the human genome.* Nat Genet, 2008. **40**(7): p. 897-903.
194. Musselman, C.A., et al., *Perceiving the epigenetic landscape through histone readers.* Nat Struct Mol Biol, 2012. **19**(12): p. 1218-27.
195. Su, Z. and J.M. Denu, *Reading the Combinatorial Histone Language.* ACS Chem Biol, 2016. **11**(3): p. 564-74.
196. DouglasHanahan and R.A. Weinberg, *The Hallmarks of Cancer.* Cell, 2000. **100**(1): p. 57-70.
197. Hanahan, D. and R.A. Weinberg, *Hallmarks of cancer: the next generation.* Cell, 2011. **144**(5): p. 646-74.
198. Yamada, Y. and Y. Yamada, *The causal relationship between epigenetic abnormality and cancer development: in vivo reprogramming and its future application.* Proc Jpn Acad Ser B Phys Biol Sci, 2018. **94**(6): p. 235-247.
199. Hassler, M.R. and G. Egger, *Epigenomics of cancer - emerging new concepts.* Biochimie, 2012. **94**(11): p. 2219-30.
200. Fraga, M.F., et al., *Loss of acetylation at Lys16 and trimethylation at Lys20 of histone H4 is a common hallmark of human cancer.* Nat Genet, 2005. **37**(4): p. 391-400.
201. Guo, P., et al., *The Histone Acetylation Modifications of Breast Cancer and their Therapeutic Implications.* Pathol Oncol Res, 2018. **24**(4): p. 807-813.
202. Janczar, S., et al., *The Role of Histone Protein Modifications and Mutations in Histone Modifiers in Pediatric B-Cell Progenitor Acute Lymphoblastic Leukemia.* Cancers (Basel), 2017. **9**(1).
203. Fullgrabe, J., E. Kavanagh, and B. Joseph, *Histone onco-modifications.* Oncogene, 2011. **30**(31): p. 3391-403.
204. Audia, J.E. and R.M. Campbell, *Histone Modifications and Cancer.* Cold Spring Harb Perspect Biol, 2016. **8**(4): p. a019521.
205. Barski, A., et al., *High-resolution profiling of histone methylations in the human genome.* Cell, 2007. **129**(4): p. 823-37.
206. Polak, P., et al., *Cell-of-origin chromatin organization shapes the mutational landscape of cancer.* Nature, 2015. **518**(7539): p. 360-364.
207. Moran, B., et al., *Epigenetics of malignant melanoma.* Semin Cancer Biol, 2018. **51**: p. 80-88.
208. Kim, K.H. and C.W. Roberts, *Targeting EZH2 in cancer.* Nat Med, 2016. **22**(2): p. 128-34.
209. Li, B. and W.J. Chng, *EZH2 abnormalities in lymphoid malignancies: underlying mechanisms and therapeutic implications.* J Hematol Oncol, 2019. **12**(1): p. 118.
210. French, C.A., et al., *BRD4-NUT Fusion Oncogene.* Cancer research, 2003. **63**(2): p. 304-307.
211. Souroullas, G.P., et al., *An oncogenic Ezh2 mutation induces tumors through global redistribution of histone 3 lysine 27 trimethylation.* Nat Med, 2016. **22**(6): p. 632-40.

212. Morin, R.D., et al., *Somatic mutations altering EZH2 (Tyr641) in follicular and diffuse large B-cell lymphomas of germinal-center origin.* Nat Genet, 2010. **42**(2): p. 181-5.
213. Yap, D.B., et al., *Somatic mutations at EZH2 Y641 act dominantly through a mechanism of selectively altered PRC2 catalytic activity, to increase H3K27 trimethylation.* Blood, 2011. **117**(8): p. 2451-9.
214. McCabe, M.T., et al., *Mutation of A677 in histone methyltransferase EZH2 in human B-cell lymphoma promotes hypertrimethylation of histone H3 on lysine 27 (H3K27).* Proc Natl Acad Sci U S A, 2012. **109**(8): p. 2989-94.
215. Bödör, C., et al., *EZH2 mutations are frequent and represent an early event in follicular lymphoma.* Blood, 2013. **122**(18): p. 3165-8.
216. Ntziachristos, P., et al., *Genetic inactivation of the polycomb repressive complex 2 in T cell acute lymphoblastic leukemia.* Nat Med, 2012. **18**(2): p. 298-301.
217. Mallen-St Clair, J., et al., *EZH2 couples pancreatic regeneration to neoplastic progression.* Genes Dev, 2012. **26**(5): p. 439-44.
218. Smith, E., C. Lin, and A. Shilatifard, *The super elongation complex (SEC) and MLL in development and disease.* Genes Dev, 2011. **25**(7): p. 661-72.
219. Liu, H., E.H. Cheng, and J.J. Hsieh, *MLL fusions: pathways to leukemia.* Cancer Biol Ther, 2009. **8**(13): p. 1204-11.
220. Milne, T.A., *Mouse models of MLL leukemia: recapitulating the human disease.* Blood, 2017. **129**(16): p. 2217-2223.
221. Rao, R.C. and Y. Dou, *Hijacked in cancer: the KMT2 (MLL) family of methyltransferases.* Nat Rev Cancer, 2015. **15**(6): p. 334-46.
222. Takeda, S., et al., *HGF-MET signals via the MLL-ETS2 complex in hepatocellular carcinoma.* J Clin Invest, 2013. **123**(7): p. 3154-65.
223. Sierra, J., et al., *The APC tumor suppressor counteracts beta-catenin activation and H3K4 methylation at Wnt target genes.* Genes Dev, 2006. **20**(5): p. 586-600.
224. Bui, N., et al., *Disruption of NSD1 in Head and Neck Cancer Promotes Favorable Chemotherapeutic Responses Linked to Hypomethylation.* Mol Cancer Ther, 2018. **17**(7): p. 1585-1594.
225. Bianco-Miotto, T., et al., *Global levels of specific histone modifications and an epigenetic gene signature predict prostate cancer progression and development.* Cancer Epidemiol Biomarkers Prev, 2010. **19**(10): p. 2611-22.
226. Peri, S., et al., *NSD1- and NSD2-damaging mutations define a subset of laryngeal tumors with favorable prognosis.* Nat Commun, 2017. **8**(1): p. 1772.
227. Ettel, M., et al., *Expression and prognostic value of NSD1 and SETD2 in pancreatic ductal adenocarcinoma and its precursor lesions.* Pathology, 2019. **51**(4): p. 392-398.
228. Wang, G.G., et al., *NUP98-NSD1 links H3K36 methylation to Hox-A gene activation and leukaemogenesis.* Nat Cell Biol, 2007. **9**(7): p. 804-12.
229. Kivioja, J.L., et al., *Chimeric NUP98-NSD1 transcripts from the cryptic t(5;11)(q35.2;p15.4) in adult de novo acute myeloid leukemia.* Leuk Lymphoma, 2018. **59**(3): p. 725-732.
230. Shiba, N., et al., *NUP98-NSD1 gene fusion and its related gene expression signature are strongly associated with a poor prognosis in pediatric acute myeloid leukemia.* Genes Chromosomes Cancer, 2013. **52**(7): p. 683-93.
231. Hollink, I.H., et al., *NUP98/NSD1 characterizes a novel poor prognostic group in acute myeloid leukemia with a distinct HOX gene expression pattern.* Blood, 2011. **118**(13): p. 3645-56.
232. Bennett, R.L., et al., *The Role of Nuclear Receptor-Binding SET Domain Family Histone Lysine Methyltransferases in Cancer.* Cold Spring Harb Perspect Med, 2017. **7**(6).
233. Swaroop, A., et al., *An activating mutation of the NSD2 histone methyltransferase drives oncogenic*

reprogramming in acute lymphocytic leukemia. Oncogene, 2019. **38**(5): p. 671-686.

234. Oyer, J.A., et al., *Point mutation E1099K in MMSET/NSD2 enhances its methyltranferase activity and leads to altered global chromatin methylation in lymphoid malignancies.* Leukemia, 2014. **28**(1): p. 198-201.
235. Pierro, J., et al., *The NSD2 p.E1099K Mutation Is Enriched at Relapse and Confers Drug Resistance in a Cell Context-Dependent Manner in Pediatric Acute Lymphoblastic Leukemia.* Mol Cancer Res, 2020. **18**(8): p. 1153-1165.
236. Li, J., et al., *NSD2-E1099K Mutation Leads to Glucocorticoid-Resistant B Cell Lymphocytic Leukemia in Mice.* Blood, 2020. **136**(Supplement 1): p. 3-4.
237. Martinez-Garcia, E., et al., *The MMSET histone methyl transferase switches global histone methylation and alters gene expression in t(4;14) multiple myeloma cells.* Blood, 2011. **117**(1): p. 211-20.
238. Hudlebusch, H.R., et al., *MMSET is highly expressed and associated with aggressiveness in neuroblastoma.* Cancer Res, 2011. **71**(12): p. 4226-35.
239. Suzuki, S., et al., *NSD3-NUT-expressing midline carcinoma of the lung: first characterization of primary cancer tissue.* Pathol Res Pract, 2015. **211**(5): p. 404-8.
240. Rosati, R., et al., *NUP98 is fused to the NSD3 gene in acute myeloid leukemia associated with t(8;11)(p11.2;p15).* Blood, 2002. **99**(10): p. 3857-60.
241. Taketani, T., et al., *NUP98-NSD3 fusion gene in radiation-associated myelodysplastic syndrome with t(8;11)(p11;p15) and expression pattern of NSD family genes.* Cancer Genet Cytogenet, 2009. **190**(2): p. 108-12.
242. Fang, R., et al., *Human LSD2/KDM1b/AOF1 regulates gene transcription by modulating intragenic H3K4me2 methylation.* Mol Cell, 2010. **39**(2): p. 222-33.
243. Zhang, Q., et al., *Structural Mechanism of Transcriptional Regulator NSD3 Recognition by the ET Domain of BRD4.* Structure, 2016. **24**(7): p. 1201-8.
244. Yang, Z.Q., et al., *Transforming properties of 8p11-12 amplified genes in human breast cancer.* Cancer Res, 2010. **70**(21): p. 8487-97.
245. Network, C.G.A.R., *Comprehensive molecular characterization of clear cell renal cell carcinoma.* Nature, 2013. **499**(7456): p. 43-9.
246. Fontebasso, A.M., et al., *Chromatin remodeling defects in pediatric and young adult glioblastoma: a tale of a variant histone 3 tail.* Brain Pathol, 2013. **23**(2): p. 210-6.
247. Yuan, H., et al., *Histone methyltransferase SETD2 modulates alternative splicing to inhibit intestinal tumorigenesis.* J Clin Invest, 2017. **127**(9): p. 3375-3391.
248. Daugaard, M., et al., *LEDGF (p75) promotes DNA-end resection and homologous recombination.* Nat Struct Mol Biol, 2012. **19**(8): p. 803-10.
249. Musselman, C.A., et al., *Molecular basis for H3K36me3 recognition by the Tudor domain of PHF1.* Nat Struct Mol Biol, 2012. **19**(12): p. 1266-72.
250. Li, F., et al., *The histone mark H3K36me3 regulates human DNA mismatch repair through its interaction with MutSα.* Cell, 2013. **153**(3): p. 590-600.
251. Luco, R.F., et al., *Regulation of alternative splicing by histone modifications.* Science, 2010. **327**(5968): p. 996-1000.
252. Wen, H., et al., *ZMYND11 links histone H3.3K36me3 to transcription elongation and tumour suppression.* Nature, 2014. **508**(7495): p. 263-8.
253. Zhang, P., et al., *Structure of human MRG15 chromo domain and its binding to Lys36-methylated histone H3.* Nucleic Acids Res, 2006. **34**(22): p. 6621-8.
254. Skucha, A., et al., *Li, 2017MLL-fusion-driven leukemia requires SETD2 to safeguard genomic integrity.* Nat Commun, 2018. **9**(1): p. 1983.
255. Li, L. and Y. Wang, *Cross-talk between the H3K36me3 and H4K16ac histone epigenetic marks in DNA double-*

strand break repair. J Biol Chem, 2017. **292**(28): p. 11951-11959.

256. Bernt, K.M., et al., *MLL-rearranged leukemia is dependent on aberrant H3K79 methylation by DOT1L.* Cancer Cell, 2011. **20**(1): p. 66-78.
257. Skucha, A., J. Ebner, and F. Grebien, *Roles of SETD2 in Leukemia-Transcription, DNA-Damage, and Beyond.* Int J Mol Sci, 2019. **20**(5).
258. Petrovchich, I. and J.M. Ford, *Genetic predisposition to gastric cancer.* Semin Oncol, 2016. **43**(5): p. 554-559.
259. Wood, K., M. Tellier, and S. Murphy, *DOT1L and H3K79 Methylation in Transcription and Genomic Stability.* Biomolecules, 2018. **8**(1): p. 11.
260. Rao, V.K., A. Pal, and R. Taneja, *A drive in SUVs: From development to disease.* Epigenetics, 2017. **12**(3): p. 177-186.
261. Cai, L., et al., *Aberrant histone methylation and the effect of Suv39H1 siRNA on gastric carcinoma.* Oncol Rep, 2014. **31**(6): p. 2593-600.
262. Kim, G., et al., *SUV39H1/DNMT3A-dependent methylation of the RB1 promoter stimulates PIN1 expression and melanoma development.* Faseb j, 2018. **32**(10): p. 5647-5660.
263. Rodrigues, C., et al., *A SUV39H1-low chromatin state characterises and promotes migratory properties of cervical cancer cells.* Exp Cell Res, 2019. **378**(2): p. 206-216.
264. Ferreira, M.J., et al., *SETDB2 and RIOX2 are differentially expressed among renal cell tumor subtypes, associating with prognosis and metastization.* Epigenetics, 2017. **12**(12): p. 1057-1064.
265. Lin, C.H., et al., *SETDB2 Links E2A-PBX1 to Cell-Cycle Dysregulation in Acute Leukemia through CDKN2C Repression.* Cell Rep, 2018. **23**(4): p. 1166-1177.
266. Casciello, F., et al., *G9a drives hypoxia-mediated gene repression for breast cancer cell survival and tumorigenesis.* Proc Natl Acad Sci U S A, 2017. **114**(27): p. 7077-7082.
267. Yin, C., et al., *G9a promotes cell proliferation and suppresses autophagy in gastric cancer by directly activating mTOR.* Faseb j, 2019. **33**(12): p. 14036-14050.
268. Wang, Y.F., et al., *G9a regulates breast cancer growth by modulating iron homeostasis through the repression of ferroxidase hephaestin.* Nat Commun, 2017. **8**(1): p. 274.
269. Ding, J., et al., *The histone H3 methyltransferase G9A epigenetically activates the serine-glycine synthesis pathway to sustain cancer cell survival and proliferation.* Cell Metab, 2013. **18**(6): p. 896-907.
270. Kim, K.B., et al., *H3K9 methyltransferase G9a negatively regulates UHRF1 transcription during leukemia cell differentiation.* Nucleic Acids Res, 2015. **43**(7): p. 3509-23.
271. Avgustinova, A., et al., *Loss of G9a preserves mutation patterns but increases chromatin accessibility, genomic instability and aggressiveness in skin tumours.* Nat Cell Biol, 2018. **20**(12): p. 1400-1409.
272. Li, L.X., et al., *Lysine methyltransferase SMYD2 promotes triple negative breast cancer progression.* Cell Death Dis, 2018. **9**(3): p. 326.
273. Oliveira-Santos, W., et al., *Residual expression of SMYD2 and SMYD3 is associated with the acquisition of complex karyotype in chronic lymphocytic leukemia.* Tumour Biol, 2016. **37**(7): p. 9473-81.
274. Sakamoto, L.H., et al., *SMYD2 is highly expressed in pediatric acute lymphoblastic leukemia and constitutes a bad prognostic factor.* Leuk Res, 2014. **38**(4): p. 496-502.
275. Wang, Y., et al., *Amplification of SMYD3 promotes tumorigenicity and intrahepatic metastasis of hepatocellular carcinoma via upregulation of CDK2 and MMP2.* Oncogene, 2019. **38**(25): p. 4948-4961.
276. Fei, X., et al., *Overexpression of SMYD3 Is Predictive of Unfavorable Prognosis in Hepatocellular Carcinoma.* Tohoku J Exp Med, 2017. **243**(3): p. 219-226.
277. Sarris, M.E., et al., *Smyd3 Is a Transcriptional Potentiator of Multiple Cancer-Promoting Genes and Required for Liver and Colon Cancer Development.* Cancer Cell, 2016. **29**(3): p. 354-366.
278. Giakountis, A., et al., *Smyd3-associated regulatory pathways in cancer.* Semin Cancer Biol, 2017. **42**: p. 70-80.

279. Liao, T., et al., *Histone methyltransferase KMT5A gene modulates oncogenesis and lipid metabolism of papillary thyroid cancer in vitro.* Oncol Rep, 2018. **39**(5): p. 2185-2192.
280. Huang, R., et al., *Monomethyltransferase SETD8 regulates breast cancer metabolism via stabilizing hypoxia-inducible factor 1α.* Cancer Lett, 2017. **390**: p. 1-10.
281. Duan, B., et al., *Histone-lysine N-methyltransferase SETD7 is a potential serum biomarker for colorectal cancer patients.* EBioMedicine, 2018. **37**: p. 134-143.
282. Song, Y., et al., *SET7/9 inhibits oncogenic activities through regulation of Gli-1 expression in breast cancer.* Tumour Biol, 2016. **37**(7): p. 9311-22.
283. Gu, Y., et al., *SET7/9 promotes hepatocellular carcinoma progression through regulation of E2F1.* Oncol Rep, 2018. **40**(4): p. 1863-1874.
284. Tarighat, S.S., et al., *The dual epigenetic role of PRMT5 in acute myeloid leukemia: gene activation and repression via histone arginine methylation.* Leukemia, 2016. **30**(4): p. 789-99.
285. Schulte, J.H., et al., *Lysine-Specific Demethylase 1 Is Strongly Expressed in Poorly Differentiated Neuroblastoma: Implications for Therapy.* Cancer Research, 2009. **69**(5): p. 2065-2071.
286. Hosseini, A. and S. Minucci, *A comprehensive review of lysine-specific demethylase 1 and its roles in cancer.* Epigenomics, 2017. **9**(8): p. 1123-1142.
287. Majello, B., et al., *Expanding the Role of the Histone Lysine-Specific Demethylase LSD1 in Cancer.* Cancers (Basel), 2019. **11**(3).
288. Harris, W.J., et al., *The histone demethylase KDM1A sustains the oncogenic potential of MLL-AF9 leukemia stem cells.* Cancer Cell, 2012. **21**(4): p. 473-87.
289. Somervaille, T.C. and M.L. Cleary, *Identification and characterization of leukemia stem cells in murine MLL-AF9 acute myeloid leukemia.* Cancer Cell, 2006. **10**(4): p. 257-68.
290. Yatim, A., et al., *NOTCH1 nuclear interactome reveals key regulators of its transcriptional activity and oncogenic function.* Mol Cell, 2012. **48**(3): p. 445-58.
291. Liu, J., et al., *Arginine methylation-dependent LSD1 stability promotes invasion and metastasis of breast cancer.* EMBO Rep, 2020. **21**(2): p. e48597.
292. Wang, Y., et al., *LSD1 is a subunit of the NuRD complex and targets the metastasis programs in breast cancer.* Cell, 2009. **138**(4): p. 660-72.
293. Hu, X., et al., *LSD1 suppresses invasion, migration and metastasis of luminal breast cancer cells via activation of GATA3 and repression of TRIM37 expression.* Oncogene, 2019. **38**(44): p. 7017-7034.
294. Yang, Y., et al., *LSD1 coordinates with the SIN3A/HDAC complex and maintains sensitivity to chemotherapy in breast cancer.* J Mol Cell Biol, 2018. **10**(4): p. 285-301.
295. Zehir, A., et al., *Mutational landscape of metastatic cancer revealed from prospective clinical sequencing of 10,000 patients.* Nat Med, 2017. **23**(6): p. 703-713.
296. Gao, J., et al., *Integrative analysis of complex cancer genomics and clinical profiles using the cBioPortal.* Sci Signal, 2013. **6**(269): p. pl1.
297. Benyoucef, A., et al., *UTX inhibition as selective epigenetic therapy against TAL1-driven T-cell acute lymphoblastic leukemia.* Genes Dev, 2016. **30**(5): p. 508-21.
298. Zheng, L., et al., *Utx loss causes myeloid transformation.* Leukemia, 2018. **32**(6): p. 1458-1465.
299. Ler, L.D., et al., *Loss of tumor suppressor KDM6A amplifies PRC2-regulated transcriptional repression in bladder cancer and can be targeted through inhibition of EZH2.* Sci Transl Med, 2017. **9**(378).
300. Ezponda, T., et al., *UTX/KDM6A Loss Enhances the Malignant Phenotype of Multiple Myeloma and Sensitizes Cells to EZH2 inhibition.* Cell Rep, 2017. **21**(3): p. 628-640.
301. Pereira, F., et al., *KDM6B/JMJD3 histone demethylase is induced by vitamin D and modulates its effects in colon cancer cells.* Hum Mol Genet, 2011. **20**(23): p. 4655-65.
302. Agger, K., et al., *The H3K27me3 demethylase JMJD3 contributes to the activation of the INK4A-ARF locus in*

response to oncogene- and stress-induced senescence. Genes Dev, 2009. **23**(10): p. 1171-6.

303. Ntziachristos, P., et al., *Contrasting roles of histone 3 lysine 27 demethylases in acute lymphoblastic leukaemia.* Nature, 2014. **514**(7523): p. 513-7.
304. Li, S.H., et al., *JMJD3 expression is an independent prognosticator in patients with esophageal squamous cell carcinoma.* Surgery, 2019. **165**(5): p. 946-952.
305. Zhang, Y., et al., *JMJD3 enhances invasiveness and migratory capacity of non-small cell lung cancer cell via activating EMT signaling pathway.* Eur Rev Med Pharmacol Sci, 2019. **23**(11): p. 4784-4792.
306. Li, Q., et al., *KDM6B induces epithelial-mesenchymal transition and enhances clear cell renal cell carcinoma metastasis through the activation of SLUG.* Int J Clin Exp Pathol, 2015. **8**(6): p. 6334-44.
307. Zou, S., et al., *JMJD3 promotes the epithelial-mesenchymal transition and migration of glioma cells via the CXCL12/CXCR4 axis.* Oncol Lett, 2019. **18**(6): p. 5930-5940.
308. Ohguchi, H., et al., *KDM6B modulates MAPK pathway mediating multiple myeloma cell growth and survival.* Leukemia, 2017. **31**(12): p. 2661-2669.
309. Noort, S., et al., *The clinical and biological characteristics of NUP98-KDM5A in pediatric acute myeloid leukemia.* Haematologica, 2020.
310. de Rooij, J.D., et al., *Pediatric non-Down syndrome acute megakaryoblastic leukemia is characterized by distinct genomic subsets with varying outcomes.* Nat Genet, 2017. **49**(3): p. 451-456.
311. Feng, T., et al., *KDM5A promotes proliferation and EMT in ovarian cancer and closely correlates with PTX resistance.* Mol Med Rep, 2017. **16**(3): p. 3573-3580.
312. Oser, M.G., et al., *The KDM5A/RBP2 histone demethylase represses NOTCH signaling to sustain neuroendocrine differentiation and promote small cell lung cancer tumorigenesis.* Genes Dev, 2019. **33**(23-24): p. 1718-1738.
313. Dai, B., et al., *Histone demethylase KDM5A inhibits glioma cells migration and invasion by down regulating ZEB1.* Biomed Pharmacother, 2018. **99**: p. 72-80.
314. Kuo, K.T., et al., *Histone demethylase JARID1B/KDM5B promotes aggressiveness of non-small cell lung cancer and serves as a good prognostic predictor.* Clin Epigenetics, 2018. **10**(1): p. 107.
315. Huang, D., et al., *KDM5B overexpression predicts a poor prognosis in patients with squamous cell carcinoma of the head and neck.* J Cancer, 2018. **9**(1): p. 198-204.
316. Wang, Z., et al., *KDM5B is overexpressed in gastric cancer and is required for gastric cancer cell proliferation and metastasis.* Am J Cancer Res, 2015. **5**(1): p. 87-100.
317. Tumber, A., et al., *Potent and Selective KDM5 Inhibitor Stops Cellular Demethylation of H3K4me3 at Transcription Start Sites and Proliferation of MM1S Myeloma Cells.* Cell Chem Biol, 2017. **24**(3): p. 371-380.
318. Li, Y., et al., *NEK2 promotes proliferation, migration and tumor growth of gastric cancer cells via regulating KDM5B/H3K4me3.* Am J Cancer Res, 2019. **9**(11): p. 2364-2378.
319. Zhang, Z.G., et al., *KDM5B promotes breast cancer cell proliferation and migration via AMPK-mediated lipid metabolism reprogramming.* Exp Cell Res, 2019. **379**(2): p. 182-190.
320. Liu, X., et al., *KDM5B Promotes Drug Resistance by Regulating Melanoma-Propagating Cell Subpopulations.* Mol Cancer Ther, 2019. **18**(3): p. 706-717.
321. Guo, G., et al., *Frequent mutations of genes encoding ubiquitin-mediated proteolysis pathway components in clear cell renal cell carcinoma.* Nat Genet, 2011. **44**(1): p. 17-9.
322. Stein, J., et al., *KDM5C is overexpressed in prostate cancer and is a prognostic marker for prostate-specific antigen-relapse following radical prostatectomy.* Am J Pathol, 2014. **184**(9): p. 2430-7.
323. Wang, Q., et al., *Histone demethylase JARID1C promotes breast cancer metastasis cells via down regulating BRMS1 expression.* Biochem Biophys Res Commun, 2015. **464**(2): p. 659-66.
324. Xu, L., et al., *Enhancement of Proliferation and Invasion of Gastric Cancer Cell by KDM5C Via Decrease in p53 Expression.* Technol Cancer Res Treat, 2017. **16**(2): p. 141-149.

325. Zhan, D., et al., *Whole exome sequencing identifies novel mutations of epigenetic regulators in chemorefractory pediatric acute myeloid leukemia.* Leuk Res, 2018. **65**: p. 20-24.
326. Li, N., et al., *JARID1D Is a Suppressor and Prognostic Marker of Prostate Cancer Invasion and Metastasis.* Cancer Res, 2016. **76**(4): p. 831-43.
327. Komura, K., et al., *ATR inhibition controls aggressive prostate tumors deficient in Y-linked histone demethylase KDM5D.* J Clin Invest, 2018. **128**(7): p. 2979-2995.
328. Komura, K., et al., *Resistance to docetaxel in prostate cancer is associated with androgen receptor activation and loss of KDM5D expression.* Proc Natl Acad Sci U S A, 2016. **113**(22): p. 6259-64.
329. Cai, L.S., et al., *ETV4 promotes the progression of gastric cancer through regulating KDM5D.* Eur Rev Med Pharmacol Sci, 2020. **24**(5): p. 2442-2451.
330. Shen, X., et al., *KDM5D inhibit epithelial-mesenchymal transition of gastric cancer through demethylation in the promoter of Cul4A in male.* J Cell Biochem, 2019. **120**(8): p. 12247-12258.
331. Inthal, A., et al., *CREBBP HAT domain mutations prevail in relapse cases of high hyperdiploid childhood acute lymphoblastic leukemia.* Leukemia, 2012. **26**(8): p. 1797-803.
332. Mullighan, C.G., et al., *CREBBP mutations in relapsed acute lymphoblastic leukaemia.* Nature, 2011. **471**(7337): p. 235-9.
333. Juskevicius, D., et al., *Mutations of CREBBP and SOCS1 are independent prognostic factors in diffuse large B cell lymphoma: mutational analysis of the SAKK 38/07 prospective clinical trial cohort.* J Hematol Oncol, 2017. **10**(1): p. 70.
334. Ohshima, T., T. Suganuma, and M. Ikeda, *A novel mutation lacking the bromodomain of the transcriptional coactivator p300 in the SiHa cervical carcinoma cell line.* Biochem Biophys Res Commun, 2001. **281**(2): p. 569-75.
335. Sobulo, O.M., et al., *MLL is fused to CBP, a histone acetyltransferase, in therapy-related acute myeloid leukemia with a t(11;16)(q23;p13.3).* Proc Natl Acad Sci U S A, 1997. **94**(16): p. 8732-7.
336. Satake, N., et al., *Novel MLL-CBP fusion transcript in therapy-related chronic myelomonocytic leukemia with a t(11;16)(q23;p13) chromosome translocation.* Genes Chromosomes Cancer, 1997. **20**(1): p. 60-3.
337. Taki, T., et al., *The t(11;16)(q23;p13) translocation in myelodysplastic syndrome fuses the MLL gene to the CBP gene.* Blood, 1997. **89**(11): p. 3945-50.
338. Ohnishi, H., et al., *A complex t(1;22;11)(q44;q13;q23) translocation causing MLL-p300 fusion gene in therapy-related acute myeloid leukemia.* Eur J Haematol, 2008. **81**(6): p. 475-80.
339. Ida, K., et al., *Adenoviral E1A-associated protein p300 is involved in acute myeloid leukemia with t(11;22)(q23;q13).* Blood, 1997. **90**(12): p. 4699-704.
340. Kitabayashi, I., et al., *Fusion of MOZ and p300 histone acetyltransferases in acute monocytic leukemia with a t(8;22)(p11;q13) chromosome translocation.* Leukemia, 2001. **15**(1): p. 89-94.
341. Crowley, J.A., et al., *Detection of MOZ-CBP fusion in acute myeloid leukemia with 8;16 translocation.* Leukemia, 2005. **19**(12): p. 2344-5.
342. Iyer, N.G., H. Ozdag, and C. Caldas, *p300/CBP and cancer.* Oncogene, 2004. **23**(24): p. 4225-31.
343. Meyer, S.N., et al., *Unique and Shared Epigenetic Programs of the CREBBP and EP300 Acetyltransferases in Germinal Center B Cells Reveal Targetable Dependencies in Lymphoma.* Immunity, 2019. **51**(3): p. 535-547.e9.
344. Jiang, Y., et al., *CREBBP Inactivation Promotes the Development of HDAC3-Dependent Lymphomas.* Cancer Discov, 2017. **7**(1): p. 38-53.
345. Horton, S.J., et al., *Early loss of Crebbp confers malignant stem cell properties on lymphoid progenitors.* Nat Cell Biol, 2017. **19**(9): p. 1093-1104.
346. Pasqualucci, L., et al., *Inactivating mutations of acetyltransferase genes in B-cell lymphoma.* Nature, 2011. **471**(7337): p. 189-95.
347. Kitabayashi, I., et al., *Activation of AML1-mediated transcription by MOZ and inhibition by the MOZ-CBP*

fusion protein. Embo j, 2001. **20**(24): p. 7184-96.

348. Chan, E.M., et al., *MOZ and MOZ-CBP cooperate with NF-kappaB to activate transcription from NF-kappaB-dependent promoters.* Exp Hematol, 2007. **35**(12): p. 1782-92.
349. Rokudai, S., et al., *MOZ increases p53 acetylation and premature senescence through its complex formation with PML.* Proc Natl Acad Sci U S A, 2013. **110**(10): p. 3895-900.
350. Bosic, M.M., et al., *Expression of p300 and p300/CBP associated factor (PCAF) in actinic keratosis and squamous cell carcinoma of the skin.* Exp Mol Pathol, 2016. **100**(3): p. 378-85.
351. Armas-Pineda, C., et al., *Expression of PCAF, p300 and Gcn5 and more highly acetylated histone H4 in pediatric tumors.* J Exp Clin Cancer Res, 2007. **26**(2): p. 269-76.
352. Frank, S.R., et al., *Binding of c-Myc to chromatin mediates mitogen-induced acetylation of histone H4 and gene activation.* Genes Dev, 2001. **15**(16): p. 2069-82.
353. Yin, Y.W., et al., *The Histone Acetyltransferase GCN5 Expression Is Elevated and Regulated by c-Myc and E2F1 Transcription Factors in Human Colon Cancer.* Gene Expr, 2015. **16**(4): p. 187-96.
354. Martínez-Balbás, M.A., et al., *Regulation of E2F1 activity by acetylation.* Embo j, 2000. **19**(4): p. 662-71.
355. Marzio, G., et al., *E2F family members are differentially regulated by reversible acetylation.* J Biol Chem, 2000. **275**(15): p. 10887-92.
356. Qiao, L., et al., *The lysine acetyltransferase GCN5 contributes to human papillomavirus oncoprotein E7-induced cell proliferation via up-regulating E2F1.* J Cell Mol Med, 2018. **22**(11): p. 5333-5345.
357. Shin, S. and I.M. Verma, *BRCA2 cooperates with histone acetyltransferases in androgen receptor-mediated transcription.* Proc Natl Acad Sci U S A, 2003. **100**(12): p. 7201-6.
358. Zheng, X., et al., *Histone acetyltransferase PCAF up-regulated cell apoptosis in hepatocellular carcinoma via acetylating histone H4 and inactivating AKT signaling.* Mol Cancer, 2013. **12**(1): p. 96.
359. Avvakumov, N. and J. Cote, *The MYST family of histone acetyltransferases and their intimate links to cancer.* Oncogene, 2007. **26**(37): p. 5395-407.
360. Collins, H.M., et al., *MOZ-TIF2 alters cofactor recruitment and histone modification at the RARbeta2 promoter: differential effects of MOZ fusion proteins on CBP- and MOZ-dependent activators.* J Biol Chem, 2006. **281**(25): p. 17124-33.
361. Yang, R., et al., *LASP2 suppressed malignancy and Wnt/β-catenin signaling pathway activation in bladder cancer.* Experimental and therapeutic medicine, 2018. **16**(6): p. 5215-5223.
362. Hu, X., et al., *Genetic alterations and oncogenic pathways associated with breast cancer subtypes.* Mol Cancer Res, 2009. **7**(4): p. 511-22.
363. Wang, Y., et al., *High-Expression HBO1 Predicts Poor Prognosis in Gastric Cancer.* Am J Clin Pathol, 2019. **152**(4): p. 517-526.
364. Song, B., et al., *Plk1 phosphorylation of orc2 and hbo1 contributes to gemcitabine resistance in pancreatic cancer.* Mol Cancer Ther, 2013. **12**(1): p. 58-68.
365. Kahali, B., et al., *Identifying targets for the restoration and reactivation of BRM.* Oncogene, 2014. **33**(5): p. 653-64.
366. Hayashi, Y., et al., *NUP98-HBO1-fusion generates phenotypically and genetically relevant chronic myelomonocytic leukemia pathogenesis.* Blood Adv, 2019. **3**(7): p. 1047-1060.
367. Sykes, S.M., et al., *Acetylation of the p53 DNA-binding domain regulates apoptosis induction.* Mol Cell, 2006. **24**(6): p. 841-51.
368. Tang, Y., et al., *Tip60-dependent acetylation of p53 modulates the decision between cell-cycle arrest and apoptosis.* Mol Cell, 2006. **24**(6): p. 827-39.
369. Awasthi, S., et al., *A human T-cell lymphotropic virus type 1 enhancer of Myc transforming potential stabilizes Myc-TIP60 transcriptional interactions.* Mol Cell Biol, 2005. **25**(14): p. 6178-98.
370. Hobbs, C.A., et al., *Tip60 protein isoforms and altered function in skin and tumors that overexpress ornithine*

decarboxylase. Cancer Res, 2006. **66**(16): p. 8116-22.

371. Li, Y. and E. Seto, *HDACs and HDAC Inhibitors in Cancer Development and Therapy.* Cold Spring Harb Perspect Med, 2016. **6**(10).
372. Rettig, I., et al., *Selective inhibition of HDAC8 decreases neuroblastoma growth in vitro and in vivo and enhances retinoic acid-mediated differentiation.* Cell Death Dis, 2015. **6**(2): p. e1657.
373. Mithraprabhu, S., et al., *Dysregulated Class I histone deacetylases are indicators of poor prognosis in multiple myeloma.* Epigenetics, 2014. **9**(11): p. 1511-20.
374. Ropero, S., et al., *A truncating mutation of HDAC2 in human cancers confers resistance to histone deacetylase inhibition.* Nat Genet, 2006. **38**(5): p. 566-9.
375. Jin, Z., et al., *Decreased expression of histone deacetylase 10 predicts poor prognosis of gastric cancer patients.* Int J Clin Exp Pathol, 2014. **7**(9): p. 5872-9.
376. Nakagawa, M., et al., *Expression profile of class I histone deacetylases in human cancer tissues.* Oncol Rep, 2007. **18**(4): p. 769-74.
377. Weichert, W., *HDAC expression and clinical prognosis in human malignancies.* Cancer Lett, 2009. **280**(2): p. 168-76.
378. Cang, S., et al., *Deficient histone acetylation and excessive deacetylase activity as epigenomic marks of prostate cancer cells.* Int J Oncol, 2009. **35**(6): p. 1417-22.
379. Shin, H.J., et al., *Inhibition of histone deacetylase activity increases chromosomal instability by the aberrant regulation of mitotic checkpoint activation.* Oncogene, 2003. **22**(25): p. 3853-8.
380. Hug, B.A. and M.A. Lazar, *ETO interacting proteins.* Oncogene, 2004. **23**(24): p. 4270-4.
381. Falkenberg, K.J. and R.W. Johnstone, *Histone deacetylases and their inhibitors in cancer, neurological diseases and immune disorders.* Nat Rev Drug Discov, 2014. **13**(9): p. 673-91.
382. Hagelkruys, A., et al., *The biology of HDAC in cancer: the nuclear and epigenetic components.* Handb Exp Pharmacol, 2011. **206**: p. 13-37.
383. Yamaguchi, T., et al., *Histone deacetylases 1 and 2 act in concert to promote the G1-to-S progression.* Genes Dev, 2010. **24**(5): p. 455-69.
384. Zupkovitz, G., et al., *The cyclin-dependent kinase inhibitor p21 is a crucial target for histone deacetylase 1 as a regulator of cellular proliferation.* Mol Cell Biol, 2010. **30**(5): p. 1171-81.
385. Fan, J., et al., *Down-regulation of HDAC5 inhibits growth of human hepatocellular carcinoma by induction of apoptosis and cell cycle arrest.* Tumour Biol, 2014. **35**(11): p. 11523-32.
386. Spurling, C.C., et al., *HDAC3 overexpression and colon cancer cell proliferation and differentiation.* Mol Carcinog, 2008. **47**(2): p. 137-47.
387. Mottet, D., et al., *HDAC4 represses p21(WAF1/Cip1) expression in human cancer cells through a Sp1-dependent, p53-independent mechanism.* Oncogene, 2009. **28**(2): p. 243-56.
388. Micheli, L., et al., *HDAC1, HDAC4, and HDAC9 Bind to PC3/Tis21/Btg2 and Are Required for Its Inhibition of Cell Cycle Progression and Cyclin D1 Expression.* J Cell Physiol, 2017. **232**(7): p. 1696-1707.
389. Wilson, A.J., et al., *Histone deacetylase 3 (HDAC3) and other class I HDACs regulate colon cell maturation and p21 expression and are deregulated in human colon cancer.* J Biol Chem, 2006. **281**(19): p. 13548-58.
390. Li, Y., L. Peng, and E. Seto, *Histone Deacetylase 10 Regulates the Cell Cycle G2/M Phase Transition via a Novel Let-7-HMGA2-Cyclin A2 Pathway.* Mol Cell Biol, 2015. **35**(20): p. 3547-65.
391. Kim, M.J., et al., *Novel SIRT Inhibitor, MHY2256, Induces Cell Cycle Arrest, Apoptosis, and Autophagic Cell Death in HCT116 Human Colorectal Cancer Cells.* Biomol Ther (Seoul), 2020. **28**(6): p. 561-568.
392. Serrano, L., et al., *The tumor suppressor SirT2 regulates cell cycle progression and genome stability by modulating the mitotic deposition of H4K20 methylation.* Genes Dev, 2013. **27**(6): p. 639-53.
393. Inoue, T., et al., *SIRT2, a tubulin deacetylase, acts to block the entry to chromosome condensation in response to mitotic stress.* Oncogene, 2007. **26**(7): p. 945-57.

394. Inoue, T., et al., *The molecular biology of mammalian SIRT proteins: SIRT2 in cell cycle regulation.* Cell Cycle, 2007. **6**(9): p. 1011-8.
395. Li, H., et al., *SIRT3 regulates cell proliferation and apoptosis related to energy metabolism in non-small cell lung cancer cells through deacetylation of NMNAT2.* Int J Oncol, 2013. **43**(5): p. 1420-30.
396. Li, S., et al., *p53-induced growth arrest is regulated by the mitochondrial SirT3 deacetylase.* PLoS One, 2010. **5**(5): p. e10486.
397. Huang, Z., et al., *Identification of a cellularly active SIRT6 allosteric activator.* Nat Chem Biol, 2018. **14**(12): p. 1118-1126.
398. Häcker, S., et al., *Histone deacetylase inhibitors cooperate with IFN-gamma to restore caspase-8 expression and overcome TRAIL resistance in cancers with silencing of caspase-8.* Oncogene, 2009. **28**(35): p. 3097-110.
399. Singh, T.R., S. Shankar, and R.K. Srivastava, *HDAC inhibitors enhance the apoptosis-inducing potential of TRAIL in breast carcinoma.* Oncogene, 2005. **24**(29): p. 4609-23.
400. Schuchmann, M., et al., *Histone deacetylase inhibition by valproic acid down-regulates c-FLIP/CASH and sensitizes hepatoma cells towards CD95- and TRAIL receptor-mediated apoptosis and chemotherapy.* Oncol Rep, 2006. **15**(1): p. 227-30.
401. Pathil, A., et al., *HDAC inhibitor treatment of hepatoma cells induces both TRAIL-independent apoptosis and restoration of sensitivity to TRAIL.* Hepatology, 2006. **43**(3): p. 425-34.
402. Inoue, S., et al., *Inhibition of histone deacetylase class I but not class II is critical for the sensitization of leukemic cells to tumor necrosis factor-related apoptosis-inducing ligand-induced apoptosis.* Cancer Res, 2006. **66**(13): p. 6785-92.
403. Schüler, S., et al., *HDAC2 attenuates TRAIL-induced apoptosis of pancreatic cancer cells.* Mol Cancer, 2010. **9**: p. 80.
404. Zhang, C., et al., *SIRT6 regulates the proliferation and apoptosis of hepatocellular carcinoma via the ERK1/2 signaling pathway.* Mol Med Rep, 2019. **20**(2): p. 1575-1582.
405. Zhu, Y., et al., *Knockout of SIRT4 decreases chemosensitivity to 5-FU in colorectal cancer cells.* Oncol Lett, 2018. **16**(2): p. 1675-1681.
406. Amann, J.M., et al., *ETO, a target of t(8;21) in acute leukemia, makes distinct contacts with multiple histone deacetylases and binds mSin3A through its oligomerization domain.* Mol Cell Biol, 2001. **21**(19): p. 6470-83.
407. Atsumi, A., et al., *Histone deacetylase 3 (HDAC3) is recruited to target promoters by PML-RARalpha as a component of the N-CoR co-repressor complex to repress transcription in vivo.* Biochem Biophys Res Commun, 2006. **345**(4): p. 1471-80.
408. Phelps, M.P., et al., *CRISPR screen identifies the NCOR/HDAC3 complex as a major suppressor of differentiation in rhabdomyosarcoma.* Proc Natl Acad Sci U S A, 2016. **113**(52): p. 15090-15095.
409. Sharif, T., et al., *HDAC6 differentially regulates autophagy in stem-like versus differentiated cancer cells.* Autophagy, 2019. **15**(4): p. 686-706.
410. Miller, K.M., et al., *Human HDAC1 and HDAC2 function in the DNA-damage response to promote DNA nonhomologous end-joining.* Nat Struct Mol Biol, 2010. **17**(9): p. 1144-51.
411. Roos, W.P. and A. Krumm, *The multifaceted influence of histone deacetylases on DNA damage signalling and DNA repair.* Nucleic Acids Res, 2016. **44**(21): p. 10017-10030.
412. Chen, C.C., et al., *Dihydrocoumarin, an HDAC Inhibitor, Increases DNA Damage Sensitivity by Inhibiting Rad52.* Int J Mol Sci, 2017. **18**(12).
413. Zhang, M., et al., *HDAC6 deacetylates and ubiquitinates MSH2 to maintain proper levels of MutSα.* Mol Cell, 2014. **55**(1): p. 31-46.
414. Radhakrishnan, R., et al., *Histone deacetylase 10 regulates DNA mismatch repair and may involve the deacetylation of MutS homolog 2.* J Biol Chem, 2015. **290**(37): p. 22795-804.
415. Mostoslavsky, R., et al., *Genomic instability and aging-like phenotype in the absence of mammalian SIRT6.*

Cell, 2006. **124**(2): p. 315-29.

416. Van Meter, M., et al., *JNK Phosphorylates SIRT6 to Stimulate DNA Double-Strand Break Repair in Response to Oxidative Stress by Recruiting PARP1 to DNA Breaks.* Cell Rep, 2016. **16**(10): p. 2641-2650.
417. Mao, Z., et al., *SIRT6 promotes DNA repair under stress by activating PARP1.* Science, 2011. **332**(6036): p. 1443-6.
418. Hayashi, A., et al., *Type-specific roles of histone deacetylase (HDAC) overexpression in ovarian carcinoma: HDAC1 enhances cell proliferation and HDAC3 stimulates cell migration with downregulation of E-cadherin.* Int J Cancer, 2010. **127**(6): p. 1332-46.
419. Peinado, H., D. Olmeda, and A. Cano, *Snail, Zeb and bHLH factors in tumour progression: an alliance against the epithelial phenotype?* Nat Rev Cancer, 2007. **7**(6): p. 415-28.
420. von Burstin, J., et al., *E-cadherin regulates metastasis of pancreatic cancer in vivo and is suppressed by a SNAIL/HDAC1/HDAC2 repressor complex.* Gastroenterology, 2009. **137**(1): p. 361-71, 371.e1-5.
421. Sun, L., et al., *MPP8 and SIRT1 crosstalk in E-cadherin gene silencing and epithelial-mesenchymal transition.* EMBO Rep, 2015. **16**(6): p. 689-99.
422. Byles, V., et al., *SIRT1 induces EMT by cooperating with EMT transcription factors and enhances prostate cancer cell migration and metastasis.* Oncogene, 2012. **31**(43): p. 4619-29.
423. Simic, P., et al., *SIRT1 suppresses the epithelial-to-mesenchymal transition in cancer metastasis and organ fibrosis.* Cell Rep, 2013. **3**(4): p. 1175-86.
424. Chen, Y., et al., *Identification of druggable cancer driver genes amplified across TCGA datasets.* PLoS One, 2014. **9**(5): p. e98293.
425. Li, Y., et al., *SIRT2 Promotes the Migration and Invasion of Gastric Cancer through RAS/ERK/JNK/MMP-9 Pathway by Increasing PEPCK1-Related Metabolism.* Neoplasia, 2018. **20**(7): p. 745-756.
426. Geng, C.H., et al., *Overexpression of Sirt6 is a novel biomarker of malignant human colon carcinoma.* J Cell Biochem, 2018. **119**(5): p. 3957-3967.
427. Qian, D.Z., et al., *Class II histone deacetylases are associated with VHL-independent regulation of hypoxia-inducible factor 1 alpha.* Cancer Res, 2006. **66**(17): p. 8814-21.
428. Kim, S.H., et al., *Regulation of the HIF-1alpha stability by histone deacetylases.* Oncol Rep, 2007. **17**(3): p. 647-51.
429. Chen, S., et al., *AMPK-HDAC5 pathway facilitates nuclear accumulation of HIF-1α and functional activation of HIF-1 by deacetylating Hsp70 in the cytosol.* Cell Cycle, 2015. **14**(15): p. 2520-36.
430. Geng, H., et al., *HDAC4 protein regulates HIF1α protein lysine acetylation and cancer cell response to hypoxia.* J Biol Chem, 2011. **286**(44): p. 38095-102.
431. Yao, Z.G., et al., *LBH589 Inhibits Glioblastoma Growth and Angiogenesis Through Suppression of HIF-1α Expression.* J Neuropathol Exp Neurol, 2017. **76**(12): p. 1000-1007.
432. Ray, A., M. Alalem, and B.K. Ray, *Loss of epigenetic Kruppel-like factor 4 histone deacetylase (KLF-4-HDAC)-mediated transcriptional suppression is crucial in increasing vascular endothelial growth factor (VEGF) expression in breast cancer.* J Biol Chem, 2013. **288**(38): p. 27232-42.
433. Seo, H.W., et al., *Transcriptional activation of hypoxia-inducible factor-1alpha by HDAC4 and HDAC5 involves differential recruitment of p300 and FIH-1.* FEBS Lett, 2009. **583**(1): p. 55-60.
434. Urbich, C., et al., *HDAC5 is a repressor of angiogenesis and determines the angiogenic gene expression pattern of endothelial cells.* Blood, 2009. **113**(22): p. 5669-79.
435. Chang, S., et al., *Histone deacetylase 7 maintains vascular integrity by repressing matrix metalloproteinase 10.* Cell, 2006. **126**(2): p. 321-34.
436. Ribatti, D. and R. Tamma, *Epigenetic control of tumor angiogenesis.* Microcirculation, 2020. **27**(3): p. e12602.
437. Kaluza, D., et al., *Class IIb HDAC6 regulates endothelial cell migration and angiogenesis by deacetylation of cortactin.* Embo j, 2011. **30**(20): p. 4142-56.

438. Dong, J., et al., *A novel HDAC6 inhibitor exerts an anti-cancer effect by triggering cell cycle arrest and apoptosis in gastric cancer.* Eur J Pharmacol, 2018. **828**: p. 67-79.
439. Lv, Z., et al., *Downregulation of HDAC6 promotes angiogenesis in hepatocellular carcinoma cells and predicts poor prognosis in liver transplantation patients.* Mol Carcinog, 2016. **55**(5): p. 1024-33.
440. Lim, J.H., et al., *Sirtuin 1 modulates cellular responses to hypoxia by deacetylating hypoxia-inducible factor 1alpha.* Mol Cell, 2010. **38**(6): p. 864-78.
441. Qu, W., et al., *Emodin inhibits HMGB1-induced tumor angiogenesis in human osteosarcoma by regulating SIRT1.* Int J Clin Exp Med, 2015. **8**(9): p. 15054-64.
442. Kunhiraman, H., et al., *2-Deoxy Glucose Modulates Expression and Biological Activity of VEGF in a SIRT-1 Dependent Mechanism.* J Cell Biochem, 2017. **118**(2): p. 252-262.
443. Lappas, M., *Anti-inflammatory properties of sirtuin 6 in human umbilical vein endothelial cells.* Mediators Inflamm, 2012. **2012**: p. 597514.
444. Xie, H.J., et al., *HDAC1 inactivation induces mitotic defect and caspase-independent autophagic cell death in liver cancer.* PLoS One, 2012. **7**(4): p. e34265.
445. Lee, J.Y., et al., *Inhibition of HDAC3- and HDAC6-Promoted Survivin Expression Plays an Important Role in SAHA-Induced Autophagy and Viability Reduction in Breast Cancer Cells.* Front Pharmacol, 2016. **7**: p. 81.
446. Lee, J.Y., et al., *HDAC6 controls autophagosome maturation essential for ubiquitin-selective quality-control autophagy.* Embo j, 2010. **29**(5): p. 969-80.
447. Lee, J.Y., et al., *Disease-causing mutations in parkin impair mitochondrial ubiquitination, aggregation, and HDAC6-dependent mitophagy.* J Cell Biol, 2010. **189**(4): p. 671-9.
448. Oehme, I., et al., *Histone deacetylase 10 promotes autophagy-mediated cell survival.* Proc Natl Acad Sci U S A, 2013. **110**(28): p. E2592-601.
449. Lee, I.H., et al., *A role for the NAD-dependent deacetylase Sirt1 in the regulation of autophagy.* Proc Natl Acad Sci U S A, 2008. **105**(9): p. 3374-9.
450. Huang, R., et al., *Deacetylation of nuclear LC3 drives autophagy initiation under starvation.* Mol Cell, 2015. **57**(3): p. 456-66.
451. Lei, W., et al., *Enhancing therapeutic efficacy of oncolytic vaccinia virus armed with Beclin-1, an autophagic Gene in leukemia and myeloma.* Biomed Pharmacother, 2020. **125**: p. 110030.
452. Guha, P., et al., *IPMK Mediates Activation of ULK Signaling and Transcriptional Regulation of Autophagy Linked to Liver Inflammation and Regeneration.* Cell Rep, 2019. **26**(10): p. 2692-2703.e7.
453. Tae, I.H., et al., *Novel SIRT1 inhibitor 15-deoxy-Δ12,14-prostaglandin J2 and its derivatives exhibit anticancer activity through apoptotic or autophagic cell death pathways in SKOV3 cells.* Int J Oncol, 2018. **53**(6): p. 2518-2530.
454. Garva, R., et al., *Sirtuin Family Members Selectively Regulate Autophagy in Osteosarcoma and Mesothelioma Cells in Response to Cellular Stress.* Front Oncol, 2019. **9**: p. 949.
455. Torrens-Mas, M., et al., *SIRT3 Silencing Sensitizes Breast Cancer Cells to Cytotoxic Treatments Through an Increment in ROS Production.* J Cell Biochem, 2017. **118**(2): p. 397-406.
456. Li, M., et al., *Non-oncogene Addiction to SIRT3 Plays a Critical Role in Lymphomagenesis.* Cancer Cell, 2019. **35**(6): p. 916-931.e9.
457. Shi, L., et al., *SIRT5-mediated deacetylation of LDHB promotes autophagy and tumorigenesis in colorectal cancer.* Mol Oncol, 2019. **13**(2): p. 358-375.
458. Wang, L., et al., *Aberrant SIRT6 expression contributes to melanoma growth: Role of the autophagy paradox and IGF-AKT signaling.* Autophagy, 2018. **14**(3): p. 518-533.
459. Garcia-Peterson, L.M., et al., *SIRT6 histone deacetylase functions as a potential oncogene in human melanoma.* Genes Cancer, 2017. **8**(9-10): p. 701-712.
460. Huang, N., et al., *Sirtuin 6 plays an oncogenic role and induces cell autophagy in esophageal cancer cells.*

Tumour Biol, 2017. **39**(6): p. 1010428317708532.

461. Han, L.L., et al., *Sirtuin6 (SIRT6) Promotes the EMT of Hepatocellular Carcinoma by Stimulating Autophagic Degradation of E-Cadherin.* Mol Cancer Res, 2019. **17**(11): p. 2267-2280.
462. Iachettini, S., et al., *Pharmacological activation of SIRT6 triggers lethal autophagy in human cancer cells.* Cell Death Dis, 2018. **9**(10): p. 996.
463. Donati, B., E. Lorenzini, and A. Ciarrocchi, *BRD4 and Cancer: going beyond transcriptional regulation.* Mol Cancer, 2018. **17**(1): p. 164.
464. Erb, M.A., et al., *Transcription control by the ENL YEATS domain in acute leukaemia.* Nature, 2017. **543**(7644): p. 270-274.
465. Perlman, E.J., et al., *MLLT1 YEATS domain mutations in clinically distinctive Favourable Histology Wilms tumours.* Nat Commun, 2015. **6**: p. 10013.
466. Wan, L., et al., *Impaired cell fate through gain-of-function mutations in a chromatin reader.* Nature, 2020. **577**(7788): p. 121-126.
467. Devaiah, B.N., et al., *BRD4 is an atypical kinase that phosphorylates serine2 of the RNA polymerase II carboxy-terminal domain.* Proc Natl Acad Sci U S A, 2012. **109**(18): p. 6927-32.
468. Allen, B.L. and D.J. Taatjes, *The Mediator complex: a central integrator of transcription.* Nat Rev Mol Cell Biol, 2015. **16**(3): p. 155-66.
469. Devaiah, B.N., et al., *BRD4 is a histone acetyltransferase that evicts nucleosomes from chromatin.* Nat Struct Mol Biol, 2016. **23**(6): p. 540-8.
470. French, C.A., *Pathogenesis of NUT midline carcinoma.* Annu Rev Pathol, 2012. **7**: p. 247-65.
471. Reynoird, N., et al., *Oncogenesis by sequestration of CBP/p300 in transcriptionally inactive hyperacetylated chromatin domains.* EMBO J, 2010. **29**(17): p. 2943-52.
472. Delmore, J.E., et al., *BET bromodomain inhibition as a therapeutic strategy to target c-Myc.* Cell, 2011. **146**(6): p. 904-17.
473. Mertz, J.A., et al., *Targeting MYC dependence in cancer by inhibiting BET bromodomains.* Proc Natl Acad Sci U S A, 2011. **108**(40): p. 16669-74.
474. Ba, M., et al., *BRD4 promotes gastric cancer progression through the transcriptional and epigenetic regulation of c-MYC.* J Cell Biochem, 2018. **119**(1): p. 973-982.
475. Otto, C., et al., *Targeting bromodomain-containing protein 4 (BRD4) inhibits MYC expression in colorectal cancer cells.* Neoplasia, 2019. **21**(11): p. 1110-1120.
476. Wu, X., et al., *BRD4 Regulates EZH2 Transcription through Upregulation of C-MYC and Represents a Novel Therapeutic Target in Bladder Cancer.* Mol Cancer Ther, 2016. **15**(5): p. 1029-42.
477. Devaiah, B.N., et al., *MYC protein stability is negatively regulated by BRD4.* Proc Natl Acad Sci U S A, 2020. **117**(24): p. 13457-13467.
478. Zhang, Z., et al., *BET Bromodomain Inhibition as a Therapeutic Strategy in Ovarian Cancer by Downregulating FoxM1.* Theranostics, 2016. **6**(2): p. 219-30.
479. Nerlakanti, N., et al., *Targeting the BRD4-HOXB13 Coregulated Transcriptional Networks with Bromodomain-Kinase Inhibitors to Suppress Metastatic Castration-Resistant Prostate Cancer.* Mol Cancer Ther, 2018. **17**(12): p. 2796-2810.
480. Del Gaudio, N., et al., *BRD9 binds cell type-specific chromatin regions regulating leukemic cell survival via STAT5 inhibition.* Cell Death Dis, 2019. **10**(5): p. 338.
481. Sabari, B.R., et al., *Coactivator condensation at super-enhancers links phase separation and gene control.* Science, 2018. **361**(6400).
482. Milkovic, N.M. and T. Mittag, *Determination of Protein Phase Diagrams by Centrifugation.* Methods Mol Biol, 2020. **2141**: p. 685-702.
483. Lovén, J., et al., *Selective inhibition of tumor oncogenes by disruption of super-enhancers.* Cell, 2013. **153**(2):

p. 320-34.

484. Uppal, S., et al., *The Bromodomain Protein 4 Contributes to the Regulation of Alternative Splicing.* Cell Rep, 2019. **29**(8): p. 2450-2460.e5.
485. Hussong, M., et al., *The bromodomain protein BRD4 regulates splicing during heat shock.* Nucleic Acids Res, 2017. **45**(1): p. 382-394.
486. Yang, L., et al., *Repression of BET activity sensitizes homologous recombination-proficient cancers to PARP inhibition.* Sci Transl Med, 2017. **9**(400).
487. Li, X., et al., *BRD4 Promotes DNA Repair and Mediates the Formation of TMPRSS2-ERG Gene Rearrangements in Prostate Cancer.* Cell Rep, 2018. **22**(3): p. 796-808.
488. Stanlie, A., et al., *Chromatin reader Brd4 functions in Ig class switching as a repair complex adaptor of nonhomologous end-joining.* Mol Cell, 2014. **55**(1): p. 97-110.
489. Zhang, J., et al., *BRD4 facilitates replication stress-induced DNA damage response.* Oncogene, 2018. **37**(28): p. 3763-3777.
490. Floyd, S.R., et al., *The bromodomain protein Brd4 insulates chromatin from DNA damage signalling.* Nature, 2013. **498**(7453): p. 246-50.
491. Lam, F.C., et al., *BRD4 prevents the accumulation of R-loops and protects against transcription-replication collision events and DNA damage.* Nat Commun, 2020. **11**(1): p. 4083.
492. Sun, C., et al., *BRD4 Inhibition Is Synthetic Lethal with PARP Inhibitors through the Induction of Homologous Recombination Deficiency.* Cancer Cell, 2018. **33**(3): p. 401-416.e8.
493. Wang, S., et al., *BRD4 inhibitors block telomere elongation.* Nucleic Acids Res, 2017. **45**(14): p. 8403-8410.
494. Horn, S., et al., *TERT promoter mutations in familial and sporadic melanoma.* Science, 2013. **339**(6122): p. 959-61.
495. Vinagre, J., et al., *Frequency of TERT promoter mutations in human cancers.* Nat Commun, 2013. **4**: p. 2185.
496. Akıncılar, S.C., et al., *Long-Range Chromatin Interactions Drive Mutant TERT Promoter Activation.* Cancer Discov, 2016. **6**(11): p. 1276-1291.
497. Park, S.W. and J.M. Lee, *Emerging Roles of BRD7 in Pathophysiology.* Int J Mol Sci, 2020. **21**(19).
498. Drost, J., et al., *BRD7 is a candidate tumour suppressor gene required for p53 function.* Nat Cell Biol, 2010. **12**(4): p. 380-9.
499. Harte, M.T., et al., *BRD7, a subunit of SWI/SNF complexes, binds directly to BRCA1 and regulates BRCA1-dependent transcription.* Cancer Res, 2010. **70**(6): p. 2538-47.
500. Niu, W., et al., *BRD7 suppresses invasion and metastasis in breast cancer by negatively regulating YB1-induced epithelial-mesenchymal transition.* J Exp Clin Cancer Res, 2020. **39**(1): p. 30.
501. Hohmann, A.F., et al., *Sensitivity and engineered resistance of myeloid leukemia cells to BRD9 inhibition.* Nat Chem Biol, 2016. **12**(9): p. 672-9.
502. Huang, H., et al., *miR-140-3p functions as a tumor suppressor in squamous cell lung cancer by regulating BRD9.* Cancer Lett, 2019. **446**: p. 81-89.
503. Ji, S., Y. Zhang, and B. Yang, *YEATS Domain Containing 4 Promotes Gastric Cancer Cell Proliferation and Mediates Tumor Progression via Activating the Wnt/β-Catenin Signaling Pathway.* Oncol Res, 2017. **25**(9): p. 1633-1641.
504. Lübbert, M., et al., *Decitabine improves progression-free survival in older high-risk MDS patients with multiple autosomal monosomies: results of a subgroup analysis of the randomized phase III study 06011 of the EORTC Leukemia Cooperative Group and German MDS Study Group.* Ann Hematol, 2016. **95**(2): p. 191-9.
505. Fenaux, P., et al., *Efficacy of azacitidine compared with that of conventional care regimens in the treatment of higher-risk myelodysplastic syndromes: a randomised, open-label, phase III study.* Lancet Oncol, 2009. **10**(3): p. 223-32.

506. Schoeler, K., et al., *TET enzymes control antibody production and shape the mutational landscape in germinal centre B cells.* Febs j, 2019. **286**(18): p. 3566-3581.
507. Jones, P.A., J.P. Issa, and S. Baylin, *Targeting the cancer epigenome for therapy.* Nat Rev Genet, 2016. **17**(10): p. 630-41.
508. Gao, S., et al., *Preclinical and Clinical Studies of Chidamide (CS055/HBI-8000), An Orally Available Subtype-selective HDAC Inhibitor for Cancer Therapy.* Anticancer Agents Med Chem, 2017. **17**(6): p. 802-812.
509. McClure, J.J., X. Li, and C.J. Chou, *Advances and Challenges of HDAC Inhibitors in Cancer Therapeutics.* Adv Cancer Res, 2018. **138**: p. 183-211.
510. Stephens, A.D., et al., *Chromatin histone modifications and rigidity affect nuclear morphology independent of lamins.* Mol Biol Cell, 2018. **29**(2): p. 220-233.
511. Qu, K., et al., *Chromatin Accessibility Landscape of Cutaneous T Cell Lymphoma and Dynamic Response to HDAC Inhibitors.* Cancer Cell, 2017. **32**(1): p. 27-41.e4.
512. Krug, B., et al., *Pervasive H3K27 Acetylation Leads to ERV Expression and a Therapeutic Vulnerability in H3K27M Gliomas.* Cancer Cell, 2019. **35**(5): p. 782-797.e8.
513. Raynal, N.J., et al., *Repositioning FDA-Approved Drugs in Combination with Epigenetic Drugs to Reprogram Colon Cancer Epigenome.* Mol Cancer Ther, 2017. **16**(2): p. 397-407.
514. Daskalakis, M., et al., *Demethylation of a hypermethylated P15/INK4B gene in patients with myelodysplastic syndrome by 5-Aza-2'-deoxycytidine (decitabine) treatment.* Blood, 2002. **100**(8): p. 2957-64.
515. Aparicio, A., et al., *LINE-1 methylation in plasma DNA as a biomarker of activity of DNA methylation inhibitors in patients with solid tumors.* Epigenetics, 2009. **4**(3): p. 176-84.
516. Prebet, T., et al., *Azacitidine with or without Entinostat for the treatment of therapy-related myeloid neoplasm: further results of the E1905 North American Leukemia Intergroup study.* Br J Haematol, 2016. **172**(3): p. 384-91.
517. Iveland, T.S., et al., *HDACi mediate UNG2 depletion, dysregulated genomic uracil and altered expression of oncoproteins and tumor suppressors in B- and T-cell lines.* J Transl Med, 2020. **18**(1): p. 159.
518. Nebbioso, A., et al., *c-Myc Modulation and Acetylation Is a Key HDAC Inhibitor Target in Cancer.* Clin Cancer Res, 2017. **23**(10): p. 2542-2555.
519. Anastas, J.N., et al., *Re-programing Chromatin with a Bifunctional LSD1/HDAC Inhibitor Induces Therapeutic Differentiation in DIPG.* Cancer Cell, 2019. **36**(5): p. 528-544.e10.
520. Bruyer, A., et al., *DNMTi/HDACi combined epigenetic targeted treatment induces reprogramming of myeloma cells in the direction of normal plasma cells.* Br J Cancer, 2018. **118**(8): p. 1062-1073.
521. Topper, M.J., et al., *Epigenetic Therapy Ties MYC Depletion to Reversing Immune Evasion and Treating Lung Cancer.* Cell, 2017. **171**(6): p. 1284-1300.e21.
522. Nguyen, T.T.T., et al., *HDAC inhibitors elicit metabolic reprogramming by targeting super-enhancers in glioblastoma models.* J Clin Invest, 2020. **130**(7): p. 3699-3716.
523. Suraweera, A., K.J. O'Byrne, and D.J. Richard, *Combination Therapy With Histone Deacetylase Inhibitors (HDACi) for the Treatment of Cancer: Achieving the Full Therapeutic Potential of HDACi.* Front Oncol, 2018. **8**: p. 92.
524. Zhao, L., et al., *Preclinical Studies Support Combined Inhibition of BET Family Proteins and Histone Deacetylases as Epigenetic Therapy for Cutaneous T-Cell Lymphoma.* Neoplasia, 2019. **21**(1): p. 82-92.
525. Fiskus, W., et al., *Superior efficacy of cotreatment with BET protein inhibitor and BCL2 or MCL1 inhibitor against AML blast progenitor cells.* Blood Cancer J, 2019. **9**(2): p. 4.
526. Genta, S., M.C. Pirosa, and A. Stathis, *BET and EZH2 Inhibitors: Novel Approaches for Targeting Cancer.* Curr Oncol Rep, 2019. **21**(2): p. 13.
527. Guo, L., et al., *A combination strategy targeting enhancer plasticity exerts synergistic lethality against BETi-resistant leukemia cells.* Nat Commun, 2020. **11**(1): p. 740.

528. Pawar, A., et al., *Resistance to BET Inhibitor Leads to Alternative Therapeutic Vulnerabilities in Castration-Resistant Prostate Cancer.* Cell Rep, 2018. **22**(9): p. 2236-2245.
529. Krivtsov, A.V., et al., *A Menin-MLL Inhibitor Induces Specific Chromatin Changes and Eradicates Disease in Models of MLL-Rearranged Leukemia.* Cancer Cell, 2019. **36**(6): p. 660-673.e11.
530. McLean, C.M., I.D. Karemaker, and F. van Leeuwen, *The emerging roles of DOT1L in leukemia and normal development.* Leukemia, 2014. **28**(11): p. 2131-8.
531. Stein, E.M., et al., *The DOT1L inhibitor pinometostat reduces H3K79 methylation and has modest clinical activity in adult acute leukemia.* Blood, 2018. **131**(24): p. 2661-2669.
532. Daigle, S.R., et al., *Selective killing of mixed lineage leukemia cells by a potent small-molecule DOT1L inhibitor.* Cancer Cell, 2011. **20**(1): p. 53-65.
533. Mohammad, H.P., et al., *A DNA Hypomethylation Signature Predicts Antitumor Activity of LSD1 Inhibitors in SCLC.* Cancer Cell, 2015. **28**(1): p. 57-69.
534. Cusan, M., et al., *LSD1 inhibition exerts its antileukemic effect by recommissioning PU.1- and C/EBPα-dependent enhancers in AML.* Blood, 2018. **131**(15): p. 1730-1742.
535. Turkalp, Z., J. Karamchandani, and S. Das, *IDH mutation in glioma: new insights and promises for the future.* JAMA Neurol, 2014. **71**(10): p. 1319-25.
536. Waitkus, M.S., B.H. Diplas, and H. Yan, *Biological Role and Therapeutic Potential of IDH Mutations in Cancer.* Cancer Cell, 2018. **34**(2): p. 186-195.
537. McCabe, M.T., et al., *EZH2 inhibition as a therapeutic strategy for lymphoma with EZH2-activating mutations.* Nature, 2012. **492**(7427): p. 108-12.
538. Khan, S.N., et al., *Multiple mechanisms deregulate EZH2 and histone H3 lysine 27 epigenetic changes in myeloid malignancies.* Leukemia, 2013. **27**(6): p. 1301-9.
539. Wong, M., et al., *The Histone Methyltransferase DOT1L Promotes Neuroblastoma by Regulating Gene Transcription.* Cancer Res, 2017. **77**(9): p. 2522-2533.
540. Vatapalli, R., et al., *Histone methyltransferase DOT1L coordinates AR and MYC stability in prostate cancer.* Nat Commun, 2020. **11**(1): p. 4153.
541. Ishiguro, K., et al., *DOT1L inhibition blocks multiple myeloma cell proliferation by suppressing IRF4-MYC signaling.* Haematologica, 2019. **104**(1): p. 155-165.
542. Yang, L., et al., *Silencing or inhibition of H3K79 methyltransferase DOT1L induces cell cycle arrest by epigenetically modulating c-Myc expression in colorectal cancer.* Clin Epigenetics, 2019. **11**(1): p. 199.
543. Morera, L., M. Lubbert, and M. Jung, *Targeting histone methyltransferases and demethylases in clinical trials for cancer therapy.* Clin Epigenetics, 2016. **8**: p. 57.
544. Mentch, S.J. and J.W. Locasale, *One-carbon metabolism and epigenetics: understanding the specificity.* Ann N Y Acad Sci, 2016. **1363**: p. 91-8.
545. Mentch, S.J., et al., *Histone Methylation Dynamics and Gene Regulation Occur through the Sensing of One-Carbon Metabolism.* Cell Metab, 2015. **22**(5): p. 861-73.
546. Yu, W., et al., *One-Carbon Metabolism Supports S-Adenosylmethionine and Histone Methylation to Drive Inflammatory Macrophages.* Molecular Cell, 2019. **75**(6): p. 1147-1160.e5.
547. Dann, S.G., et al., *Reciprocal regulation of amino acid import and epigenetic state through Lat1 and EZH2.* EMBO J, 2015. **34**(13): p. 1773-85.
548. Li, X., et al., *Regulation of chromatin and gene expression by metabolic enzymes and metabolites.* Nat Rev Mol Cell Biol, 2018. **19**(9): p. 563-578.
549. Zeisel, S., *Choline, Other Methyl-Donors and Epigenetics.* Nutrients, 2017. **9**(5).
550. Kim, H. and Y.J. Park, *Links between Serine Biosynthesis Pathway and Epigenetics in Cancer Metabolism.* Clinical Nutrition Research, 2018. **7**(3): p. 153.
551. Maddocks, O.D., et al., *Serine Metabolism Supports the Methionine Cycle and DNA/RNA Methylation*

through De Novo ATP Synthesis in Cancer Cells. Mol Cell, 2016. **61**(2): p. 210-21.

552. Wu, Q., et al., *YAP/TAZ-mediated activation of serine metabolism and methylation regulation is critical for LKB1-deficient breast cancer progression.* Bioscience Reports, 2017. **37**(5).
553. Kottakis, F., et al., *LKB1 loss links serine metabolism to DNA methylation and tumorigenesis.* Nature, 2016. **539**(7629): p. 390-395.
554. Li, S., et al., *Serine and SAM Responsive Complex SESAME Regulates Histone Modification Crosstalk by Sensing Cellular Metabolism.* Mol Cell, 2015. **60**(3): p. 408-21.
555. Sivanand, S., I. Viney, and K.E. Wellen, *Spatiotemporal Control of Acetyl-CoA Metabolism in Chromatin Regulation.* Trends Biochem Sci, 2018. **43**(1): p. 61-74.
556. Lee, J.V., et al., *Akt-dependent metabolic reprogramming regulates tumor cell histone acetylation.* Cell Metab, 2014. **20**(2): p. 306-319.
557. Liu, X., et al., *The structural basis of protein acetylation by the p300/CBP transcriptional coactivator.* Nature, 2008. **451**(7180): p. 846-50.
558. Langer, M.R., et al., *Modulating acetyl-CoA binding in the GCN5 family of histone acetyltransferases.* J Biol Chem, 2002. **277**(30): p. 27337-44.
559. Jozaki, K., et al., *Glucose regulates the histone acetylation of gene promoters in decidualizing stromal cells.* Reproduction, 2019. **157**(5): p. 457-464.
560. Campbell, S.L. and K.E. Wellen, *Metabolic Signaling to the Nucleus in Cancer.* Mol Cell, 2018. **71**(3): p. 398-408.
561. Cluntun, A.A., et al., *The rate of glycolysis quantitatively mediates specific histone acetylation sites.* Cancer Metab, 2015. **3**: p. 10.
562. McDonnell, E., et al., *Lipids Reprogram Metabolism to Become a Major Carbon Source for Histone Acetylation.* Cell Rep, 2016. **17**(6): p. 1463-1472.
563. Zhao, S., et al., *ATP-Citrate Lyase Controls a Glucose-to-Acetate Metabolic Switch.* Cell Rep, 2016. **17**(4): p. 1037-1052.
564. Sebastian, C. and R. Mostoslavsky, *The Various Metabolic Sources of Histone Acetylation.* Trends Endocrinol Metab, 2017. **28**(2): p. 85-87.
565. Madiraju, P., et al., *Mitochondrial acetylcarnitine provides acetyl groups for nuclear histone acetylation.* Epigenetics, 2009. **4**(6): p. 399-403.
566. Galdieri, L. and A. Vancura, *Acetyl-CoA carboxylase regulates global histone acetylation.* J Biol Chem, 2012. **287**(28): p. 23865-76.
567. Rios Garcia, M., et al., *Acetyl-CoA Carboxylase 1-Dependent Protein Acetylation Controls Breast Cancer Metastasis and Recurrence.* Cell Metab, 2017. **26**(6): p. 842-855 e5.
568. Yucel, N., et al., *Glucose Metabolism Drives Histone Acetylation Landscape Transitions that Dictate Muscle Stem Cell Function.* Cell Rep, 2019. **27**(13): p. 3939-3955 e6.
569. Kopinski, P.K., et al., *Regulation of nuclear epigenome by mitochondrial DNA heteroplasmy.* Proc Natl Acad Sci U S A, 2019. **116**(32): p. 16028-16035.
570. Wellen, K.E., et al., *ATP-citrate lyase links cellular metabolism to histone acetylation.* Science, 2009. **324**(5930): p. 1076-80.
571. Gao, X., et al., *Acetate functions as an epigenetic metabolite to promote lipid synthesis under hypoxia.* Nat Commun, 2016. **7**: p. 11960.
572. Lauterbach, M.A., et al., *Toll-like Receptor Signaling Rewires Macrophage Metabolism and Promotes Histone Acetylation via ATP-Citrate Lyase.* Immunity, 2019. **51**(6): p. 997-1011.e7.
573. Li, X., X. Qian, and Z. Lu, *Local histone acetylation by ACSS2 promotes gene transcription for lysosomal biogenesis and autophagy.* Autophagy, 2017. **13**(10): p. 1790-1791.
574. Theillet, F.X., et al., *Physicochemical properties of cells and their effects on intrinsically disordered proteins*

(IDPs). Chem Rev, 2014. **114**(13): p. 6661-714.

575. Diehl, K.L. and T.W. Muir, *Chromatin as a key consumer in the metabolite economy.* Nat Chem Biol, 2020. **16**(6): p. 620-629.
576. Bulusu, V., et al., *Acetate Recapturing by Nuclear Acetyl-CoA Synthetase 2 Prevents Loss of Histone Acetylation during Oxygen and Serum Limitation.* Cell Rep, 2017. **18**(3): p. 647-658.
577. Mews, P., et al., *Acetyl-CoA synthetase regulates histone acetylation and hippocampal memory.* Nature, 2017. **546**(7658): p. 381-386.
578. Sivanand, S., et al., *Nuclear Acetyl-CoA Production by ACLY Promotes Homologous Recombination.* Mol Cell, 2017. **67**(2): p. 252-265 e6.
579. Sutendra, G., et al., *A nuclear pyruvate dehydrogenase complex is important for the generation of acetyl-CoA and histone acetylation.* Cell, 2014. **158**(1): p. 84-97.
580. Zhou, W., et al., *Nuclear accumulation of pyruvate dehydrogenase alpha 1 promotes histone acetylation and is essential for zygotic genome activation in porcine embryos.* Biochim Biophys Acta Mol Cell Res, 2020. **1867**(4): p. 118648.
581. Chen, L.Y., et al., *Modulation of matrix metabolism by ATP-citrate lyase in articular chondrocytes.* J Biol Chem, 2018. **293**(31): p. 12259-12270.
582. Lee, J.V., et al., *Acetyl-CoA promotes glioblastoma cell adhesion and migration through Ca(2+)-NFAT signaling.* Genes Dev, 2018. **32**(7-8): p. 497-511.
583. Jiang, Y., et al., *Galdieri, 2016AMP-activated protein kinase links acetyl-CoA homeostasis to BRD4 recruitment in acute myeloid leukemia.* Blood, 2019. **134**(24): p. 2183-2194.
584. Schrader, M., M. Kamoshita, and M. Islinger, *Organelle interplay-peroxisome interactions in health and disease.* J Inherit Metab Dis, 2020. **43**(1): p. 71-89.
585. Schulz, H., *Fatty Acid Oxidation.* 2013: p. 281-284.
586. Nowinski, S.M., et al., *Mitochondrial fatty acid synthesis coordinates oxidative metabolism in mammalian mitochondria.* Elife, 2020. **9**.
587. Fang, Y., et al., *Histone crotonylation promotes mesoendodermal commitment of human embryonic stem cells.* Cell Stem Cell, 2021.
588. Violante, S., et al., *Substrate specificity of human carnitine acetyltransferase: Implications for fatty acid and branched-chain amino acid metabolism.* Biochim Biophys Acta, 2013. **1832**(6): p. 773-9.
589. Choi, S., et al., *Oxoglutarate dehydrogenase and acetyl-CoA acyltransferase 2 selectively associate with H2A.Z-occupied promoters and are required for histone modifications.* Biochim Biophys Acta Gene Regul Mech, 2019. **1862**(10): p. 194436.
590. Westin, M.A., M.C. Hunt, and S.E. Alexson, *The identification of a succinyl-CoA thioesterase suggests a novel pathway for succinate production in peroxisomes.* J Biol Chem, 2005. **280**(46): p. 38125-32.
591. Goudarzi, A., et al., *Starvation promotes histone lysine butyrylation in the liver of male but not female mice.* Gene, 2020. **745**: p. 144647.
592. Newman, J.C. and E. Verdin, *Ketone bodies as signaling metabolites.* Trends Endocrinol Metab, 2014. **25**(1): p. 42-52.
593. Tan, J., et al., *The role of short-chain fatty acids in health and disease.* Adv Immunol, 2014. **121**: p. 91-119.
594. Smestad, J., et al., *Chromatin Succinylation Correlates with Active Gene Expression and Is Perturbed by Defective TCA Cycle Metabolism.* iScience, 2018. **2**: p. 63-75.
595. Ringel, A.E., S.A. Tucker, and M.C. Haigis, *Chemical and Physiological Features of Mitochaondrial Acylation.* Molecular cell, 2018. **72**(4): p. 610-624.
596. Murphy, M.P. and L.A.J. O'Neill, *Krebs Cycle Reimagined: The Emerging Roles of Succinate and Itaconate as Signal Transducers.* Cell, 2018. **174**(4): p. 780-784.
597. Trefely, S., et al., *Compartmentalised acyl-CoA metabolism and roles in chromatin regulation.* Molecular

Metabolism, 2020. **38**: p. 100941.

598. Nikiforov, A., V. Kulikova, and M. Ziegler, *The human NAD metabolome: Functions, metabolism and compartmentalization.* Crit Rev Biochem Mol Biol, 2015. **50**(4): p. 284-97.
599. Kuribayashi, H., et al., *Roles of Nmnat1 in the survival of retinal progenitors through the regulation of pro-apoptotic gene expression via histone acetylation.* Cell Death Dis, 2018. **9**(9): p. 891.
600. Ryall, J.G., et al., *The NAD(+)-dependent SIRT1 deacetylase translates a metabolic switch into regulatory epigenetics in skeletal muscle stem cells.* Cell Stem Cell, 2015. **16**(2): p. 171-83.
601. Karch, K.R., et al., *The nucleosomal surface is the main target of histone ADP-ribosylation in response to DNA damage.* Mol Biosyst, 2017. **13**(12): p. 2660-2671.
602. Forneris, F., et al., *LSD1: oxidative chemistry for multifaceted functions in chromatin regulation.* Trends Biochem Sci, 2008. **33**(4): p. 181-9.
603. Giancaspero, T.A., et al., *FAD synthesis and degradation in the nucleus create a local flavin cofactor pool.* J Biol Chem, 2013. **288**(40): p. 29069-80.
604. Carey, B.W., et al., *Intracellular alpha-ketoglutarate maintains the pluripotency of embryonic stem cells.* Nature, 2015. **518**(7539): p. 413-6.
605. Xiao, M., et al., *Inhibition of α-KG-dependent histone and DNA demethylases by fumarate and succinate that are accumulated in mutations of FH and SDH tumor suppressors.* Genes Dev, 2012. **26**(12): p. 1326-38.
606. Yang, W., et al., *PKM2 Phosphorylates Histone H3 and Promotes Gene Transcription and Tumorigenesis.* Cell, 2014. **158**(5): p. 1210.
607. Xia, L., et al., *Pyruvate kinase M2 phosphorylates H2AX and promotes genomic instability in human tumor cells.* Oncotarget, 2017. **8**(65): p. 109120-109134.
608. Xu, W., et al., *Oncometabolite 2-hydroxyglutarate is a competitive inhibitor of α-ketoglutarate-dependent dioxygenases.* Cancer Cell, 2011. **19**(1): p. 17-30.
609. Figueroa, M.E., et al., *Leukemic IDH1 and IDH2 mutations result in a hypermethylation phenotype, disrupt TET2 function, and impair hematopoietic differentiation.* Cancer Cell, 2010. **18**(6): p. 553-67.
610. Lu, C., et al., *IDH mutation impairs histone demethylation and results in a block to cell differentiation.* Nature, 2012. **483**(7390): p. 474-8.
611. Pavlova, N.N. and C.B. Thompson, *The Emerging Hallmarks of Cancer Metabolism.* Cell Metab, 2016. **23**(1): p. 27-47.
612. Warburg, O., *On the Origin of Cancer Cells.* Science, 1956. **123**(3191): p. 309-314.
613. Sun, L., et al., *Metabolic reprogramming for cancer cells and their microenvironment: Beyond the Warburg Effect.* Biochim Biophys Acta Rev Cancer, 2018. **1870**(1): p. 51-66.
614. Anastasiou, D., et al., *Inhibition of pyruvate kinase M2 by reactive oxygen species contributes to cellular antioxidant responses.* Science, 2011. **334**(6060): p. 1278-83.
615. Kim, J.W., et al., *HIF-1-mediated expression of pyruvate dehydrogenase kinase: a metabolic switch required for cellular adaptation to hypoxia.* Cell Metab, 2006. **3**(3): p. 177-85.
616. Sheng, H. and W. Tang, *Glycolysis Inhibitors for Anticancer Therapy: A Review of Recent Patents.* Recent Pat Anticancer Drug Discov, 2016. **11**(3): p. 297-308.
617. Su, Q., et al., *The role of pyruvate kinase M2 in anticancer therapeutic treatments.* Oncol Lett, 2019. **18**(6): p. 5663-5672.
618. Barthel, A., et al., *Regulation of GLUT1 gene transcription by the serine/threonine kinase Akt1.* J Biol Chem, 1999. **274**(29): p. 20281-6.
619. Wieman, H.L., J.A. Wofford, and J.C. Rathmell, *Cytokine stimulation promotes glucose uptake via phosphatidylinositol-3 kinase/Akt regulation of Glut1 activity and trafficking.* Mol Biol Cell, 2007. **18**(4): p. 1437-46.
620. Deprez, J., et al., *Phosphorylation and activation of heart 6-phosphofructo-2-kinase by protein kinase B and*

other protein kinases of the insulin signaling cascades. J Biol Chem, 1997. **272**(28): p. 17269-75.

621. Gottlob, K., et al., *Inhibition of early apoptotic events by Akt/PKB is dependent on the first committed step of glycolysis and mitochondrial hexokinase.* Genes Dev, 2001. **15**(11): p. 1406-18.
622. Papandreou, I., et al., *HIF-1 mediates adaptation to hypoxia by actively downregulating mitochondrial oxygen consumption.* Cell Metab, 2006. **3**(3): p. 187-97.
623. Lee, G., et al., *Oxidative Dimerization of PHD2 is Responsible for its Inactivation and Contributes to Metabolic Reprogramming via HIF-1α Activation.* Sci Rep, 2016. **6**: p. 18928.
624. Semenza, G.L., *Hypoxia-inducible factors in physiology and medicine.* Cell, 2012. **148**(3): p. 399-408.
625. Luo, W., et al., *Pyruvate kinase M2 is a PHD3-stimulated coactivator for hypoxia-inducible factor 1.* Cell, 2011. **145**(5): p. 732-44.
626. Mekhail, K., et al., *HIF activation by pH-dependent nucleolar sequestration of VHL.* Nat Cell Biol, 2004. **6**(7): p. 642-7.
627. Chaneton, B., et al., *Serine is a natural ligand and allosteric activator of pyruvate kinase M2.* Nature, 2012. **491**(7424): p. 458-462.
628. Christofk, H.R., et al., *The M2 splice isoform of pyruvate kinase is important for cancer metabolism and tumour growth.* Nature, 2008. **452**(7184): p. 230-3.
629. Kennedy, K.M. and M.W. Dewhirst, *Tumor metabolism of lactate: the influence and therapeutic potential for MCT and CD147 regulation.* Future Oncol, 2010. **6**(1): p. 127-48.
630. Feron, O., *Pyruvate into lactate and back: from the Warburg effect to symbiotic energy fuel exchange in cancer cells.* Radiother Oncol, 2009. **92**(3): p. 329-33.
631. Kuşoğlu, A. and Ç. Biray Avcı, *Cancer stem cells: A brief review of the current status.* Gene, 2019. **681**: p. 80-85.
632. Ebinger, S., et al., *Characterization of Rare, Dormant, and Therapy-Resistant Cells in Acute Lymphoblastic Leukemia.* Cancer Cell, 2016. **30**(6): p. 849-862.
633. LeBleu, V.S., et al., *PGC-1α mediates mitochondrial biogenesis and oxidative phosphorylation in cancer cells to promote metastasis.* Nat Cell Biol, 2014. **16**(10): p. 992-1003, 1-15.
634. Viale, A., et al., *Oncogene ablation-resistant pancreatic cancer cells depend on mitochondrial function.* Nature, 2014. **514**(7524): p. 628-32.
635. Testa, U., et al., *Oxidative stress and hypoxia in normal and leukemic stem cells.* Exp Hematol, 2016. **44**(7): p. 540-60.
636. Eagle, H., *The minimum vitamin requirements of the L and HeLa cells in tissue culture, the production of specific vitamin deficiencies, and their cure.* J Exp Med, 1955. **102**(5): p. 595-600.
637. Rivera, S., et al., *Amino acid metabolism in tumour-bearing mice.* Biochem J, 1988. **249**(2): p. 443-9.
638. Yuneva, M.O., et al., *The metabolic profile of tumors depends on both the responsible genetic lesion and tissue type.* Cell Metab, 2012. **15**(2): p. 157-70.
639. Gaglio, D., et al., *Glutamine deprivation induces abortive s-phase rescued by deoxyribonucleotides in k-ras transformed fibroblasts.* PLoS One, 2009. **4**(3): p. e4715.
640. Still, E.R. and M.O. Yuneva, *Hopefully devoted to Q: targeting glutamine addiction in cancer.* Br J Cancer, 2017. **116**(11): p. 1375-1381.
641. Yang, L., S. Venneti, and D. Nagrath, *Glutaminolysis: A Hallmark of Cancer Metabolism.* Annu Rev Biomed Eng, 2017. **19**: p. 163-194.
642. Richman, E.L., et al., *Choline intake and risk of lethal prostate cancer: incidence and survival.* Am J Clin Nutr, 2012. **96**(4): p. 855-63.
643. Ying, J., et al., *Associations between dietary intake of choline and betaine and lung cancer risk.* PLoS One, 2013. **8**(2): p. e54561.
644. Zhang, C.X., et al., *Choline and betaine intake is inversely associated with breast cancer risk: a two-stage*

case-control study in China. Cancer Sci, 2013. **104**(2): p. 250-8.

645. Wang, R., et al., *The transcription factor Myc controls metabolic reprogramming upon T lymphocyte activation.* Immunity, 2011. **35**(6): p. 871-82.
646. Wise, D.R., et al., *c.* Proc Natl Acad Sci U S A, 2008. **105**(48): p. 18782-7.
647. Eberhardy, S.R. and P.J. Farnham, *c-Myc mediates activation of the cad promoter via a post-RNA polymerase II recruitment mechanism.* J Biol Chem, 2001. **276**(51): p. 48562-71.
648. Gao, P., et al., *c-Myc suppression of miR-23a/b enhances mitochondrial glutaminase expression and glutamine metabolism.* Nature, 2009. **458**(7239): p. 762-5.
649. Mannava, S., et al., *Direct role of nucleotide metabolism in C-MYC-dependent proliferation of melanoma cells.* Cell Cycle, 2008. **7**(15): p. 2392-400.
650. Reynolds, M.R., et al., *Control of glutamine metabolism by the tumor suppressor Rb.* Oncogene, 2014. **33**(5): p. 556-66.
651. Faubert, B., et al., *Loss of the tumor suppressor LKB1 promotes metabolic reprogramming of cancer cells via HIF-1α.* Proc Natl Acad Sci U S A, 2014. **111**(7): p. 2554-9.
652. Son, J., et al., *Glutamine supports pancreatic cancer growth through a KRAS-regulated metabolic pathway.* Nature, 2013. **496**(7443): p. 101-5.
653. Csibi, A., et al., *The mTORC1 pathway stimulates glutamine metabolism and cell proliferation by repressing SIRT4.* Cell, 2013. **153**(4): p. 840-54.
654. Suzuki, S., et al., *Phosphate-activated glutaminase (GLS2), a p53-inducible regulator of glutamine metabolism and reactive oxygen species.* Proc Natl Acad Sci U S A, 2010. **107**(16): p. 7461-6.
655. Bryan, H.K., et al., *The Nrf2 cell defence pathway: Keap1-dependent and -independent mechanisms of regulation.* Biochem Pharmacol, 2013. **85**(6): p. 705-17.
656. El-Hattab, A.W., *Serine biosynthesis and transport defects.* Mol Genet Metab, 2016. **118**(3): p. 153-9.
657. Mattaini, K.R., M.R. Sullivan, and M.G. Vander Heiden, *The importance of serine metabolism in cancer.* J Cell Biol, 2016. **214**(3): p. 249-57.
658. Labuschagne, C.F., et al., *Serine, but not glycine, supports one-carbon metabolism and proliferation of cancer cells.* Cell Rep, 2014. **7**(4): p. 1248-58.
659. Jain, M., et al., *Metabolite profiling identifies a key role for glycine in rapid cancer cell proliferation.* Science, 2012. **336**(6084): p. 1040-4.
660. Possemato, R., et al., *Functional genomics reveal that the serine synthesis pathway is essential in breast cancer.* Nature, 2011. **476**(7360): p. 346-50.
661. Ye, J., et al., *Serine catabolism regulates mitochondrial redox control during hypoxia.* Cancer Discov, 2014. **4**(12): p. 1406-17.
662. Liu, J., et al., *Phosphoglycerate dehydrogenase induces glioma cells proliferation and invasion by stabilizing forkhead box M1.* J Neurooncol, 2013. **111**(3): p. 245-55.
663. Krall, A.S., et al., *Asparagine promotes cancer cell proliferation through use as an amino acid exchange factor.* Nat Commun, 2016. **7**: p. 11457.
664. Maddocks, O.D., et al., *Serine starvation induces stress and p53-dependent metabolic remodelling in cancer cells.* Nature, 2013. **493**(7433): p. 542-6.
665. Tavana, O. and W. Gu, *The Hunger Games: p53 regulates metabolism upon serine starvation.* Cell Metab, 2013. **17**(2): p. 159-61.
666. Sun, L., et al., *cMyc-mediated activation of serine biosynthesis pathway is critical for cancer progression under nutrient deprivation conditions.* Cell Res, 2015. **25**(4): p. 429-44.
667. Ananieva, E.A. and A.C. Wilkinson, *Branched-chain amino acid metabolism in cancer.* Curr Opin Clin Nutr Metab Care, 2018. **21**(1): p. 64-70.
668. Mayers, J.R., et al., *Tissue of origin dictates branched-chain amino acid metabolism in mutant Kras-driven*

cancers. Science, 2016. **353**(6304): p. 1161-5.

669. Tönjes, M., et al., *BCAT1 promotes cell proliferation through amino acid catabolism in gliomas carrying wild-type IDH1.* Nat Med, 2013. **19**(7): p. 901-908.
670. Hattori, A., et al., *Cancer progression by reprogrammed BCAA metabolism in myeloid leukaemia.* Nature, 2017. **545**(7655): p. 500-504.
671. Yu, C.P., et al., *Targeting TDO in cancer immunotherapy.* Med Oncol, 2017. **34**(5): p. 73.
672. Pilotte, L., et al., *Reversal of tumoral immune resistance by inhibition of tryptophan 2,3-dioxygenase.* Proc Natl Acad Sci U S A, 2012. **109**(7): p. 2497-502.
673. Buck, M.D., D. O'Sullivan, and E.L. Pearce, *T cell metabolism drives immunity.* J Exp Med, 2015. **212**(9): p. 1345-60.
674. Opitz, C.A., et al., *An endogenous tumour-promoting ligand of the human aryl hydrocarbon receptor.* Nature, 2011. **478**(7368): p. 197-203.
675. Hill, J.M., et al., *L-asparaginase therapy for leukemia and other malignant neoplasms. Remission in human leukemia.* Jama, 1967. **202**(9): p. 882-8.
676. Pieters, R., et al., *L-asparaginase treatment in acute lymphoblastic leukemia: a focus on Erwinia asparaginase.* Cancer, 2011. **117**(2): p. 238-49.
677. Li, J. and J.X. Cheng, *Direct visualization of de novo lipogenesis in single living cells.* Sci Rep, 2014. **4**: p. 6807.
678. Menendez, J.A. and R. Lupu, *Fatty acid synthase and the lipogenic phenotype in cancer pathogenesis.* Nat Rev Cancer, 2007. **7**(10): p. 763-77.
679. Chajès, V., et al., *Acetyl-CoA carboxylase alpha is essential to breast cancer cell survival.* Cancer Res, 2006. **66**(10): p. 5287-94.
680. Flavin, R., et al., *Fatty acid synthase as a potential therapeutic target in cancer.* Future Oncol, 2010. **6**(4): p. 551-62.
681. Migita, T., et al., *ATP citrate lyase: activation and therapeutic implications in non-small cell lung cancer.* Cancer Res, 2008. **68**(20): p. 8547-54.
682. Rysman, E., et al., *De novo lipogenesis protects cancer cells from free radicals and chemotherapeutics by promoting membrane lipid saturation.* Cancer Res, 2010. **70**(20): p. 8117-26.
683. Hensley, C.T., et al., *Metabolic Heterogeneity in Human Lung Tumors.* Cell, 2016. **164**(4): p. 681-94.
684. Chen, Y.J., et al., *Lactate metabolism is associated with mammalian mitochondria.* Nat Chem Biol, 2016. **12**(11): p. 937-943.
685. Huang, D., et al., *HIF-1-mediated suppression of acyl-CoA dehydrogenases and fatty acid oxidation is critical for cancer progression.* Cell Rep, 2014. **8**(6): p. 1930-1942.
686. Yang, L., et al., *Targeting Stromal Glutamine Synthetase in Tumors Disrupts Tumor Microenvironment-Regulated Cancer Cell Growth.* Cell Metab, 2016. **24**(5): p. 685-700.
687. Spinelli, J.B., et al., *Metabolic recycling of ammonia via glutamate dehydrogenase supports breast cancer biomass.* Science, 2017. **358**(6365): p. 941-946.
688. Potapova, I.A., et al., *Phosphorylation of recombinant human ATP:citrate lyase by cAMP-dependent protein kinase abolishes homotropic allosteric regulation of the enzyme by citrate and increases the enzyme activity. Allosteric activation of ATP:citrate lyase by phosphorylated sugars.* Biochemistry, 2000. **39**(5): p. 1169-79.
689. Galdieri, L., et al., *Activation of AMP-activated Protein Kinase by Metformin Induces Protein Acetylation in Prostate and Ovarian Cancer Cells.* J Biol Chem, 2016. **291**(48): p. 25154-25166.
690. Chiang, E.P., et al., *Effects of insulin and glucose on cellular metabolic fluxes in homocysteine transsulfuration, remethylation, S-adenosylmethionine synthesis, and global deoxyribonucleic acid methylation.* J Clin Endocrinol Metab, 2009. **94**(3): p. 1017-25.
691. Shyh-Chang, N., et al., *Influence of threonine metabolism on S-adenosylmethionine and histone methylation.* Science, 2013. **339**(6116): p. 222-6.

692. Towbin, B.D., et al., *Step-wise methylation of histone H3K9 positions heterochromatin at the nuclear periphery.* Cell, 2012. **150**(5): p. 934-47.
693. Chang, S., S. Yim, and H. Park, *The cancer driver genes IDH1/2, JARID1C/ KDM5C, and UTX/ KDM6A: crosstalk between histone demethylation and hypoxic reprogramming in cancer metabolism.* Exp Mol Med, 2019. **51**(6): p. 1-17.
694. Jabbour, E., et al., *New insights into the pathophysiology and therapy of adult acute lymphoblastic leukemia.* Cancer, 2015. **121**(15): p. 2517-28.
695. Liu, Y.F., et al., *Genomic Profiling of Adult and Pediatric B-cell Acute Lymphoblastic Leukemia.* EBioMedicine, 2016. **8**: p. 173-183.
696. Foà, R., et al., *Dasatinib-Blinatumomab for Ph-Positive Acute Lymphoblastic Leukemia in Adults.* N Engl J Med, 2020. **383**(17): p. 1613-1623.
697. Dai, H., et al., *Bispecific CAR-T cells targeting both CD19 and CD22 for therapy of adults with relapsed or refractory B cell acute lymphoblastic leukemia.* J Hematol Oncol, 2020. **13**(1): p. 30.
698. Heng, G., et al., *Sustained Therapeutic Efficacy of Humanized Anti-CD19 Chimeric Antigen Receptor T Cells in Relapsed/Refractory Acute Lymphoblastic Leukemia.* Clin Cancer Res, 2020. **26**(7): p. 1606-1615.
699. Aldoss, I. and A.S. Stein, *Advances in adult acute lymphoblastic leukemia therapy.* Leuk Lymphoma, 2018. **59**(5): p. 1033-1050.
700. Khan, M., R. Siddiqi, and T.H. Tran, *Philadelphia chromosome-like acute lymphoblastic leukemia: A review of the genetic basis, clinical features, and therapeutic options.* Semin Hematol, 2018. **55**(4): p. 235-241.
701. Baylin, S.B. and P.A. Jones, *Epigenetic Determinants of Cancer.* Cold Spring Harb Perspect Biol, 2016. **8**(9).
702. Rousseaux, S., J. Wang, and S. Khochbin, *Cancer hallmarks sustained by ectopic activations of placenta/male germline genes.* Cell Cycle, 2013. **12**(15): p. 2331-2.
703. Van Tongelen, A., A. Loriot, and C. De Smet, *Oncogenic roles of DNA hypomethylation through the activation of cancer-germline genes.* Cancer Lett, 2017. **396**: p. 130-137.
704. Ana Janic, L.M., Salud Llamazares, David Rossell, Cayetano Gonzalez, *Ectopic Expression of Germline Genes Drives Malignant Brain Tumor Growth in Drosophila.* SCIENCE, 2010. **330**: p. 1824-1827.
705. Gibbs, Z.A. and A.W. Whitehurst, *Emerging Contributions of Cancer/Testis Antigens to Neoplastic Behaviors.* Trends Cancer, 2018. **4**(10): p. 701-712.
706. Chen, X., et al., *Expression and prognostic relevance of MAGE-A3 and MAGE-C2 in non-small cell lung cancer.* Oncol Lett, 2017. **13**(3): p. 1609-1618.
707. Rousseaux, S., et al., *Ectopic Activation of Germline and Placental Genes Identifies Aggressive Metastasis-Prone Lung Cancers.* Science Translational Medicine, 2013. **5**(186): p. 1-11.
708. Emadali, A., et al., *Identification of a novel BET bromodomain inhibitor-sensitive, gene regulatory circuit that controls Rituximab response and tumour growth in aggressive lymphoid cancers.* EMBO molecular medicine, 2013. **5**(8): p. 1180-1195.
709. Lu, Y.C., et al., *Treatment of Patients With Metastatic Cancer Using a Major Histocompatibility Complex Class II-Restricted T-Cell Receptor Targeting the Cancer Germline Antigen MAGE-A3.* J Clin Oncol, 2017. **35**(29): p. 3322-3329.
710. Gordeeva, O., *Cancer-testis antigens: Unique cancer stem cell biomarkers and targets for cancer therapy.* Semin Cancer Biol, 2018. **53**: p. 75-89.
711. Jin Wang, et al., *A six gene expression signature defnes aggressive subtypes and predicts outcome in childhood and adult acute lymphoblastic leukemia.* Oncotarget, 2015: p. 1-16.
712. Barchiesi, A. and C. Vascotto, *Transcription, Processing, and Decay of Mitochondrial RNA in Health and Disease.* Int J Mol Sci, 2019. **20**(9).
713. Bonekamp, N.A. and N.G. Larsson, *SnapShot: Mitochondrial Nucleoid.* Cell, 2018. **172**(1-2): p. 388-388.e1.
714. Nicholls, T.J. and M. Minczuk, *In D-loop: 40 years of mitochondrial 7S DNA.* Exp Gerontol, 2014. **56**: p. 175-

81.

715. Sousa, J.S., E. D'Imprima, and J. Vonck, *Mitochondrial Respiratory Chain Complexes*, in *Membrane Protein Complexes: Structure and Function*, J.R. Harris and E.J. Boekema, Editors. 2018, Springer Singapore: Singapore. p. 167-227.
716. Mirko, S.B.Đ., *Interaction between mitochondrial and nuclear genomes: the role in life-history evolution. .* Biologia Serbica, 2017. **39**(1): p. 32-40.
717. Hubackova, S., et al., *Mitochondria-driven elimination of cancer and senescent cells.* Biol Chem, 2019. **400**(2): p. 141-148.
718. Ashton, T.M., et al., *Oxidative Phosphorylation as an Emerging Target in Cancer Therapy.* Clin Cancer Res, 2018. **24**(11): p. 2482-2490.
719. Simarro, M., et al., *Fast kinase domain-containing protein 3 is a mitochondrial protein essential for cellular respiration.* Biochem Biophys Res Commun, 2010. **401**(3): p. 440-6.
720. Lee, I. and W. Hong, *RAP--a putative RNA-binding domain.* Trends Biochem Sci, 2004. **29**(11): p. 567-70.
721. Boehm, E., et al., *FASTKD1 and FASTKD4 have opposite effects on expression of specific mitochondrial RNAs, depending upon their endonuclease-like RAP domain.* Nucleic Acids Res, 2017. **45**(10): p. 6135-6146.
722. Popow, J., et al., *FASTKD2 is an RNA-binding protein required for mitochondrial RNA processing and translation.* Rna, 2015. **21**(11): p. 1873-84.
723. Jourdain, A.A., et al., *A mitochondria-specific isoform of FASTK is present in mitochondrial RNA granules and regulates gene expression and function.* Cell Rep, 2015. **10**(7): p. 1110-21.
724. Ghezzi, D., et al., *FASTKD2 nonsense mutation in an infantile mitochondrial encephalomyopathy associated with cytochrome c oxidase deficiency.* Am J Hum Genet, 2008. **83**(3): p. 415-23.
725. Marshall, K.D., et al., *The novel cyclophilin-D-interacting protein FASTKD1 protects cells against oxidative stress-induced cell death.* Am J Physiol Cell Physiol, 2019. **317**(3): p. C584-c599.
726. Emadali, A., et al., *Identification of a novel BET bromodomain inhibitor-sensitive, gene regulatory circuit that controls Rituximab response and tumour growth in aggressive lymphoid cancers.* EMBO Mol Med, 2013. **5**(8): p. 1180-95.
727. Goudarzi, A., et al., *Dynamic Competing Histone H4 K5K8 Acetylation and Butyrylation Are Hallmarks of Highly Active Gene Promoters.* Mol Cell, 2016. **62**(2): p. 169-180.
728. Sanjana, N.E., O. Shalem, and F. Zhang, *Improved vectors and genome-wide libraries for CRISPR screening.* Nat Methods, 2014. **11**(8): p. 783-784.
729. Weber, K., et al., *A multicolor panel of novel lentiviral "gene ontology" (LeGO) vectors for functional gene analysis.* Mol Ther, 2008. **16**(4): p. 698-706.
730. Spinck, M., et al., *Evolved, Selective Erasers of Distinct Lysine Acylations.* Angew Chem Int Ed Engl, 2020. **59**(27): p. 11142-11149.
731. Dull, T., et al., *A third-generation lentivirus vector with a conditional packaging system.* J Virol, 1998. **72**(11): p. 8463-71.
732. Dobin, A., et al., *STAR: ultrafast universal RNA-seq aligner.* Bioinformatics, 2013. **29**(1): p. 15-21.
733. Langmead, B. and S.L. Salzberg, *Fast gapped-read alignment with Bowtie 2.* Nat Methods, 2012. **9**(4): p. 357-9.
734. Anders, S., P.T. Pyl, and W. Huber, *HTSeq--a Python framework to work with high-throughput sequencing data.* Bioinformatics, 2015. **31**(2): p. 166-9.
735. Schneider, C.A., W.S. Rasband, and K.W. Eliceiri, *NIH Image to ImageJ: 25 years of image analysis.* Nat Methods, 2012. **9**(7): p. 671-5.
736. Barral, S., et al., *Histone Variant H2A.L.2 Guides Transition Protein-Dependent Protamine Assembly in Male Germ Cells.* Mol Cell, 2017. **66**(1): p. 89-101.e8.
737. Dai, B., et al., *Detection of post-translational modifications on native intact nucleosomes by ELISA.* Journal of

visualized experiments : JoVE, 2011(50): p. 2593.

738. Boehm, E., et al., *Role of FAST Kinase Domains 3 (FASTKD3) in Post-transcriptional Regulation of Mitochondrial Gene Expression.* J Biol Chem, 2016. **291**(50): p. 25877-25887.
739. Antonicka, H. and E.A. Shoubridge, *Mitochondrial RNA Granules Are Centers for Posttranscriptional RNA Processing and Ribosome Biogenesis.* Cell Rep, 2015. **10**(6): p. 920-932.
740. Han, S., et al., *Proximity Biotinylation as a Method for Mapping Proteins Associated with mtDNA in Living Cells.* Cell Chem Biol, 2017. **24**(3): p. 404-414.
741. Testa U., et al., *Oxidative stress and hypoxia in normal and leukemic stem cells.* Exp Hematol, 2016. **44**(7): p. 540-60.
742. Wang Y. H., et al., *Cell-state-specific metabolic dependency in hematopoiesis and leukemogenesis.* Cell, 2014. **158**(6): p. 1309-1323.
743. Hoang-Minh, L.B., et al., *Infiltrative and drug-resistant slow-cycling cells support metabolic heterogeneity in glioblastoma.* EMBO J, 2018. **37**(23).
744. Herrera, J.E., et al., *The histone acetyltransferase activity of human GCN5 and PCAF is stabilized by coenzymes.* J Biol Chem, 1997. **272**(43): p. 27253-8.
745. Imhof, A., et al., *Acetylation of general transcription factors by histone acetyltransferases.* Curr Biol, 1997. **7**(9): p. 689-92.
746. Zhang, K., et al., *Histone acetylation and deacetylation: identification of acetylation and methylation sites of HeLa histone H4 by mass spectrometry.* Mol Cell Proteomics, 2002. **1**(7): p. 500-8.
747. Thorne, A.W., et al., *Patterns of histone acetylation.* Eur J Biochem, 1990. **193**(3): p. 701-13.
748. Garcia, B.A., et al., *Organismal differences in post-translational modifications in histones H3 and H4.* J Biol Chem, 2007. **282**(10): p. 7641-55.
749. Schübeler, D., M. Groudine, and M.A. Bender, *The murine beta-globin locus control region regulates the rate of transcription but not the hyperacetylation of histones at the active genes.* Proc Natl Acad Sci U S A, 2001. **98**(20): p. 11432-7.
750. Louphrasitthiphol, P., et al., *Tuning Transcription Factor Availability through Acetylation-Mediated Genomic Redistribution.* Mol Cell, 2020. **79**(3): p. 472-487 e10.
751. Yuan, G.C., et al., *Genome-scale identification of nucleosome positions in S. cerevisiae.* Science, 2005. **309**(5734): p. 626-30.
752. Lorch, Y. and R.D. Kornberg, *Chromatin-remodeling for transcription.* Q Rev Biophys, 2017. **50**: p. e5.
753. Schones, D.E., et al., *Dynamic regulation of nucleosome positioning in the human genome.* Cell, 2008. **132**(5): p. 887-98.
754. Nizovtseva, E.V., et al., *Nucleosome-free DNA regions differentially affect distant communication in chromatin.* Nucleic Acids Res, 2017. **45**(6): p. 3059-3067.